UNIVERSIDADE DE BRASÍLIA - UNB

INSTITUTO DE GEOCIÊNCIAS - IG

COMPLEXOS ACAMADADOS DA SERRA DA ONÇA E SERRA DO PUMA: GEOLOGIA E PETROLOGIA DE DUAS INTRUSÕES MÁFICO-ULTRAMÁFICAS COM SEQUENCIA DE CRISTALIZAÇÃO DISTINTA NA PROVÍNCIA ARQUEANA DE CARAJÁS, BRASIL.

WOLNEY DUTRA ROSA

DISSERTAÇÃO DE MESTRADO Nº 331

Brasília

2014

UNIVERSIDADE DE BRASÍLIA - UNB
INSTITUTO DE GEOCIÊNCIAS - IG

COMPLEXOS ACAMADADOS DA SERRA DA ONÇA E SERRA DO PUMA: GEOLOGIA E PETROLOGIA DE DUAS INTRUSÕES MÁFICO-ULTRAMÁFICAS COM SEQUENCIA DE CRISTALIZAÇÃO DISTINTA NA PROVÍNCIA ARQUEANA DE CARAJÁS, BRASIL.

Wolney Dutra Rosa

Dissertação de Mestrado Nº 331

Orientador: Prof. Dr. Cesar Fonseca Ferreira Filho (IG-UnB)

Examinadores:

Prof. Dr. Cesar F. Ferreira Filho IG-UnB (orientador)

Prof. Dr[a]. Juliana Charão Marques - IG-IFRGS (membro externo)

Prof. Dr. Massimo Matteini - IG-UnB (membro interno)

Prof. Dr[a]. Catarina L. Toledo (membro interno - suplente)

Brasília, agosto de 2014

AGRADECIMENTOS

Ao professor Dr. Cesar F. Ferreira Filho, por toda dedicação, vontade em transmitir seu conhecimento e comprometimento com o projeto de pesquisa;

À professora Dra. Sylvia Maria Araújo, pela revisão final no trabalho;

Ao professor Márcio M. Pimentel, pela ajuda com os estudos geocronológicos;

Ao Instituto de Geociências da Universidade de Brasília e seus professores, pela base geológica na minha graduação e pelo suporte nas diversas análises deste projeto;

A Vale S/A pelo apoio na liberação dos dados e acesso as áreas;

Ao CNPq, IG-UnB e VALE pelo suporte no custeio e nas diversas etapas de campo e laboratório deste projeto de pesquisa.

Aos meus gerentes Fernando Matos e Fernando Greco, por aprovar e apoiar o projeto de pesquisa;

Aos geólogos e amigos de trabalho, em especial a Carlos Augusto Medeiros, Rogerio Caron, Denisson Oliveira, Samuel Nunes e Cantidiano Freitas, pelo apoio em campo, discussões e disposição em ajudar;

À geóloga e amiga, Juliana Araujo, por não medir esforços na hora de ajudar e incentivar;

À geóloga e querida esposa, Rubia Schley, pela paciência, apoio incondicional, toque de arte nas figuras e força para conseguir finalizar esse projeto;

A minha irmã, Hianny, e seu anjinho Felipe, que mesmo distante transformou a vida de toda família;

Aos meus pais, José e Luzia, pela dedicação, amor, carinho e construção dos meus valores como ser humano.

ÍNDICE

ÍNDICE DE FIGURAS

ÍNDICE DE TABELAS

RESUMO

Os complexos máficos-ultramáficos da Serra da Onça e Serra do Puma estão localizados na porção SW da Província Mineral de Carajás (PMC), um dos mais importantes distritos minerais do Brasil, conhecida por abrigar várias intrusões acamadadas que possuem significantes recursos de níquel laterítico. É resultado deste estudo, a primeira caracterização detalhada destas duas intrusões na porção ocidental da PMC, que indicam uma evolução magmática notavelmente diferente para os Complexos da Serra da Onça (CSO) e Complexo da Serra do Puma (CSP). A geologia do CSO foi previamente descrito por Macambira (1997) e Macambira e Ferreira Filho (2002). A CSO é uma intrusão de direção EW, com 24 km de comprimento e aproximadamente 3,5 km de largura. A estratigrafia da CSO consiste em um grupo de borda inferior (GBI), zona ultramáfica (ZU) e zona máfica (ZM). O GBI localizado na porção norte da intrusão, forma uma estreita e descontinua camada constituída por gabronoritos (Opx+Cpx+Pl cúmulus). A ZU forma uma serra alongada e é constituída principalmente por dunitos (Ol+Chr) e camadas de ortopiroxenitos (Opx+Chr). A sequência de cristalização da ZU consiste em Ol+Chr; Ol+Opx+Chr; Opx+Chr e Opx. A ZM abrange metade de toda área exposta da CSO e consiste em sua maioria de gabronoritos (Opx+Cpx+Pl). As rochas mais fracionadas da ZM consistem em camadas pouco espessas de ilmenita-magnetita gabronorito (Pig+Cpx+Pl+Mag+Ilm cúmulus). A sequencia de cristalização da ZM é Opx+Pl; Opx+Pl+Cpx; Pig+Pl+Cpx e Pig+Pl+Cpx+Mag+Ilm. O Complexo da Serra do Puma (CSP) é uma intrusão acamadada de direção SW-NE com aproximadamente 25 km de comprimento por 3 km de largura. Sua estratigrafia é formada por um grupo de borda inferior (GBI), zona ultramáfica (ZU) e zona acamadada (ZA). O GBI forma uma zona distinta formada por gabros (Cpx+Pl) na borda norte da CSP. A ZU forma uma serra alongada e é constituída principalmente por dunitos (Ol+Chr) com menores intercalações de peridotitos com Ol+Chr cúmulus ou Ol+Cpx+Chr, e variáveis proporções de Cpx+Opx+Pl intersticial, camadas descontinuas e pouco espessas de clinopiroxenito (Cpx cúmulus). A ZA é formada principalmente por gabros (Cpx+Pl) com inúmeras intercalações de peridotitos e em menor proporção clinopiroxenitos (Cpx+Pl). Pequenas lentes de magnetita gabro pegmatoide, interpretado como porções enriquecidas em líquido residual fracionado preso dentro da ZA. A sequencia de cristalização para CSP é formada por Ol+Chr, Ol+Cpx+Chr, Ol+Cpx, Cpx e Cpx+Pl.

Sequencias de cristalização distintas para CSO (Ol+Chr > Opx+Chr > Opx > Opx+Pl > Opx+Pl+Cpx) e CSP (Ol+Chr > Ol+Cpx+Chr > Cpx > Cpx+Pl) indica que eles seguem diferentes linhas de cristalização do líquido magmático. A cristalização de Opx primeiro do que Cpx no CSO indica um magma primário saturado em sílica, no caso do CSP onde ocorre apenas a cristalização de Cpx como fase cúmulus, o magma parental deve ser insaturado em sílica. Uma composição muito primitiva (com alto conteúdo de MgO) para o magma parental da CSO e CSP é indicado pela abundância de dunitos e peridotitos (cerca de 50% nos dois complexos). O elevado conteúdo de MgO e de Ni é muito semelhante para os dunitos que são a base do minério laterítico dos dois depósitos. O range de composição dos cúmulus de Ol na ZU para o CSO ($Fo_{86.2-92.4}$) e CSP ($Fo_{88.6-87.7}$) suporta a interpretação da composição muito primitiva para o magma parental. A composição mais primitiva Fo_{92} dos cúmulus de Ol são comparáveis com as reportadas para o Great Dyke (Fo_{92}; Wilson, 1982), Niquelândia Complex (Fo_{93}; Ferreira Filho & Araújo, 2009; Ferreira Filho *et al*. 2010) e Ipueira-Medrado Sill (Fo_{93}; Marques & Ferreira Filho, 2003), todos originados de magmas parentais muito primitivo. Perfis de elementos incompatíveis e traços, normalizados ao manto, de rochas gabroicas do CSO e CSP, mostram relativo enriquecimento em ETRL e Th, com anomalias negativas de Nb e Ta. A distribuição destes elementos traços é consistente com uma mistura de fusão de manto primitivo com crosta continental. A similaridade entre os perfis de elementos incompatíveis e traços da CSO e CSP sugere que as rochas cumuláticas dos dois complexos cristalizaram a partir de um magma parental similar em conteúdo de elementos incompatíveis. Evidências adicionais de contaminação crustal são fornecidas pelos dados isotópicos de Sm-Nd, onde o CSP tem valores de $\varepsilon_{Nd\ (T=2.77\ Ga)}$ = -3,56 a 2,41 e o CSO com $\varepsilon_{Nd\ (T=2.77\ Ga)}$ = -3,33 a -2,12. O fato do CSO ter valores menos variáveis e mais negativos de $\varepsilon_{Nd\ (T=2.77\ Ga)}$ e ligeiro aumento nas razões La/Sm e Ce/Nb quando comparados as do CSP, indica uma maior contaminação crustal para o CSO. A combinação de todos os dados sugere que as composições de acordo com os magmas parentais do CSO e CSP foram derivados a partir de uma fonte semelhante, seguindo por uma contaminação variável por rochas da crosta, que é mais significativa no CSO. Dados de U-Pb em zircões ígneos, proveniente de uma magnetita gabro pegmatoide do CSP, indicaram uma idade de cristalização de 2713±30 Ma, que reforça um importante evento magmático Neoarqueno (2,76 Ga) para a PMC. Estas idades são correlatas ao vulcanismo bimodal do Grupo Grão Pará (2759±2 Ma, Machado *et al*., 1991;

2760±11 Ma, Trendall *et al*., 1998) apoiando assim a interpretação de que as rochas vulcânicas máficas e as intrusões máfica-ultramáficas resultaram de eventos coevos (Machado *et al*., 1991; Ferreira Filho *et al*., 2007). As grandes intrusões máfica-ultramáficas da CMP estão encaixadas em descontinuidades crustais profundas, que permitem a ascensão das intrusões acamadadas. Durante o processo de ascensão variáveis conteúdos de crosta continental mais antiga são assimilados, isso é esperado se o magmatismo máfico-ultramáfico em Carajás está associado com o rifteamento intra-placa de crosta mais antiga (Gibbs *et al*., 1986; Olszewski *et al*., 1989; Villas & Santos, 2001).

ABSTRACT

The mafic-ultramafic complexes of the Serra da Onça and Serra do Puma are located in the SW portion of the Carajás Mineral Province (CMP), one of the most important mineral districts of Brazil, known for hosting several layered intrusions that have significant lateritic nickel resources. It is the result of this study, the first detailed characterization of these two intrusions in the western portion of CMP, indicating a remarkably different magmatic evolution for the Serra da Onça Complexe (SOC) and Serra do Puma Complex(SPC).

The geology of the CSO was previously described by Macambira (1997) and Macambira and Ferreira Filho (2002). The SOC is an intrusion of EW direction, 24 km long and approximately 3.5 km wide. The stratigraphy of the SOC consists of a lower border group (LBG), ultramafic zone (UZ) and mafic zone (MZ). The LBG located in the northern portion of the intrusion, form a narrow and discontinuous layer consisting of gabbronorites (Opx + Cpx + Pl cumulus). The UZ form an elongated hill and is composed mainly of dunites (Ol + Chr) and orthopyroxenites layers (Opx + Chr). The sequence of crystallization of the UZ consists of Ol+Chr; Ol+Opx+Chr; Opx+Chr and Opx. The UZ covers half of the entire SOC exposed area and is characterized mostly by gabbronorites (Opx+Cpx+Pl). The most fractionated rocks of the MZ consist on slightly thick layers of ilmenite-magnetite gabbronorite (Pig+Cpx+Pl+Mag+Ilm cmulus). The crystallization sequence of the MZ is Opx+Pl; Opx+Pl+Cpx; Pig+Pl+Cpx and Pig+Pl+Cpx+Mag+Ilm. The Serra do Puma Complex (SPC) is a layered intrusion of SW-NE direction with approximately 25 km long by 3 km wide. The stratigraphy of this complex is formed by a lower border group (LBG), ultramafic zone (UZ) and layered zone (LZ). The LBG forms a distinct zone constituted by gabbros (Cpx + Pl) on the northern edge of the SPC. The UZ forms an elongated hill and is composed mainly by dunites (Ol+Chr) with minor peridotites intercalations with Ol+Chr cumulus or Ol+Cpx+Chr, and variable proportions of interstitial Cpx + Opx + Pl, discontinuous and slightly thick layers of clinopyroxenite (Cpx cumulus). The LZ is primarily composed of gabbros (Cpx + Pl) with innumerable intercalations of peridotites and clinopyroxenites in lower proportion (Cpx + Pl). Small lenses of magnetite gabbro pegmatoid are interpreted as portions enriched in fractionated residual liquid trapped inside the LZ. The crystallization sequence for the SPC is comprised of by Ol + Chr, Ol + Cpx + Chr, Ol + Cpx, Cpx

and Cpx + Pl. Distinct crystallization sequences for the SOC (Ol+Chr > Opx+Chr > Opx > Opx+Pl > Opx+Pl+Cpx) and the SPC (Ol + Chr> Ol + Cpx + Chr> Cpx> Cpx + Pl>) indicates that they follow different processes of magmatic liquid crystallization. The crystallization of Opx, first of Cpx in the SOC indicates a primary magma saturated in silica, in the case of the SPC, where occurs only the Cpx crystallization as cumulus phase, the parental magma should be unsaturated in silica. A very primitive composition (with high MgO contents) for the parental magma of the SOC and the SPC is indicated by the abundance of dunites and peridotites (about 50% in both complexes). The high content of MgO and Ni is very similar to dunites which are the basis of the lateritic ore for both deposits. The composition range of Ol cumulus in UZ for the SOC ($Fo_{86.2-92.4}$) and the SPC ($Fo_{88.6-87.7}$) supports the interpretation of the very primitive composition for the parental magma. The most primitive composition Fo_{92} of Ol cumulus are comparable with those reported for the Great Dyke (Fo_{92}; Wilson, 1982), Niquelândia Complex (Fo_{93}; Ferreira Filho & Araújo, 2009; Ferreira Filho et al. 2010) and Ipueira-Medrado Sill (Fo_{93}; Marques & Ferreira Filho, 2003), all originated from very primitive parental magmas. Profiles of incompatible elements and normalized to the mantle traces of the SOC and SPC gabbroic rocks, show relative enrichment in LREE and Th, with negative anomalies of Nb and Ta. The distribution of these trace elements is consistent with a fusion blend of primitive mantle and continental crust. The similarity between the profiles of incompatible elements and traces of the SOC and the SPC suggests that the cumulate rocks of both complexes crystallize from a similar parental magma regarding the contents of incompatible elements. Additional evidence of crustal contamination is provided by Sm-Nd isotopic data, where the SPC shows values of εNd (T=2.77 Ga) = -3.56 to 2.41 and the SOC presents εNd (T=2.77 Ga) = -3.33 to -2.12. The fact that the SOC have lower variable values and more negative values of εNd (T=2.77 Ga) and slight increase in La/Sm and Ce/Nb ratios compared to the SPC, indicates a greater crustal contamination to the SOC. The combination of all data suggests that the compositions, according to the parental magmas of the SOC and the SPC, were derived form a similar source, followed with a variable contamination by crustal rocks, which is more significant in the SOC. U-Pb data in igneous zircons from a magnetite gabbro pegmatoid of the SPC, indicated a crystallization age of 2713±30 Ma, which reinforces an important Neoarchean (2.76 Ga) magmatic event for the CMP. These ages correlate to the bimodal volcanism of the Grão Pará Group (2759±2

Ma, Machado et al., 1991; 2760±11 Ma, Trendall et al., 1998) supporting the interpretation that the mafic volcanic rocks and mafic-ultramafic intrusions resulted from coeval events (Machado et al., 1991; Ferreira Filho et al., 2007). Mafic-ultramafic large intrusions of the CMP are embedded in deep crustal discontinuities, allowing the ascension of the layered intrusions. During the ascension process, variable contents of oldest continental crust are assimilated, and this is expected if the mafic-ultramafic magmatism in Carajás is associated with the older crust intraplate rifting (Gibbs et al., 1986; Olszewski et al., 1989; Villas & Santos, 2001).

CONSIDERAÇÕES GERAIS

Introdução

A pesquisa realizada está inserida no Projeto Integrado de Pesquisa do coordenador, **"Desenvolvimento de parâmetros comparativos da fertilidade do magmatismo máfico-ultramáfico de Carajás para mineralizações magmáticas (Ni, Cu, EGP, Cr, Ti-V) com base em estudos geocronológicos, petrológicos e do seu posicionamento tectônico-estratigráfico"**, aprovado no Edital MCT/CTMineral/VALE/CNPq 12/2009, com recursos liberados em 08/2010. O projeto está inserido da Linha Temática: **"Desenvolver metodologias de exploração geológica de suporte à exploração mineral voltados às especificidades do ambiente geológico do Brasil com a finalidade de contribuir para aprimorar e ampliar o conhecimento geológico do subsolo brasileiro"**, e conta com a parceria da VALE S/A.

A exploração mineral em Carajás está chegando a um nível de maturidade que, a exemplo do que ocorre em outras províncias minerais do planeta, demanda novas metodologias tecnológicas e geológicas (ou conceituais) de exploração. Os depósitos magmáticos associados a magmas máficos e máfico-ultramáficos (UMU), incluindo Ni, Cu, EGP, Cr e Ti-V são originados a partir de processos petrológicos inerentes a estes magmas. Em vista disso a fertilidade ou probabilidade relativa dos complexos MUM para hospedar depósitos magmáticos pode ser estabelecida a partir de suas características petrológicas. Critérios petrológicos, geralmente associados a suítes específicas de magmas MUM, constituem a principal ferramenta de exploração indireta utilizada na prospecção direcionada a depósitos magmáticos de Ni-Cu-EGP-Cr-Ti-V.

Trabalhos de mapeamento geológicos diversos, incluindo os programas de levantamento geológico da CPRM e aqueles desenvolvidos por empresas de exploração mineral, indicam que associações MUM são abundantes na região de Carajás. Trabalhos geocronológicos e petrológicos são ainda muito restritos e estão em descompasso com o atual conhecimento geológico disponível. Na ausência destes trabalhos as propostas para definição de diferentes suítes MUM na região de Carajás são especulativas e passíveis de conduzir a interpretações equivocadas. O programa prospecção mineral para depósitos magmáticos de EGP e Ni-Cu desenvolvidos pela VALE em Carajás, especialmente nos últimos 10 anos, permitem estabelecer

características geológicas-estratigráficas de várias associações MUM. Estes resultados sugerem uma complexidade e diversidade de associações MUM bem maior do que é reconhecido atualmente em trabalhos publicados.

Localização e fisiografia

A área de pesquisa abrange os complexos máfico-ultramáficos da serra do Puma e Onça, localizados no sudoeste do Estado do Pará, no norte do Brasil. A menor distância entre eles, em linha direta é de 8,5 km, por estrada, 13,5 km. A parte ocidental do Complexo Puma está no município de Parauapebas. Seus dois terços orientais estão dentro da Reserva Indígena Cateté. A metade ocidental do Complexo Onça está localizada no município de São Félix do Xingú. A metade oriental no município de Ourilândia do Norte.

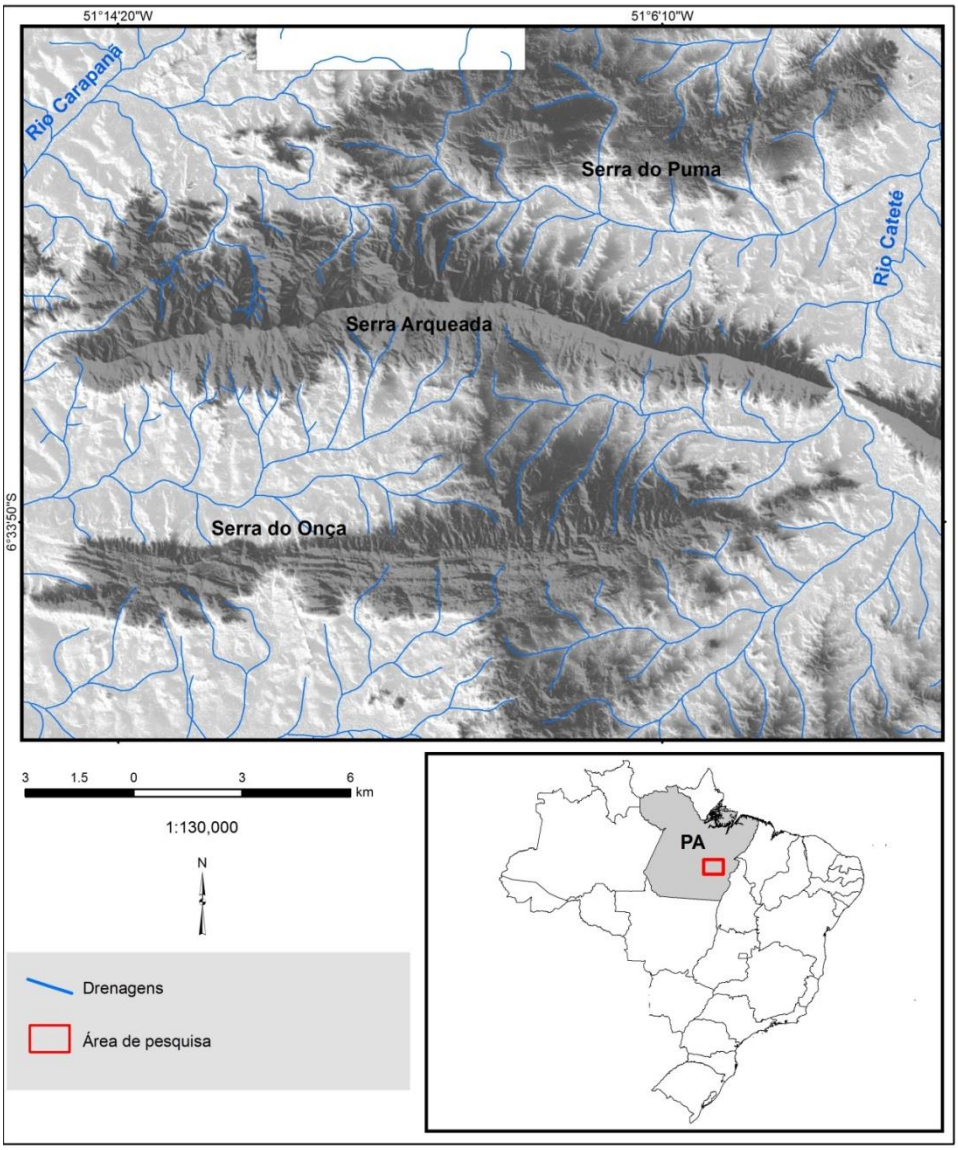

Figura i.1 – Mapa de localização da área com principais drenagens e modelo digital de terreno.

A Serra do Puma, Serra da Onça e Serra Arqueada (localizada entre as outras duas) dominam o relevo regional. Serra do Puma é uma área elevada, alongada na direção N80ºE, com um comprimento de cerca de 23 km e uma largura de 3 km. A máxima variação de cota é de aproximadamente 160 metros. A Serra da Onça tem uma tendência EW de área elevada com um comprimento de 20 km e uma largura de até 3 km. A máxima variação de cota é de cerca de 300 metros. A Serra do Puma e a parte oriental da Serra da Onça estão na bacia de drenagem do Rio Cateté, que é um afluente do Rio Itacaiúnas, que por sua vez, é um afluente do Rio Tocantins. A parte ocidental da Serra da Onça é drenada pela bacia do Rio Carapanã e Rio Fresco, afluentes do Rio Xingú.

Justificativa e objetivos

O objetivo deste estudo é fornecer informações geológicas e petrológicas, incluindo dados isotópicos, litogeoquímicos e de química mineral, que permitam caracterizar o Complexo Serra do Puma e Serra da Onça no contexto do magmatismo máfico-ultramáfico de Carajás. Uma vez que não existem dados geocronológicos e petrológicos do Complexo Serra do Puma, a sua atual caracterização como parte de uma suíte magmática maior, designada Suíte Cateté, é meramente especulativa. Trabalhos anteriores desenvolvidos na Serra do Puma e Serra da Onça indicam ainda que eles apresentam uma estratigrafia magmática, e padrão de fracionamento distintos daquele observado em outros corpos desta suíte (Macambira & Ferreira Filho 2002).

Método

Para atingir estes objetivos foi efetuada revisão bibliográfica, inclusive com a análise de mapas e relatórios internos da Vale S/A. Mapas de detalhe (1:25.000) da região que engloba o CSO e a parte oeste do CSP foi desenvolvido durante os trabalhos de exploração mineral da VALE na região (2006 a 2010), o qual foi coordenado, a partir de 2008, pelo autor desta dissertação. Procedeu-se campanhas de campo adicionais para realização de perfis, discussões de aspectos relevantes da estratigrafia e estrutura dos complexos e coleta de amostras de rocha. Estudos petrográficos foram desenvolvidos em lâminas delgadas de cerca de 120 amostras dos complexos e de suas encaixantes imediatas, o que permitiu o reconhecimento dos diversos litotipos identificados na área estudada. Deste total foram selecionadas 44

amostras distribuídas em seções representativas de cada complexo, as quais forneceram material para as diversas metodologias analíticas utilizadas neste estudo.

As análises químicas de mineral via microssonda eletrônica foram realizadas no Laboratório de Microssonda Eletrônica da Universidade de Brasília, em equipamento JEOL JXA-8230. Foram analisados de forma sistemática cristais de olivina, ortopiroxênio, clinopiroxênio, e plagioclásio. O tratamento dos dados foi feito por meio de planilha eletrônica Excel e os resultados analíticos encontram-se no Anexo 01.

A preparação e análise de amostras para litogeoquímica foram realizadas no Laboratório ActLab, usando método convencional para elementos maiores (FRX) e elementos traço (ICP-MS). Uma descrição completa dos métodos analíticos está disponível na pagina da internet: ActLab (www.actlabs.com). Um total de 44 amostras representativas de afloramentos foram analisadas. Os resultados para estas amostras são apresentados na Tabela 01 (Complexo da Serra da Onça) e Tabela 02 (Complexo da Serra do Puma).

Para este trabalho foram realizadas 15 análises isotópicas Sm–Nd (tabela 04) segundo método descrito por Gioia & Pimentel (2000) no Laboratório de Geocronologia da Universidade de Brasília.

Para as analises de U-Pb em zircões foram obtidos concentrados minerais pelo uso de técnicas convencionais e seleção manual com lupa binocular. As análises U-Pb LA-ICPMS seguiram o procedimento analítico descrito por Buhn et al. (2009) e foram realizadas no Laboratório de Geocronologia da Universidade de Brasília. Grãos de zircão com $^{206}Pb/^{204}Pb$ inferiores a 1000 foram rejeitadas. Os dados foram plotados utilizando ISOPLOT v.3 (Ludwig, 2001) e os erros para as razões isotópicas são apresentados ao nível 2σ. Resultados de U-Pb para amostra SC68 (Puma) estão apresentados na Tabela 3.

Escopo do estudo

Conforme previsto no regulamento do Curso de Pós-graduação em Geologia da Universidade de Brasília e por sugestão do Orientador, esta dissertação de mestrado apresenta-se estruturada na forma de artigo à ser submetido para publicação em periódico com corpo editorial. O artigo é apresentado na forma que será submetido, mantendo o estilo e o formato previstos no periódico.

O artigo, intitulado **"*Serra da Onça and Serra do Puma layered complexes:***

geology and petrology of two intrusions with distinct crystallization sequences in the archean Carajás province, Brazil.*"** foi elaborado durante o ano de 2014 e será submetido à revista ***Applied Earth Sciences - Institution of Mining and Metallurgy Este artigo tem como objetivo principal fornecer informações geológicas e petrológicas, incluindo dados isotópicos, litogeoquímicos e de química mineral, que permitam caracterizar o Complexo Serra do Puma e Serra da Onça no contexto do magmatismo máfico-ultramáfico de Carajás.

Referências

Buhn B., Pimentel M.M., Matteini M., Dantas E.L. 2009. High spatial resolution analysis of Pb and U isotopes for geochronology by laser ablation multi-collector inductively coupled plasma mass spectrometry (LAMC- ICP-MS). Anais da Acad. Bras. de Ciências, 1:1-16.

Ferreira Filho, C.F., Araujo, S.M., 2009. Review of Brazilian chromite deposits associated with layered intrusions: geological and petrological constraints for the origin of stratiform chromitites: Applied Earth Sciences (Trans. Inst. Min. Metall. B), v. 118, 86-100.

Ferreira Filho, C.F., Cançado, F., Correa, C., Macambira, E.M,B., Siepierski, L., Junqueira-Brod, T. C. 2007. Mineralizações estratiformes de EGP-Ni associadas a complexos acamadados em Carajás: os exemplos de Luanga e Serra da Onça, in Contribuições à Geologia da Amazônia, Sociedade Brasileira de Geologia - Núcleo Norte, 01-14.

Ferreira Filho, C.F., Pimentel, M.M., Araujo, S.M., and Laux, J.H., 2010. Layered intrusions and volcanic sequences in Central Brazil: Geological and geochronological constraints for Mesoproterozoic (1.25 Ga) and Neoproterozoic (0.79 Ga) igneous associations. Precambrian Research, v. 183, p. 617−634.

Gibbs, A.K., Wirth, K.R., Hirata, W.K., Olszewski Jr, W.J. 1986. Age and composition of the Grão Pará Group volcanics, Serra dos Carajás: Revista Brasileira de Geociências, 201-211.

Gioia, S.M.C.L., Pimentel, M.M., 2000. The Sm-Nd isotopic method in the Geochronology Laboratory of the University of Brasília. Anais Academia Brasileira de Ciências 72, 219-245.

Ludwig, K.R., 2001. Users Manual for Isoplot/Ex version 2.47. A geochronological

toolkit for Microsoft Excel. Berkeley Geochronology Center Special Publication 1a, 55p.

Macambira E.M.B. and Ferreira Filho C.F., 2002. Fracionamento Magmático dos Corpos Máfico-Ultramáficos da Suíte Intrusiva Cateté – Sul do Pará. In: Klein E.L., Vasquez M.L. & Rosa Costa L.T. (eds.) Contribuições à Geologia da Amazônia v. 3. SBG-Núcleo Norte, pp. 105-114.

Macambira, E.M.B. 1997. Geologia e aspectos metalogenéticos dos elementos do Grupo Platina no Complexo Máfico-ultramáfico da Serra da Onça, Sul do Pará. Tese de Mestrado. Universidade Federal do Pará – UFPA, Pará, Brasil.

Machado, W., Lindenmayer, Z.G., Krogh, T.E., and Lindenmayer, D. 1991. U-Pb geochronology of Archean magmatism and basement reactivation in the Carajás area, Amazon shield, Brazil. Precambrian Research, 329-354.

Marques, J.C. and Ferreira Filho, C.F., 2003. The chromite deposits of the Ipueira-Medrado Sill, Bahia, Brazil. Economic Geologt, v. 98, 87-108.

Olszewski, W.J., Wirth, K.R., Gibbs, A.K. and Gaudette, H.E., 1989. The age, origin, and tectonics of the Grão Pará Group and associated rocks, Serra dos Carajás, Brazil: Archean continental volcanism and rifting. Precam. Res. 42, 229–254.

Trendall, A.F., Basei, M.A.S., De Laeter, J.R. and Nelson, D.R., 1998. SHRIMP zircon U-Pb constraints on the age of the Carajás Formation, Grão Pará Group, Amazon Craton. J. South Am. Earth Sci. 11, 265–277.

Villas, R.N. and Santos, M.D., 2001. Gold deposits of the Carajás Mineral Province: deposit types and metallogenesis. Miner. Deposita 36, 300–331.

Wilson, A.H., 1982. The Geology of the Great 'Dyke', Zimbabwe: The Ultramafic Rocks'. Journl of Petrology, v. 23, p. 240–292.

To be submitted: Applied Earth Sciences - IMM

SERRA DA ONÇA AND SERRA DO PUMA LAYERED COMPLEXES: GEOLOGY AND PETROLOGY OF TWO INTRUSIONS WITH DISTINCT CRYSTALLIZATION SEQUENCES IN THE ARCHEAN CARAJÁS PROVINCE, BRAZIL.

Wolney Dutra Rosa, Cesar F. Ferreira Filho and Márcio Martins Pimentel

Abstract

The Serra da Onça (SOC) and Serra do Puma (SPC) mafic-ultramafic complexes are located in the SW portion of the Carajás Mineral Province (CMP), the most important mineral district of Brazil. Despite the geographical proximity and similarity in tectonic environment, these complexes have different sequences of magmatic crystallization. The SOC follows a crystallization sequence consisting of Ol+Chr > Opx+Chr > Opx > Opx+Pl > Opx+Pl+Cpx, whereas the crystallization sequence of the SPC consists of Ol+Chr > Ol+Cpx+Chr > Cpx > Cpx+Pl. The compositional range of cumulus Ol within the UZ of the SOC ($Fo_{86.2-92.4}$) and the SPC ($Fo_{88.6-87.7}$) supports a very primitive composition for their parental magmas. The early crystallization of Opx relative to Cpx in the SOC indicates that the primary magma was silica saturated, whereas the absence of Opx as a cumulus mineral in the SPC suggests that the primary magma was silica undersaturated. Very similar mantle-normalized lithophile trace element profiles for the SOC and SPC rocks suggest that cumulate rocks from both complexes crystallized from parental magmas with similar contents of incompatible elements. Mantle-normalized negative Nb and Ta anomalies characterize both the SOC and SPC, but are more significant for the SOC compared to the SPC. These features may reflect the relative enrichment of LREE associated with larger amounts of Cpx in samples of the SOC compared with those of the SPC. Both complexes have highly variable negative values of εNd (T = 2.77 Ga), but gabbroic rocks of the SOC (εNd (T = 2.77 Ga) = -3.33 to - 2.12) are more negative and less variable than the values for gabbroic rocks of the SPC (εNd (T=2.77 Ga) = -2.47 to 2.41). The combination of all data suggests that the composition of the SOC and SPC parental primitive magmas were derived from similar source, followed by variable crustal contamination. Neoarchean ages reported for layered intrusions in the eastern

portion of the Carajás Mineral Province (e.g. Luanga and Lago Grande) overlap with the age of the bimodal volcanism of the Grão Pará Group (e.g. 2759±2 Ma; 2760±11), thus supporting the interpretation that mafic volcanics and mafic-ultramafic layered intrusions resulted from coeval magmatic events. The 2713±30 Ma age reported for the SPC in this study is younger than the ages reported for the Grão Pará Group, as well as the Luanga complex, thus indicating a relatively younger intrusive event in the western portion of the CMP. Crustal contamination is expected for high temperature and Mg-rich magmas, such as the parental magmas of the SOC and SPC, which intruded into gneisses and migmatites of the ca. 3.0 Ga Xingu Complex. Results are also compatible with a higher proportion of crustal contamination for layered rocks of the SOC compared with those of the SPC. The abundance of different types primitive crustal contaminated layered intrusions in the CMP indicates a high potential for magmatic Ni-Cu-PGE deposits. Considering that previous exploration for Ni-Cu-PGE deposits mainly targeted exposed large layered intrusions, future exploration should move toward smaller or covered to poorly exposed intrusions.

Keywords: Layered intrusion, crystallization sequence, U-Pb and Sm-Nd isotopes,

1 Introduction

The Carajás Mineral Province (CMP) is known for hosting numerous large layered intrusions that host significant resources of lateritic nickel. These layered intrusions were identified during mineral exploration projects or regional studies carried out since the early 1970's (Araújo and Maia, 1991; Macambira and Vale, 1997). However, detailed petrological and geochronological studies of these layered intrusions are relatively scarce, and so far restricted to the Luanga (Machado et al., 1991; Diella et al., 1995; Ferreira Filho et al., 2007) and Lago Grande (Teixeira, 2013; Teixeira et al., submitted) complexes, all of them located in the eastern portion of the CMP. These layered intrusions have Neoarchean ages that overlap with the ca. 2.75 Ga extensive basaltic magmatism of the CMP, confirming previous interpretation by Machado et al. (1991) based on age dating of the Luanga Complex. The abundance of layered intrusions, together with their close association with mafic volcanics, leds to a suggestion that they correspond to a Large Igneous Province (LIP) by Macambira and Ferreira Filho (2002). Due to poorly constrained age dating, this suggestion was included in the LIP database (Ernst and Buchan, 2001; LIP Commission database at www.largeigneousprovinces.org) as the 2.4 Ga Cateté Event, an event remarked by the LIP Commission as poorly dated and possibly associated with continental flood basalts.

This study provides the geological, petrological, geochemical and geochronological characterization of the Serra da Onça and Serra do Puma layered complexes. Results of this study, the first detailed characterization of mafic-ultramafic intrusion in the western portion of the CMP, indicate a remarkably distinct magmatic evolution for the Serra da Onça and Serra do Puma complexes. Our results are compared with previous studies of layered intrusions developed in the eastern portion of Carajás to improve the understanding of the mafic-ultramafic magmatism and their mineral deposits in the CMP, as well as petrological processes associated with fractionation of layered intrusions worldwide. Our results also provide additional evidence for the significance of the 2.75 Ga mafic magmatic event in Carajás, thus improving the database of LIP and mineral deposits through time.

2 Exploration and Development History

The Serra da Onça and Serra do Puma layered intrusions are best known for hosting VALE's world-class nickel laterite deposit in Carajás. Nickel resources of the

Puma-Onça project, which includes open pit mine and Fe-Ni smelter, derive from these two closely located layered intrusions. Before dealing with specific aspects of these layered intrusions, it is worth revising the long exploration and development history of this project.

The discovery in the late 60' of the giant iron deposits in the Serra dos Carajás, located in the southeastern portion of Pará state, generated many exploratory opportunities in this portion of the Amazonian Craton. Pioneers exploration companies assembled mineral exploration research programs for Mn, Fe, Ni and Au. In 1973, the company Inco Ltd., through its subsidiary in Brazil, started an extensive mineral exploration in targets selected based on interpretation of aerial photographs and radar image. With the confirmation that these targets consist of large mafic-ultramafic complexes, where grades higher than 2% Ni were identified in laterites developed over serpentinized dunite, the company developed an advanced project in the Serra do Onça and the Serra do Puma complexes. This project allowed Inco to establish in 1977 a total inferred resource, at a 1.5% Ni cutoff, of 30.8Mt @ 2.35% Ni (Reported as part of the Feasibility Study of Canico Resource Corp. in 2005). In 2002, Canico Resource Corp. settled an agreement with Inco for further development of these resources. After a detailed drilling program and new resource evaluation, a feasibility study was concluded in 2005, reporting estimated resources of 194.8Mt @ 1.16% Ni (Feasibility Study of Canico Resource Corp). Currently the deposit is operated by Vale S/A, which effected the acquisition in 2005. After additional extensive detailed drilling and processing studies by Vale S/A, the first iron-nickel mine in Carajás was developed. The total blocked resources (measured and indicated resources) are 198.7 Mt @ 1.36% Ni (Vale 2013 Annual Report; in www.vale.com). The Puma-Onça project produced 5,400 t of nickel contained in ferronickel in the first quarter of 2014, reaching 86% of its nominal capacity for a single furnace operation (Vale 1Q14 Report; in www.vale.com).

3 Regional Setting

3.1 The Carajás Mineral Province

The study area is located in the southwest portion of the Carajás Mineral Province (CMP), one of the most important mineral districts in Brazil, with world-class deposits of Fe, Mn, Cu, Au and Ni. The CMP is located in the southern part of the Amazonian Craton, between the Araguaia Belt to the east and Paleoproterozoic

terrains of the Uatumã Supergroup to the west (Docegeo, 1988; Huhn et al., 1988) (Fig. 1). This mineral province comprises two Archean tectonic blocks (Fig. 1), the southern Rio Maria granitoid–greenstone terrain, represented by rocks of the Andorinhas Supergroup (Huhn et al., 1988), and the northern Itacaiúnas Belt, comprising the Itacaiúnas Supergroup of the Carajás Basin (Araújo et al., 1988). The structural evolution of the CMP is attributed to the development of regional E-W trending, steeply dipping fault zones, reactivated in several episodes in the Archean and Paleoproterozoic (Holdsworth and Pinheiro, 2000). Paleoproterozoic (ca. 1.87-1.88) extension events of the Amazonian Craton were indicated by dyke swarms in the CMP (Rivalenti et al., 1998).

The southwest region of the CMP (Fig. 2), focus of this study, consists mainly of gneiss, migmatite and granulite of the Xingu Complex (Docegeo, 1988). U-Pb zircon ages (Machado et al., 1991) indicate that these rocks were formed in 2,859 ± 2 Ma and migmatized in 2,851 ± 4 Ma. Fragments of granite-greenstone terrains, characterized by supracrustal rocks of the Tucumã Group (Araújo and Maia, 1991), consist of metavolcanosedimentary sequences comprising mafic and felsic metavolcanic rocks and interlayered metasediments (Macambira and Vale, 1997). U-Pb zircon dating of a felsic metavolcanic rock of this sequence and of a metagranodiorite indicate ages of 2,868 ± 8 Ma and 2,852 ± 16 Ma, respectively. These data concur with the suggestion that the development of sialic crust in the south portion of CMP occurred between 3.0-2.85 Ga (Avelar et al., 1999).

Several large felsic plutons, such as deformed Neoarchean (ca. 2.7 Ga) alkaline granites of the Plaquê Suite (Araújo et al. 1994; Macambira et al., 1996) and Paeloproterozoic granites (ca. 1.88 Ga; Gibbs et al., 1986; Machado et al., 1991; Macambira and Lafon, 1995) intrude the Xingú Complex. The Neoarchean plutons indicate a robust felsic magmatic event concomitant with the mafic volcanism of the Itacaiúnas Supergroup rocks (Barros et al., 2001; Santos et al., 2001).

Mafic-ultramafic complexes consist of several elongated medium to large intrusions following EW and NS regional trends (Macambira and Ferreira Filho, 2002). These mafic-ultramafic complexes are known to contain significant lateritic Ni deposits, such as Onça, Puma, Jacaré, Jacarezinho and Mundial, developed over large ultramafic zones where dunite predominates. Even though these intrusions were originally interpreted as part of a magmatic suite (Cateté Suite; Macambira and Vale,

1997), different crystallization sequences were identified in these complexes (Macambira and Ferreira Filho, 2002).

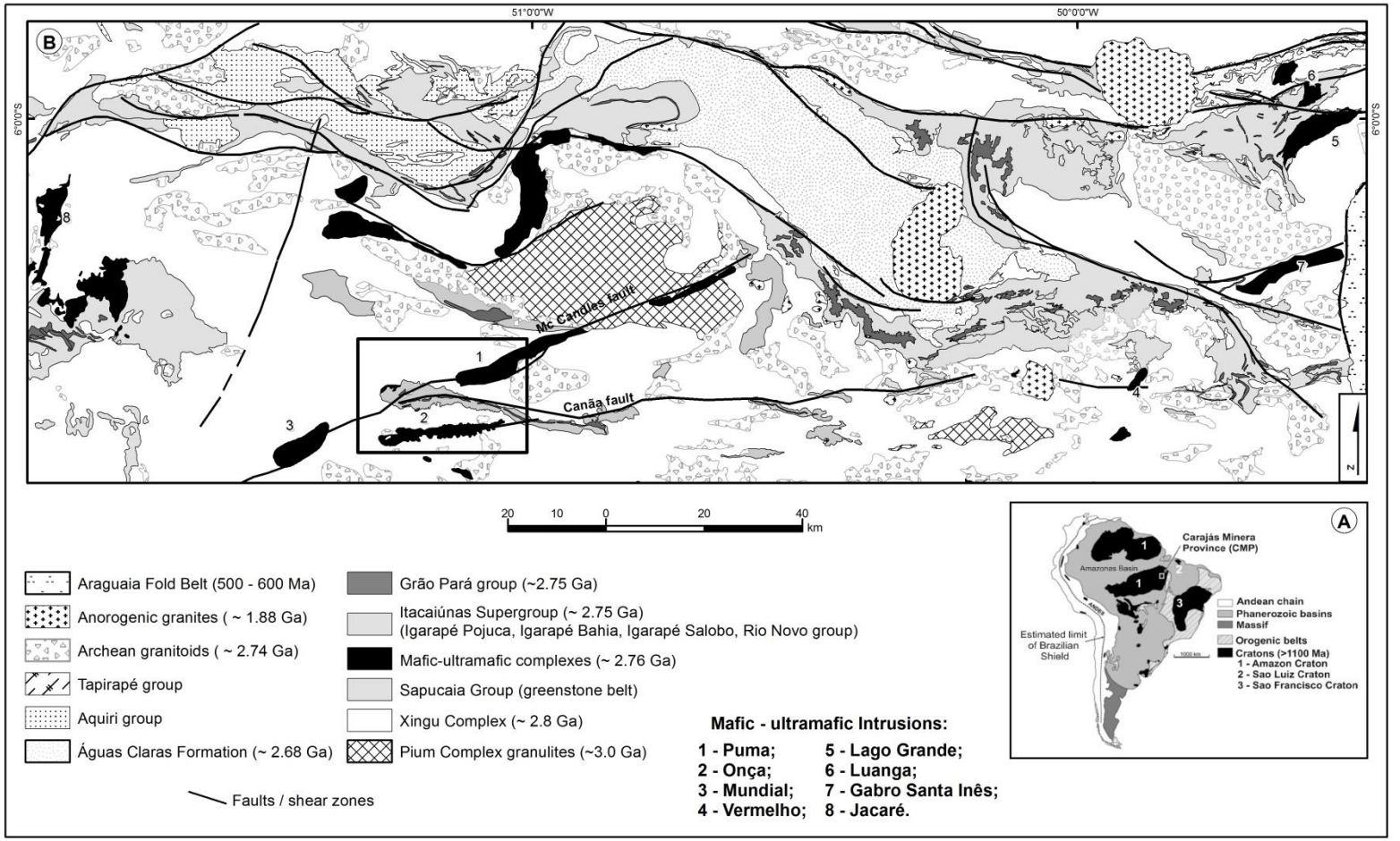

Figure 1 - A) Location of the Carajás Mineral Province. B) Geological map of Carajás Mineral Province (Modified from CPRM 2008). The area of the Serra da Onça and Serra do Puma complexes (indicated in the map) is detailed in figures 2 and 3.

3.2 Layered intrusions

The Cateté Intrusive Suite (Macambira and Vale, 1997) corresponds to a set of large to medium-size mafic-ultramafic intrusions located in the west portion of the CMP (Fig. 1 and 2). This Suite intruded in Archean rocks of the Xingu Complex, Plaquê Granite and São Félix Group (Fig. 2), considered by the authors as part of an anorogenic extensional system. As reported by Macambira and Ferreira Filho (2002), these layered intrusions have thick ultramafic zones at the base of the igneous stratigraphy, where Ni laterite deposits developed over serpentinized dunite, and show extensive fractionation toward mafic cumulates upward in the stratigraphy. Based on different crystallization sequences, these layered intrusions were divided in two distinct groups (Macambira and Ferreira Filho, 2002). One group, comprising the Serra da Onça, Jacaré and Jacarezinho complexes, has abundant orthopyroxene as a cumulus mineral and consists mainly of dunite, harzburgite, orthopyroxenite, norite and gabbronorite. Another group, comprising the Serra do Puma and Carapanã, does not crystallize orthopyroxene as a cumulus mineral and consists mainly of dunite, wehrlite, clinopyroxenite and gabbro. The abundance of ultramafic rocks, as well as the very primitive composition of cumulus olivine (Fo content up to 92 mol. %; Ferreira Filho et al., 2007), indicates that a large amount of primitive mantle-derived magmas intruded sialic crust in the southwestern portion of the CMP. Except for disruptions along shear zones, these undeformed and unmetamorphosed layered intrusions have nicely preserved igneous structure, fabric and mineralogy.

The age of these layered intrusions is poorly constrained in previous study. Published geochronological results, restricted to the Serra da Onça Complex, consist of one whole-rock Sm-Nd isochron (2,378±55 Ma; Macambira, 1997) and one SHRIMP U-Pb zircon age for a gabbroic rock (2,766±6 Ma; unpublished data reported by Lafon et al., 2000). The first age was used to suggest the ca. 2.4 Ga age for the Cateté Suite (Macambira and Ferreira Filho, 2002; Ernst and Buchan, 2001), but is inconsistent with new geological and geochronological results to be presented and discussed in this paper. The Neoarchean age indicated by Lafon et al. (2000) is consistent with the new data reported in this study, as well as recent data obtained for layered intrusions in the eastern portion of the CMP (Teixeira, 2013; Teixeira et al., submitted). Age constraints for these layered intrusions will be further addressed in the following discussions of this study.

The area of the Serra da Onça and Serra do Puma complexes were mapped by VALE during exploration programs developed in 2006-2010 (Fig. 2). The eastern portion of the Serra do Puma Complex (SPC) is located within a native people reserve and was not mapped during VALE's exploration program. The location of the layered complexes is controlled by major EW, NW-SE amd NE-SW regional trends of the Itacaiúnas Shear Belt. These trends are associated with dip crustal discontinuities that represent preferred sites of location of magma transferred from the mantle to the crust. The Serra da Onça Complex (SOC) is located along the EW Canaã lineament, whereas the Serra do Puma Complex (SPC) is located along the NE-SW McCandles fault (Fig. 1). The SOC and SPC are intrusive into banded gneiss-migmatite of the Xingú Complex or slightly foliated granitic intrusions of the Plaquê Suite (Fig. 2).

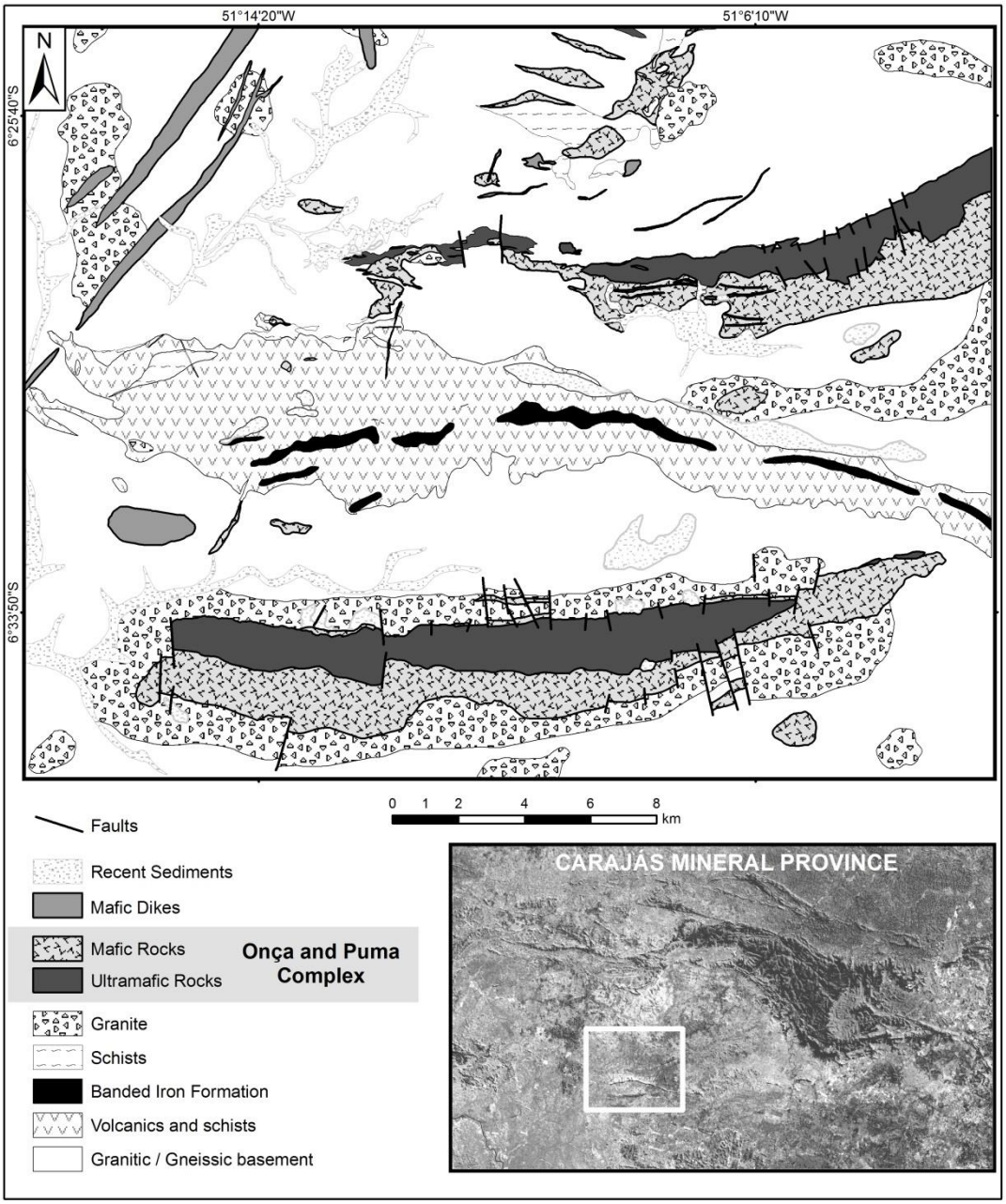

Figure 2 - Geological map of the area of the Serra da Onça and Serra do Puma complexes (partially modified from Vale's unpublished internal reports).

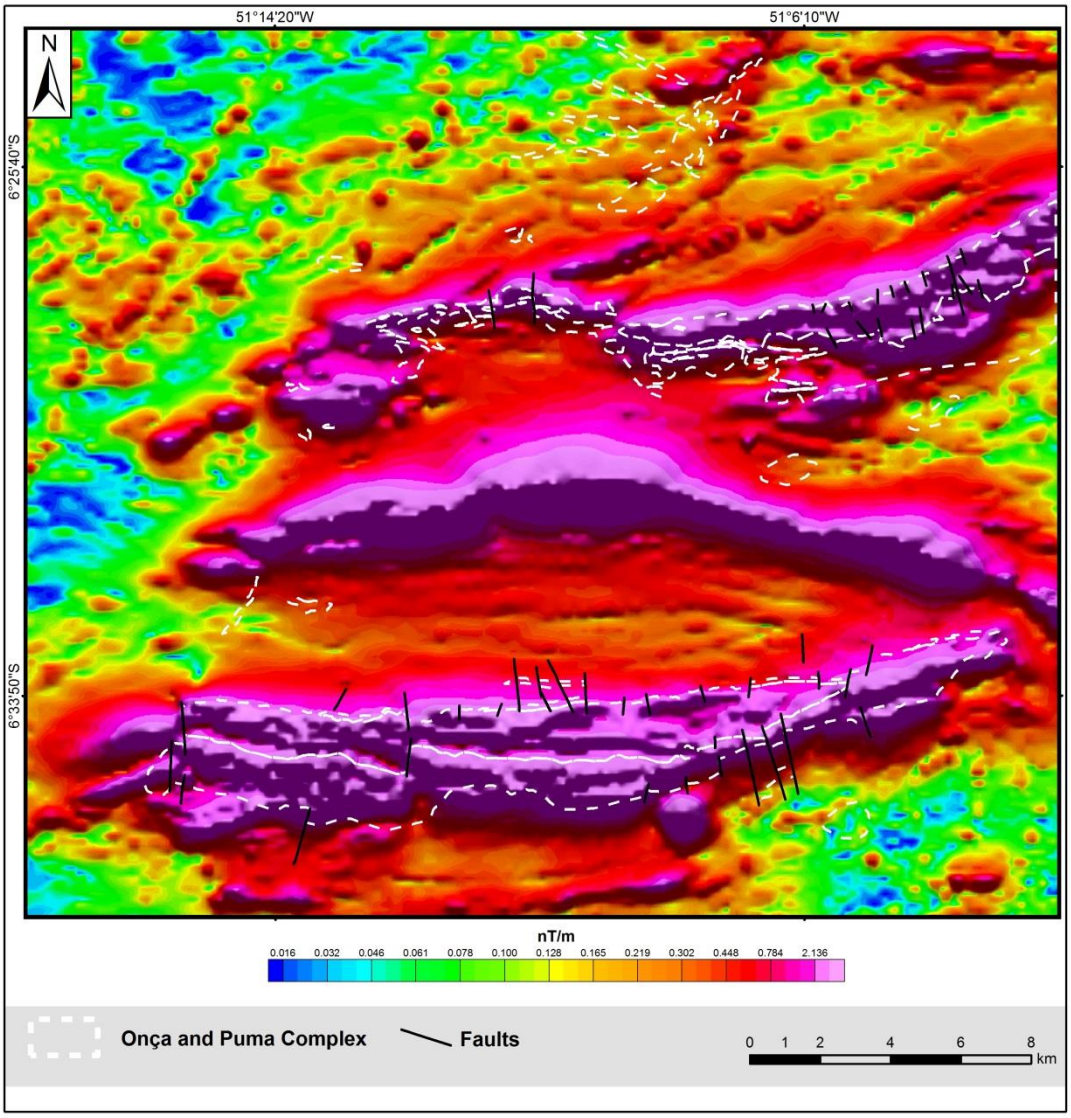

Figure 3 - Analytical signal amplitude of the area indicated in Fig. 2 (partially modified from Vale's unpublished internal reports). Dashed lines indicate mapped mafic-ultramafic intrusions.

4 Analytical Procedures

4.1 Microprobe analyses

Mineral analyses were performed on polished thin section using a 5-spectrometer JEOL JXA-8230 SuperProbe at the Electron Microprobe Laboratory of the University of Brasília (Brazil). The wavelength dispersive (WDS) analyses were performed at an accelerating voltage of 15 kV and a beam current of 10 nA. Both synthetic and natural mineral standards were used for the analyses and the same standards and procedure were retained throughout the analytical work. Systematic WDS analyses were obtained for olivine, pyroxene, and plagioclase. Representative analyses of olivine, pyroxene and plagioclase are included in Appendix 01.

4.2 Bulk rock lithochemical analyses

Sample preparation and lithogeochemistry analyses were performed at ActLab Laboratory using conventional major (XRF) and trace (ICP-MS) element routines. A complete description of analytical methods is available in the ActLab Home Page (www.actlabs.com). A total of 44 representative samples from outcrops were analysed in the ActLab Laboratory. Results for these samples are shown in Table 01 (Serra da Onça Complex) and Table 02 (Serra do Puma Complex).

4.3 Sm-Nd isotopic analyses

Sm-Nd isotopic analyses followed the method described by Gioia and Pimentel (2000) and were carried out at the Geochronology Laboratory of the University of Brasília (UnB). Whole-rock powders (~ 3000 mg) were mixed with ^{149}Sm-^{150}Nd spike solution and dissolved in Savillex bombs. Sm and Nd extraction of whole-rock samples followed conventional cation exchange techniques. The isotopic measurements were carried out on a multi-collector Finnigan MAT 262 mass spectrometer in static mode. The $^{143}Nd/^{144}Nd$ ratios were normalized to $^{146}Nd/^{144}Nd$ of 0.7219 and the decay constant used was 6.54 × 10-12 a-1. The TDM values were calculated using the model of DePaolo (1981). Nd procedure blanks were better than 100 pg. Sm-Nd results for 15 samples of the SOC and SPC are shown in Table 3.

4.4 LA-ICPMS U-Pb zircon analyses

Zircon concentrates were extracted from ca. 10-20 kg rock samples using conventional gravimetric and magnetic techniques at the Geochronology Laboratory of the University of Brasília. Mineral fractions were handpicked under a binocular microscope to obtain fractions of similar size, shape and color. Before every micro-analytical procedure, mounts were cleaned with dilute (2%) HNO_3. Backscattered electron and cathodoluminescence images were obtained using a FEI-QUANTA 450 SEM working at 15 kV at the University of Brasília. For U-Pb isotopic LA-ICPMS analyses, the sample was mounted in an especially adapted laser cell and loaded into a New Wave UP213 Nd:YAG laser (λ = 213 nm), linked to a Thermo Finnigan Neptune Multi-collector ICPMS. The laser was run at a frequency of 10 Hz and energy of ~100 mJ/cm2 with a spot diameter of 30μm for U-Pb systematics. The U-Pb LA-ICPMS analyses followed the analytical procedure described by Buhn et al. (2009) and were carried out at the Geochronology Laboratory of the University of

Brasília. Two international zircon standards were used. A fragment of zircon standard GJ-1 (Jackson et al., 2004) was used as the primary reference material in a standard-sample bracketing method, accounting for mass bias and drift correction (Albarède et al., 2004). An internal standard was run at the start and at the end of each analytical session, yielding accuracy around 2% and a precision in the range of 1% (1σ). Uncertainties in sample analyses were propagated by quadratic addition of the external uncertainty observed for the standards to the reproducibility and within-run precision of each unknown analysis. Zircon grains with $^{206}Pb/^{204}Pb$ lower than 1000 were rejected. Plotting of U–Pb data was performed using ISOPLOT v.3 (Ludwig, 2001) and errors for isotopic ratios are presented at the 2σ level. U-Pb results for sample SC68 are shown in Table 3.

5 Serra da Onça Layered Mafic-Ultramafic Complex

5.1 Geology and Petrography

The geology of the Serra da Onça Complex (SOC) was previously described by Macambira (1997) and Macambira and Ferreira Filho (2002). Extensive mapping and drilling, together with geochemical and geophysical surveys for mining or brownfield exploration, provided new significant constraints on the geology and stratigraphy of the layered sequence. The SOC consists of a 24 km-long and less than 3.5 km-wide EW trending intrusion (Fig. 3 and 4). Magmatic layering has consistent moderate dip of 40-45° to the south (Fig. 4), as indicated by outcrops of layered rocks, drill holes and geophysical modeling.

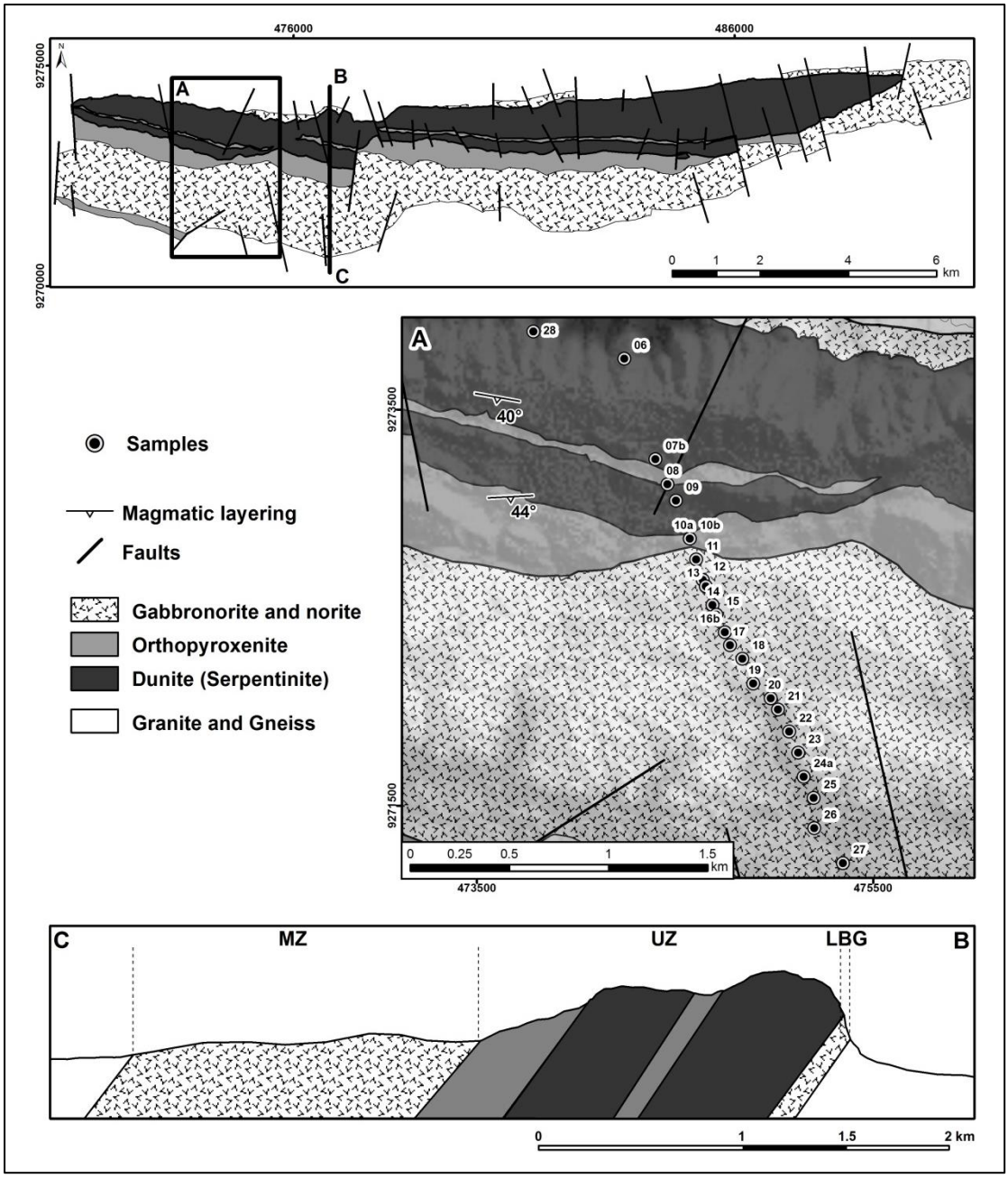

Figure 4 - Geological map and section of the Serra da Onça Complex.

The stratigraphy of the SOC consists of a Lower Border Group (LBG), an Ultramafic Zone (UZ) and a Mafic Zone (MZ) (Fig. 4 and 6). The maximum estimated thickness, considering the widest portion of the intrusion, is about 2.6 km. Primary igneous minerals and textures are largely preserved in the SOC, except for the serpentinization of olivine-rich rocks. Extensive replacement of igneous minerals occurs along discrete shear zones and/or hydrothermal alteration, a feature that is not considered in the following petrographic description.

The LBG forms a thin and discontinuous zone of abundant medium- to fine-grained gabbronorite (Opx + Cpx + Pl cumulate) located at the northern limit of the SOC (Fig. 5A). This zone is located at the base of the hill sustained by silica-rich laterites developed over ultramafic rocks, such that boulders of laterites and transported soil from ultramafic rocks partially cover the LBG. The stratigraphy of the LBG is not constrained by geological traverses with abundant outcrops or layered in situ outcrops. Scattered outcrops of harzburgite (Ol + Chr cumulate with large Opx oikocrysts) and melanorite (Opx cumulate with intercumulus Pl) close to dunite of the UZ are likely to correspond to an upward transition toward the UZ. This is similar to what is described at the base of several layered intrusions (Eales et al., 1996; McBirney, 1996; McCallum, 1996; Latypov, 2003). Considering that the LBG has the same dip of the UZ and MZ, the maximum estimated thickness for this border zone is about 125 meters (Fig. 4).

The UZ forms an elongated hill (Fig. 5A) and consists mainly of dunite (Ol + Chr cumulate) and orthopyroxenite (Opx + Chr cumulate). Medium-grained dunite with adcumulate texture predominates at the lower portion of the UZ (Fig. 5B and 5C), whereas medium- to coarse-grained adcumulate orthopyroxenite characterize the upper portion (Fig. 3 and 4). Even though dunite is extensively to moderately serpentinized, relicts of igneous olivine is eventually preserved in unweathered outcrops. Orthopyroxenite is just lightly serpentinized and igneous Opx is largely preserved in most outcrops (Fig. 5D). Two main layers of orthopyroxenite are recognized. A lower thin one and an upper thick layer in the upper contact of the UZ (Fig. 4). Chromite is a ubiquitous accessory mineral (0.5 to 3.0 vol. %) in dunite and orthopyroxenite. The amount of chromite in orthopyroxenite decreases upward in the stratigraphy and the uppermost orthopyroxenites do not have cumulus chromite. Intercumulus minerals in dunite consist of large interstitial Opx and Cpx in dunite, and Cpx and Pl in orthopyroxenite. The crystallization sequence of the UZ consists of Ol+Chr; Ol+Opx+Chr; Opx+Chr and Opx.

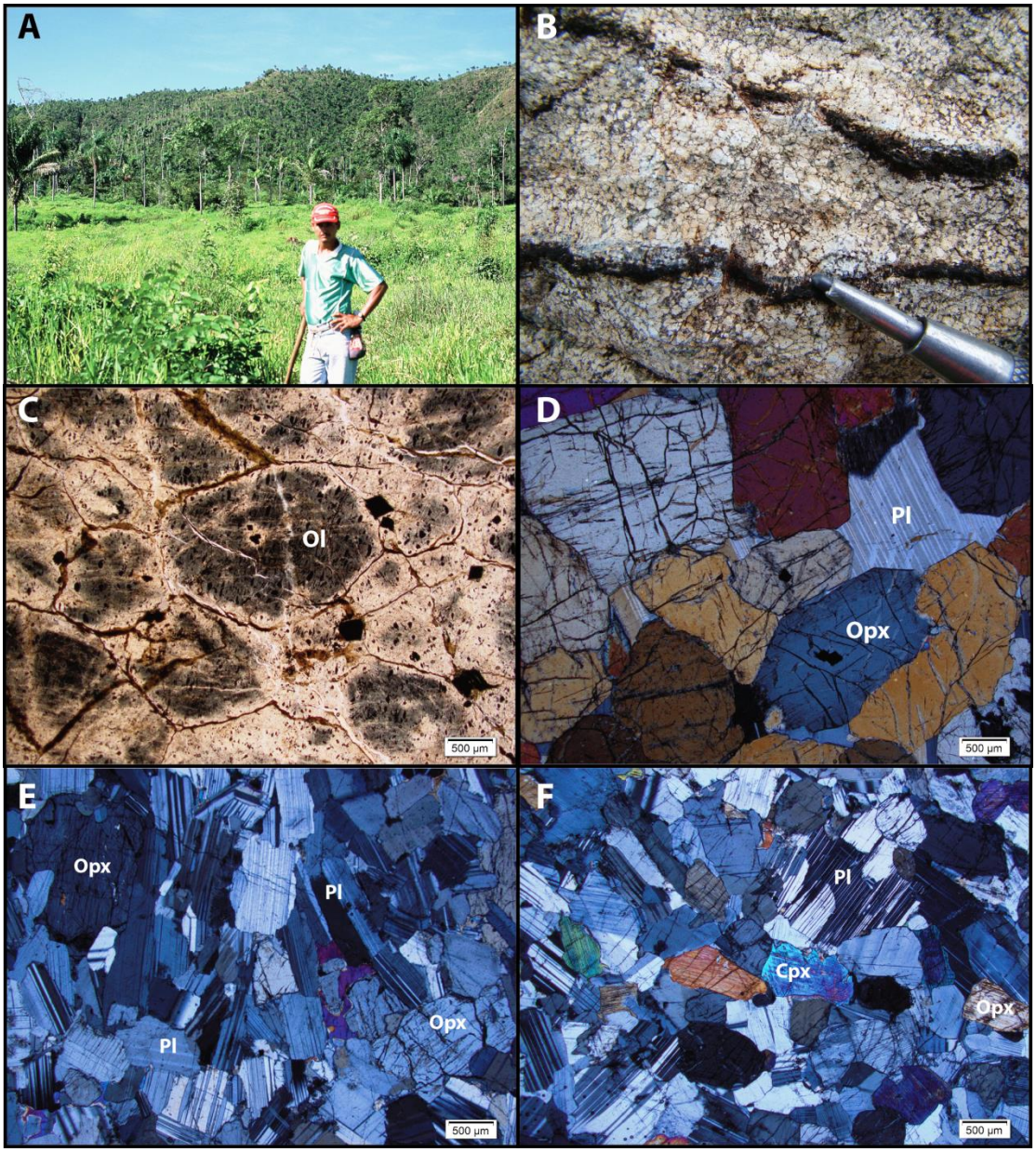

Figure 5 - A) View from north to south of the Serra da Onça Complex. The hill correspond to the base of the UZ. The LBG forms a narrow zone at the base of the hill. B) Weathered medium-grained adcumulate dunite of the UZ. C) Photomicrograph of medium-grained dunite. The sample consists of serpentinized olivine (Ol) and euhedral chromite (opaques). D) Photomicrograph of plagioclase orthopyroxenite of the UZ. The sample consists of cumulus Opx and intercumulus plagioclase (Pl). E) Photomicrograph of norite of the MZ. The sample is an Opx and plagioclase (Pl) cumulate with minor intercumulus Cpx (anhedral crystals with higher birefringence). F) Gabbronorite of the MZ. The sample is an adcumulate with cumulus Opx, Cpx and plagioclase (Pl).

The MZ consists mainly of medium-grained gabbronorite and covers about half of the exposed area of the SOC (Fig. 4). Complete sections of the lower contact of the MZ are exposed in three drill cores developed for exploration of Pt-Pd anomalies in the central portion of the SOC (Ferreira Filho et al., 2007). This transition zone consists of orthopyroxenite (Opx cumulate) of the UZ, followed by

sharp contacts to norite (Opx + Pl cumulate; Fig. 5E) and gabbronorite (Opx + Cpx + Pl cumulate; Fig. 5F) upward in the stratigraphy. The MZ is wider and has abundant outcrops in the western and central portion of the complex. In this portion Opx is replaced by pigeonite (identified as inverted pigeonite) upward in the stratigraphy (Pig + Cpx + Pl cumulate). The most fractionated rocks consist of layer of ilmenite-magnetite-bearing gabbronorite (Pig + Cpx + Pl + Mag + Ilm cumulate) located in the central portion of the MZ. This magnetite-ilmenite-bearing gabbronorite forms a thin (< 50 meter-wide) stratigraphic marker, indicated by Ti and V anomalies in soil geochemistry surveys. In these rocks accessory magnetite is a cumulus phase, while ilmenite occur as a cumulus phase or as exsolution lamellae within cumulus magnetite crystals. Primary layering, defined by different modal proportions of plagioclase and pyroxene, and igneous lamination, defined by oriented plagioclase crystals, are common features in the MZ.

A discontinuous layer and scattered outcrops of orthopyroxenite and orthocumulate norite (cumulus Opx with intercumulus Pl) occur in the southern and uppermost portion of the MZ. The upper contact of the MZ with foliated granites is poorly constrained due to scattered outcrops. The reappearance of Opx cumulates in the southern portion of the SOC, in contact with host granitic rocks, suggests that they may represent an Upper Border Group of the layered intrusion.

Repeated sequences of cumulates within the MZ suggests the existence of multiple injections of parental magma during the magmatic fractionation of the magma chamber. The crystallization sequence of the MZ consists of Opx+Pl; Opx+Pl+Cpx; Pig+Pl+Cpx and Pig+Pl+Cpx+Mag+Ilm. The complete sequence of crystallization for the SOC is indicated by the following scheme:

olivine + chromite
olivine + orthopyroxene + chromite
orthopyroxene + chromite
orthopyroxene
orthopyroxene + plagioclase
orthopyroxene + clinopiroxene + plagioclase
pigeonite + clinopyroxene + plagioclase
pigeonite + clinopyroxene + plagioclase + magnetite + ilmenite

The contact between the UZ and the MZ is exposed in three drill cores drilled during exploration for PGE in the SOC by CANICO (Ferreira Filho et al., 2007). In

the drill cores the contact between the UZ and MZ is sharp, characterized by Opx adcumulate at the upper portion of the UZ followed by norite (Opx + Pl cumulate) at the base of the MZ, separated by a thin (< 3 meter-thick) zone of orthopyroxenite with interstitial plagioclase. These drill cores also show a sharp upward transition from an about 50 meter-thick layer of norite (Opx+Pl cumulate) to gabbronorite (Opx+Cpx+Pl).

The upper contact of the SOC is poorly exposed. The occurrence of an orthopyroxenite layer in the western portion of the intrusion (Fig. 4), as well as scattered outcrops of relatively more primitive rocks (norite, harzburgite) close to the upper contact with host granite, suggest that they belong to an upper border group (i.e., UBG in Fig. 6).

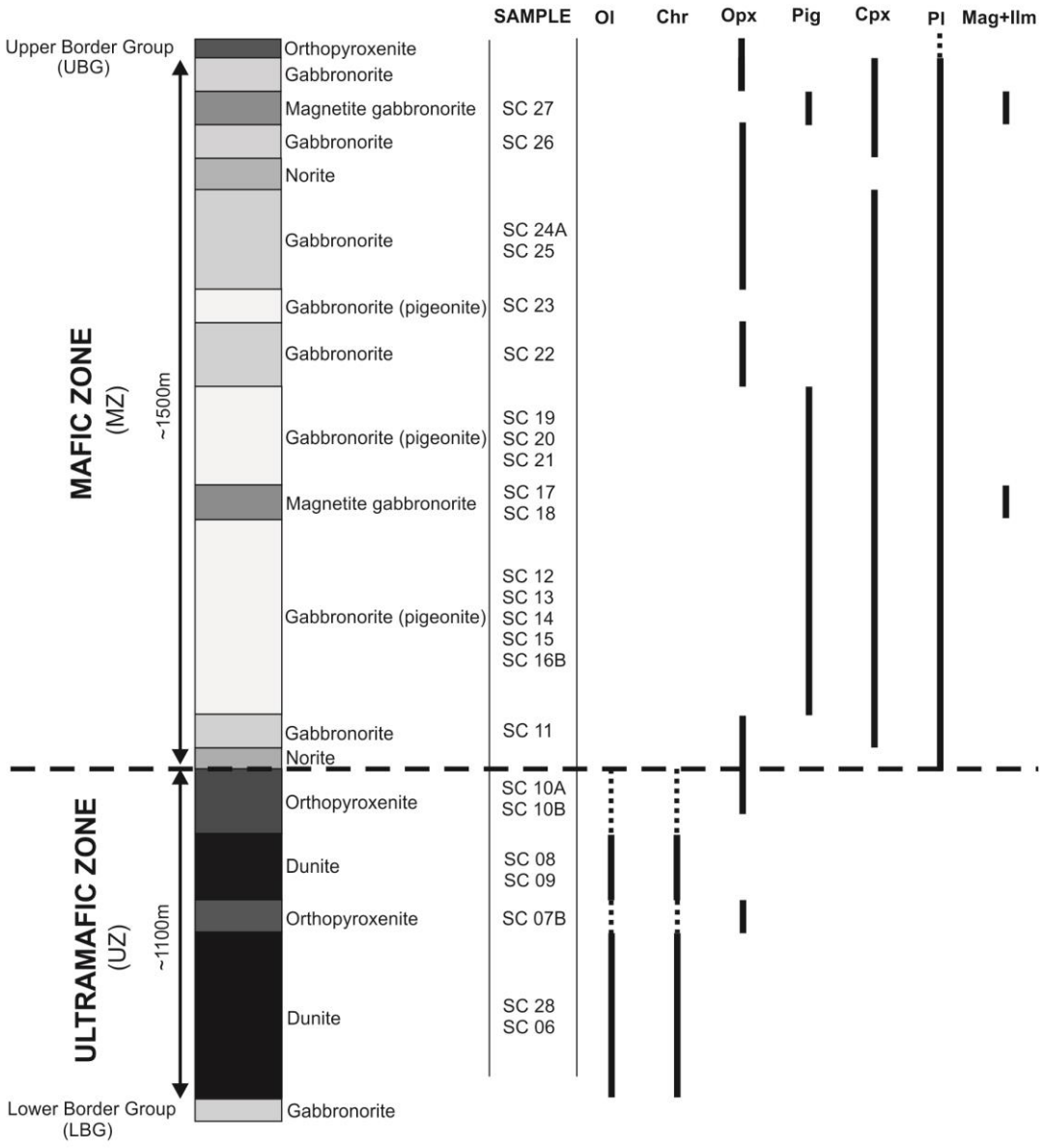

Figure 6 - Stratigraphy of the Serra da Onça Complex.

5.2 Mineral Chemistry

Systematic analyses of olivine, orthopyroxene and plagioclase crystals were performed in unweathered samples through a complete section of the SOC (see Fig. 4 for location of samples). Due to extensive weathering and/or serpentinization, analyses of olivine in the UZ are limited to a few samples. Representative microprobe analyses for minerals of the SOC are provided in Appendix 1.

The composition of olivine crystals in dunite and olivine orthopyroxenite samples from the UZ ranges from $Fo_{92.4}$ to $Fo_{86.2}$, indicating very primitive (i.e., very high Fo content) to primitive compositions. The small number of samples does not provide a systematic cryptic variation of olivine in the UZ. The results however suggest the existence of significant reversals, as indicated by very primitive composition of olivine (Fo_{92}) in the upper portion of the UZ (Fig. 7). Ni contents in olivine range from 3,280-4,190 ppm in dunite and 2,150-2,600 ppm in olivine orthopyroxenite (Fig. 8). Ni contents in olivine are not positively correlated as indicated by highly variable Ni contents for olivine with similar Fo content (~ Fo_{92}). This may indicate depletion of Ni associated with sulfide segregation during the magmatic evolution of the SOC or new influxes of Ni depleted magma.

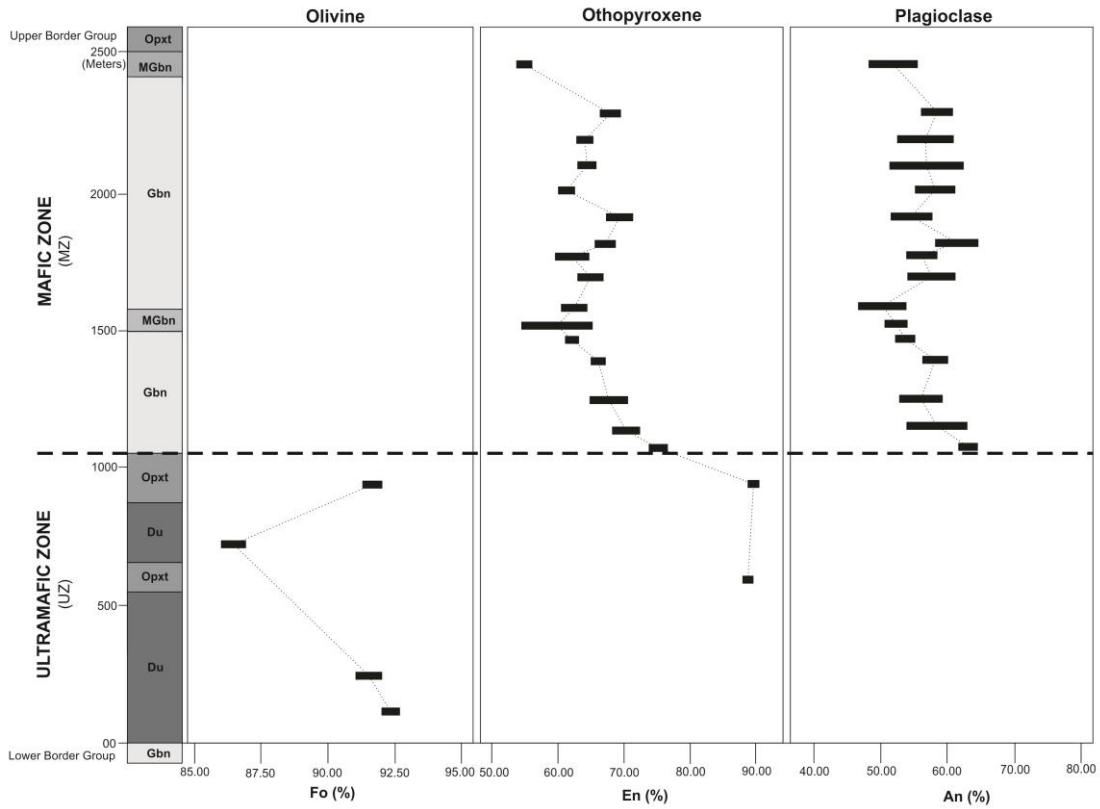

Figure 7 - Compositional variation of olivine, orthopyroxene and plagioclase throughout the stratigraphy of the SOC.

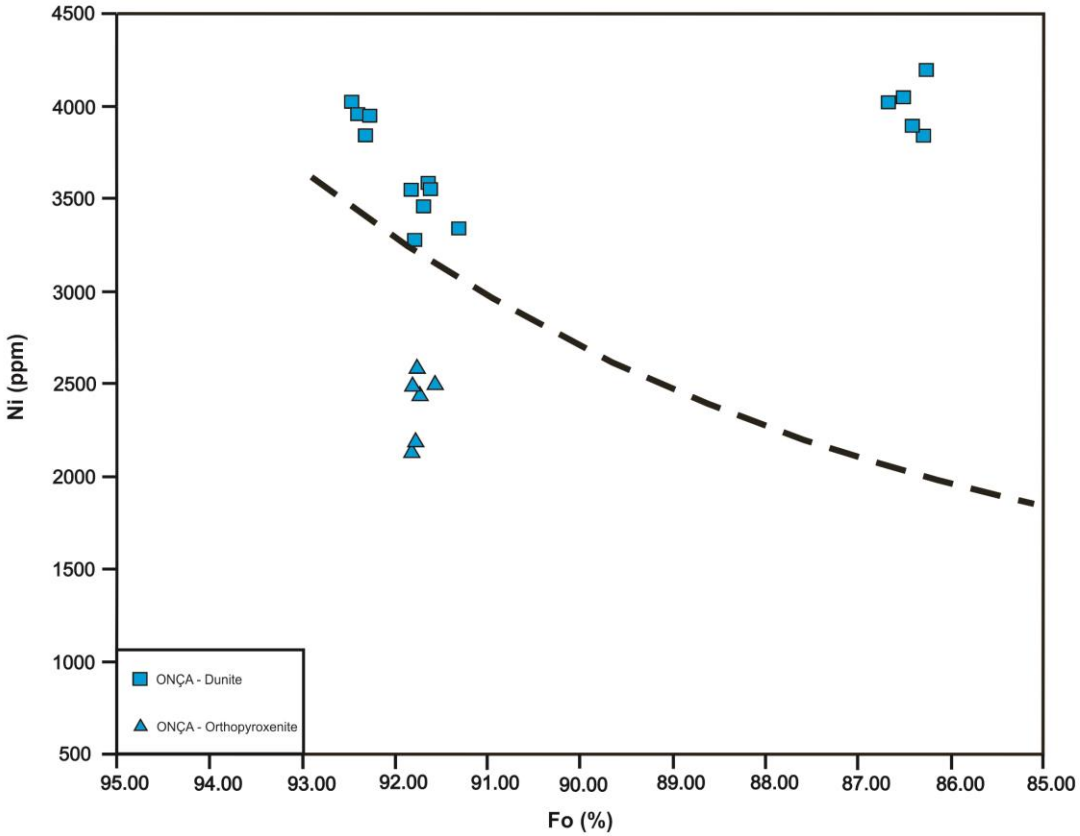

Figure 8 - Plot of Fo versus Ni content of olivine of the SOC. The dashed line is the compositional trend for olivine from layered complexes (Simkin and Smith, 1970).

Opx compositions in few samples of orthopyroxenite of the UZ are very primitive and range from $En_{89.8}$ to $En_{88.7}$. These compositions the UZ contrast with more fractionated compositions of Opx in gabbroic rocks of the MZ (Fig. 07). Systematic analyses of Opx in gabbroic rocks provide cryptic variation data for the MZ (Fig. 7). Opx compositions in the MZ range from $En_{75.9}$ to $En_{54.3}$, following a trend characterized by several reversals (Fig. 7). Opx compositions in the lower portion of the MZ follow a continuous fractionation trend, a feature consistent with the continuous crystallization sequence (from Opx cumulate, to Opx+Pl cumulate and Opx+Cpx+Pl cumulate) investigated in drill cores where the contact of the UZ to the MZ is exposed. Successive reversals in the fractionation of Opx in the MZ are likely to result from new influxes of primitive magma in a dynamic magma chamber.

Plagioclase compositions in the MZ range from $An_{63.7}$ to $An_{47.4}$ and follow the same pattern of cryptic variation indicated by Opx compositions (Fig. 7). Similar cryptic variation pattern for Opx and Pl in the MZ of the SOC is consistent with their crystallization as cumulus minerals throughout the MZ.

6 Serra do Puma Layered Mafic-Ultramafic Complex

6.1 Geology and Petrography

The Serra do Puma Complex (SPC) consists of a 25 km-long and less than 3 km-wide SW-NE trending layered intrusion (Fig. 1). The eastern half of the complex is located within a native people (Xikrin Group) reserve where exploration activities and mapping are not allowed. Extensive mapping and drilling, together with geochemical and geophysical surveys for mining or brownfield exploration, provided a detailed map for the western half of the SPC (Fig. 9). Magmatic layering has consistent moderate dip of 30-40° to the southeast (Fig. 9), as indicated by outcrops of layered rocks and geophysical modeling.

The SPC consists of a Lower Border Group (LBG), an Ultramafic Zone (UZ) and a Layered Zone (LZ) (Fig. 9 and 11). The maximum estimated thickness of the eastern portion of the SPC, considering the widest portion of the intrusion, is about 2.1 km (Fig. 9 and 11). Primary igneous minerals and textures are largely preserved in the SPC, except for the serpentinization of olivine-rich rocks. Extensive replacement of igneous minerals occurs along discrete shear zones and/or hydrothermal alteration, a feature that is not considered in the following petrographic description.

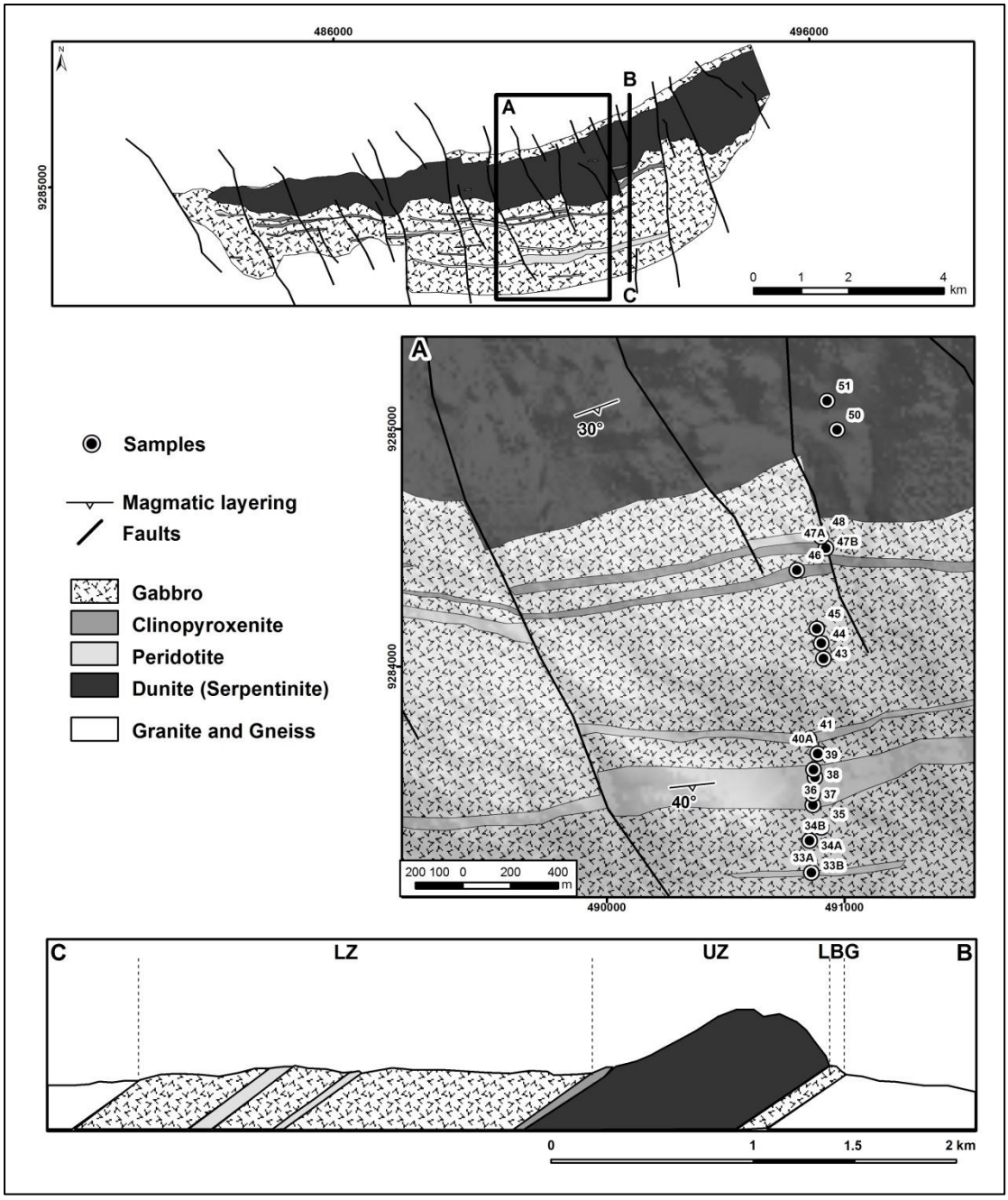

Figure 9 - Geological map and section of the Serra do Puma Complex.

The LBG forms a thin but distinct zone of gabbroic rocks located in the northern border of the SPC (Fig. 9). Similar to the SOC, this border group is located at the base of the hill sustained by silica-rich laterites, such that outcrops are scarce in this partially covered area. The LBG consists mainly of fine- to medium-grained gabbro (Cpx + Pl cumulate), has an estimated thickness of 110 meters and is located at the base of the layered intrusion.

The UZ forms an elongated hill (Fig. 10A) and consists mainly of dunite with minor interlayered peridotite and clinopyroxenite. The UZ has an estimated thickness

of up to 950 meters in the area mapped in detail of the SPC (Fig. 9 and 11). Dunite occurs as medium-grained adcumulate rocks with cumulus olivine and chromite. Dunite is extensively serpentinized and/or weathered and primary olivine is rarely preserved in the UZ. Chromite, a ubiquitous accessory mineral (0.5 to 3.0 vol. %) in dunite of the UZ, occurs as fine-grained euhedral crystals, generally located between larger olivine crystals. Intercumulus minerals in dunite consist of Opx and Cpx that form large (up to few centimeters) oikocrysts enclosing several olivine crystals. Layers of peridotite consist of Ol + Chr cumulates with abundant interstitial Cpx and minor Opx (usually wehrlite or lherzolite), or Ol + Cpx cumulate with minor intercumulus Opx and Pl (usually wehrlite). The latter, together with clinopyroxenite (Cpx cumulate), form thin (up to 100 meter-thick) and discontinuous layers in the UZ. The amount of interlayered peridotites and clinopyroxenite increases toward the upper portion of the UZ.

The Layered Zone (LZ) consists mainly of gabbro (Cpx + Pl cumulate) with abundant interlayered peridotite and minor clinopyroxenite. The LZ has an estimated thickness of up to 1,050 meters in the area mapped in detail of the SPC (Fig. 9 and 11). Gabbro occurs as medium-grained adcumulates, consisting of cumulus Pl and Cpx (Fig. 10F). Modal layering, consisting of variable proportions of Cpx and Pl (from gabbro to leucogabbro), is frequent in large outcrops of gabbroic rocks of the LZ (Fig. 10B). These rhythmic layers vary from few centimeters up to few meters thick. Igneous lamination, defined by oriented tabular plagioclase crystals (Fig. 10F), is also frequent in outcrops of gabbroic rocks of the LZ. Few pockets of pegmatoidal magnetite-gabbro occur within medium-grained gabbro of the LZ. These pockets (up to 1-2 meters) are interpreted as portions enriched in fractionated residual trapped liquid within the LZ. Clinopyroxenite consists of medium- to coarse-grained Cpx cumulate with variable proportions of interstitial (intercumulus) plagioclase (Fig. 10E). Depending on the amount of interstitial plagioclase the texture varies from adcumulate to mesocumulate. Clinopyroxenite layers are up to 100 meters thick and include transitional compositions to wehrlite (i.e. olivine clinopyroxenite; Fig. 10D) or gabbro (i.e. melagabbro). Peridotites have variable modal compositions and occur interlayered with gabbro throughout the LZ. Individual layers of peridotite are up to 150 meters thick, but thinner layers (usually 10-50 meters thick) predominate. Xenoliths of gabbro are frequent in peridotite layers. These xenoliths occur as irregular or elongated whitish blocks enclosed in dark colored peridotite (Fig. 10C).

Xenoliths of gabbro have irregular or rounded borders indicating that they are partially melted and reabsorbed by the ultramafic rock. Peridotites are medium- to coarse-grained Ol + Chr cumulates (or Ol + Cpx + Chr cumulates) with variable proportions of interstitial minerals (Cpx, Opx and Pl). The texture varies from mesocumulate to orthocumulate depending on the amount of interstitial minerals. Peridotites are usually wehrlite (Ol+Chr cumulate with abundant intercumulus Cpx, or an Ol+Cpx+Chr cumulate), but lherzolite (Ol + Chr cumulate with abundant intercumulus Cpx and Opx), plagioclase wehrlite or plagioclase lherzolite (with Pl as an additional intercumulus mineral) are frequent rock types. Peridotites frequently have both Cpx and Opx, but the modal amounts of Cpx are systematically much greater than Opx. Chromite is a ubiquitous accessory mineral (0.5 to 3.0 vol. %) in peridotites of the LZ and occurs as fine-grained euhedral crystals, generally enclosed in Cpx, Opx or Pl oikocrysts. Cotetic crystallization of olivine and chromite, indicating an Ol + Chr cumulate, occurs in dunite of the UZ and most peridotites of the UZ and LZ, but chromite usually disappear in Cpx + Ol cumulates.

The upper contact of the SPC to the southeast is poorly exposed. The contact zone is characterized by boulders of gabbro and associated peridotite of the SPC to the north, interpreted as a zone of interlayered gabbro and peridotite, and a quartz-rich soil with scattered boulders of gneiss of the host rock to the south.

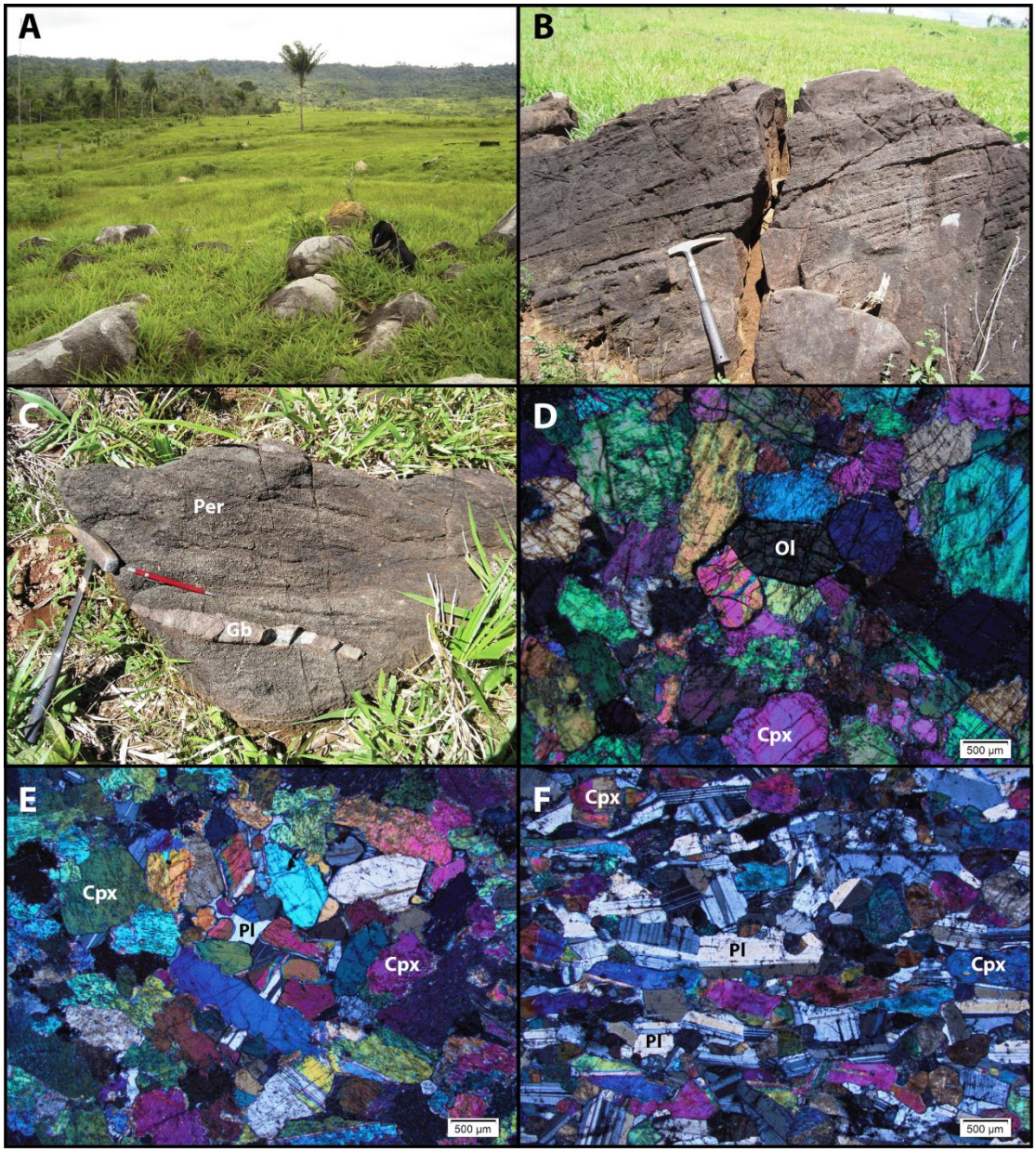

Figure 10 - A) View from south to north of the Serra do Puma Complex. The hill correspond to the UZ. The boulders in the front view consist of gabbro from the upper portion of the LZ. B) Layered gabbro of the LZ. C) Elongated xenolith of gabbro within peridotite of the LZ. D) Photomicrograph of olivine clinopyroxenite with adcumulate textute of the LZ. The sample consists of cumulus Cpx and olivine (Ol) . E) Photomicrograph of clinopyroxenite of the UZ. The sample is an Cpx cumulate with minor intercumulus plagioclase (Pl). F) Gabbro of the LZ with igneous lamination. The sample is an adcumulate with cumulus Cpx and plagioclase (Pl).

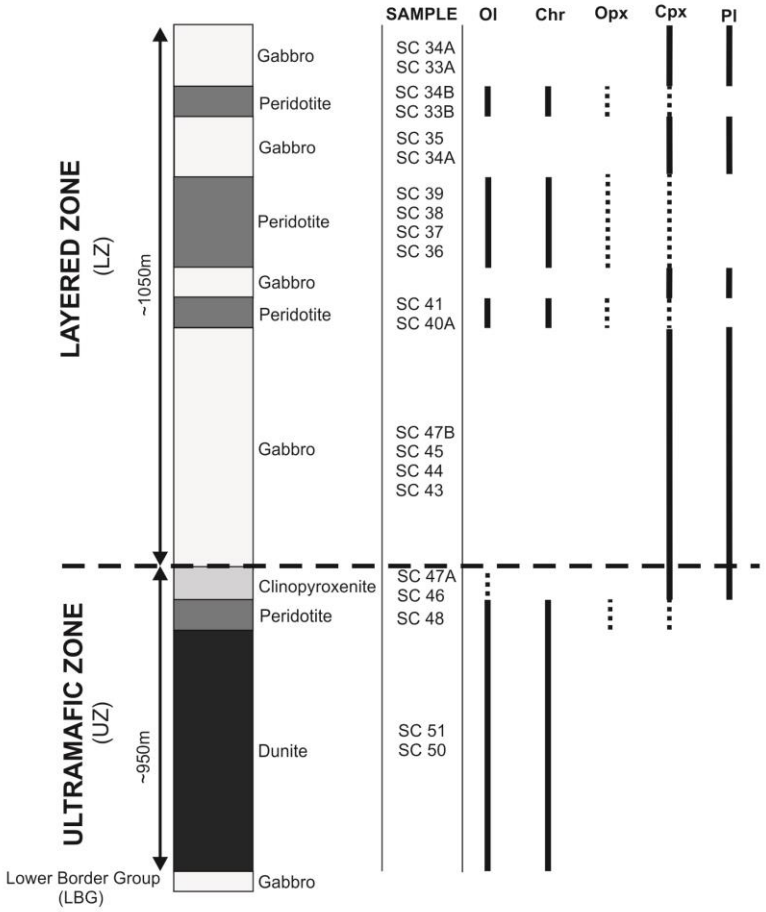

Figure 11 - Stratigraphy of the Serra do Puma Complex.

Frequent interlayer of gabbro and peridotite in the LZ suggests the existence of multiple injections of parental magma during the magmatic fractionation of the magma chamber. Partially reabsorbed xenoliths of gabbro within peridotite layers indicate magmatic erosion of previously crystallized layers of gabbro by new injections of parental magma. This indicates that the LZ developed in a dynamic magma chamber with successive influxes of parental magma. The crystallization sequence of the SPC consists of Ol+Chr, Ol+Cpx+Chr, Ol+Cpx, Cpx and Cpx+Pl, The complete sequence of crystallization for the SPC is indicated by the following scheme:

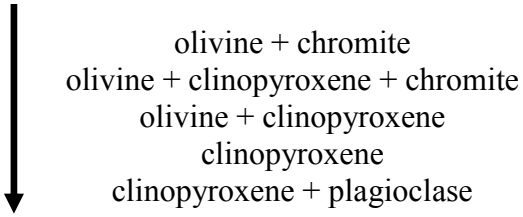

6.2 Mineral Chemistry

Systematic analyses of olivine, clinopyroxene and plagioclase were performed in unweathered samples through a complete section of the SPC (see Fig. 9 for the location of samples). Representative microprobe analyses for minerals of the SPC are provided in Appendix 1.

Due to extensive weathering and/or serpentinization analyses of olivine crystals are limited to just one sample of dunite from the UZ (Fig. 12). Olivine composition of this sample is primitive ($Fo_{88.6}$ to $Fo_{87.7}$) and enriched in nickel (2,840 to 3,210 ppm). This sample is located in the upper half portion of the UZ and, therefore, should not be considered as the most primitive olivine of the SPC. Systematic analyses of olivine crystals in peridotites (11 samples) and olivine-bearing clinopyroxenite (01 sample) from the upper portion of the UZ and throughout the LZ provide cryptic variation data for this stratigraphic interval of the SPC (Fig. 12). Olivine compositions in this interval are moderately primitive and range from $Fo_{85.0}$ to $Fo_{76.2}$, with higher contents of Fo in one sample located in the upper portion of the UZ and another in the upper portion of the MZ (Fig. 12). These results indicate several reversals and do not provide evidence for progressive fractionation of olivine throughout the MZ. The compositional variation of olivine in the LZ is likely to result from successive new influxes of parental magma, thus reinforcing the geological evidences for a dynamic magma chamber. Nickel contents in olivine crystals from peridotites and olivine-bearing clinopyroxenite range from 1,525 to 3,525 ppm. Nickel contents in olivine of samples from the SPC (including one dunite) are positively correlated with Fo contents (Fig. 13). These results are consistent with compositions of nickel-undepleted olivine for layered intrusions (Fig. 13).

Clinopyroxene and plagioclase compositions of samples from the upper portion of the UZ and throughout the LZ are indicated in Figure 12. In general these results follow the same pattern of cryptic variation indicated by olivine compositions (Fig. 12). Compared with the compositions of olivine, results for plagioclase and Cpx have larger range of compositions for specific samples. These highly variable compositions occur in samples where these minerals are interstitial (intercumulus).

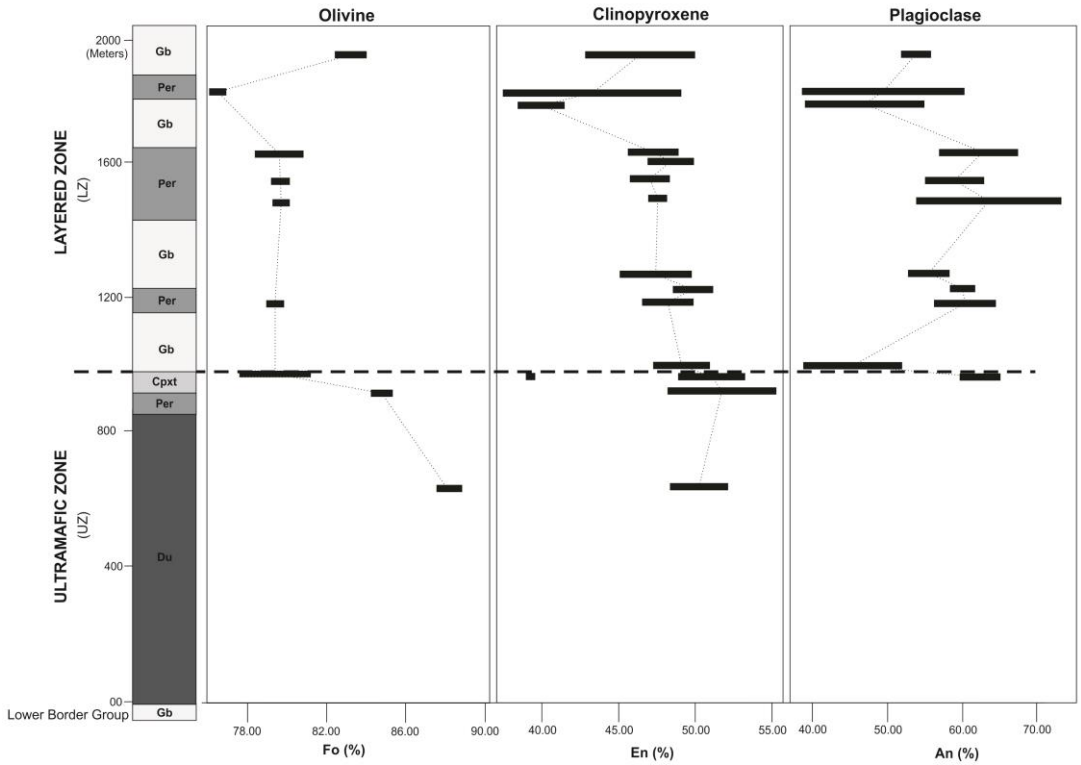

Figure 12 - Compositional variation of olivine, clinopyroxene and plagioclase throughout the stratigraphy of the SPC.

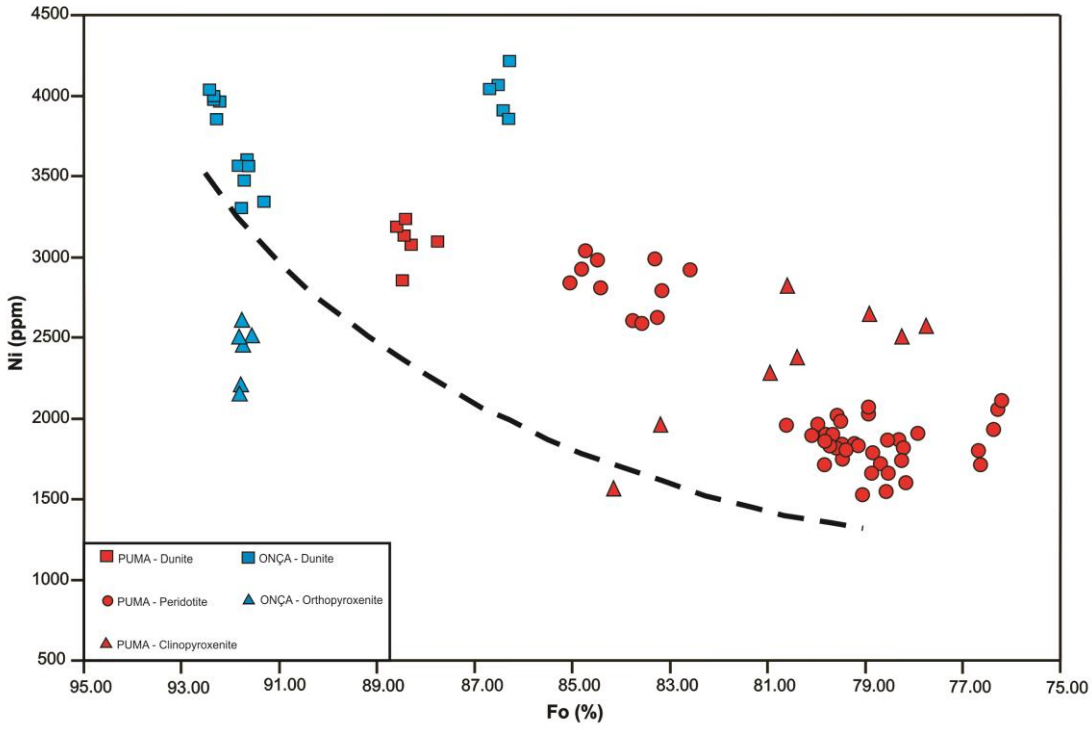

Figure 13 - Plot of Fo versus Ni content of olivine of the SPC. The dashed line is the compositional trend for olivine from layered complexes (Simkin and Smith, 1970).

7 Bulk Rock Geochemistry

7.1 Major and Minor Elements

Whole-rock chemical compositions of the Serra da Onça and Serra do Puma complexes samples are listed in Table 1 and 2, respectively. Because these layered complexes consist of cumulate rocks, their major and minor element compositions are dominantly controlled by the type of cumulus minerals. The plot of selected major and minor elements against Mg# (i.e. MgO/[MgO+FeO_t]) indicates the predominance of olivine, pyroxene and plagioclase cumulates (Fig. 14).

The large variation of Mg# is consistent with petrographic and mineral chemistry data for cumulate rocks of both complexes. Samples of dunite and peridotite of the SOC have higher Mg# (79.8 to 86.8 %) compared with those of the SPC (62.6 to 79.4 %). Higher Mg# for samples of the SOC may reflect the lack of analyses of ultramafic samples from the lower portion of the UZ of the SPC. On the other hand, the extensive fractionation of ultramafic rocks of the SPC result from interlayered peridotites throughout the upper portions of the stratigraphy, a feature that does not occur at the SOC. High contents of Ni and Cr in samples of ultramafic rocks of both complexes are controlled by olivine and accessory chromite, respectively (Fig. 14). High Cr contents (up to > 1 wt. %) are consistent with the occurrence of cumulus chromite in dunite and peridotites in samples from these complexes. Samples of gabbroic rocks of the SPC have higher Mg# (45.6 to 78.1 %) compared with those of the SOC (28.1 to 65.3 %), which reflect the sharp transition from the lower UZ to the upper MZ in the SOC, as well as the extensive fractionation of the gabbroic rocks. The latter is well indicated by cryptic variation data for the SOC (Fig. 7). Distinct contents of TiO2 for samples of the SOC and SPC reflect the abundance of Cpx as a cumulus mineral in the latter (Fig. 14). The difference in the crystallization sequence is nicely illustrated by the MgO-CaO plot for pyroxenites and gabbroic rocks, as indicated by distinct trends for samples of the SOC and SPC (Fig. 15).

Sample	SC 28	SC 06	SC 07B	SC 08	SC 09	SC 10A	SC 10B	SC 11	SC 12	SC 13	SC 14	SC 15	SC 16B	SC 17	SC 18	SC 19	SC 20	SC 21	SC 22	SC 23	SC 24A	SC 25	SC 26	SC 27
Stratigraphy *	100.50	230.00	580.00	710.00	780.00	920.00	920.00	1060.00	1120.00	1135.00	1225.00	1370.00	1445.00	1500.00	1565.00	1670.00	1748.00	1800.00	1898.00	1987.00	2081.00	2171.00	2278.00	2448.00
Rock code	Du	Du	Opxt	Du	Du	Opxt	Opxt	Gbn	Gbn	Gbn	Gbn	Gbn	Gbn	MGbn	MGbn	Gbn	Gbn	Gbn	Gbn	Gbn	Gbn	Gbn	Gbn	MGbn
SiO_2	32.46	32.86	56.38	33.11	38.44	50.15	56.99	52.46	53.18	52.81	52.89	53.28	52.78	48.71	48.69	53.26	53.16	52.91	53.12	52.46	52.58	52.49	53.31	52.86
Al_2O_3	0.46	0.92	0.79	0.08	0.22	0.95	1.20	17.51	16.98	17.13	17.08	17.20	11.45	17.03	17.35	17.68	17.26	15.60	13.57	16.23	11.32	13.12	8.34	15.04
$Fe_2O_{3\ total}$	6.48	7.33	7.32	10.52	9.17	6.46	6.06	4.91	6.40	6.28	6.60	7.00	11.95	14.37	13.15	6.99	7.40	7.96	9.47	8.08	12.99	10.10	13.64	10.71
MnO	0.09	0.09	0.14	0.15	0.13	0.10	0.12	0.12	0.12	0.12	0.12	0.13	0.24	0.14	0.12	0.15	0.15	0.14	0.16	0.15	0.22	0.22	0.22	0.18
MgO	42.57	41.93	34.55	41.46	36.70	36.86	34.36	9.23	8.82	8.45	8.21	7.77	11.37	5.61	5.58	7.36	7.60	9.56	12.62	7.62	13.32	11.67	16.62	6.94
CaO	0.17	0.34	0.57	0.15	0.05	0.60	0.93	12.31	12.16	12.10	11.46	11.70	10.19	10.35	10.60	11.61	11.62	10.97	8.69	12.49	7.86	8.68	6.20	9.99
Na_2O	0.02	0.13	0.04	0.03	0.01	0.03	0.04	2.22	2.33	2.47	2.48	2.53	1.81	2.97	2.96	2.70	2.66	2.30	1.97	2.38	1.64	1.91	1.22	2.78
K_2O	0.08	0.10	0.01	0.04	0.01	0.01	0.01	0.18	0.05	0.14	0.24	0.20	0.16	0.14	0.20	0.11	0.14	0.17	0.26	0.16	0.18	0.24	0.25	0.40
TiO_2	0.01	0.04	0.03	0.00	0.01	0.03	0.05	0.07	0.10	0.10	0.12	0.13	0.17	0.61	0.45	0.13	0.12	0.16	0.16	0.16	0.19	0.20	0.26	0.45
P_2O_5	-0.01	0.01	0.01	-0.01	0.01	0.01	0.02	0.02	0.02	0.01	0.02	0.01	0.01	0.01	0.01	0.01	0.01	0.02	0.02	0.02	0.01	0.01	0.03	0.08
LOI	17.30	16.10	-0.03	14.36	14.28	4.12	0.25	1.32	0.07	0.68	0.80	0.20	-0.02	-0.01	-0.06	0.09	0.26	0.34	0.02	0.01	-0.20	0.35	-0.20	0.58
TOTAL	99.65	99.85	99.81	99.92	99.03	99.32	99.95	100.35	100.23	100.27	100.02	100.16	100.13	99.92	99.05	100.08	100.38	100.14	100.05	99.75	100.12	98.99	99.87	100.00
V	17.64	22.65	30.13	9.60	14.52	35.42	35.08	75.46	95.15	97.60	99.54	107.94	166.35	829.59	1790.00	99.00	109.16	92.14	76.27	134.74	145.06	129.26	124.33	135.29
Cr	8510.00	7080.00	4270.00	824.03	3600.00	7000.00	3930.00	171.92	79.17	100.07	124.70	114.65	94.41	45.63	23.14	93.97	66.25	410.38	711.45	58.74	818.62	632.12	1000.00	153.27
Co	96.09	118.49	76.84	143.07	86.60	88.99	71.20	37.04	46.41	42.72	45.48	47.96	84.98	77.49	85.38	47.88	47.89	48.17	34.89	48.54	85.34	55.91	78.12	48.10
Ni	1810.00	2300.00	609.08	2450.00	6050.00	830.59	572.10	256.68	163.88	152.52	137.33	130.90	133.56	106.23	45.93	130.69	102.48	213.11	129.02	103.48	334.15	186.07	375.18	86.76
Cu	-10.00	12.10	-10.00	-10.00	-10.00	-10.00	11.47	12.80	186.55	147.43	273.34	171.68	148.49	54.68	360.23	100.98	118.55	110.80	45.52	121.67	143.47	63.55	70.67	64.84
Zn	51.96	47.16	47.01	65.26	58.61	62.52	38.63	43.07	37.66	91.19	57.59	44.24	72.62	50.00	51.59	-30.00	47.92	52.53	-30.00	51.05	115.31	39.45	104.03	101.11
Ga	1.11	1.71	1.07	-1.00	-1.00	1.58	1.65	14.01	14.62	15.13	15.81	16.65	12.20	22.06	20.77	17.00	15.75	14.76	10.43	16.03	13.15	12.26	10.95	18.61
Ge	0.49	1.03	1.86	0.93	0.94	1.49	1.58	1.41	1.26	1.22	1.38	1.52	1.80	1.02	1.43	0.78	1.45	1.49	-0.50	1.55	1.81	0.88	1.82	1.42
As	-5.00	-5.00	-5.00	-5.00	-5.00	-5.00	-5.00	-5.00	-5.00	-5.00	-5.00	-5.00	-5.00	-5.00	-5.00	-5.00	-5.00	-5.00	-5.00	-5.00	-5.00	-5.00	-5.00	-5.00
Rb	1.43	4.95	-1.00	1.09	1.15	-1.00	-1.00	8.84	1.54	4.31	7.33	3.05	2.85	2.19	2.68	1.60	2.24	5.61	2.35	1.89	4.89	5.87	8.53	10.34
Sr	3.89	10.13	2.12	2.78	-2.00	3.23	4.53	243.61	234.79	255.80	272.43	283.16	202.15	367.61	273.36	342.49	281.86	293.26	261.95	267.93	221.42	251.19	158.41	364.26
Y	-0.50	1.07	-0.50	-0.50	-0.50	-0.50	0.51	1.62	2.75	2.92	4.86	3.77	4.81	1.97	2.00	2.79	3.27	4.29	3.29	5.37	4.24	3.32	6.57	10.55
Zr	1.76	3.57	1.35	0.93	-1.00	1.00	1.57	2.90	2.36	4.00	11.43	5.14	5.32	2.67	2.77	2.41	3.00	7.38	4.88	5.28	5.20	4.75	15.58	25.38
Nb	0.38	0.84	0.31	0.48	-0.20	-0.20	-0.20	-0.20	0.21	-0.20	0.20	0.21	-0.20	-0.20	-0.20	-0.20	-0.20	0.29	-0.20	-0.20	0.48	0.98	1.18	1.52
Mo	5.69	7.04	-2.00	7.72	-2.00	-2.00	-2.00	-2.00	-2.00	-2.00	-2.00	-2.00	-2.00	-2.00	-2.00	-2.00	-2.00	-2.00	-2.00	-2.00	11.16	-2.00	-2.00	-2.00
Ag	-0.50	-0.50	-0.50	-0.50	-0.50	-0.50	-0.50	-0.50	-0.50	-0.50	-0.50	-0.50	-0.50	-0.50	-0.50	-0.50	-0.50	-0.50	-0.50	-0.50	-0.50	-0.50	-0.50	-0.50
In	-0.10	-0.10	-0.10	-0.10	-0.10	-0.10	-0.10	-0.10	-0.10	-0.10	-0.10	-0.10	-0.10	-0.10	-0.10	-0.10	-0.10	-0.10	-0.10	-0.10	-0.10	-0.10	-0.10	-0.10
Sn	-1.00	-1.00	2.81	-1.00	-1.00	-1.00	-1.00	-1.00	-1.00	-1.00	-1.00	-1.00	-1.00	-1.00	-1.00	-1.00	-1.00	-1.00	-1.00	-1.00	-1.00	-1.00	-1.00	-1.00
Sb	10.00	-0.20	-0.20	-0.20	2.04	-0.20	-0.20	-0.20	-0.20	-0.20	-0.20	-0.20	-0.20	-0.20	-0.20	-0.20	-0.20	-0.20	-0.20	-0.20	-0.20	-0.20	-0.20	-0.20
Cs	0.10	0.24	-0.10	0.14	0.25	-0.10	-0.10	0.25	-0.10	0.15	0.24	0.15	0.15	0.14	0.20	-0.10	0.11	0.23	0.19	0.10	0.25	0.21	0.41	0.47
Ba	7.39	15.33	5.69	11.78	7.72	9.03	11.71	78.37	63.27	75.63	132.88	103.59	95.96	94.03	91.55	99.28	97.99	131.31	91.67	86.20	90.33	172.69	133.53	326.25
La	0.09	0.87	0.13	-0.05	0.06	0.06	0.10	0.40	0.64	0.74	1.05	1.31	1.08	0.65	0.68	1.14	0.96	1.83	1.46	1.38	1.22	1.29	2.64	7.46
Ce	0.19	1.98	0.36	0.12	0.08	0.13	0.25	0.82	1.38	1.54	2.12	2.72	2.42	1.21	1.29	2.28	2.00	4.03	3.04	3.33	2.51	2.66	5.51	16.07
Pr	0.02	0.22	0.04	-0.01	-0.01	0.01	0.03	0.11	0.17	0.19	0.27	0.33	0.31	0.15	0.16	0.27	0.24	0.48	0.36	0.46	0.30	0.33	0.68	1.92
Nd	0.08	0.94	0.22	-0.05	-0.05	0.07	0.13	0.50	0.79	0.89	1.30	1.51	1.50	0.76	0.74	1.29	1.18	2.13	1.59	2.27	1.43	1.49	2.94	7.96
Sm	0.02	0.18	0.05	0.01	-0.01	0.02	0.04	0.17	0.23	0.27	0.37	0.41	0.46	0.21	0.23	0.34	0.37	0.53	0.41	0.68	0.39	0.42	0.70	1.85
Eu	0.01	0.05	0.01	-0.01	-0.01	-0.01	0.01	0.12	0.23	0.26	0.29	0.30	0.28	0.15	0.16	0.29	0.30	0.34	0.30	0.36	0.27	0.28	0.33	0.80
Gd	0.02	0.18	0.03	0.01	-0.01	0.01	0.04	0.19	0.34	0.35	0.46	0.52	0.59	0.27	0.27	0.43	0.47	0.67	0.49	0.82	0.47	0.44	0.79	1.73
Tb	-0.01	0.02	-0.01	-0.01	-0.01	-0.01	-0.01	0.04	0.07	0.07	0.09	0.10	0.12	0.06	0.06	0.07	0.09	0.12	0.09	0.15	0.09	0.09	0.17	0.31
Dy	0.02	0.19	0.04	0.01	-0.01	0.04	0.07	0.25	0.43	0.43	0.60	0.62	0.79	0.35	0.36	0.48	0.57	0.71	0.58	0.95	0.69	0.55	1.03	1.86
Ho	-0.01	0.03	-0.01	-0.01	-0.01	-0.01	0.02	0.05	0.09	0.09	0.12	0.13	0.17	0.07	0.07	0.10	0.12	0.14	0.12	0.19	0.14	0.11	0.23	0.38
Er	0.02	0.12	0.03	0.02	-0.01	0.04	0.06	0.17	0.29	0.29	0.38	0.41	0.53	0.22	0.22	0.31	0.37	0.47	0.39	0.59	0.49	0.39	0.78	1.16
Tm	-0.01	0.02	0.01	-0.01	-0.01	0.01	0.01	0.03	0.05	0.04	0.06	0.06	0.08	0.03	0.03	0.05	0.06	0.07	0.06	0.08	0.07	0.06	0.12	0.16
Yb	0.03	0.12	0.03	0.02	0.02	0.05	0.08	0.17	0.28	0.30	0.37	0.38	0.55	0.20	0.22	0.29	0.36	0.43	0.38	0.53	0.49	0.38	0.79	1.04
Lu	0.00	0.02	0.01	0.00	0.00	0.01	0.02	0.03	0.05	0.05	0.06	0.06	0.09	0.03	0.03	0.05	0.06	0.07	0.06	0.08	0.08	0.06	0.13	0.16
Hf	-0.10	-0.10	-0.10	-0.10	-0.10	-0.10	-0.10	0.10	-0.10	0.13	0.26	0.19	0.20	0.11	0.11	0.10	0.13	0.25	0.18	0.22	0.19	0.16	0.47	0.80
Ta	0.61	0.05	-0.01	-0.01	-0.01	-0.01	-0.01	0.03	0.02	-0.01	-0.01	-0.01	-0.01	-0.01	-0.01	-0.01	-0.01	0.02	-0.01	-0.01	-0.01	-0.01	0.04	0.08
W	-0.50	0.60	-0.50	-0.50	-0.50	-0.50	-0.50	-0.50	-0.50	-0.50	-0.50	-0.50	-0.50	-0.50	-0.50	-0.50	-0.50	-0.50	-0.50	-0.50	-0.50	-0.50	-0.50	-0.50
Tl	-0.05	-0.05	-0.05	-0.05	-0.05	-0.05	-0.05	-0.05	-0.05	-0.05	0.06	-0.05	-0.05	-0.05	-0.05	-0.05	-0.05	-0.05	-0.05	-0.05	-0.05	-0.05	-0.05	0.06
Pb	10.53	17.87	-5.00	11.45	-5.00	-5.00	-5.00	-5.00	-5.00	-5.00	-5.00	-5.00	-5.00	-5.00	-5.00	-5.00	-5.00	-5.00	-5.00	-5.00	17.25	-5.00	-5.00	5.78
Bi	-0.10	-0.10	-0.10	-0.10	-0.10	-0.10	-0.10	-0.10	-0.10	-0.10	0.11	0.11	0.17	-0.10	0.28	-0.10	-0.10	-0.10	-0.10	0.20	-0.10	-0.10	-0.10	-0.10
Th	-0.05	0.20	-0.05	-0.05	-0.05	-0.05	-0.05	0.05	0.07	0.08	0.12	0.14	0.12	-0.05	-0.05	0.06	0.06	0.30	0.18	0.09	0.13	0.08	0.74	1.16
U	0.01	0.04	-0.01	0.02	0.02	-0.01	0.01	0.02	0.02	0.03	0.05	0.04	0.03	0.01	-0.01	0.02	0.04	0.09	0.05	0.03	0.05	0.04	0.21	0.35

Major element oxides in weight percent, trace elements in parts per million; total iron reported as Fe_2O_3
LOI: loss on ignition
Rock code: Du dunite, Opxt orthopyroxenite, Gbn gabbronorite, MGbn magnetite-gabbronorite
* Indicated location (meters) in Fig. 6

Table 01 – Whole-rock analyses of representative samples from the Serra da Onça Complex.

Sample	SC 33A	SC 33B	SC 34A	SC 34B	SC 35	SC 36	SC 37	SC 38	SC 39	SC 40A	SC 41	SC 43	SC 44	SC 45	SC 46	SC 47A	SC 47B	SC 48	SC 50	SC 51
Stratigraphy *	2391.00	2391.00	2254.00	2254.00	2210.00	2130.00	2073.00	2029.00	1998.00	1930.00	1850.00	1585.00	1526.00	1473.00	1213.00	1184.00	1184.00	1145.00	790.00	661.00
Rock code	Gb	Per	Gb	Pl-Per	Gb	Per	Per	Pl-Per	Pl-Per	Pl-Per	Pl-Per	Gb	Gb	Gb	Cpxt	Cpxt	Gb	Per	Du	Du
SiO_2	50.87	41.14	52.28	42.44	53.11	40.37	41.49	40.41	39.46	37.36	40.29	51.85	51.73	52.28	52.56	53.30	52.43	41.83	37.62	37.53
Al_2O_3	15.91	4.23	13.37	4.37	15.52	7.33	7.67	7.69	6.78	2.70	7.15	8.60	16.14	10.34	3.62	6.51	11.66	2.22	0.85	0.38
$Fe_2O_{3\ total}$	5.51	12.36	10.14	14.88	7.11	13.47	14.44	13.67	14.10	15.88	13.12	5.94	3.70	4.85	6.15	4.42	3.50	10.89	10.19	10.78
MnO	0.11	0.17	0.14	0.23	0.11	0.21	0.23	0.21	0.22	0.21	0.21	0.12	0.08	0.10	0.13	0.11	0.08	0.16	0.15	0.13
MgO	9.11	31.74	8.50	24.94	7.11	25.48	25.87	26.04	25.96	31.93	26.56	13.88	9.33	12.63	17.43	15.50	12.45	33.10	39.21	34.93
CaO	12.10	4.40	10.96	6.82	11.11	5.16	5.00	4.94	4.90	2.19	5.73	15.87	15.31	16.53	18.06	18.93	16.84	6.44	0.61	0.16
Na_2O	2.40	0.50	2.76	0.44	3.41	0.77	0.85	0.61	0.48	0.14	0.58	1.40	2.32	1.57	0.73	0.88	1.59	0.21	0.06	0.04
K_2O	1.16	0.22	0.42	0.12	0.34	0.44	0.22	0.23	0.30	0.10	0.28	0.27	0.21	0.46	0.04	0.11	0.32	0.06	0.06	0.04
TiO_2	0.24	0.22	0.54	0.28	0.44	0.19	0.18	0.15	0.13	0.17	0.16	0.24	0.13	0.19	0.30	0.15	0.13	0.09	0.04	0.02
P_2O_5	0.03	0.03	0.03	0.02	0.05	0.02	0.02	0.02	0.01	0.01	0.02	0.02	0.01	0.01	0.02	0.01	0.02	0.01	0.01	0.01
LOI	2.60	4.77	1.23	5.09	1.49	5.54	4.37	5.93	7.19	8.89	5.41	1.79	1.45	1.24	0.80	0.42	1.27	4.84	11.07	14.98
TOTAL	100.03	99.77	100.36	99.63	99.81	98.98	100.35	99.91	99.52	99.57	99.52	99.97	100.41	100.21	99.84	100.33	100.27	99.86	99.87	99.00
V	118.10	85.68	255.43	138.01	158.35	70.78	66.03	54.14	63.82	87.61	63.52	180.52	106.23	161.34	204.52	156.91	117.59	70.02	32.84	35.14
Cr	251.27	2530.00	304.69	2720.00	256.24	1560.00	1200.00	1190.00	1450.00	2930.00	1440.00	439.20	215.62	818.80	2320.00	1320.00	680.61	2970.00	4520.00	>10,000
Co	30.75	114.12	43.57	121.13	32.68	51.64	120.51	90.77	140.60	167.58	122.71	45.84	26.28	34.04	43.80	31.03	26.36	114.02	140.24	186.33
Ni	206.11	1870.00	263.62	848.89	171.65	340.62	868.07	625.18	987.55	1200.00	932.36	294.24	242.35	308.28	388.20	323.97	284.64	1630.00	2130.00	1850.00
Cu	33.84	33.47	38.54	31.44	66.74	23.59	26.04	-10.00	12.74	-10.00	47.15	49.66	16.51	30.34	38.41	21.00	31.30	-10.00	40.50	-10.00
Zn	69.68	109.52	45.05	104.97	37.07	-30.00	161.19	37.59	109.79	101.21	107.47	41.18	-30.00	-30.00	33.09	36.37	-30.00	46.46	105.11	88.61
Ga	12.22	5.41	15.18	5.96	16.65	4.22	6.69	4.93	6.11	3.92	6.24	7.52	11.07	8.54	5.55	5.77	8.08	2.55	1.62	1.33
Ge	1.45	1.57	1.81	1.72	1.53	-0.50	1.42	0.40	1.59	1.62	1.38	2.36	1.57	1.99	2.35	2.59	1.05	1.44	1.17	1.15
As	-5.00	-5.00	-5.00	-5.00	-5.00	-5.00	-5.00	-5.00	-5.00	-5.00	-5.00	-5.00	-5.00	-5.00	-5.00	-5.00	-5.00	-5.00	-5.00	-5.00
Rb	46.16	8.97	11.98	3.02	10.19	3.15	4.58	3.43	4.21	1.33	7.59	11.12	8.74	19.37	3.84	3.96	13.72	1.65	1.84	-1.00
Sr	289.88	63.34	209.62	40.69	231.03	67.95	61.93	72.48	58.31	22.24	85.97	107.41	181.81	156.12	34.37	64.85	165.89	23.66	4.08	-2.00
Y	10.55	5.37	15.97	7.14	15.45	4.20	4.30	3.67	4.18	4.12	4.27	9.81	4.22	6.48	9.27	5.19	4.35	2.51	0.89	-0.50
Zr	20.74	13.18	29.70	18.89	33.66	11.01	12.15	9.18	8.35	21.32	8.74	9.75	5.40	7.81	15.06	4.89	5.97	3.26	3.33	1.31
Nb	1.08	1.17	1.63	0.84	2.14	0.78	0.89	0.74	0.69	0.66	0.66	0.64	0.43	0.52	0.75	0.34	0.50	0.43	0.35	0.37
Mo	-2.00	12.87	-2.00	-2.00	-2.00	-2.00	-2.00	2.00	-2.00	-2.00	9.34	-2.00	-2.00	-2.00	-2.00	6.57	-2.00	-2.00	11.08	-2.00
Ag	-0.50	1.09	-0.50	-0.50	-0.50	-0.50	1.71	-0.50	-0.50	-0.50	-0.50	-0.50	-0.50	-0.50	-0.50	-0.50	-0.50	-0.50	-0.50	-0.50
In	-0.10	-0.10	-0.10	-0.10	-0.10	-0.10	-0.10	-0.10	-0.10	-0.10	-0.10	-0.10	-0.10	-0.10	-0.10	-0.10	-0.10	-0.10	-0.10	-0.10
Sn	-1.00	-1.00	-1.00	-1.00	-1.00	-1.00	-1.00	-1.00	-1.00	2.33	-1.00	-1.00	-1.00	-1.00	-1.00	1.34	-1.00	-1.00	-1.00	-1.00
Sb	-0.20	0.23	0.25	-0.20	-0.20	-0.20	0.78	-0.20	-0.20	-0.20	11.94	-0.20	-0.20	-0.20	-0.20	0.21	-0.20	-0.20	-0.20	-0.20
Cs	0.24	0.26	0.27	0.11	0.12	-0.10	-0.10	0.14	-0.10	-0.10	0.27	0.15	0.13	0.20	0.16	0.31	0.11	-0.10	-0.10	-0.10
Ba	256.52	144.70	157.36	96.30	185.71	192.66	198.29	186.85	157.28	68.31	205.49	110.72	65.21	120.96	45.87	46.43	129.95	34.70	11.39	5.56
La	2.51	2.59	2.55	1.27	3.71	1.24	1.55	1.29	1.98	0.88	1.10	1.63	0.79	1.00	1.66	0.53	0.74	0.45	0.23	-0.05
Ce	4.07	4.95	7.14	2.88	11.79	2.57	3.13	2.36	2.59	1.88	2.28	3.10	1.85	2.50	4.15	1.44	1.86	0.98	0.66	0.09
Pr	0.58	0.54	1.14	0.40	1.81	0.36	0.38	0.30	0.34	0.26	0.27	0.52	0.26	0.37	0.57	0.20	0.25	0.14	0.06	0.01
Nd	2.79	2.50	5.46	1.96	8.42	1.54	1.67	1.31	1.50	1.31	1.42	2.65	1.39	2.08	2.89	1.24	1.33	0.66	0.34	0.06
Sm	0.78	0.63	1.49	0.67	2.12	0.45	0.46	0.37	0.38	0.41	0.43	0.91	0.45	0.69	0.96	0.48	0.45	0.25	0.09	0.03
Eu	0.37	0.25	0.66	0.30	0.83	0.22	0.24	0.20	0.21	0.13	0.20	0.35	0.27	0.29	0.35	0.20	0.23	0.10	0.05	-0.01
Gd	1.03	0.75	1.89	0.87	2.28	0.54	0.57	0.46	0.54	0.53	0.55	1.28	0.59	0.91	1.32	0.65	0.61	0.35	0.11	0.03
Tb	0.20	0.14	0.37	0.18	0.42	0.12	0.11	0.10	0.10	0.11	0.10	0.25	0.12	0.19	0.26	0.14	0.13	0.07	0.02	-0.01
Dy	1.27	0.94	2.30	1.15	2.62	0.70	0.74	0.61	0.62	0.69	0.71	1.59	0.77	1.16	1.63	0.91	0.81	0.43	0.14	0.04
Ho	0.26	0.19	0.49	0.25	0.55	0.15	0.14	0.12	0.13	0.15	0.15	0.34	0.16	0.25	0.33	0.19	0.16	0.09	0.03	-0.01
Er	0.83	0.64	1.59	0.80	1.72	0.51	0.51	0.41	0.42	0.49	0.47	1.00	0.46	0.73	1.02	0.60	0.48	0.28	0.10	0.03
Tm	0.11	0.09	0.22	0.11	0.24	0.07	0.07	0.06	0.06	0.08	0.07	0.13	0.07	0.11	0.14	0.08	0.07	0.04	0.02	0.01
Yb	0.65	0.59	1.32	0.73	1.50	0.44	0.49	0.38	0.38	0.44	0.42	0.79	0.39	0.60	0.84	0.47	0.40	0.25	0.10	0.04
Lu	0.10	0.08	0.20	0.11	0.23	0.07	0.07	0.06	0.06	0.08	0.07	0.12	0.06	0.09	0.13	0.07	0.06	0.04	0.01	0.01
Hf	0.56	0.40	0.88	0.51	0.98	0.32	0.36	0.26	0.25	0.55	0.28	0.37	0.20	0.29	0.50	0.20	0.21	0.12	-0.10	-0.10
Ta	0.04	0.05	0.09	0.03	0.14	0.07	0.03	0.03	0.03	0.02	0.03	0.02	-0.01	-0.01	0.03	-0.01	0.01	0.02	-0.01	-0.01
W	-0.50	-0.50	-0.50	-0.50	-0.50	-0.50	-0.50	-0.50	-0.50	-0.50	-0.50	-0.50	-0.50	-0.50	-0.50	-0.50	-0.50	-0.50	22.78	-0.50
Tl	0.11	-0.05	-0.05	-0.05	-0.05	-0.05	-0.05	-0.05	-0.05	-0.05	-0.05	-0.05	-0.05	0.05	-0.05	-0.05	-0.05	-0.05	-0.05	-0.05
Pb	28.35	39.54	-5.00	-5.00	-5.00	-5.00	-5.00	-5.00	-5.00	-5.00	19.53	5.72	-5.00	-5.00	-5.00	15.02	-5.00	-5.00	36.16	-5.00
Bi	-0.10	0.24	-0.10	-0.10	-0.10	-0.10	0.20	-0.10	-0.10	-0.10	0.11	-0.10	-0.10	-0.10	-0.10	-0.10	-0.10	-0.10	-0.10	-0.10
Th	0.37	0.37	0.81	0.23	1.44	0.18	0.22	0.12	0.16	0.17	0.16	0.21	0.05	0.13	0.33	0.05	0.16	0.07	0.05	-0.05
U	0.10	0.26	0.17	0.07	0.23	0.07	0.14	0.05	0.06	0.07	0.04	0.05	0.02	0.04	0.10	0.04	0.04	0.03	0.03	0.02

Major element oxides in weight percent, trace elements in parts per million; total iron reported as Fe_2O_3
LOI: loss on ignition
Rock code: Du dunite, Cpxt Clinopyroxenite, Gb gabbro, Per Peridotite, Pl-Per Plagioclase- Peridotite
* Indicated location (meters) in Fig. 11

Table 02 – Whole-rock analyses of representative samples from the Serra do Puma Complex.

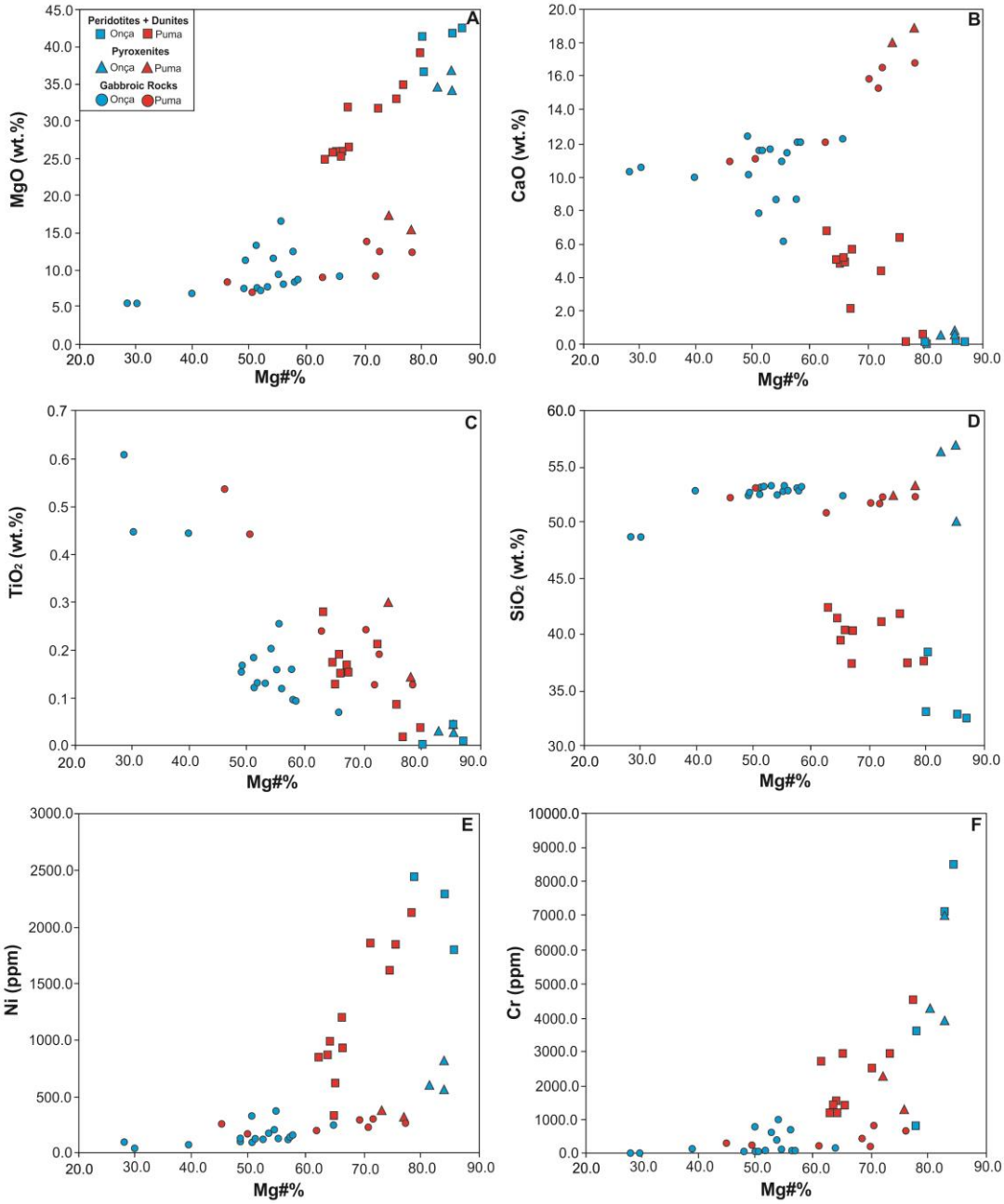

Figure 14 - Plot of Mg# versus selected major and minor element contents for rocks of the Serra da Onça and Serra do Puma complexes. Data from Table 1 and Table 2.

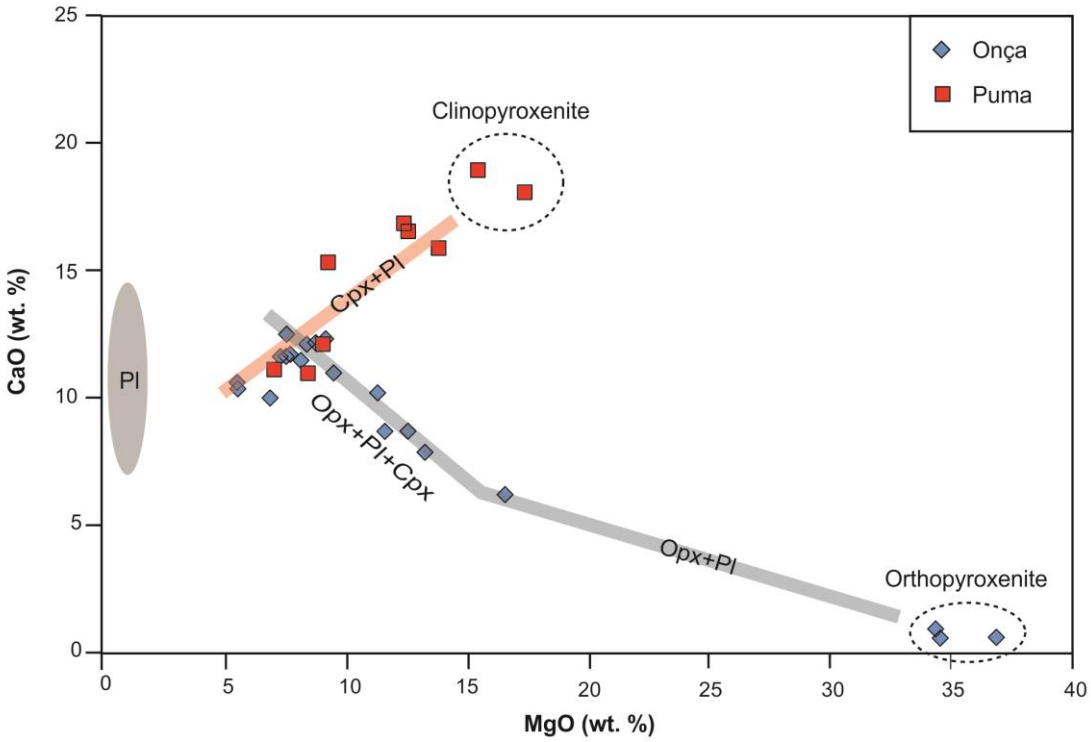

Figure 15 - Plot of MgO versus CaO contents for pyroxenites and gabbroic rocks of the Serra da Onça and Serra do Puma complexes. Data from Table 1 and Table 2. Field of plagioclase is based upon microprobe data for cumulus plagioclase from both complexes (reported in this study). Thick solid lines indicate the cristalization sequence for the SOC (bluish color) and SPC (reddish color) complexes.

7.2 Trace Elements

The contents of incompatible trace elements in the mafic-ultramafic rocks of the SOC and SPC are generally low (Tables 1 and 2), as expected for cumulates consisting mainly by olivine, pyroxene and plagioclase. Variations in contents of incompatible trace elements in mafic-ultramafic cumulates in layered complexes result from the combined effect of variable assemblages of cumulate minerals, fractionation of the parental magma and variable amounts of trapped intercumulus liquid (Barnes, 1986; Ferreira Filho et al., 1998). Mafic-ultramafic rocks of the SOC and SPC are predominantly adcumulates, such that the amount of incompatible trace elements contained in cumulate minerals is relevant for their concentration in these rocks. Therefore, results for trace elements are considered for different types of cumulate rocks.

Distinct mantle-normalized rare earth element (REE) profiles characterize different cumulate rocks of the SOC and SPC (Fig. 16). REE profiles for clinopyroxenites (Cpx cumulate) of the SPC and orthopyroxenites (Opx cumulate) of the SOC indicate the significance of different cumulate minerals in the distribution of REE

in these rocks (Fig. 16B). Because partition coefficients of REE for Cpx are significantly higher than Opx (Godel et al., 2011; Ferreira Filho et al., 1998), clinopyroxenites of the SPC have significantly higher REE contents when compared with orthopyroxenites of the SOC. Therefore, different REE contents and REE profiles for pyroxenites of the SOC and SPC should be evaluated considering the effect of different cumulus minerals. The same reasoning should be used when considering the distribution of REE of gabbroic rocks of the SOC and SPC (Fig. 16A). Gabbroic rocks of the SOC and SPC have similar amounts of plagioclase but consist of different propostions of Cpx and Opx. REE profiles for gabbroic rocks of the SOC (Opx+Cpx+Pl cumulates) have positive slopes for LREE and HREE (i.e. progressive enrichment toward lighter REE) and very distinct positive Eu anomalies (Fig. 16A). On the other hand, REE profiles for gabbroic rocks of the SPC (Cpx+Pl cumulates) have flat to slightly positive slopes for LREE, mainly flat HREE profile and discrete positive Eu anomalies (Fig. 16A). Different REE profiles for gabbroic rocks of the SOC and SPC result in distinct La/Sm and Gd/Yb ratios (Fig. 17). Because the modal proportion of Cpx is higher in gabbroic rocks of the SPC than gabbroic rocks from the SOC, these differences should partially result from distinct modal proportions. However, plots of La/Sm vs Ce and La/Sm vs Yb (Fig. 18) indicate that higher La/Sm ratios for gabbroic samples of the SOC compared with gabbroic samples of the SPC are independent of the total amount of REE elements. These indicate that higher La/Sm ratios of the SOC gabbroic rocks should not result just of distinct modal proportion of Cpx, and distinct compositions of parental magmas for the SOC and SPC should be involved. The conclusion derived from this reasoning indicates that the parental magma of the SOC has a relatively higher La/Yb ratio compared to the parental magma of the SPC.

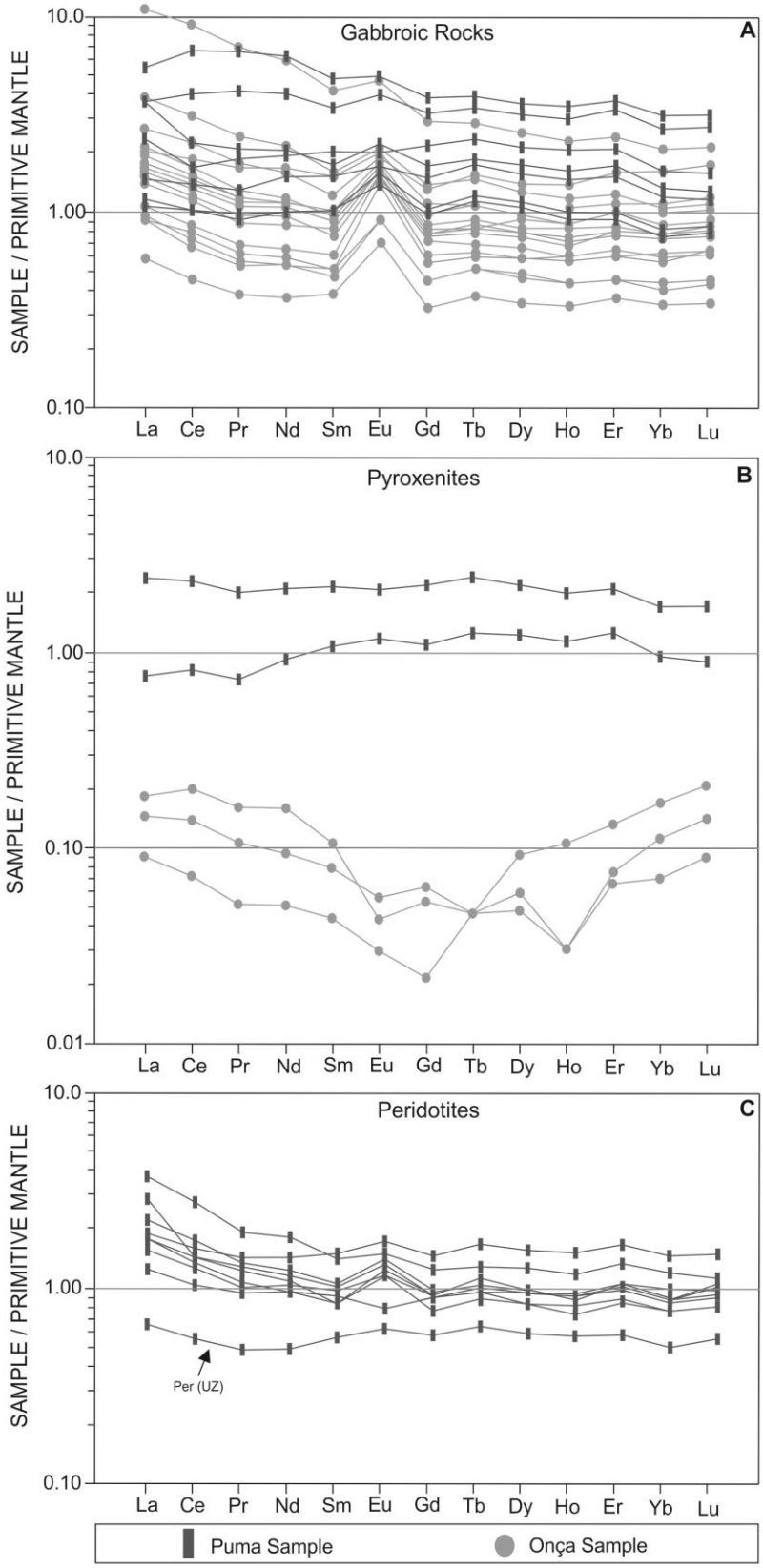

Figure 16 - Primitive mantle-normalized REE profiles for samples of the SOC and SPC. A) Samples of gabbroic rocks. B) Samples of pyroxenites. C) Samples of peridotites. Data from Tables 1 and 2. Primitive mantle normalization values are from Sun and McDonough (1989).

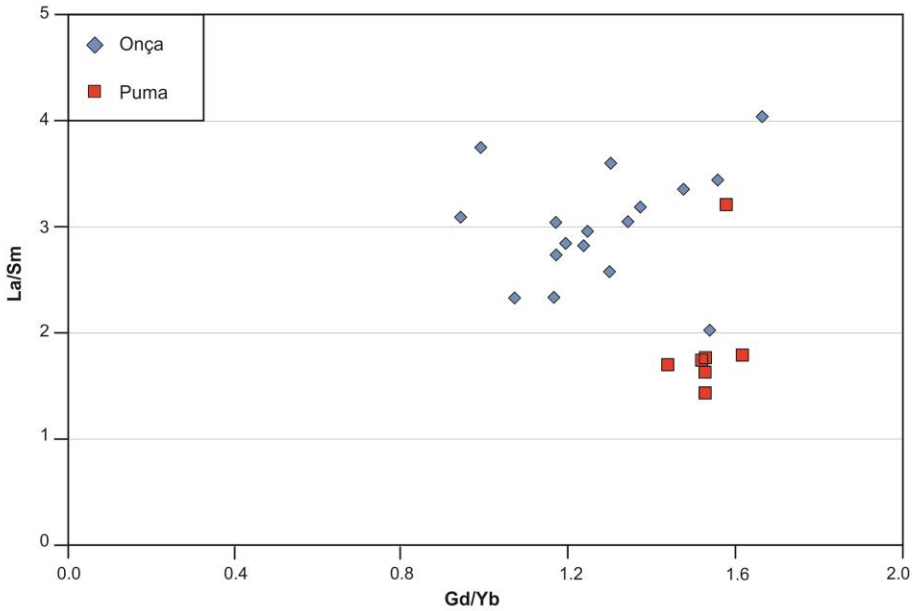

Figure 17 - Gd/Yb vs La/Sm plot for gabbroic rocks of the SOC and SPC. Same samples plotted in Fig. 16A.

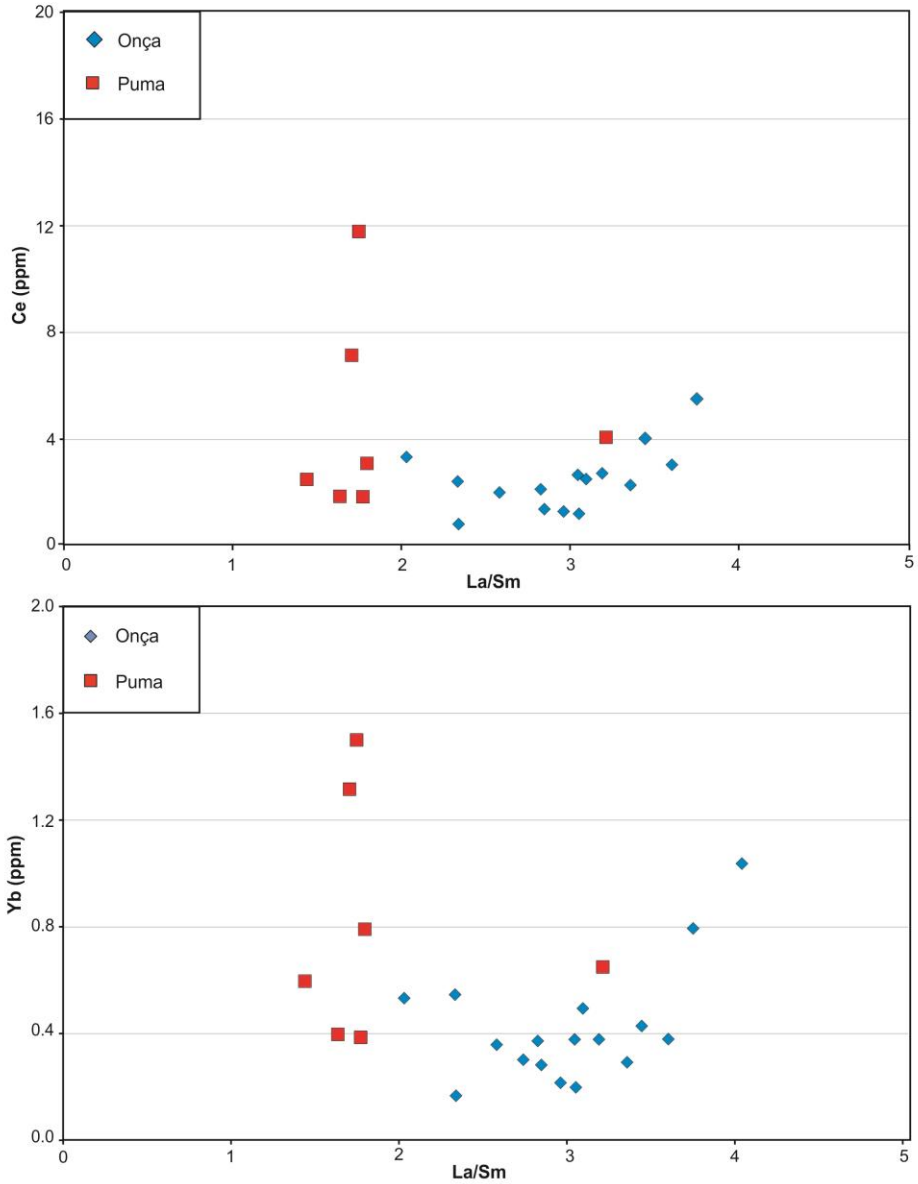

Figure 18 - La/Sm vs Ce and La/Sm vs Yb plots for gabbroic rocks of the SOC and SPC. Same samples plotted in Fig. 16A.

Contents for several highly incompatible high field strength cations, including Ta, Nb, Th and Hf, in cumulate rocks of the SOC and SPC are close to or below detection limits for most samples, especially for dunites and peridotites (Table 1 and 2). To avoid scattering due to results close to detection limits, mantle-normalized lithophile trace element profiles of the SOC and SPC are plot just for gabbroic rocks with higher contents of incompatible trace elements (Fig. 19A and 19B). These profiles are very similar and are consistent with profiles obtained for rocks with lower trace element contents, including peridotites and pyroxenites. Distinct profiles are restricted to samples of ilmenite-magnetite bearing gabbronorites of the SOC, which are characterized by

significant Ti anomalies. Mantle-normalized alteration-resistant trace element profiles are more fractionated for gabbroic samples of the SOC, as indicated by relative enrichment in LREE (Fig. 19A). Gabbroic samples from the SOC and SPC have pronounced negative Nb and Ta anomalies (Fig. 19). It is worth to mention that Nb and Ta anomalies are more significant for the SOC compared to the SPC, which reflects the relative enrichment of LREE in samples of the SOC. Very similar mantle-normalized lithophile trace element profiles for the SOC and SPC rocks suggest that cumulate rocks from both complexes crystallized from parental magmas with similar contents of incompatible elements.

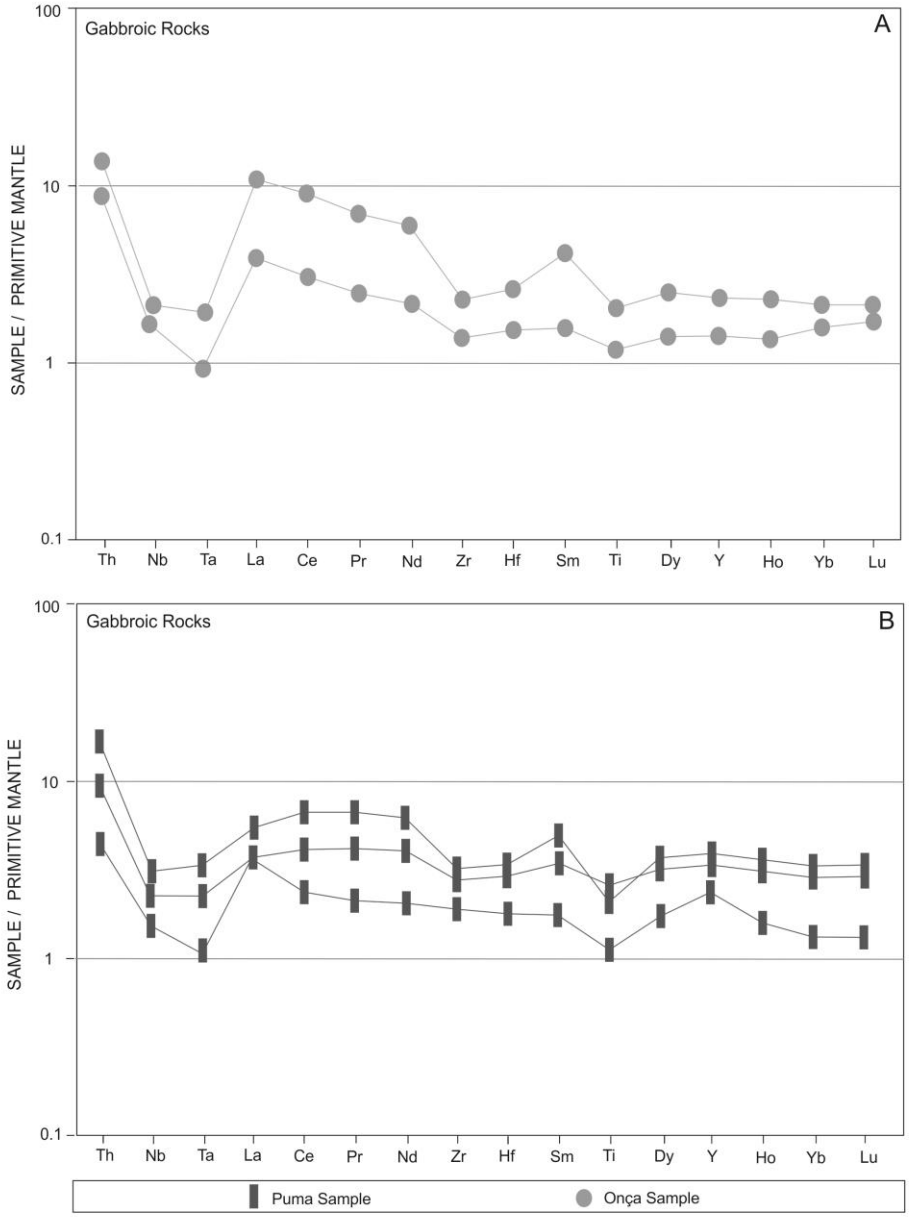

Figure 19 - Primitive mantle-normalized alteration-resistant trace elements profiles for samples of gabbroic rocks of the SOC and SPC. Data from Tables 1 and 2. Primitive mantle normalization values are from Sun and McDonough (1989).

8 U-Pb and Sm-Nd isotopes

8.1 U-Pb geochronology

Extensive sampling for zircon U-Pb geochronology was carried on in the SOC (07 samples), SPC (02 samples) and smaller nearby layered complexes (01 sample of the Carapanã complex and 02 samples of the Guepardo Complex). Sampling was focused on fractionated gabbroic rocks, including pegmatoidal facies representing clusters enriched in trapped residual liquid, as well as orthocumulate peridotites. Out of 12 samples collected, just one sample from the SPC produced a concentrate of minerals (zircons) appropriated for U-Pb geochronology. U-Pb isotope data for this sample (SC68) are presented in Table 3. Sample SC68 corresponds to a pegmatoid gabbro of the SPC, interpreted as representative of the most evolved rocks of the LZ. This pegmatoidal gabbro occurs as an irregular pod within medium-grained gabbro. Except for the coarser grain size and minor interstitial quartz, sample SC68 is similar to gabbroic rocks of the Layered Zone of the SPC

U-Pb isotopic analyses of zircon crystals render several concordant to slightly discordant U-Pb dates (Table 3; Fig. 20). Twenty-two spot analyses define a Discordia line with an upper intercept age of 2713±30 Ma (MSWD=6.5). This age is interpreted as the crystallization age of zircons and, therefore, the age of magmatic crystallization of the SPC.

Spot	U(ppm)	Th(ppm)	Th/U	206Pb/204Pb	Ratio 7/6*	2s (%)	Age 7/6	2s (Ma)	Ratio 7/5*	2s (%)	Age 7/5	2s (Ma)	Ratio 6/8*	2s (%)	Age 6/8	2s (Ma)
011-Z06	75.80	254.38	3.36	26404.95	0.18372	0.9	2686.7	14.7	13.17897	2.1	2692.6	19.5	0.52028	1.9	2700.3	41.6
023-Z14	205.72	270.96	1.32	6512.66	0.18359	1.0	2685.6	15.8	13.33840	2.5	2703.9	23.5	0.52694	2.3	2728.5	51.4
006-Z03	143.60	422.05	2.94	95396.79	0.18545	0.7	2702.2	11.7	13.65417	1.7	2726.0	16.1	0.53401	1.6	2758.3	34.8
040-Z25	85.84	138.78	1.62	21392.91	0.18222	1.0	2673.2	17.0	13.77303	1.5	2734.2	14.0	0.54820	1.1	2817.7	24.3
010-Z05	108.89	250.54	2.30	45443.52	0.18494	0.7	2697.6	12.2	13.93074	1.8	2745.0	17.1	0.54633	1.7	2809.9	37.7
015-Z08	179.05	576.51	3.22	13676.21	0.18349	1.1	2684.6	17.6	14.00756	1.6	2750.2	14.6	0.55368	1.1	2840.5	25.8
004-Z01	202.15	192.52	0.95	135466.46	0.19045	0.9	2746.0	14.5	14.11876	1.4	2757.7	12.9	0.53768	1.0	2773.7	23.5
022-Z13	95.78	274.17	2.86	42614.31	0.18790	1.2	2723.9	19.4	14.23198	2.0	2765.3	18.4	0.54934	1.6	2822.4	35.4
029-Z18	155.23	278.20	1.79	56809.94	0.18869	1.0	2730.7	16.2	14.26258	1.4	2767.3	13.5	0.54822	1.0	2817.8	23.5
027-Z16	203.85	587.88	2.88	94839.88	0.18885	1.1	2732.2	17.5	14.31241	1.5	2770.6	14.4	0.54966	1.1	2823.7	24.8
034-Z21	203.34	248.75	1.22	55977.80	0.18963	0.8	2738.9	12.4	14.30676	1.1	2770.3	10.8	0.54719	0.9	2813.5	19.7
036-Z23	117.20	424.10	3.62	67203.92	0.19258	1.0	2764.3	16.1	14.36272	1.6	2774.0	15.4	0.54091	1.3	2787.2	29.3
030-Z19	176.36	411.90	2.34	8603.05	0.18603	0.8	2707.4	13.1	14.24778	1.1	2766.3	10.4	0.55548	0.8	2847.9	17.3
045-Z27	165.08	339.16	2.05	43083.11	0.19051	1.2	2746.6	20.0	14.36058	1.8	2773.8	17.0	0.54670	1.3	2811.4	30.2
018-Z11	55.42	99.37	1.79	7118.03	0.18807	1.4	2725.3	22.7	14.29130	3.1	2769.2	29.1	0.55114	2.8	2829.9	63.4
039-Z24	171.22	376.16	2.20	51349.78	0.18835	1.0	2727.8	16.7	14.43487	1.7	2778.7	16.0	0.55584	1.4	2849.4	31.3
024-Z15	155.53	267.45	1.72	41493.90	0.18701	0.9	2716.0	15.2	14.52526	1.5	2784.7	14.0	0.56333	1.2	2880.4	26.7
035-Z22	75.67	300.17	3.97	14763.90	0.18673	0.9	2713.6	15.2	14.48589	1.6	2782.1	15.5	0.56264	1.4	2877.5	31.4
005-Z02	114.75	113.88	0.99	79961.72	0.18811	0.8	2725.7	13.7	14.55620	1.9	2786.7	18.1	0.56122	1.7	2871.7	39.9
012-Z07	117.68	569.84	4.84	23573.97	0.18937	1.1	2736.7	17.9	14.59045	2.2	2788.9	20.5	0.55881	1.9	2861.7	43.5
048-Z30	109.18	236.82	2.17	41184.51	0.19271	1.0	2765.4	15.7	14.64029	2.0	2792.2	18.4	0.55100	1.7	2829.3	38.8
016-Z09	113.53	264.01	2.33	51429.51	0.18934	1.0	2736.4	16.5	14.93847	2.4	2811.3	22.4	0.57222	2.2	2916.9	50.5

Table 03 - U-Pb LA-MC-ICPMS data for sample SC68.

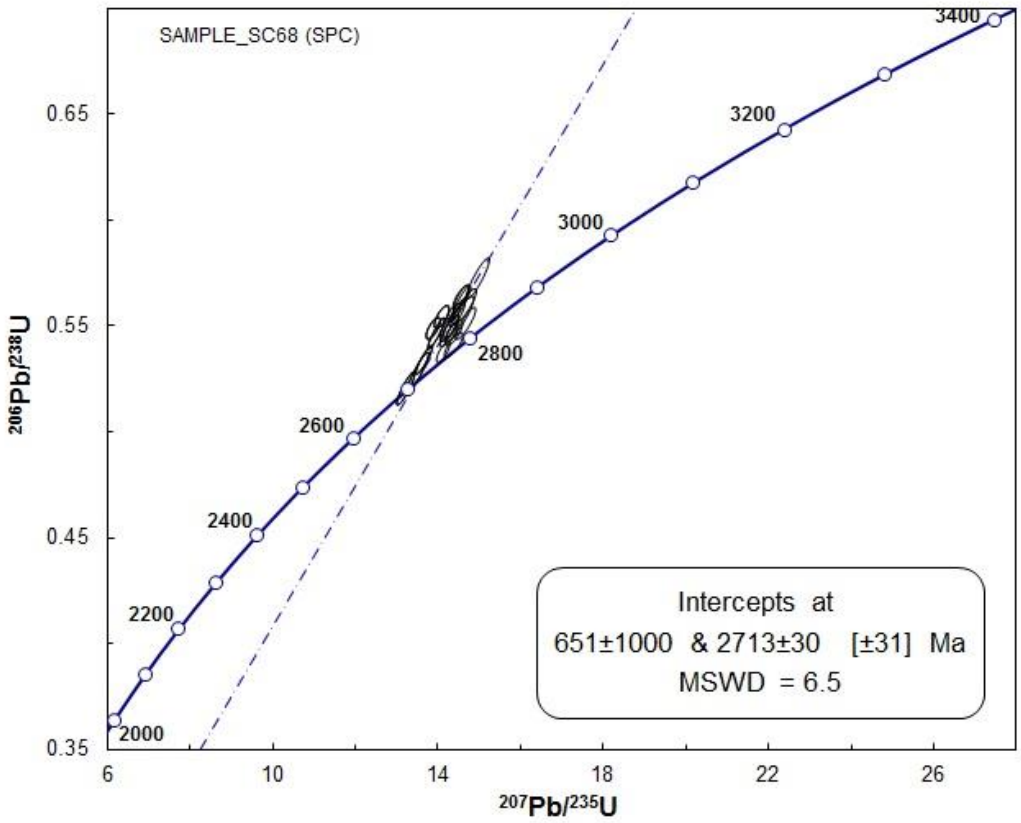

Figure 20 - LA-MC-ICPMS U-Pb plot for sample SC68. See text for explanation.

8.2 Sm-Nd systematics

The Sm-Nd isotopic data of the SOC and SPC are listed in Table 04. Nd isotopic data obtained for different mafic (gabbro, leucogabbro, gabbro pegmatoid) and ultramafic (clinopyroxenite, plagioclase peridotite and peridotite) lithotypes of the SPC render variably positive to negative εNd (T=2.77 Ga) values (-3.56 to 2.41). Plotted against the stratigraphy, the Sm–Nd data of the SPC are scattered and do not correlate with the layering sequence or the fractionation trend. Peridotites of the SPC generally have more negative εNd (T=2.77 Ga) values (-3.56 to -0.64) than interlayered gabbroic rocks (-2.47 to 2.41) (Fig. 21). Nd isotopic data for gabbronorite and Mag gabbronorite of the SOC have negative εNd (T=2.77 Ga) values (-3.33 to -2.12). Plotted against the stratigraphy, the Sm–Nd data of the SOC are scattered and do not correlate with the layering sequence or the fractionation trend. Compared with isotopic data of the SPC, gabbroic rocks of the SOC have more negative and less variable εNd (T=2.77 Ga) values as well as generally higher La/Sm and Ce/Nb ratios (Fig. 21).

Sample	Rock	Complex	Nd (ppm)	Sm (ppm)	Sm/Nd	$^{147}Sm/^{144}Nd$	$^{143}Nd/^{144}Nd$	±(2SE)	$(^{143}Nd/^{144}Nd)i$	ε(0)	ε(2.77Ga)
SC33A	Gabbro	Puma	2.793	0.780	0.279	0.1689	0.512201	10	0.509114	-8.52	1.38
SC34B	Pl Peridotite	Puma	1.957	0.665	0.340	0.2056	0.512699	12	0.508941	1.19	-2.02
SC35B	Gabbro Peg	Puma	8.419	2.124	0.252	0.1525	0.511955	9	0.509167	-13.32	2.41
SC37	Peridotite	Puma	1.665	0.464	0.278	0.1683	0.511984	13	0.508907	-12.76	-2.70
SC38	Pl-Peridotite	Puma	1.306	0.370	0.283	0.1711	0.511991	14	0.508863	-12.62	-3.56
SC43	Gabbro	Puma	2.648	0.906	0.342	0.2069	0.512701	12	0.508918	1.23	-2.47
SC44	Leucogabbro	Puma	1.392	0.448	0.322	0.1944	0.512620	16	0.509067	-0.35	0.45
SC46	Clinopyroxenite	Puma	2.888	0.962	0.333	0.2014	0.512790	17	0.509107	2.97	1.24
SC48	Peridotite	Puma	0.663	0.249	0.376	0.2273	0.513166	20	0.509011	10.30	-0.64
SC68	Gabbro Pegmatoid	Puma	5.800	1.530	0.264	0.1595	0.511956	21	0.509041	-13.30	-0.06
SC12	Gabbronorite	Onça	0.795	0.226	0.285	0.1721	0.512021	21	0.508874	-12.04	-3.33
SC17	Mag Gabbronorite	Onça	0.764	0.212	0.277	0.1675	0.511965	18	0.508902	-13.13	-2.78
SC22	Gabbronorite	Onça	1.586	0.406	0.256	0.1548	0.511712	14	0.508882	-18.06	-3.17
SC25	Gabbronorite	Onça	1.491	0.424	0.284	0.1719	0.512031	14	0.508889	-11.84	-3.04
SC27	Mag Gabbronorite	Onça	7.961	1.847	0.232	0.1402	0.511499	12	0.508936	-22.22	-2.12

Table 04 - Sm–Nd isotopic data for the SOC and SPC.

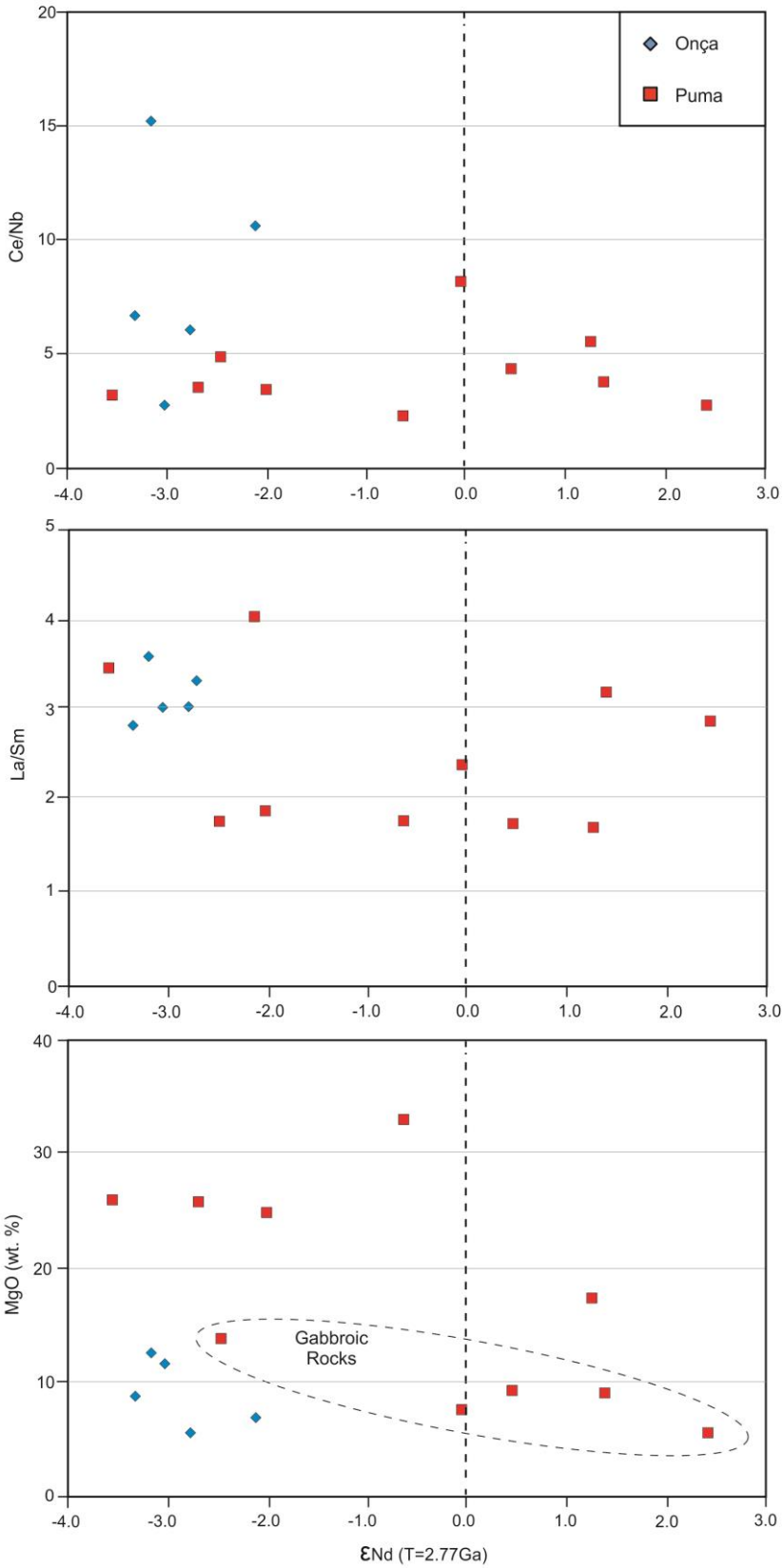

Figure 21 - $\varepsilon_{Nd\ (T=2.77\ Ga)}$ vs Ce/Nb and La/Sm and $\varepsilon_{Nd\ (T=2.77\ Ga)}$ vs MgO plots for rocks of the SOC and SPC. Data from Table 01, 02 and 04.

9 Discussion

9.1 Parental Magma

The characterization of the parental magmas of layered intrusions is of great interest because this provide clues on the nature of the mantle source, the potential assimilation of older crustal rocks and the prospectivity of an igneous suite to host magmatic mineral deposits.

The composition of the parental magmas of the SOC and SPC is not constrained by common approaches used to define their composition (e.g., chilled margin, bulk composition, extrusive equivalents, related dykes, and melt inclusions), as illustrated by several studies of extensively investigated layered intrusions (e.g. Cawthorn, 1996). Whenever a direct composition of the parental magma is not possible in layered intrusions, the nature of the parental magma has been inferred from the crystallization sequences of the intrusions and the geochemistry of cumulate minerals and rocks (e.g. Chai and Naldrett, 1992; Ferreira Filho et al. 1998; Godel et al. 2011). Distinct crystallization sequences described for the SOC and SPC suggests that each complex evolved from a different parental magma, and the reason behind the existence of such difference becomes a relevant question as far as the characterization of magmatic suites in the CMP is concerned. A very primitive composition (i.e., high MgO content) for the parental magma of the SOC and SPC is indicated by the abundance of dunite and peridotite, as well as the relatively high proportion of ultramafic rocks (about 50 %) in the stratigraphy of both complexes. The compositional range of cumulus Ol within the UZ of the SOC ($Fo_{86.2-92.4}$) and the SPC ($Fo_{88.6-87.7}$) supports a very primitive composition for their parental magmas. It is worth remembering that due to extensive weathering and/or serpentinization analyses of olivine crystals are limited to just one sample of dunite from the UZ of the SPC (Fig. 12). Therefore, this composition should not be considered as representative of the most primitive olivine of the SPC, and highly primitive olivine compositions (~ Fo_{92}) should be considered for both complexes. Primitive compositions and similar compositional range for olivine of the UZ in both complexes are supported by comparable bulk rock MgO and Ni contents for bedrock dunite of Ni laterite deposits of the SOC and SPC, as indicated by systematic data collected for resources evaluation. The composition of the most primitive cumulus Ol in the SOC is comparable with those reported for the Great Dyke (Fo_{92} ; Wilson, 1982), Niquelândia Complex (Fo_{93} ; Ferreira Filho and Araújo, 2009; Ferreira Filho et al. 2010)

and Ipueira-Medrado Sill (Fo_{93} ; Marques and Ferreira Filho, 2003), all of them originated from highly primitive parental magmas.

Distinct crystallization sequences for the SOC (Ol+Chr > Opx+Chr > Opx > Opx+Pl > Opx+Pl+Cpx) and SPC (Ol+Chr > Ol+Cpx+Chr > Cpx > Cpx+Pl >) indicate that they follow different liquid lines of descent. The crystallization sequence of the SOC is similar to those of the major PGE-bearing intrusions (e.g. Bushveld, Stillwater, Great Dyke) in which Opx precedes Cpx (Eales and Cawthorn, 1996). The early crystallization of Opx relative to Cpx in the SOC indicates that the primary magma was silica saturated, whereas the absence of Opx as a cumulus mineral in the SPC suggests that the primary magma was silica undersaturated. The origin of chemically distinct magmas, such as those of the SOC and SPC, are interpreted in different ways, but these interpretations converge along two trains of thought:

i. They are different primitive mantle melts and therefore should be considered as part of two distinct magmatic suites in the CMP.

ii. They represent similar primitive mantle melt modified by variable differentiation and contamination processes.

The contrasting processes cannot be readily distinguished using isotope and trace element data. However, the broad similarity in the trace element data for the SOC and SPC suggests that they were derived from a similar source, possibly followed by variable contamination with crustal rocks, a subject to be addressed in the following topic.

9.2 Assimilation

Mantle-normalized alteration-resistant trace element profiles of gabbroic rocks of the SOC and SPC are fractionated, as indicated by relative enrichment in LREE and Th, with pronounced negative Nb and Ta anomalies (Fig. 19). Mantle-normalized negative Nb and Ta anomalies are a characteristic feature for the upper and lower crust (Wedepohl, 1995). The alteration-resistant element profiles obtained for the SOC and SPC are comparable with average composition of the B1 rocks of the chilled margins of the Bushveld Complex (Barnes et al., 2010). The B1 magma is interpreted as the product of a mixture of a primitive mantle melt mixed with continental crust, and has been successfully modeled as the parental magma of the cumulate rocks of Lower and Lower Critical Zone of the Bushveld Complex (Barnes et al., 2010; Godel et al., 2011). The distribution of alteration-resistant elements in the SOC and SPC is therefore consistent with a mixture of a primitive mantle melt with continental crust. Mantle-normalized

negative Nb and Ta anomalies are more significant for the SOC compared to the SPC, which partially reflects the relative enrichment of LREE in samples of the SOC (Fig. 17 and 18). Very similar mantle-normalized lithophile trace element profiles for the SOC and SPC rocks suggest that cumulate rocks from both complexes crystallized from parental magmas with similar contents of incompatible elements.

Additional evidence for crustal contamination of the parental magma of the SOC and SPC is provided by Sm-Nd isotopic data (Table 04). Nd isotopic data obtained for different rock types of the SPC render variably positive to negative εNd (T=2.77 Ga) values (-3.56 to 2.41), while gabbroic rocks of the SOC have negative and less variable εNd (T=2.77 Ga) values (-3.33 to - 2.12). Nd data of the SPC and SOC are scattered and do not correlate with the layering sequence or the fractionation trend of these layered complexes. These results are consistent with an original mantle melt variably contaminated with older continental crust. Crustal contamination is expected for high temperature and Mg-rich magmas, like the parental magmas of the SOC and SPC, intruded into gneisses and migmatites of the ca. 3.0 Ga Xingu Complex. Compared with isotopic data of the SPC, gabbroic rocks of the SOC have more negative and less variable εNd (T=2.77 Ga) values as well as generally higher La/Sm and Ce/Nb ratios (Fig. 21). These features are compatible with a higher proportion of crustal contamination for layered rocks of the SOC compared with those of the SPC. However, considering the data for each layered intrusion, εNd (T=2.77 Ga) values are poorly correlated with La/Sm and Ce/Nb ratios (Fig. 21). Poor correlation between εNd (T=2.77 Ga) values with La/Sm and Ce/Nb ratios persists even if the data are limited to gabbroic rocks, a group of samples likely to be less affected by compositional variations produced by variable contents of REE in cumulate minerals.

The evaluation of the importance of crustal contamination based upon isotope and trace element data of cumulate rocks is not straightforward. Because the compositions of the parental magmas are not known (i.e., based on chilled margins or volcanic equivalents) and the compositions of potential contaminants are poorly constraint, the latter statement is particularly significant for the SOC and SPC. However, the combined data thus suggest that the compositions of the parental magmas of the SOC and SPC were derived from a similar source, followed by variable contamination with crustal rocks, which are more significant for the SOC.

9.3 The petro-tectonic setting of the Serra da Onça and Serra do Puma layered complexes

The 2713±30 Ma U-Pb zircon age obtained in this study for the SPC provides an additional age for layered intrusions of the Carajás Mineral Province. Reported U-Pb zircon ages for these layered intrusions (Fig. 22) indicate that they all have Neoarchean ages broadly bracket between 2680-2780 Ma. U-Pb zircon ages for the Luanga (2763±6 Ma; Machado et al., 1991), Lago Grande (2722±53 Ma; Teixeira, 2013; Teixeira et al., submitted) and Serra da Onça (2766±6Ma; unpublished data reported by Lafon et al., 2000) complexes overlap with precise ages of the bimodal volcanism of the Grão Pará Group (2759±2 Ma, Machado et al., 1991; 2760±11 Ma, Trendall et al., 1998), thus supporting the interpretation that mafic volcanics and mafic-ultramafic layered intrusions resulted from coeval magmatic events (Machado et al., 1991; Ferreira Filho et al., 2007). The age reported for the SPC in this study is younger than the ages reported for the Grão Pará Group, as well as the Luanga and SOC complexes, thus indicating a relatively younger intrusive event. Considering that the reported age of the SOC is based upon unpublished zircon U-Pb SHRIMP data for one gabbroic sample, together with our difficulties to get concentrate of minerals (zircons) appropriated for U-Pb geochronology in seven investigated samples, the interpretation of reported ages for the SOC should be considered with caution. Obtained results for the SOC and SPC may be interpreted in two different ways:

i. The reported 2766±6Ma U-Pb zircon age corresponds to the magmatic age of the SOC. Following this interpretation, the silica unsaturated and less contaminated magma of the SPC would have intruded later than the SOC, thus representing a younger intrusion compared to dated layered complexes and volcanics from the eastern portion of the CMP (Fig. 22).

ii. The reported 2766±6Ma U-Pb zircon age corresponds to ages of inherited zircons, eventually assimilated from syntectonic granites (ca 2.76-2.74 Ga; Dall'Agnol et al. 1994; Avelar et al. 1999). Geological support for this alleged contamination is provided the abundance of large Neoarchean granites (Plaquê plutons) in the area close to the SOC and SPC (Fig. 02). This interpretation opens the possibility that younger ages of mafic-ultramafic complexes may be a characteristic feature of the western portion of the CMP, as indicated by the 2713±30 Ma age reported in this study.

These two contrasting interpretation are currently being investigated through additional sampling for U-Pb geochronology of several layered intrusions in the western

portion of the CMP. At this point in time we suggest that the layered intrusions of the CMP are part of a major Neoarchean (ca 2.76 Ga) magmatic event, which has a spread of ages that still need to be fully investigated. Based on recent U-Pb zircon ages obtained for layered intrusions of the CMP (summarized in Fig. 22), we suggest that the alleged 2.4 Ga Cateté Event indicated in the LIP Commission (www.largeigneousprovinces.org) should be reported a Neoarchean event (ca 2.76 Ga).

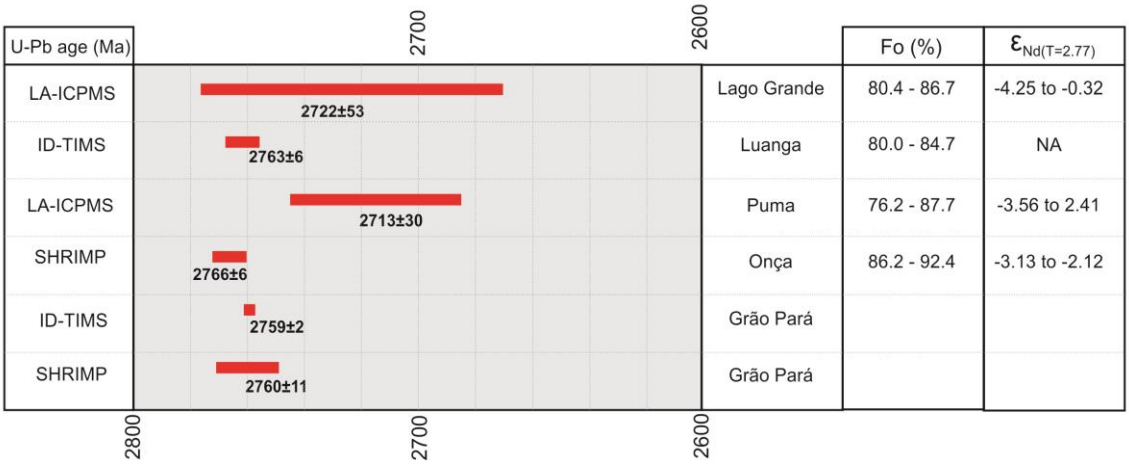

Figure 22 - Summary of U-Pb zircon ages, Fo contents of olivine and Sm-Nd isotopes for layered intrusions of the CMP. Data from the following references: Lago Grande (Teixeira, 2013; Teixeira *et al*., submitted); Luanga (Machado *et al*., 1991; Ferreira Filho *et al*., 2007); Luanga and Puma (this study), Grão Pará (Machado *et al.* 1991; Trendall *et al*., 1998).

The location of the layered complexes in the CMP is controlled by major regional faults, a feature that is particularly evident in aerogeophysical features along EW (e.g. Canaã shear zone) and NE-SW (e.g. MacCandles shear zone) trends (Fig. 1 and 23). Geophysical features associated with these regional trends are interrupted or largely attenuated in areas covered by the Itacaiúnas Supergroup, Aquiri Group and Águas Clara Formation, indicating that they represent dip crustal discontinuities older than the Neoarchean supra-crustal sequences (Fig. 23). The larger and most primitive layered intrusions in the CMP (e.g. SOC, SPC, Vermelho Complex and Serra do Jacaré Complex), all of them characterized by a thick pile of ultramafic rocks and world class Ni-laterite resources, are emplaced within older terrains of the Xingú Complex. These intrusions were located along dip crustal discontinuities that represent preferred sites of location of magma transferred from the mantle to the crust.

The assimilation of older continental crust during the ascent and/or emplacement of the mafic-ultramafic magma of the SOC and SPC (this study), as well as the Lago

Grande Complex (Teixeira, 2013; Teixeira et al., submitted), is suggested by trace element contents and Sm-Nd isotopes. Fo contents for layered complexes summarized in Figure 22 indicate highly to moderately primitive compositions, while negative εNd (T=2.77 Ga) values suggest contamination with old silaic crust. This suggestion is consistent with a large volume of primitive to moderately primitive magma being transferred through continental crust in the Carajás region. This is expected if mafic-ultramafic magmatism in Carajás is associated with intra-plate rifting of older continental crust (Gibbs et al., 1986; Olszewski et al., 1989; Villas and Santos, 2001).

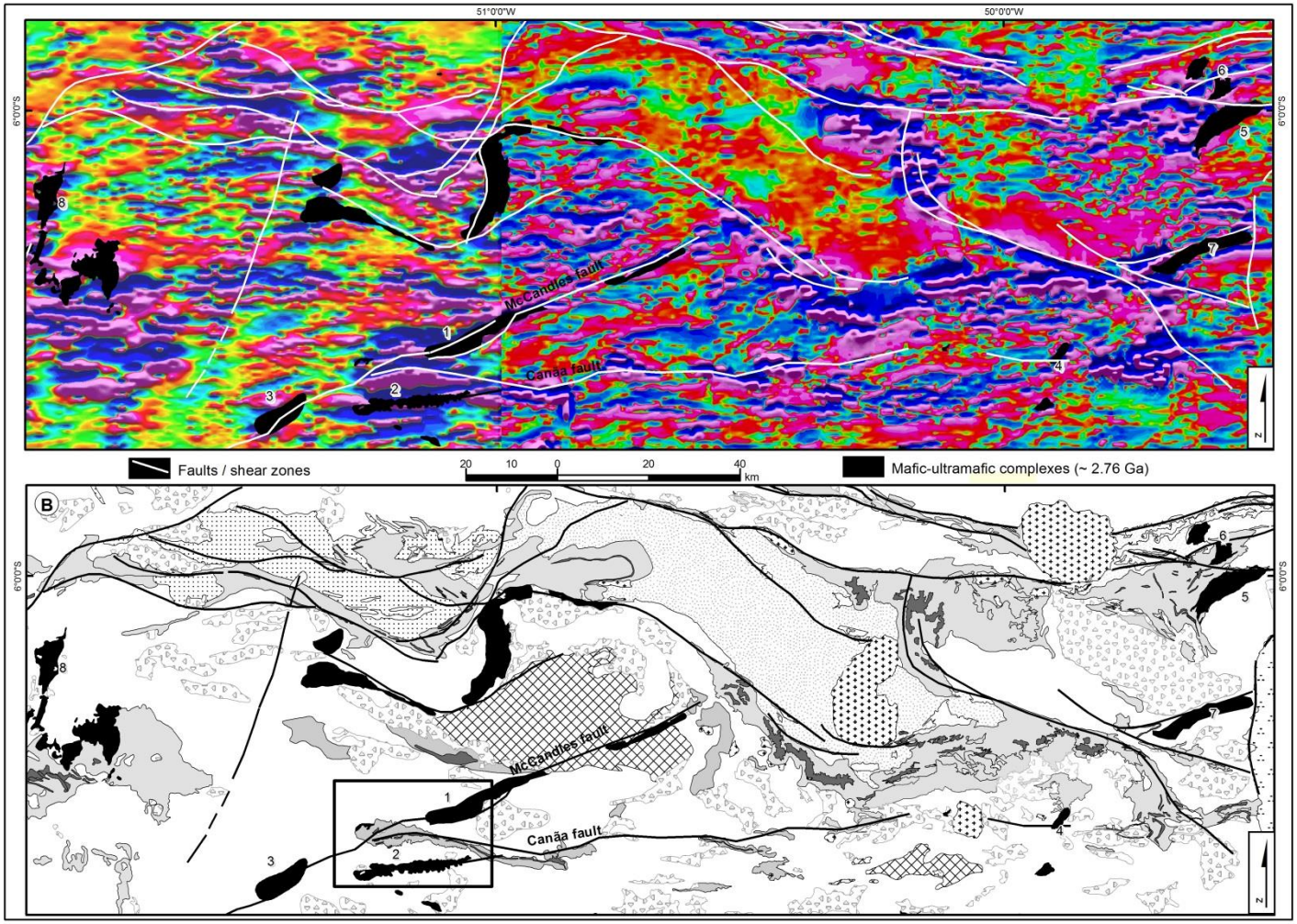

Figure 23 - A) Analytical signal image for the CMP (geophysical data processes from PGBC and Carajás 1 regional surveys). B) Geological map of the CMP (see captions in Fig. 1).

9.4 The potential for Ni-Cu-PGE deposits

Large events of mafic-ultramafic magmatism are responsible for the concentration of most world-class Ni-Cu-PGE deposits in the world (Naldrett 2004, and references therein). Apart from the abundance of mafic-ultramafic intrusions of different compositions and sizes in the CMP, reported magmatic Ni-Cu-PGE mineralization is so far limited to PGE resources (with no disclosed figures) in the Luanga and SOC complexes (Ferreira Filho et al., 2007). The CMP has been exposed to moderate exploration for Ni-Cu-PGE deposits in the last decade, such that the paucity of primary Ni-Cu-PGE mineralization in the region cannot be credit solely to underexploration anymore. Therefore, the prospectivity of the CMP for Ni-Cu-PGE deposits should now be considered taking into account previous results obtained for investigated layered complexes and the exploration tools applied. In broad terms past exploration for Ni-Cu-PGE deposits in the CMP has been focused on results provided by regional surveys (e.g. stream sediments, different aerogeophysical surveys) or detailed investigation of exposed large layered intrusions. The latter has been mainly targeted for reef type PGE deposits, as illustrated by the Luanga and Serra da Onça complexes (Ferreira Filho et al., 2007). Future exploration should move toward smaller or covered/poorly exposed intrusions, as well as the application of new exploration tools or models.

10. Conclusions

The main conclusions of this study are as follows:

1. Despite the geographical proximity and similarity in tectonic environment of the SOC and SPC, they have different sequence of magmatic crystallization. The SOC follows a crystallization sequence consisting of Ol+Chr > Opx+Chr > Opx > Opx+Pl > Opx+Pl+Cpx, whereas the crystallization sequence of the SPC consists of Ol+Chr > Ol+Cpx+Chr > Cpx > Cpx+Pl.
2. The abundance of ultramafic rocks (dunite and peridotites) and the composition of cumulus olivine (up to Fo_{92}) indicate very primitive parental magma for both complexes.
3. The early crystallization of Opx relative to Cpx in the SOC indicates that the primary magma was silica saturated, whereas the absence of

Opx as a cumulus mineral in the SPC suggests that the primary magma was silica undersaturated.

4. Whole rock analytical results for the major elements reflect the relative abundance of cumulus minerals of each complex, and are consistent with distinct crystallization sequences for the SOC and SPC.
5. Very similar mantle-normalized lithophile trace element profiles for the SOC and SPC rocks suggest that cumulate rocks from both complexes crystallized from parental magmas with similar contents of incompatible elements.
6. The enrichment in LREE and mantle-normalized negative Nb and Ta anomalies, suggest a contamination of the primitive parental magma by continental crust.
7. Both complexes have highly variable negative values of εNd (T = 2.77 Ga), but gabbroic rocks of the SOC (εNd (T = 2.77 Ga) = -3.33 to -2.12) are more negative and less variable than the values for the SPC (εNd (T=2.77 Ga) = -2.47 to 2.41).
8. The combinations of several evidences suggest that the parental magma of both complexes is derived from a similar source, followed by a variable contamination by continental crust that is more significant in the SOC.
9. The 2713±30 Ma age reported for the SPC in this study is younger than the ages reported for the Grão Pará Group, as well as the Luanga complex, thus indicating a relatively younger intrusive event in the western portion of the CMP.
10. The large mafic-ultramafic intrusions of the CMP emplaced into deep crustal discontinuities. During the ascension process, variables contents of oldest continental crust are assimilated. This is expected if mafic-ultramafic magmatism in Carajás is associated with intra-plate rifting of older continental crust.
11. The abundance of primitive crustal contaminated layered intrusions in the CMP indicates a high potential for magmatic Ni-Cu-PGE deposits in this reagion.

Acknowledgments

This study was supported by CNPq (Conselho Nacional de Desenvolvimento Científico e Teconológico) and VALE S.A. (Projeto 550398/2010-4). Analytical facilities of the Instituto de Geociências of the University of Brasília (UnB) provided additional support for this research. The authors acknowledge Fernando Martins Matos, Lincoln Siepierski, Samuel Nunes and Denisson Oliveira from VALE for their support during fieldwork and interpretation of exploration data, as well as stimulating discussions on the geology of the Carajás Mineral Province. Cesar F. Ferreira Filho is a Research Fellow of CNPq since 1996, and acknowledges the continuous support through research grants and scholarships for the "Metalogenênese de Depósitos Associados ao Magmatismo Máfico-Ultramáfico" Research Group. This study is part of the first author's (Wolney Dutra Rosa) M.Sc dissertation developed at the Instituto de Geociências (UnB).

References

Albarede, F. et al., 2004. Precise and accu-rate isotopic measurements using multi-ple collector ICPMS. Geochimica et Cosmochimica Acta, 68: 2725-2744.

Araújo, O.J.B., Macambira, E.M.B., Vale, A.G., Oliveira, J.R., Silva Neto, C.S., Costa, E.J., Santos, A., Pena Filho, J.I de C., Neves, A.P., João, X.S.J., Costa, J.B.S. 1994. Primeira integração das investigações geológicas do programa Grande Carajás na região SE do Estado do Pará, in Simpósio Geologia Amazônica, 4, Belém, 299-300.

Araújo, O.J.B., Maia, R.G.N. 1991. Programa Grande Carajás, Serra dos Carajás, Folha SB.22-Z-A, Estado do Pará. DNPM-CPRM. Brasília.

Araújo, O.J.B., Maia, R.G.N., João, X.S.J., Costa, J.B.S. 1988. A megaestruturação arqueana da Folha Serra dos Carajás: in Congresso Latino Americano de Geologia, Anais, 324-338, Belém, Brasil.

Avelar, V.G., Lafon, J.M., Correia J.R., FC, Macambira, E.M.B. 1999. O magmatismo arqueano da região de Tucumã-Provínica Mineral de Carajás: Novos dados geocronológicos, Revista Brasileira de Geociências, 453-460.

Barnes, S.J., 1986. The effect of trapped liquid crystallization on cumulus mineral

compositions in layered intrusions. Contributions to Mineralogy and Petrology, v. 93, 524–531.

Barnes, S.-J., Maier, W.D., Curl, E.A., 2010. Composition of the marginal rocks and sills of the Rustenburg Layered Suite, Bushveld Complex, South Africa: implications for the formation of the platinum-group element deposits. Economic Geology, v. 105, 1491-1511.

Barros, C.E.M., Sardinha, A.S., Barbosa, J.P.O., Krimski, R. and Macambira, M.J.B. 2001. Pb–Pb and U–Pb zircon ages of Archean syntectonic granites of the Carajás metallogenic province, northern Brazil: in South American Symposium on Isotopic Geology, 3, Proceedings, 94-97.

Buhn B., Pimentel M.M., Matteini M., Dantas E.L. 2009. High spatial resolution analysis of Pb and U isotopes for geochronology by laser ablation multi-collector inductively coupled plasma mass spectrometry (LAMC- ICP-MS). Anais da Acad. Bras. de Ciências, 1:1-16.

Chai G. and Naldrett A.J., 1992. Characteristics of Ni–Cu–PGE mineralization and genesis of the Jinchuan deposit, northwest China. Economic Geology, 47:1475–1495

Cawthorn, R.G., 1996. Layered intrusions. Developments in Petrology, v. 15, Elsevier, 531 pp.

Dall'Agnol, R., Lafon, J.M. and Macambira, M.J.B., 1994. Proterozoic anorogenic magmatism in the Central Amazonian Province, Amazonian Craton: geochronological, petrological and geochemical aspects. Mineral Petrol 50:113–118

DePaolo, DJ. Neodymium isotopes in the Colorado front rage and implications for crust formation and mantle evolution in the Proterozoic. Nature; 1981. p. 193-197.

Diella V., Ferrario A., Girardi V.A.V. 1995. PGE and PGM in the Luanga mafic ultramafic intrusion in Serra dos Carajás (Pará State, Brazil). Ore Geology Reviews, 9, 443-453.

Docegeo - Rio Doce Geologia e Mineração. 1988. Revisão Litoestratigráfica da Província Mineral de Carajás. In: Congresso Brasileiro de Geologia, 11-59.

Eales, H.V. and Cawthorn, R.G., 1996. The Bushveld Complex. In: Cawthorn, R.G. (Ed.),

Layered Intrusions. Developments in Petrology, vol. 15. Elsevier Science B. V., pp. 181–229.

Ernst and Buchan, 2001; LIP Commission database at www.largeigneousprovinces.com

Ferreira Filho, C.F., Araujo, S.M., 2009. Review of Brazilian chromite deposits associated with layered intrusions: geological and petrological constraints for the origin of stratiform chromitites: Applied Earth Sciences (Trans. Inst. Min. Metall. B), v. 118, 86-100.

Ferreira Filho, C.F., Cançado, F., Correa, C., Macambira, E.M,B., Siepierski, L., Junqueira-Brod, T. C. 2007. Mineralizações estratiformes de EGP-Ni associadas a complexos acamadados em Carajás: os exemplos de Luanga e Serra da Onça, in Contribuições à Geologia da Amazônia, Sociedade Brasileira de Geologia - Núcleo Norte, 01-14.

Ferreira Filho, C.F., Naldrett, A.J. and Gorton, M.P., 1998. REE and pyroxene compositional variation across the Niquelândia layered intrusion, Brazil: petrological and metallogenetic implications. Applied Earth Sciences (Trans. Inst. Min. Metall. B) 107, 1-22.

Ferreira Filho, C.F., Pimentel, M.M., Araujo, S.M., and Laux, J.H., 2010. Layered intrusions and volcanic sequences in Central Brazil: Geological and geochronological constraints for Mesoproterozoic (1.25 Ga) and Neoproterozoic (0.79 Ga) igneous associations. Precambrian Research, v. 183, p. 617−634.

Gibbs, A.K., Wirth, K.R., Hirata, W.K., Olszewski Jr, W.J. 1986. Age and composition of the Grão Pará Group volcanics, Serra dos Carajás: Revista Brasileira de Geociências, 201-211.

Gioia, SMCL, Pimentel, MM. The Sm-Nd isotopic method in the geochronology laboratory of University of Brasilia. Anais da Academia Brasileira de Ciências; 2000. p. 219-245.

Godel G., Sarah-Jane Barnes S-J. and Maier, W.D., 2011. Parental magma composition inferred from trace element in cumulus and intercumulus silicate minerals: An example from the Lower and Lower Critical Zones of the Bushveld Complex, South-Africa. Lithos 125, 537–552

Holdsworth, R.E., Pinheiro, R.V.L. 2000. The anatomy of shallow-crustal transpressional structures: insights from the Archean Carajás fault zone, Amazon, Brazil, Journal

Structural Geology, 1105-1123.

Huhn, S.R.B., Santos, A.B.S., Amaral, A.F., Ledsham, E.J., Gouveia, J.L., Martins, et al. 1988. O terreno granito-greenstone da região de Rio Maria-Sul do Pará: in Congresso Brasileiro de Geologia, 35, Anais, Sociedade Brasileira de Geologia, 1438-1452.

Jackson, SE, Pearson, NJ, Griffin, WL, Belousova, EA. The application of laser ablation inductively coupled plasma mass spectrometry to in situ U-Pb zircon geochronology. Chemical Geology; 2004. p. 47-69.

Lafon J.M., Macambira M.J.B., Pidgeon R.T. 2000. Zircon U-Pb SHRIMP dating of Neoarchean magmatism in the southwestern part of the Carajás Province (eastern Amazonian Craton, Brazil). In: International Geological Congress, 30, Abstract Volume, CD-ROM.

Latypov, R.M., 2003. The origin of marginal compositional reversals in basic-ultrabasic sills and layered intrusions by Soret fractionation. Journal of Petrology 44, 1579-1618.

Ludwig, K.R., 2001. Users Manual for Isoplot/Ex version 2.47. A geochronological toolkit for Microsoft Excel. Berkeley Geochronology Center Special Publication 1a, 55p.

Macambira, E.M.B. 1997. Geologia e aspectos metalogenéticos dos elementos do Grupo Platina no Complexo Máfico-ultramáfico da Serra da Onça, Sul do Pará. Tese de Mestrado. Universidade Federal do Pará – UFPA, Pará, Brasil.

Macambira E.M.B. and Ferreira Filho C.F., 2002. Fracionamento Magmático dos Corpos Máfico-Ultramáficos da Suíte Intrusiva Cateté – Sul do Pará. In: Klein E.L., Vasquez M.L. & Rosa Costa L.T. (eds.) Contribuições à Geologia da Amazônia v. 3. SBG-Núcleo Norte, pp. 105-114.

Macambira, E. M. B., Jorge João, X. da S. and Souza, E. C. 1996. Aspectos Geológicos e Petroquímicos do Granito Plaquê - Sul do Estado do Pará. Symposium Archean terranes of the South American plataform, Brasília, Extended Abstracts, 73-75.

Macambira, M. J. B. and Lafon, J.M. 1995. Geocronologia da Síntese dos Dados e Novos Desafios. Boletim do Museu Paraense Emílio Goeldi, 7, 263-288.

Macambira E.M.B. and Vale G., 1997. Programa Levantamentos Geológicos Básicos do Brasil. São Felix do Xingu. Folha SB.22-Y-B. Estado do Pará. Brasília. DNPM/CPRM. 384pp.

Machado, W., Lindenmayer, Z.G., Krogh, T.E., and Lindenmayer, D. 1991. U-Pb geochronology of Archean magmatism and basement reactivation in the Carajás area, Amazon shield, Brazil. Precambrian Research, 329-354.

Marques, J.C. and Ferreira Filho, C.F., 2003. The chromite deposits of the Ipueira-Medrado Sill, Bahia, Brazil. Economic Geologt, v. 98, 87–108.

McBirney, A.R., 1996. The Skaergaard Intrusion. In: Cawthorn, R.G. (Ed.), Layered Intrusions. Developments in Petrology, vol. 15. Elsevier Science B. V., pp. 147–180.

McCallum, I.S., 1996. The Stillwater Complex. In: Cawthorn, R.G. (Ed.), Layered Intrusions. Developments in Petrology, vol. 15. Elsevier Science B. V., pp. 441–483.

Naldrett, A.J., 2004, Magmatic sulfide deposits: Geology, Geochemistry and Exploration: Heidelberg, Springer Verlag, 728 pp.

Olszewski, W.J., Wirth, K.R., Gibbs, A.K. and Gaudette, H.E., 1989. The age, origin, and tectonics of the Grão Pará Group and associated rocks, Serra dos Carajás, Brazil: Archean continental volcanism and rifting. Precam. Res. 42, 229–254.

Rivalenti, G., Mazzucchelli, M., Gerardi, V.A.V., Cavazzini, G., Finatti, C., Barbieri, M.A., Texeira, W. 1998. Petrogenesis of the Paleoproterozoic basalt–andesite–rhyolite dyke association on the Carajás region, Amazonian craton. Lithos, 235-265.

Santos, J.O.S., Groves, D.I., Hartmann, L.A., Moura, M.A., Mc-Naughton, N.J. 2001. Gold deposits of the Tapajós and Alta Floresta domains, Tapajós-Parima orogenic belt, Amazon craton, Brazil: Mineralium Deposita, 278-299.

Simkin, T. and Smith, J.V., 1970. Minor-element distribution in olivine. Journal of Geology 78: 304-325.

Sun S.S. and McDonough W.F., 1989. Chemical and isotopic systematics of oceanic basalts: implications for mantle composition and processes. In: Saunders AD, Norry MJ (Eds.), Magmatism in the Ocean Basins. Geological Society Special Publication, pp. 313–345.

Teixeira, A.S., Ferreira Filho, C.F., DellaGiustina, M.E.S., Araújo, S.M., Silva, H.H.A.D. submitted. Geology, Petrology and Geochronology of the Lago Grande Layered Complex: Evidence for a PGE-Mineralized Magmatic Suite in The Carajás Province, Brazil. Submitted to Ore Geology Reviews.

Teixeira, A.S., 2013. Geologia, Petrologia e Geocronologia do Complexo Acamadado Lago Grande: Evidência para uma Suite Magmática Mineralizada a PGE na Província Carajás – Brasil. Unpbl. M.Sc. thesis, Universidade de Brasília, Brazil, 108 pp.

Trendall, A.F., Basei, M.A.S., De Laeter, J.R. and Nelson, D.R., 1998. SHRIMP zircon U-Pb constraints on the age of the Carajás Formation, Grão Pará Group, Amazon Craton. J. South Am. Earth Sci. 11, 265–277.

Vale 1Q14 Report; in www.vale.com.

Vale 2013 Annual Report; in www.vale.com.

Villas, R.N. and Santos, M.D., 2001. Gold deposits of the Carajás Mineral Province: deposit types and metallogenesis. Miner. Deposita 36, 300–331.

Wedepohl, K.H., 1995. The composition of the continental crust. Geochimica Cosmochimica Acta, v. 59, 1217-1232.

Wilson, A.H., 1982. The Geology of the Great 'Dyke', Zimbabwe: The Ultramafic Rocks'. Journl of Petrology, v. 23, p. 240–292.

CONCLUSÕES

As principais conclusões alcançadas com este estudo são listadas a seguir:

1. Apesar da proximidade geográfica e similaridade do ambiente tectónico das duas intrusões, os dois complexos apresentam uma sequencia de cristalização magmática completamente distinta. O Complexo da Serra da Onça (CSO) é caracterizado por Ol+Chr > Opx+Chr > Opx > Opx+Pl > Opx+Pl+Cpx, já o Complexo da Serra do Puma (CSP) por Ol+Chr > Ol+Cpx+Chr > Cpx > Cpx+Pl .
2. A abundancia de rochas ultramáficas (dunitos e peridotitos), elevado teor de MgO e o range composicional dos cúmulus de olivina (Fo_{92}) são evidencias de um magma parental muito primitivo para os dois complexos.
3. A cristalização de Opx antes da formação de Cpx no CSO indica que o magma parental era saturado em sílica, enquanto que a ausência de Opx como mineral cúmulus no CSP, sugere um magma primário não saturado em sílica.
4. Os resultados analíticos de rocha total, para elementos maiores, refletem a abundancia dos minerais cúmulus nos dois complexos, e são consistentes com a sequência de cristalização distinta para o CSO e CSP.
5. Uma distribuição muito semelhante de elementos incompatíveis e traços, normatizados ao manto, para as rochas do CSO e CSP sugere que estas rochas cumuláticas cristalizaram a partir de magmas parentais com conteúdos similares de elementos incompatíveis.
6. O enriquecimento em ETRL e as anomalias negativas de Nb e Ta, normatizados ao manto, sugerem uma contaminação por crosta continental do magma parental primitivo.
7. Os dois complexos apresentam valores negativos de εNd (T = 2.77 Ga), mas as rochas gabróicas do CSO (εNd (T = 2.77 Ga) = -3.33 to - 2.12) são mais negativas e menos variáveis do que as do CSP (εNd (T=2.77 Ga) = -2.47 to 2.41).
8. A combinação das diversas evidências sugere que o magma parental dos dois complexos é derivado de uma fonte similar, seguido de variável contaminação por crosta continental, que é mais significativa no CSO.
9. A idade de 2713±30 Ma registrada para o SPC neste estudo é mais jovem que

as idades registradas para o Grupo Grão Pará, bem como para o complexo Luanga, indicando assim um evento intrusivo mais jovem na porção oeste da PMC.

10. A grande quantidade de intrusões máficas-ultramáficas estão encaixadas em descontinuidades crustais profundas. Durante o processo de ascensão, variáveis conteúdos de crosta continental antiga são assimilados. Isso é esperado se o magmatismo máfico-ultramáfico de Carajás for associado com um rifteamento intraplaca de crosta continental antiga.
11. A grande quantidade de intrusões acamadadas formadas por magma parental primitivo com evidências de contaminação crustal na PMC indica o alto potencial para depósitos magmáticos de Ni-Cu-PGE na região.

ANEXOS

(Resultados de química mineral – micro sonda – olivina (Ol), ortopiroxênio (Opx), clinopiroxênio (Cpx) e plagioclásio (Pl) dos Complexos da Serra do Onça e Serra do Puma).

SERRA DO ONÇA COMPLEX	Sample		SC06	SC06	SC06	SC06	SC06	SC06	SC08	SC08	SC08	SC08	SC08	SC28	SC28	SC28	SC28	SC28	SC28	SC10A	SC10A	SC10A	SC10A	SC10A	SC10A	SC10A
	Analysis		OL1.1	OL1.2	OL2.1	OL2.2	OL3.1	OL3.2	OL1.1	OL1.2	OL2.1	OL2.2	OL3.1	OL1.1	OL1.2	OL2.1	OL2.2	OL3.1	OL3.2	OL2.1	OL2.2	OL3.1	OL3.2	OL4.1	OL4.2	OL5.1
	Location	(m)	230.0	230.0	230.0	230.0	230.0	230.0	710.0	710.0	710.0	710.0	710.0	100.5	100.5	100.5	100.5	100.5	100.5	920.0	920.0	920.0	920.0	920.0	920.0	920.0
	SiO2	(wt.%)	41.53	42.00	42.24	41.88	41.83	41.82	41.40	41.30	41.22	41.53	41.07	40.76	40.50	42.44	41.83	41.64	41.87	41.96	42.06	41.24	41.20	41.74	42.14	41.79
	Al2O3	(wt.%)	0.02	0.02	0.01	0.06	<0.01	0.03	<0.01	0.02	0.03	<0.01	<0.01	0.03	0.01	<0.01	<0.01	<0.01	<0.01	0.03	<0.01	0.03	0.01	0.01	0.03	0.02
	MgO	(wt.%)	50.09	50.75	51.23	50.01	50.97	50.89	46.74	46.70	46.79	47.36	46.89	50.43	50.34	51.27	51.77	51.42	51.25	51.16	51.16	50.43	50.66	50.86	50.83	50.70
	FeO	(wt.%)	7.99	8.19	8.05	8.39	8.04	8.20	12.90	13.04	13.11	13.03	12.66	7.42	7.25	7.45	7.53	7.46	7.57	8.07	8.13	8.20	8.00	7.99	8.06	8.03
	NiO	(wt.%)	0.44	0.45	0.45	0.42	0.42	0.46	0.50	0.49	0.53	0.51	0.51	0.49	0.51	0.50	0.51	0.50	0.50	0.32	0.31	0.32	0.32	0.27	0.33	0.28
	Cr2O3	(wt.%)	0.07	<0.01	0.02	0.02	0.02	0.05	0.02	0.04	0.12	0.03	<0.01	0.01	0.04	0.01	<0.01	0.04	0.04	0.02	<0.01	0.01	0.03	0.02	0.06	<0.01
	MnO	(wt.%)	0.11	0.08	0.09	0.09	0.09	0.09	0.20	0.18	0.17	0.14	0.18	0.06	0.06	0.10	0.09	0.09	0.10	0.06	0.08	0.08	0.06	0.09	0.07	0.06
	Total	(wt.%)	100.24	101.49	102.09	100.87	101.38	101.52	101.75	101.77	101.97	102.61	101.31	99.19	98.71	101.77	101.73	101.16	101.33	101.61	101.74	100.30	100.27	100.98	101.52	100.88
	Si	*	1.01	1.01	1.01	1.01	1.00	1.00	1.01	1.01	1.01	1.01	1.01	1.00	1.00	1.01	1.00	1.00	1.00	1.00	1.00	1.00	1.00	1.00	1.01	1.01
	Al	*	0.00	0.00	0.00	0.00	0.00	0.00	0.00	0.00	0.00	0.00	0.00	0.00	0.00	0.00	0.00	0.00	0.00	0.00	0.00	0.00	0.00	0.00	0.00	0.00
	Mg	*	1.81	1.81	1.82	1.80	1.82	1.82	1.70	1.70	1.70	1.71	1.71	1.84	1.85	1.82	1.84	1.84	1.83	1.82	1.82	1.82	1.83	1.82	1.81	1.82
	Fe	*	0.16	0.16	0.16	0.17	0.16	0.16	0.26	0.27	0.27	0.26	0.26	0.15	0.15	0.15	0.15	0.15	0.15	0.16	0.16	0.17	0.16	0.16	0.16	0.16
	Ni	*	0.01	0.01	0.01	0.01	0.01	0.01	0.01	0.01	0.01	0.01	0.01	0.01	0.01	0.01	0.01	0.01	0.01	0.01	0.01	0.01	0.01	0.01	0.01	0.01
	Cr	*	0.00	0.00	0.00	0.00	0.00	0.00	0.00	0.00	0.00	0.00	0.00	0.00	0.00	0.00	0.00	0.00	0.00	0.00	0.00	0.00	0.00	0.00	0.00	0.00
	Mn	*	0.00	0.00	0.00	0.00	0.00	0.00	0.00	0.00	0.00	0.00	0.00	0.00	0.00	0.00	0.00	0.00	0.00	0.00	0.00	0.00	0.00	0.00	0.00	0.00
	Total	*	2.99	2.99	2.99	2.99	3.00	3.00	2.99	2.99	2.99	2.99	2.99	3.00	3.00	2.99	3.00	3.00	3.00	3.00	3.00	3.00	3.00	3.00	2.99	2.99
	Fo	%	91.69	91.62	91.81	91.32	91.78	91.63	86.41	86.29	86.26	86.50	86.68	92.32	92.47	92.37	92.37	92.39	92.26	91.81	91.74	91.57	91.81	91.82	91.77	91.78
	Fa	%	8.20	8.30	8.10	8.59	8.13	8.28	13.38	13.51	13.56	13.35	13.13	7.62	7.47	7.53	7.53	7.53	7.65	8.12	8.18	8.36	8.13	8.09	8.16	8.15
SERRA DO PUMA COMPLEX	Sample		SC33b	SC33b	SC33b	SC33b	SC33b	SC33b	SC34b	SC34b	SC34b	SC34b	SC34b	SC36	SC36	SC36	SC36	SC36	SC36	SC37	SC37	SC37	SC37	SC37	SC37	SC38
	Analysis		OL1.1	OL1.2	OL1.3	OL2.1	OL2.2	OL3.1	OL1.1	OL1.2	OL2.1	OL2.2	OL3.1	OL1.1	OL1.2	OL2.1	OL2.2	OL3.1	OL3.2	OL1.1	OL1.2	OL2.1	OL2.2	OL3.1	OL3.2	OL1.1
	Location	(m)	2391.0	2391.0	2391.0	2391.0	2391.0	2391.0	2254.0	2254.0	2254.0	2254.0	2254.0	2130.0	2130.0	2130.0	2130.0	2130.0	2130.0	2073.0	2073.0	2073.0	2073.0	2073.0	2073.0	2029.0
	SiO2	(wt.%)	39.00	38.86	39.35	40.19	40.83	40.74	39.62	39.34	38.96	39.01	39.31	39.95	39.83	39.85	40.28	39.95	40.22	38.97	39.08	39.69	39.75	39.52	39.38	39.99
	Al2O3	(wt.%)	0.01	0.01	<0.01	0.04	<0.01	0.01	<0.01	0.01	<0.01	<0.01	<0.01	0.01	0.04	0.04	0.02	<0.01	0.01	<0.01	0.01	<0.01	0.01	0.01	0.01	0.01
	MgO	(wt.%)	44.24	44.38	44.47	44.42	44.58	44.86	39.79	39.59	39.71	39.85	39.63	41.70	40.70	42.40	42.37	41.89	41.92	40.86	40.28	41.06	40.87	40.84	40.47	41.25
	FeO	(wt.%)	15.57	15.78	15.37	16.49	15.78	15.30	21.81	21.16	21.71	21.37	21.52	19.32	19.88	18.65	18.47	18.94	19.26	19.98	20.00	19.97	19.60	19.62	19.85	19.36
	NiO	(wt.%)	0.38	0.35	0.33	0.37	0.33	0.33	0.27	0.23	0.26	0.22	0.25	0.23	0.22	0.25	0.24	0.25	0.23	0.23	0.24	0.24	0.20	0.24	0.20	0.26
	Cr2O3	(wt.%)	<0.01	0.02	0.03	0.02	0.03	<0.01	0.02	<0.01	0.02	0.02	0.01	0.01	0.02	<0.01	<0.01	<0.01	0.02	<0.01	<0.01	<0.01	0.01	<0.01	0.01	<0.01
	MnO	(wt.%)	0.20	0.21	0.18	0.19	0.19	0.20	0.28	0.28	0.28	0.28	0.30	0.27	0.25	0.27	0.28	0.27	0.22	0.25	0.31	0.29	0.26	0.26	0.28	0.26
	Total	(wt.%)	99.38	99.60	99.73	101.71	101.73	101.45	101.77	100.61	100.93	100.75	101.01	101.50	100.95	101.46	101.66	101.31	101.87	100.30	99.93	101.25	100.69	100.48	100.19	101.14
	Si	*	0.99	0.99	0.99	1.00	1.01	1.01	1.01	1.01	1.00	1.00	1.01	1.01	1.01	1.00	1.01	1.01	1.01	1.00	1.01	1.01	1.01	1.01	1.01	1.01
	Al	*	0.00	0.00	0.00	0.00	0.00	0.00	0.00	0.00	0.00	0.00	0.00	0.00	0.00	0.00	0.00	0.00	0.00	0.00	0.00	0.00	0.00	0.00	0.00	0.00
	Mg	*	1.68	1.68	1.68	1.65	1.64	1.66	1.51	1.52	1.52	1.53	1.51	1.57	1.54	1.59	1.58	1.58	1.57	1.56	1.55	1.55	1.55	1.55	1.55	1.56
	Fe	*	0.33	0.34	0.33	0.34	0.33	0.32	0.46	0.45	0.47	0.46	0.46	0.41	0.42	0.39	0.39	0.40	0.40	0.43	0.43	0.42	0.42	0.42	0.43	0.41
	Ni	*	0.01	0.01	0.01	0.01	0.01	0.01	0.01	0.01	0.01	0.00	0.01	0.01	0.01	0.01	0.01	0.01	0.01	0.01	0.01	0.01	0.00	0.01	0.00	0.01
	Cr	*	0.00	0.00	0.00	0.00	0.00	0.00	0.00	0.00	0.00	0.00	0.00	0.00	0.00	0.00	0.00	0.00	0.00	0.00	0.00	0.00	0.00	0.00	0.00	0.00
	Mn	*	0.00	0.00	0.00	0.00	0.00	0.00	0.01	0.01	0.01	0.01	0.01	0.01	0.01	0.01	0.01	0.01	0.01	0.01	0.01	0.01	0.01	0.01	0.01	0.01
	Total	*	3.01	3.01	3.01	3.00	2.99	2.99	2.99	3.00	3.00	2.99	2.99	2.99	2.99	3.00	2.99	2.99	2.99	3.00	2.99	2.99	2.99	2.99	2.99	2.99
	Fo	%	83.34	83.18	83.59	82.60	83.27	83.76	76.25	76.69	76.30	76.63	76.40	79.14	78.28	79.97	80.11	79.53	79.32	78.26	77.94	78.32	78.57	78.55	78.19	78.93
	Fa	%	16.45	16.60	16.21	17.20	16.53	16.03	23.45	23.00	23.40	23.06	23.28	20.57	21.45	19.74	19.60	20.18	20.45	21.47	21.71	21.37	21.14	21.17	21.51	20.79
SERRA DO PUMA COMPLEX	Sample		SC38	SC38	SC38	SC38	SC39	SC39	SC39	SC39	SC39	SC40A	SC40A	SC40A	SC40A	SC40A	SC40A	SC41	SC41	SC41	SC41	SC41	SC41	SC48	SC48	SC48
	Analysis		OL1.2	OL2.1	OL2.2	OL3.1	OL1.1	OL1.2	OL2.1	OL3.1	OL4.1	OL1.1	OL1.2	OL2.1	OL2.2	OL3.1	OL3.2	OL1.1	OL1.2	OL2.1	OL2.2	OL3.1	OL3.2	OL1.1	OL1.2	OL2.1
	Location	(m)	2029.0	2029.0	2029.0	2029.0	1998.0	1998.0	1998.0	1998.0	1998.0	1930.0	1930.0	1930.0	1930.0	1930.0	1930.0	1850.0	1850.0	1850.0	1850.0	1850.0	1850.0	1145.0	1145.0	1145.0
	SiO2	(wt.%)	39.93	40.04	39.78	40.14	39.95	39.77	39.98	39.98	39.97	39.64	40.01	39.80	39.73	39.73	39.35	39.68	39.56	39.86	39.74	39.72	39.67	40.44	40.68	40.95
	Al2O3	(wt.%)	<0.01	0.01	0.01	0.02	0.01	0.01	0.01	0.02	<0.01	<0.01	<0.01	<0.01	<0.01	<0.01	0.04	0.02	0.02	0.01	0.01	0.01	0.01	0.03	0.02	0.01
	MgO	(wt.%)	41.52	42.49	41.90	41.80	41.17	41.35	41.35	41.74	41.36	41.26	41.92	41.96	41.68	41.69	41.33	41.89	41.76	41.81	41.54	41.88	42.05	45.21	45.26	45.49
	FeO	(wt.%)	19.31	17.96	18.71	19.25	19.76	19.51	19.40	19.86	19.45	18.81	18.58	18.82	18.82	18.77	18.84	18.78	18.97	18.51	18.87	18.61	18.67	14.38	14.03	14.40
	NiO	(wt.%)	0.19	0.25	0.23	0.23	0.21	0.23	0.26	0.22	0.21	0.23	0.24	0.24	0.26	0.23	0.23	0.24	0.22	0.24	0.23	0.24	0.22	0.38	0.36	0.39
	Cr2O3	(wt.%)	0.03	0.01	<0.01	0.02	<0.01	0.01	0.03	<0.01	<0.01	0.04	<0.01	<0.01	0.01	<0.01	0.02	0.03	0.01	<0.01	<0.01	0.02	0.03	0.02	<0.01	0.02
	MnO	(wt.%)	0.27	0.28	0.25	0.28	0.28	0.24	0.26	0.26	0.26	0.25	0.23	0.20	0.22	0.25	0.22	0.26	0.24	0.25	0.24	0.25	0.25	0.16	0.14	0.21
	Total	(wt.%)	101.25	101.05	100.88	101.74	101.38	101.10	101.28	102.06	101.25	100.22	100.98	101.02	100.72	100.67	100.03	100.90	100.78	100.68	100.65	100.73	100.89	100.62	100.49	101.45
	Si	*	1.01	1.01	1.01	1.01	1.01	1.01	1.01	1.01	1.01	1.01	1.01	1.01	1.01	1.01	1.01	1.01	1.00	1.01	1.01	1.01	1.00	1.01	1.01	1.01
	Al	*	0.00	0.00	0.00	0.00	0.00	0.00	0.00	0.00	0.00	0.00	0.00	0.00	0.00	0.00	0.00	0.00	0.00	0.00	0.00	0.00	0.00	0.00	0.00	0.00
	Mg	*	1.56	1.59	1.58	1.57	1.55	1.56	1.56	1.56	1.56	1.57	1.58	1.58	1.58	1.58	1.57	1.58	1.58	1.58	1.57	1.58	1.59	1.68	1.68	1.67
	Fe	*	0.41	0.38	0.40	0.41	0.42	0.41	0.41	0.42	0.41	0.40	0.39	0.40	0.40	0.40	0.40	0.40	0.40	0.39	0.40	0.39	0.40	0.30	0.29	0.30
	Ni	*	0.00	0.01	0.01	0.01	0.00	0.01	0.01	0.00	0.00	0.01	0.01	0.01	0.01	0.01	0.01	0.01	0.01	0.01	0.01	0.01	0.00	0.01	0.01	0.01
	Cr	*	0.00	0.00	0.00	0.00	0.00	0.00	0.00	0.00	0.00	0.00	0.00	0.00	0.00	0.00	0.00	0.00	0.00	0.00	0.00	0.00	0.00	0.00	0.00	0.00
	Mn	*	0.01	0.01	0.01	0.01	0.01	0.01	0.01	0.01	0.01	0.01	0.00	0.00	0.01	0.01	0.01	0.01	0.01	0.01	0.01	0.01	0.00	0.00	0.00	0.00
	Total	*	2.99	2.99	2.99	2.99	2.99	2.99	2.99	2.99	2.99	2.99	2.99	2.99	2.99	2.99	3.00	3.00	2.99	2.99	2.99	2.99	2.99	2.99	2.99	2.99
	Fo	%	79.08	80.59	79.75	79.23	78.55	78.87	78.94	78.71	78.90	79.41	79.89	79.72	79.59	79.62	79.44	79.68	79.49	79.89	79.48	79.83	79.84	84.71	85.06	84.74
	Fa	%	20.63	19.11	19.98	20.47	21.15	20.88	20.78	21.01	20.82	20.31	19.87	20.06	20.17	20.12	20.32	20.05	20.25	19.84	20.26	19.90	19.89	15.12	14.79	15.05
SERRA DO PUMA COMPLEX	Sample		SC48	SC48	SC48	SC50	SC50	SC50	SC50	SC50	SC50	SC45	SC45	SC45	SC45	SC45	SC45	SC46	SC46	SC46	SC46	SC46	SC46	SC46	SC46	SC46
	Analysis		OL2.2	OL3.1	OL3.2	OL1.1	OL1.2	OL2.1	OL2.2	OL3.1	OL3.2	OLIV1.1	OLIV1.2	OLIV1.3	OLIV2.1	OLIV2.2	OL1.1	OL1.2	OL1.3	OL2.1	OL2.2	OL3.1	OL3.2	OL3.3		
	Location	(m)	1145	1145	1145	790	790	790	790	790	790	1473	1473	1473	1473	1473	1213	1213	1213	1213	1213	1213	1213	1213		
	SiO2	(wt.%)	40.97	40.70	40.86	41.25	41.42	41.40	41.33	41.31	41.68	39.82	39.79	39.87	39.67	39.57	39.85	39.19	39.65	36.18	38.25	40.12	40.18	40.14		
	Al2O3	(wt.%)	<0.01	0.02	0.01	<0.01	0.05	0.01	0.01	0.01	0.02	0.01	0.01	<0.01	<0.01	<0.01	0.01	<0.01	0.01	<0.01	<0.01	<0.01	0.01	<0.01		
	MgO	(wt.%)	45.29	44.85	45.37	47.82	47.40	48.20	47.72	48.00	47.77	41.31	41.39	41.48	41.26	41.52	41.05	40.36	40.96	40.27	41.90	42.15	42.19	42.49		
	FeO	(wt.%)	14.28	14.57	14.68	11.03	11.65	10.90	10.91	11.01	11.13	19.13	19.16	18.86	18.96	18.76	19.34	20.31	20.10	13.38	14.92	18.10	17.89	17.58		
	NiO	(wt.%)	0.37	0.36	0.38	0.41	0.39	0.40	0.36	0.40	0.39	0.30	0.33	0.32	0.35	0.32	0.34	0.33	0.32	0.20	0.25	0.30	0.36	0.29		
	Cr2O3	(wt.%)	0.01	0.01	0.01	<0.01	0.09	0.01	<0.01	<0.01	0.01	<0.01	<0.01	<0.01	0.01	<0.01	<0.01	0.01	<0.01	0.01	0.02	<0.01	<0.01	0.02		
	MnO	(wt.%)	0.16	0.16	0.18	0.14	0.16	0.19	0.17	0.18	0.18	0.25	0.22	0.20	0.23	0.23	0.20	0.27	0.21	0.13	0.16	0.21	0.22	0.22		
	Total	(wt.%)	101.07	100.66	101.48	100.64	101.16	101.12	100.49	100.90	101.18	100.82	100.90	100.72	100.47	100.39	100.78	100.47	101.24	90.17	95.49	100.88	100.84	100.73		
	Si	*	1.01	1.01	1.01	1.01	1.01	1.01	1.01	1.01	1.01	1.01	1.01	1.01	1.01	1.01	1.01	1.01	1.01	1.01	1.01	1.01	1.01	1.01		
	Al	*	0.00	0.00	0.00	0.00	0.00	0.00	0.00	0.00	0.00	0.00	0.00	0.00	0.00	0.00	0.00	0.00	0.00	0.00	0.00	0.00	0.00	0.00		
	Mg	*	1.67	1.66	1.67	1.74	1.73	1.75	1.74	1.75	1.73	1.56	1.56	1.57	1.57	1.58	1.55	1.54	1.55	1.67	1.65	1.58	1.59	1.60		
	Fe	*	0.30	0.30	0.30	0.23	0.24	0.22	0.22	0.23	0.23	0.41	0.41	0.40	0.40	0.40	0.41	0.44	0.43	0.31	0.33	0.38	0.38	0.37		
	Ni	*	0.01	0.01	0.01	0.01	0.01	0.01	0.01	0.01	0.01	0.01	0.01	0.01	0.01	0.01	0.01	0.01	0.01	0.00	0.01	0.01	0.01	0.01		
	Cr	*	0.00	0.00	0.00	0.00	0.00	0.00	0.00	0.00	0.00	0.00	0.00	0.00	0.00	0.00	0.00	0.00	0.00	0.00	0.00	0.00	0.00	0.00		
	Mn	*	0.00	0.00	0.00	0.00	0.00	0.00	0.00	0.00	0.00	0.01	0.01	0.00	0.01	0.01	0.00	0.01	0.00	0.00	0.00	0.00	0.01	0.01		
	Total	*	2.99	2.99	2.99	2.99	2.99	2.99	2.99	2.99	2.99	2.99	2.99	2.99	2.99	3.00	2.99	2.99	2.99	2.99	2.99	2.99	2.99	2.99		
	Fo	%	84.83	84.44	84.48	88.42	87.74	88.57	88.48	88.44	88.27	79.16	79.19	79.51	79.31	79.58	78.92	77.75	78.24	84.16	83.20	80.40	80.59	80.96		
	Fa	%	15.01	15.39	15.33	11.44	12.10	11.24	11.35	11.38	11.54	20.57	20.57	20.28	20.44	20.17	20.86	21.95	21.54	15.69	16.62	19.38	19.17	18.79		

SERRA DO ONÇA COMPLEX

Sample		SC22	SC22	SC22	SC22	SC22	SC22	SC22	SC22	SC22	SC23	SC23	SC23	SC23	SC23	SC24A	SC24A	SC24A	SC24A	SC24A	SC11	SC11	SC11	SC11	SC11
Analysis		OPX1.1	OPX1.2	OPX1.3	OPX2.1	OPX2.2	OPX%.1	CPX3.1	OPX4.1	OPX6.1	OPX1.1	OPX1.2	OPX1.3	OPX2.1	OPX2.2	OPX1.1	OPX2.1	OPX2.2	OPX3.1	OPX4.1	OPX1.1	OPX1.2	OPX2.1	OPX2.2	OPX3.1
Location	(m)	1898.0	1898.0	1898.0	1898.0	1898.0	1898.0	1898.0	1898.0	1898.0	1987.0	1987.0	1987.0	1987.0	1987.0	2081.0	2081.0	2081.0	2081.0	2081.0	1060.0	1060.0	1060.0	1060.0	1060.0
Na2O	wt. %	0.04	0.05	0.04	0.01	<0.01	0.03	<0.01	<0.01	0.01	0.03	<0.01	<0.01	<0.01	<0.01	<0.01	0.01	<0.01	0.01	<0.01	<0.01	0.01	0.02	0.01	0.01
K2O	wt. %	0.01	0.01	0.02	<0.01	0.01	0.01	<0.01	0.03	<0.01	<0.01	0.01	<0.01	0.03	<0.01	0.01	0.02	<0.01	0.01	0.02	<0.01	<0.01	<0.01	<0.01	<0.01
Al2O3	wt. %	1.32	1.36	1.37	1.11	1.12	1.32	0.98	1.10	1.12	0.86	0.89	1.09	0.95	0.91	1.14	1.23	1.22	1.22	1.14	1.12	1.06	1.05	1.08	1.07
MgO	wt. %	24.95	24.24	24.63	24.76	24.95	24.37	25.02	25.10	24.50	20.97	21.30	21.41	21.66	21.76	22.61	22.85	22.57	22.31	22.47	27.17	27.31	27.06	27.59	27.19
SiO2	wt. %	53.22	53.36	53.35	53.17	53.19	52.73	52.98	52.94	52.92	51.48	51.53	52.04	52.24	52.49	52.22	52.36	52.36	52.60	51.85	54.22	54.09	54.20	54.14	54.56
CaO	wt. %	3.07	3.21	2.03	1.24	0.97	2.66	1.12	1.36	1.73	5.46	1.01	1.04	1.20	1.62	1.68	1.94	1.96	1.91	1.05	2.34	1.97	2.51	2.04	2.53
MnO	wt. %	0.32	0.29	0.32	0.27	0.34	0.32	0.33	0.29	0.27	0.44	0.41	0.45	0.43	0.45	0.38	0.33	0.41	0.34	0.40	0.23	0.28	0.25	0.24	0.25
TiO2	wt. %	0.16	0.15	0.16	0.22	0.21	0.19	0.21	0.22	0.24	0.19	0.20	0.20	0.19	0.16	0.20	0.23	0.24	0.24	0.22	0.10	0.09	0.10	0.10	0.08
FeO	wt. %	14.802	16.011	16.825	17.321	17.476	15.847	17.085	16.594	17.263	16.747	22.073	22.443	21.951	21.557	19.703	19.116	19.623	19.885	20.308	13.032	13.113	12.992	12.681	13.055
NiO	wt. %	0.05	0.06	0.06	0.05	0.05	0.05	0.07	0.05	0.05	0.02	0.03	0.01	0.02	0.04	0.06	0.07	0.04	0.06	0.06	0.13	0.12	0.12	0.10	0.12
Cr2O3	wt. %	0.24	0.27	0.25	0.19	0.20	0.22	0.23	0.23	0.21	<0.01	<0.01	<0.01	<0.01	0.02	0.17	0.16	0.17	0.17	0.16	0.05	0.03	0.03	0.06	0.06
Fe2O3	wt. %	1.60	0.28	0.10	<0.01	<0.01	0.88	0.51	0.74	0.37	3.08	0.20	0.11	0.82	0.82	0.15	0.52	0.37	<0.01	0.20	<0.01	0.25	0.05	0.52	<0.01
Total	wt. %	99.78	99.30	99.14	98.34	98.51	98.63	98.54	98.65	98.67	99.27	97.65	98.80	99.50	99.82	98.32	98.82	98.97	98.74	97.88	98.39	98.32	98.38	98.56	98.92
Na	*	<0.01	<0.01	<0.01	<0.01	<0.01	<0.01	<0.01	<0.01	<0.01	<0.01	<0.01	<0.01	<0.01	<0.01	<0.01	<0.01	<0.01	<0.01	<0.01	<0.01	<0.01	<0.01	<0.01	<0.01
K	*	<0.01	<0.01	<0.01	<0.01	<0.01	<0.01	<0.01	<0.01	<0.01	<0.01	<0.01	<0.01	<0.01	<0.01	<0.01	<0.01	<0.01	<0.01	<0.01	<0.01	<0.01	<0.01	<0.01	<0.01
Al	*	0.06	0.06	0.06	0.05	0.05	0.06	0.04	0.05	0.05	0.04	0.04	0.05	0.04	0.04	0.05	0.05	0.05	0.05	0.05	0.05	0.05	0.05	0.05	0.05
Mg	*	1.36	1.33	1.35	1.37	1.38	1.35	1.38	1.38	1.35	1.17	1.22	1.21	1.21	1.21	1.27	1.27	1.26	1.25	1.27	1.47	1.48	1.47	1.49	1.47
Si	*	1.94	1.96	1.96	1.97	1.97	1.95	1.96	1.96	1.96	1.93	1.97	1.97	1.96	1.96	1.96	1.96	1.96	1.97	1.96	1.97	1.97	1.97	1.97	1.98
Ca	*	0.12	0.13	0.08	0.05	0.04	0.11	0.05	0.05	0.07	0.22	0.04	0.04	0.05	0.07	0.07	0.08	0.08	0.08	0.04	0.09	0.08	0.10	0.08	0.10
Mn	*	0.01	0.01	0.01	0.01	0.01	0.01	0.01	0.01	0.01	0.01	0.01	0.01	0.01	0.01	0.01	0.01	0.01	0.01	0.01	0.01	0.01	0.01	0.01	0.01
Ti	*	<0.01	<0.01	<0.01	0.01	0.01	0.01	0.01	0.01	0.01	0.01	0.01	0.01	0.01	<0.01	0.01	0.01	0.01	0.01	0.01	<0.01	<0.01	<0.01	<0.01	<0.01
Fe	*	0.45	0.49	0.52	0.54	0.54	0.49	0.53	0.51	0.54	0.53	0.71	0.71	0.69	0.67	0.62	0.60	0.61	0.62	0.64	0.40	0.40	0.40	0.39	0.40
Ni	*	<0.01	<0.01	<0.01	<0.01	<0.01	<0.01	<0.01	<0.01	<0.01	<0.01	<0.01	<0.01	<0.01	<0.01	<0.01	<0.01	<0.01	<0.01	<0.01	<0.01	<0.01	<0.01	<0.01	<0.01
Cr	*	0.01	0.01	0.01	0.01	0.01	0.01	0.01	0.01	0.01	<0.01	<0.01	<0.01	<0.01	<0.01	0.01	0.01	0.01	0.01	0.01	<0.01	<0.01	<0.01	<0.01	<0.01
Fe3+	*	0.04	0.01	<0.01	<0.01	<0.01	0.03	0.01	0.02	0.01	0.09	0.01	<0.01	0.02	0.02	<0.01	0.02	0.01	<0.01	0.01	<0.01	0.01	<0.01	0.01	<0.01
Total	*	4.00	4.00	4.00	4.00	4.00	4.00	4.00	4.00	4.00	4.00	4.00	4.00	4.00	4.00	4.00	4.00	4.00	4.00	4.00	4.00	4.00	4.00	4.00	4.00
WO	%	6.19	6.47	4.08	2.52	1.96	5.41	2.27	2.76	3.49	11.36	2.10	2.14	2.46	3.30	3.45	3.97	4.01	3.91	2.16	4.64	3.91	4.97	4.04	4.99
EN	%	70.00	67.91	68.98	69.69	69.99	68.93	70.28	70.60	68.86	60.72	61.49	61.17	61.74	61.69	64.44	64.99	64.08	63.69	64.49	74.86	75.35	74.55	75.98	74.54
FS	%	23.81	25.62	26.94	27.79	28.05	25.66	27.45	26.65	27.65	27.93	36.42	36.69	35.80	35.01	32.12	31.05	31.91	32.40	33.35	20.50	20.74	20.48	19.98	20.47

SERRA DO ONÇA COMPLEX

Sample		SC11	SC12	SC12	SC12	SC12	SC12	SC12	SC13	SC13	SC13	SC13	SC13	SC14	SC14	SC14	SC14	SC14	SC14	SC15	SC15	SC15	SC15	SC15	SC15
Analysis		OPX3.2	OPX1.1	OPX1.2	OPX1.3	OPX2.1	OPX2.2	OPX2.3	OPX1.1	OPX1.2	OPX1.3	OPX2.1	OPX2.2	OPX1.1	OPX1.2	OPX1.3	OPX2.1	OPX2.2	OPX2.3	OPX1.1	OPX1.2	OPX1.3	OPX2.1	OPX2.2	OPX3.1
Location	(m)	1060.0	1120.0	1120.0	1120.0	1120.0	1120.0	1120.0	1135.0	1135.0	1135.0	1135.0	1135.0	1225.0	1225.0	1225.0	1225.0	1225.0	1225.0	1370.0	1370.0	1370.0	1370.0	1370.0	1370.0
Na2O	wt. %	<0.01	<0.01	0.02	0.01	<0.01	<0.01	<0.01	<0.01	<0.01	<0.01	<0.01	<0.01	<0.01	<0.01	<0.01	<0.01	<0.01	<0.01	<0.01	<0.01	<0.01	<0.01	<0.01	0.01
K2O	wt. %	<0.01	<0.01	<0.01	<0.01	0.02	<0.01	<0.01	<0.01	<0.01	0.01	<0.01	<0.01	0.01	0.01	0.01	<0.01	<0.01	<0.01	<0.01	<0.01	<0.01	<0.01	0.01	0.01
Al2O3	wt. %	1.00	0.91	0.94	0.91	0.85	0.96	0.94	1.13	1.04	1.02	0.97	0.92	0.92	0.95	1.01	0.90	0.88	0.89	0.93	0.91	0.89	0.87	0.80	0.97
MgO	wt. %	27.19	25.70	24.69	25.00	25.40	25.68	25.78	25.69	25.40	25.50	25.64	25.71	24.77	25.01	24.74	23.21	23.41	23.45	23.47	23.31	23.57	23.48	23.43	23.45
SiO2	wt. %	53.87	53.63	53.61	53.46	53.42	53.94	54.06	54.05	54.09	53.96	54.30	54.42	53.08	53.27	53.06	53.55	53.23	53.62	53.04	52.63	52.72	52.97	52.97	53.16
CaO	wt. %	2.05	0.79	3.01	3.01	1.34	1.99	1.49	0.97	2.09	1.42	1.33	1.29	1.12	1.27	1.10	0.98	2.22	1.06	1.31	1.22	1.07	1.43	1.41	2.28
MnO	wt. %	0.23	0.25	0.31	0.26	0.31	0.32	0.31	0.29	0.35	0.31	0.31	0.32	0.31	0.29	0.28	0.33	0.35	0.35	0.35	0.37	0.43	0.36	0.39	0.40
TiO2	wt. %	0.12	0.13	0.12	0.11	0.14	0.11	0.12	0.16	0.17	0.13	0.14	0.12	0.21	0.22	0.20	0.13	0.13	0.13	0.19	0.21	0.21	0.20	0.21	0.20
FeO	wt. %	13.067	16.722	15.754	15.196	16.557	15.871	16.516	17.418	16.474	16.994	17.299	17.323	17.703	17.318	17.794	19.447	18.748	19.425	19.7	19.585	19.393	19.41	19.518	18.555
NiO	wt. %	0.11	0.08	0.06	0.08	0.07	0.08	0.06	0.03	0.06	0.04	0.04	0.05	0.05	0.05	0.03	0.07	0.03	0.03	0.03	0.05	0.03	0.05	0.03	0.04
Cr2O3	wt. %	0.02	<0.01	0.01	0.04	0.03	0.03	0.04	0.02	0.04	0.04	0.04	0.06	0.03	0.05	0.02	0.03	0.03	0.05	0.03	0.02	0.01	0.02	0.01	0.06
Fe2O3	wt. %	0.24	<0.01	<0.01	0.67	<0.01	1.05	0.53	0.51	0.81	0.76	0.45	0.47	1.07	1.12	0.69	<0.01	<0.01	<0.01	1.08	0.85	1.46	1.08	1.16	1.15
Total	wt. %	97.91	98.21	98.52	98.76	98.12	100.03	99.83	100.27	100.52	100.18	100.51	100.68	99.27	99.55	98.93	98.64	99.02	99.00	100.14	99.14	99.78	99.86	99.94	100.26
Na	*	<0.01	<0.01	<0.01	<0.01	<0.01	<0.01	<0.01	<0.01	<0.01	<0.01	<0.01	<0.01	<0.01	<0.01	<0.01	<0.01	<0.01	<0.01	<0.01	<0.01	<0.01	<0.01	<0.01	<0.01
K	*	<0.01	<0.01	<0.01	<0.01	<0.01	<0.01	<0.01	<0.01	<0.01	<0.01	<0.01	<0.01	<0.01	<0.01	<0.01	<0.01	<0.01	<0.01	<0.01	<0.01	<0.01	<0.01	<0.01	<0.01
Al	*	0.04	0.04	0.04	0.04	0.04	0.04	0.04	0.05	0.04	0.04	0.04	0.04	0.04	0.04	0.04	0.04	0.04	0.04	0.04	0.04	0.04	0.04	0.04	0.04
Mg	*	1.48	1.42	1.36	1.37	1.40	1.39	1.40	1.39	1.37	1.38	1.39	1.39	1.36	1.37	1.36	1.29	1.30	1.30	1.29	1.30	1.30	1.30	1.29	1.29
Si	*	1.97	1.98	1.98	1.97	1.98	1.96	1.97	1.96	1.96	1.96	1.97	1.97	1.96	1.96	1.96	1.99	1.98	1.99	1.96	1.96	1.95	1.96	1.96	1.96
Ca	*	0.08	0.03	0.12	0.12	0.05	0.08	0.06	0.04	0.08	0.06	0.05	0.05	0.04	0.05	0.04	0.04	0.09	0.04	0.05	0.05	0.04	0.06	0.06	0.09
Mn	*	0.01	0.01	0.01	0.01	0.01	0.01	0.01	0.01	0.01	0.01	0.01	0.01	0.01	0.01	0.01	0.01	0.01	0.01	0.01	0.01	0.01	0.01	0.01	0.01
Ti	*	<0.01	<0.01	<0.01	<0.01	<0.01	<0.01	<0.01	<0.01	0.01	<0.01	<0.01	<0.01	0.01	0.01	0.01	<0.01	<0.01	<0.01	0.01	0.01	0.01	0.01	0.01	0.01
Fe	*	0.40	0.52	0.49	0.47	0.51	0.48	0.50	0.53	0.50	0.52	0.53	0.52	0.55	0.53	0.55	0.61	0.58	0.60	0.61	0.61	0.60	0.60	0.60	0.57
Ni	*	<0.01	<0.01	<0.01	<0.01	<0.01	<0.01	<0.01	<0.01	<0.01	<0.01	<0.01	<0.01	<0.01	<0.01	<0.01	<0.01	<0.01	<0.01	<0.01	<0.01	<0.01	<0.01	<0.01	<0.01
Cr	*	<0.01	<0.01	<0.01	<0.01	<0.01	<0.01	<0.01	<0.01	<0.01	<0.01	<0.01	<0.01	<0.01	<0.01	<0.01	<0.01	<0.01	<0.01	<0.01	<0.01	<0.01	<0.01	<0.01	<0.01
Fe3+	*	0.01	<0.01	<0.01	0.02	<0.01	0.03	0.01	0.01	0.02	0.02	0.01	0.01	0.03	0.03	0.02	<0.01	<0.01	<0.01	0.03	0.02	0.04	0.03	0.03	0.03
Total	*	4.00	4.00	4.00	4.00	4.00	4.00	4.00	4.00	4.00	4.00	4.00	4.00	4.00	4.00	4.00	3.98	4.00	3.99	4.00	4.00	4.00	4.00	4.00	4.00
WO	%	4.08	1.59	6.02	6.05	2.68	3.95	2.95	1.92	4.14	2.81	2.62	2.54	2.25	2.56	2.22	2.02	4.48	2.15	2.65	2.48	2.16	2.89	2.85	4.59
EN	%	75.26	71.80	68.84	69.75	70.91	70.94	71.02	70.73	69.89	70.38	70.29	70.37	69.43	69.85	69.36	66.28	65.52	66.41	65.81	65.87	66.47	65.95	65.78	65.63
FS	%	20.66	26.61	25.14	24.20	26.42	25.11	26.03	27.35	25.97	26.80	27.09	27.09	28.32	27.60	28.43	31.70	30.01	31.44	31.55	31.65	31.37	31.17	31.37	29.77

SERRA DO ONÇA COMPLEX

Sample		SC16B	SC16B	SC16B	SC16B	SC16B	SC17	SC17	SC17	SC17	SC17	SC17	SC17	SC17	SC18	SC18	SC18	SC18	SC18	SC18	SC19	SC19	SC19	SC19	SC19
Analysis		OPX1.1	OPX1.2	OPX2.1	OPX2.2	OPX3.1	OPX1.1	OPX1.2	OPX2.2	OPX2.3	3-REPET	CPX3.2	OPX3.1	OPX3.2	OPX1.1	OPX1.2	CPX1.3	OPX2.1	OPX2.2	0PX???	OPX1.1	OPX1.2	OPX2.1	OPX2.2	OPX3.1
Location	(m)	1445.0	1445.0	1445.0	1445.0	1445.0	1500.0	1500.0	1500.0	1500.0	1500.0	1500.0	1500.0	1500.0	1565.0	1565.0	1565.0	1565.0	1565.0	1565.0	1670.0	1670.0	1670.0	1670.0	1670.0
Na2O	wt. %	<0.01	<0.01	<0.01	<0.01	<0.01	<0.01	<0.01	0.01	<0.01	0.01	0.01	0.02	0.01	<0.01	<0.01	<0.01	<0.01	0.02	0.01	<0.01	<0.01	<0.01	<0.01	<0.01
K2O	wt. %	<0.01	0.01	0.01	<0.01	0.01	<0.01	0.02	0.01	<0.01	<0.01	0.01	<0.01	<0.01	0.01	<0.01	0.01	0.01	0.01	0.01	<0.01	<0.01	0.01	<0.01	0.01
Al2O3	wt. %	0.82	0.83	0.72	0.84	0.79	1.06	1.27	1.26	1.31	1.48	1.08	1.07	1.16	1.28	1.32	1.27	1.27	1.01	1.16	0.97	0.81	0.76	0.97	1.12
MgO	wt. %	21.73	21.72	22.00	22.04	21.93	21.74	22.59	21.68	21.59	20.28	18.62	20.68	20.35	22.60	22.29	22.18	21.52	22.63	21.32	23.65	23.75	23.59	23.20	22.32
SiO2	wt. %	52.28	52.23	52.44	52.62	52.42	52.14	52.25	51.67	51.61	52.66	51.50	52.51	52.46	53.15	53.31	52.86	52.37	53.41	52.31	53.44	53.45	53.39	53.36	53.29
CaO	wt. %	1.38	1.30	0.74	0.91	1.01	0.88	1.04	1.14	1.37	1.80	0.98	2.77	3.63	0.66	2.77	0.72	3.12	3.27	1.77	0.80	0.79	0.77	1.44	0.97
MnO	wt. %	0.44	0.45	0.42	0.48	0.43	0.45	0.44	0.45	0.41	0.35	0.49	0.37	0.39	0.35	0.37	0.40	0.34	0.38	0.35	0.45	0.41	0.46	0.46	0.43
TiO2	wt. %	0.19	0.20	0.16	0.18	0.17	0.14	0.14	0.14	0.12	0.17	0.14	0.16	0.13	0.12	0.12	0.13	0.13	0.14	0.18	0.18	0.16	0.17	0.18	0.19
FeO	wt. %	21.718	21.735	22.21	22.12	21.954	22.119	20.497	21.278	21.163	22.274	25.279	21.706	20.981	21.791	19.866	22.283	19.977	18.959	21.423	20.385	20.225	20.426	20.28	21.099
NiO	wt. %	0.02	0.05	0.02	0.03	0.04	0.02	<0.01	<0.01	<0.01	0.02	0.02	<0.01	<0.01	0.01	0.02	<0.01	0.01	<0.01	0.01	0.04	0.06	0.05	0.04	0.02
Cr2O3	wt. %	0.03	0.01	0.04	0.04	0.02	<0.01	0.01	<0.01	0.02	0.02	0.01	<0.01	<0.01	<0.01	0.01	0.01	<0.01	<0.01	0.01	0.03	0.03	0.03	0.03	0.02
Fe2O3	wt. %	0.71	0.84	0.45	0.49	0.80	0.67	0.73	1.24	1.10	<0.01	<0.01	<0.01	<0.01	<0.01	<0.01	<0.01	0.51	0.23	<0.01	0.02	0.25	0.08	0.41	<0.01
Total	wt. %	99.32	99.36	99.22	99.76	99.58	99.21	98.98	98.88	98.68	99.06	98.13	99.29	99.11	99.97	100.07	99.86	99.27	100.06	98.54	99.97	99.94	99.72	100.36	99.47
Na	*	<0.01	<0.01	<0.01	<0.01	<0.01	<0.01	<0.01	<0.01	<0.01	<0.01	<0.01	<0.01	<0.01	<0.01	<0.01	<0.01	<0.01	<0.01	<0.01	<0.01	<0.01	<0.01	<0.01	<0.01
K	*	<0.01	<0.01	<0.01	<0.01	<0.01	<0.01	<0.01	<0.01	<0.01	<0.01	<0.01	<0.01	<0.01	<0.01	<0.01	<0.01	<0.01	<0.01	<0.01	<0.01	<0.01	<0.01	<0.01	<0.01
Al	*	0.04	0.04	0.03	0.04	0.04	0.05	0.06	0.06	0.06	0.07	0.05	0.05	0.05	0.06	0.06	0.06	0.06	0.04	0.05	0.04	0.04	0.03	0.04	0.05
Mg	*	1.22	1.22	1.23	1.23	1.23	1.22	1.26	1.22	1.22	1.14	1.07	1.16	1.14	1.25	1.23	1.23	1.20	1.25	1.20	1.30	1.31	1.30	1.28	1.24
Si	*	1.97	1.96	1.97	1.97	1.97	1.96	1.96	1.95	1.95	1.98	1.99	1.98	1.98	1.97	1.97	1.97	1.96	1.97	1.98	1.97	1.97	1.98	1.97	1.98
Ca	*	0.06	0.05	0.03	0.04	0.04	0.04	0.04	0.05	0.06	0.07	0.04	0.11	0.15	0.03	0.11	0.03	0.13	0.13	0.07	0.03	0.03	0.03	0.06	0.04
Mn	*	0.01	0.01	0.01	0.02	0.01	0.01	0.01	0.01	0.01	0.01	0.02	0.01	0.01	0.01	0.01	0.01	0.01	0.01	0.01	0.01	0.01	0.01	0.01	0.01
Ti	*	0.01	0.01	0.01	0.01	0.01	<0.01	<0.01	<0.01	<0.01	0.01	<0.01	<0.01	<0.01	<0.01	<0.01	<0.01	<0.01	<0.01	0.01	0.01	0.01	0.01	0.01	0.01
Fe	*	0.68	0.68	0.70	0.69	0.69	0.70	0.64	0.67	0.67	0.70	0.82	0.68	0.66	0.68	0.61	0.70	0.63	0.59	0.68	0.63	0.63	0.63	0.63	0.66
Ni	*	<0.01	<0.01	<0.01	<0.01	<0.01	<0.01	<0.01	<0.01	<0.01	<0.01	<0.01	<0.01	<0.01	<0.01	<0.01	<0.01	<0.01	<0.01	<0.01	<0.01	<0.01	<0.01	<0.01	<0.01
Cr	*	<0.01	<0.01	<0.01	<0.01	<0.01	<0.01	<0.01	<0.01	<0.01	<0.01	<0.01	<0.01	<0.01	<0.01	<0.01	<0.01	<0.01	<0.01	<0.01	<0.01	<0.01	<0.01	<0.01	<0.01
Fe3+	*	0.02	0.02	0.01	0.01	0.02	0.02	0.02	0.04	0.03	<0.01	<0.01	<0.01	<0.01	<0.01	<0.01	<0.01	0.01	0.01	<0.01	<0.01	0.01	<0.01	0.01	<0.01
Total	*	4.00	4.00	4.00	4.00	4.00	4.00	4.00	3.99	4.00	3.98	3.98	3.99	3.99	3.99	3.99	4.00	4.00	3.99	3.99	4.00	4.00	4.00	4.00	3.99
WO	%	2.82	2.67	1.51	1.86	2.06	1.81	2.13	2.37	2.83	3.78	2.08	5.68	7.46	1.33	5.58	1.47	6.38	6.55	3.66	1.60	1.58	1.54	2.88	1.99
EN	%	61.81	61.87	62.44	62.29	62.27	62.04	64.39	62.48	62.25	59.18	55.10	58.98	58.22	63.66	62.55	62.61	61.20	63.16	61.24	65.85	66.16	65.78	64.68	63.59
FS	%	35.37	35.46	36.05	35.85	35.67	36.16	33.49	35.15	34.92	37.04	42.81	35.34	34.32	35.00	31.87	35.93	32.42	30.29	35.10	32.55	32.26	32.68	32.44	34.42

SERRA DO ONÇA COMPLEX

Sample		SC19	SC20	SC20	SC20	SC20	SC20	SC20	SC21	SC21	SC21	SC21	SC25	SC25	SC25	SC25	SC25	SC25	SC25	SC26	SC26	SC26	SC26	SC26	SC27
Analysis		OPX3.2	OPX1.1	OPX1.2	OPX2.1	OPX2.2	OPX3.2	OPX4.2	OPX1.1	OPX1.2	OPX2.1	OPX2.2	OPX1.1	OPX1.2	OPX1.3	OPX3.1	OPX3.2	CPX2.1	CPX2.1	OPX1.1	OPX1.2	OPX2.1	OPX2.2	OPX3.1	OPX1.1
Location	(m)	1670.0	1748.0	1748.0	1748.0	1748.0	1748.0	1748.0	1800.0	1800.0	1800.0	1800.0	2171.0	2171.0	2171.0	2171.0	2171.0	2171.0	2171.0	2278.0	2278.0	2278.0	2278.0	2278.0	2448.0
Na2O	wt. %	0.01	<0.01	<0.01	<0.01	0.01	<0.01	<0.01	0.02	0.01	0.01	<0.01	0.02	<0.01	<0.01	<0.01	<0.01	<0.01	<0.01	<0.01	0.02	0.01	<0.01	<0.01	<0.01
K2O	wt. %	0.01	0.01	<0.01	0.01	<0.01	0.01	0.01	0.01	0.01	0.01	0.01	0.01	<0.01	<0.01	<0.01	<0.01	0.01	<0.01	<0.01	<0.01	<0.01	<0.01	0.01	0.01
Al2O3	wt. %	1.02	0.92	1.01	1.03	0.86	0.89	0.83	0.94	1.06	1.06	1.01	1.30	1.03	1.07	1.03	1.11	1.05	0.96	1.05	0.91	1.10	0.99	1.04	0.72
MgO	wt. %	23.01	21.05	21.35	21.13	20.32	22.73	22.02	24.38	23.88	24.00	24.49	22.47	22.92	22.78	22.72	22.78	22.72	23.07	24.80	24.67	24.23	24.39	23.85	19.13
SiO2	wt. %	53.16	52.99	53.05	52.21	53.03	53.09	52.78	53.92	53.76	54.06	53.58	52.77	53.08	53.27	52.79	53.26	52.75	53.25	53.67	54.04	53.85	53.70	53.10	52.11
CaO	wt. %	1.68	0.73	1.57	0.50	2.28	0.77	1.53	2.13	1.85	2.35	0.91	1.88	1.50	1.61	1.28	1.25	1.34	1.17	1.20	1.69	2.20	0.92	1.09	1.48
MnO	wt. %	0.45	0.38	0.36	0.46	0.37	0.42	0.38	0.31	0.31	0.34	0.35	0.37	0.40	0.40	0.40	0.42	0.40	0.37	0.28	0.32	0.29	0.33	0.32	0.44
TiO2	wt. %	0.19	0.18	0.18	0.16	0.18	0.17	0.15	0.21	0.17	0.17	0.20	0.29	0.34	0.20	0.28	0.28	0.30	0.30	0.23	0.21	0.20	0.26	0.31	0.32
FeO	wt. %	19.981	21.351	21.316	23.525	20.55	21.373	21.002	17.952	18.426	18.406	19.019	20.258	20.199	20.385	20.772	20.458	20.583	20.72	18.288	18.038	18.06	19.075	19.084	26.104
NiO	wt. %	0.07	0.04	0.05	0.02	0.04	0.05	0.05	0.07	0.05	0.04	0.04	0.04	0.08	0.08	0.06	0.04	0.04	0.04	0.07	0.09	0.08	0.07	0.06	0.05
Cr2O3	wt. %	0.03	0.02	0.02	0.01	0.02	0.02	0.01	0.10	0.09	0.10	0.09	0.18	0.12	0.20	0.13	0.12	0.10	0.18	0.14	0.19	0.20	0.20	0.17	0.02
Fe2O3	wt. %	0.44	<0.01	<0.01	<0.01	<0.01	<0.01	<0.01	0.43	<0.01	<0.01	0.10	<0.01	<0.01	<0.01	0.03	<0.01	<0.01	<0.01	0.36	<0.01	<0.01	<0.01	<0.01	0.12
Total	wt. %	100.03	97.66	98.90	99.06	97.67	99.51	98.75	100.48	99.63	100.54	99.78	99.57	99.66	99.98	99.49	99.72	99.29	100.06	100.10	100.17	100.21	99.93	99.03	100.48
Na	*	<0.01	<0.01	<0.01	<0.01	<0.01	<0.01	<0.01	<0.01	<0.01	<0.01	<0.01	<0.01	<0.01	<0.01	<0.01	<0.01	<0.01	<0.01	<0.01	<0.01	<0.01	<0.01	<0.01	<0.01
K	*	<0.01	<0.01	<0.01	<0.01	<0.01	<0.01	<0.01	<0.01	<0.01	<0.01	<0.01	<0.01	<0.01	<0.01	<0.01	<0.01	<0.01	<0.01	<0.01	<0.01	<0.01	<0.01	<0.01	<0.01
Al	*	0.04	0.04	0.05	0.05	0.04	0.04	0.04	0.04	0.05	0.05	0.04	0.06	0.05	0.05	0.05	0.05	0.05	0.04	0.05	0.04	0.05	0.04	0.05	0.03
Mg	*	1.27	1.19	1.19	1.19	1.15	1.26	1.23	1.33	1.31	1.31	1.34	1.25	1.27	1.26	1.26	1.26	1.26	1.27	1.35	1.34	1.32	1.34	1.32	1.08
Si	*	1.97	2.01	1.99	1.98	2.01	1.98	1.98	1.97	1.98	1.97	1.97	1.96	1.97	1.97	1.97	1.97	1.97	1.97	1.96	1.97	1.97	1.97	1.97	1.97
Ca	*	0.07	0.03	0.06	0.02	0.09	0.03	0.06	0.08	0.07	0.09	0.04	0.08	0.06	0.06	0.05	0.05	0.05	0.05	0.05	0.07	0.09	0.04	0.04	0.06
Mn	*	0.01	0.01	0.01	0.02	0.01	0.01	0.01	0.01	0.01	0.01	0.01	0.01	0.01	0.01	0.01	0.01	0.01	0.01	0.01	0.01	0.01	0.01	0.01	0.01
Ti	*	0.01	0.01	0.01	<0.01	0.01	0.01	<0.01	0.01	0.01	0.01	0.01	0.01	0.01	0.01	0.01	0.01	0.01	0.01	0.01	0.01	0.01	0.01	0.01	0.01
Fe	*	0.62	0.68	0.67	0.74	0.65	0.67	0.66	0.55	0.57	0.56	0.59	0.63	0.63	0.63	0.65	0.63	0.64	0.64	0.56	0.55	0.55	0.59	0.59	0.83
Ni	*	<0.01	<0.01	<0.01	<0.01	<0.01	<0.01	<0.01	<0.01	<0.01	<0.01	<0.01	<0.01	<0.01	<0.01	<0.01	<0.01	<0.01	<0.01	<0.01	<0.01	<0.01	<0.01	<0.01	<0.01
Cr	*	<0.01	<0.01	<0.01	<0.01	<0.01	<0.01	<0.01	<0.01	<0.01	<0.01	<0.01	0.01	<0.01	0.01	<0.01	<0.01	<0.01	0.01	<0.01	0.01	0.01	0.01	0.01	<0.01
Fe3+	*	0.01	<0.01	<0.01	<0.01	<0.01	<0.01	<0.01	0.01	<0.01	<0.01	<0.01	<0.01	<0.01	<0.01	<0.01	<0.01	<0.01	<0.01	0.01	<0.01	<0.01	<0.01	<0.01	<0.01
Total	*	4.00	3.96	3.98	3.99	3.96	4.00	3.99	3.99	3.99	3.99	3.99	4.00	3.99	4.00	3.99	3.99	3.99	4.00	3.99	4.00	4.00	4.00	3.99	4.00
WO	%	3.38	1.54	3.25	1.03	4.87	1.56	3.13	4.24	3.73	4.66	1.82	3.82	3.03	3.25	2.58	2.53	2.71	2.36	2.39	3.35	4.38	1.84	2.21	3.03
EN	%	64.48	62.33	61.63	60.45	60.30	64.01	62.70	67.42	66.84	66.29	68.00	63.48	64.46	63.98	63.97	64.37	64.08	64.53	68.73	68.17	67.10	67.86	67.14	54.52
FS	%	32.14	36.12	35.12	38.52	34.84	34.43	34.17	28.34	29.43	29.05	30.18	32.70	32.51	32.77	33.45	33.10	33.22	33.11	28.88	28.47	28.52	30.30	30.65	42.45

SERRA DO ONÇA COMPLEX

Sample		SC27	SC27	SC27	SC27	SC7B	SC7B	SC7B	SC7B	SC7B	SC7B	SC10B	SC10B	SC10B	SC10B	SC10B
Analysis		OPX1.2	OPX2.1	OPX2.2	OPX3.1	OPX1.1	OPX1.2	OPX2.1	3.1	OPX3.2	OPX4.1	OPX1.1	OPX1.2	OPX2.1	OPX3.1	OPX3.2
Location	(m)	2448.0	2448.0	2448.0	2448.0	580.0	580.0	580.0	580.0	580.0	580.0	920.0	920.0	920.0	920.0	920.0
Na2O	wt. %	<0.01	<0.01	<0.01	<0.01	0.01	0.03	0.02	0.02	0.02	0.02	0.03	0.04	0.04	0.03	0.04
K2O	wt. %	<0.01	0.01	0.01	<0.01	0.01	<0.01	<0.01	<0.01	<0.01	<0.01	<0.01	0.01	<0.01	<0.01	<0.01
Al2O3	wt. %	0.71	0.71	0.74	0.68	0.70	0.72	0.82	0.73	0.71	0.74	1.18	1.16	1.16	1.13	1.16
MgO	wt. %	19.16	18.61	18.96	19.17	33.76	33.98	33.54	33.63	33.79	33.96	34.22	34.00	34.07	33.75	33.79
SiO2	wt. %	52.09	51.27	51.69	52.13	57.95	58.03	57.63	57.72	57.69	57.88	58.17	58.04	58.04	58.08	58.03
CaO	wt. %	1.25	1.22	1.47	1.15	0.58	0.59	0.59	0.58	0.57	0.55	0.84	0.85	0.89	0.91	0.87
MnO	wt. %	0.49	0.45	0.43	0.49	0.12	0.15	0.13	0.14	0.11	0.13	0.12	0.08	0.13	0.11	0.12
TiO2	wt. %	0.32	0.31	0.30	0.20	0.04	0.02	0.03	0.03	0.03	0.04	0.04	0.05	0.04	0.07	0.04
FeO	wt. %	26.038	25.875	25.481	25.58	6.675	6.61	6.682	6.749	6.664	6.697	5.721	5.693	5.637	5.77	5.683
NiO	wt. %	0.03	0.02	0.04	0.01	0.11	0.09	0.10	0.13	0.06	0.10	0.09	0.07	0.09	0.09	0.10
Cr2O3	wt. %	0.02	0.03	<0.01	<0.01	0.58	0.62	0.72	0.65	0.61	0.66	0.69	0.67	0.65	0.69	0.66
Fe2O3	wt. %	<0.01	<0.01	<0.01	<0.01	<0.01	<0.01	<0.01	<0.01	<0.01	<0.01	<0.01	<0.01	<0.01	<0.01	<0.01
Total	wt. %	100.11	98.50	99.13	99.42	100.53	100.83	100.26	100.38	100.23	100.77	101.09	100.65	100.75	100.62	100.49
Na	*	<0.01	<0.01	<0.01	<0.01	<0.01	<0.01	<0.01	<0.01	<0.01	<0.01	<0.01	<0.01	<0.01	<0.01	<0.01
K	*	<0.01	<0.01	<0.01	<0.01	<0.01	<0.01	<0.01	<0.01	<0.01	<0.01	<0.01	<0.01	<0.01	<0.01	<0.01
Al	*	0.03	0.03	0.03	0.03	0.03	0.03	0.03	0.03	0.03	0.03	0.05	0.05	0.05	0.05	0.05
Mg	*	1.08	1.07	1.08	1.09	1.73	1.74	1.72	1.73	1.74	1.74	1.74	1.73	1.74	1.72	1.73
Si	*	1.98	1.98	1.98	1.99	1.99	1.99	1.99	1.99	1.99	1.99	1.98	1.98	1.98	1.99	1.99
Ca	*	0.05	0.05	0.06	0.05	0.02	0.02	0.02	0.02	0.02	0.02	0.03	0.03	0.03	0.03	0.03
Mn	*	0.02	0.02	0.01	0.02	<0.01	<0.01	<0.01	<0.01	<0.01	<0.01	<0.01	<0.01	<0.01	<0.01	<0.01
Ti	*	0.01	<0.01	<0.01	<0.01	<0.01	<0.01	<0.01	<0.01	<0.01	<0.01	<0.01	<0.01	<0.01	<0.01	<0.01
Fe	*	0.83	0.84	0.82	0.82	0.19	0.19	0.19	0.19	0.19	0.19	0.16	0.16	0.16	0.17	0.16
Ni	*	<0.01	<0.01	<0.01	<0.01	<0.01	<0.01	<0.01	<0.01	<0.01	<0.01	<0.01	<0.01	<0.01	<0.01	<0.01
Cr	*	<0.01	<0.01	<0.01	<0.01	0.02	0.02	0.02	0.02	0.02	0.02	0.02	0.02	0.02	0.02	0.02
Fe3+	*	<0.01	<0.01	<0.01	<0.01	<0.01	<0.01	<0.01	<0.01	<0.01	<0.01	<0.01	<0.01	<0.01	<0.01	<0.01
Total	*	4.00	3.98	3.98	3.98	3.98	3.98	3.98	3.98	3.98	3.98	3.98	3.98	3.98	3.97	3.97
WO	%	2.56	2.56	3.06	2.39	1.09	1.12	1.11	1.10	1.07	1.03	1.59	1.62	1.69	1.73	1.66
EN	%	54.83	54.32	54.86	55.36	88.87	88.95	88.77	88.70	88.93	88.94	89.81	89.83	89.79	89.51	89.70
FS	%	42.61	43.12	42.08	42.25	10.05	9.93	10.12	10.20	10.00	10.03	8.60	8.55	8.53	8.75	8.64

	Sample		SC33B	SC33B	SC33B	SC33B	SC33B	SC34B	SC34B	SC34B	SC34B	SC36	SC36	SC36	SC36	SC36	SC36	SC36	SC36	SC37	SC37	SC37	SC37	SC37	SC37	SC37
	Analysis		OPX1.1	OPX1.2	OPX1.3	OPX1.4	OPX1.5	OPX1.1	OPX1.2	OPX1.3	OPX1.4	OPX1.1	OPX1.2	OPX1.3	OPX2.1	OPX2.2	OPX2.1	OPX2.2	OPX2.3	OPX1.2	OPX3.1	OPX4.1	OPX4.2	OPX4.3	OPX4.4	OPX4.5
	Location	(m)	2391.0	2391.0	2391.0	2391.0	2391.0	2254.0	2254.0	2254.0	2254.0	2130.0	2130.0	2130.0	2130.0	2130.0	2130.0	2130.0	2130.0	2073.0	2073.0	2073.0	2073.0	2073.0	2073.0	2073.0	2073.0
SERRA DO PUMA COMPLEX	Na2O	wt. %	<0.01	<0.01	<0.01	<0.01	<0.01	0.05	0.05	0.03	0.05	<0.01	<0.01	<0.01	<0.01	0.05	0.04	<0.01	<0.01	<0.01	<0.01	<0.01	<0.01	<0.01	<0.01	<0.01	<0.01
	K2O	wt. %	0.01	0.01	0.02	0.01	0.01	<0.01	<0.01	0.01	<0.01	<0.01	0.01	0.01	<0.01	0.01	<0.01	0.01	0.01	<0.01	0.01	<0.01	<0.01	0.01	<0.01	<0.01	0.01
	Al2O3	wt. %	0.72	0.44	0.01	0.19	0.13	1.22	1.25	1.04	1.24	2.53	2.37	0.75	1.46	1.45	1.06	1.35	1.17	0.61	1.61	0.40	1.62	0.44	1.84	2.71
	MgO	wt. %	30.87	31.09	43.77	31.28	31.38	27.69	27.94	28.03	27.61	30.10	30.36	28.68	28.33	28.24	29.57	28.35	29.94	29.53	29.91	31.22	30.70	31.36	30.61	29.72
	SiO2	wt. %	56.43	56.78	39.65	57.23	57.62	54.66	54.28	55.21	54.83	54.90	55.80	55.77	54.53	54.71	55.25	54.98	56.18	56.08	56.31	57.03	56.05	57.40	56.10	55.16
	CaO	wt. %	0.20	0.20	0.02	0.23	0.23	1.99	2.00	2.04	1.99	0.06	0.07	0.18	1.97	2.03	0.09	0.06	0.09	0.13	0.08	0.09	0.09	0.07	0.10	0.06
	MnO	wt. %	0.30	0.27	0.18	0.29	0.27	0.28	0.27	0.27	0.30	0.50	0.49	0.43	0.27	0.27	0.52	0.45	0.56	0.40	0.52	0.47	0.46	0.46	0.44	0.50
	TiO2	wt. %	0.03	0.01	<0.01	0.01	<0.01	0.29	0.27	0.26	0.32	<0.01	0.01	0.02	0.35	0.35	<0.01	<0.01	<0.01	0.01	0.02	<0.01	0.02	<0.01	0.02	0.01
	FeO	wt. %	11.722	11.222	0	11.213	10.895	12.912	12.238	12.717	13.047	11.321	11.37	14.442	11.914	12.261	12.488	14.625	12.429	13.373	12.272	10.902	11.413	11.543	11.189	11.959
	NiO	wt. %	0.06	0.07	0.37	0.06	0.08	0.08	0.07	0.08	0.09	0.04	0.04	0.03	0.07	0.05	0.03	0.04	0.04	0.03	0.03	0.04	0.05	0.04	0.02	0.04
	Cr2O3	wt. %	0.05	0.05	0.02	0.06	0.08	0.39	0.30	0.32	0.37	0.03	0.02	0.08	0.41	0.45	0.05	0.03	0.04	0.13	0.04	0.04	0.05	0.03	0.05	<0.01
	Fe2O3	wt. %	<0.01	<0.01	51.89	<0.01	<0.01	<0.01	0.36	<0.01	<0.01	<0.01	<0.01	<0.01	<0.01	0.52	0.03	<0.01	0.12	<0.01	<0.01	<0.01	<0.01	<0.01	<0.01	0.00
	Total	wt. %	100.40	100.14	135.90	100.57	100.69	99.56	99.02	100.00	99.83	99.47	100.55	100.39	99.89	99.89	99.06	100.01	100.46	100.30	100.82	100.19	100.44	101.36	100.36	100.16
	Na	*	<0.01	<0.01	<0.01	<0.01	<0.01	<0.01	<0.01	<0.01	<0.01	<0.01	<0.01	<0.01	<0.01	<0.01	<0.01	<0.01	<0.01	<0.01	<0.01	<0.01	<0.01	<0.01	<0.01	<0.01
	K	*	<0.01	<0.01	<0.01	<0.01	<0.01	<0.01	<0.01	<0.01	<0.01	<0.01	<0.01	<0.01	<0.01	<0.01	<0.01	<0.01	<0.01	<0.01	<0.01	<0.01	<0.01	<0.01	<0.01	<0.01
	Al	*	0.03	0.02	<0.01	0.01	0.01	0.05	0.05	0.04	0.05	0.11	0.10	0.03	0.06	0.06	0.05	0.06	0.05	0.03	0.07	0.02	0.07	0.02	0.08	0.11
	Mg	*	1.62	1.63	1.92	1.63	1.63	1.48	1.50	1.49	1.48	1.59	1.59	1.52	1.51	1.50	1.58	1.51	1.57	1.56	1.57	1.63	1.61	1.63	1.60	1.56
	Si	*	1.99	2.00	1.17	2.00	2.01	1.97	1.96	1.97	1.97	1.95	1.96	1.99	1.95	1.96	1.98	1.97	1.98	1.99	1.98	2.00	1.97	2.00	1.97	1.95
	Ca	*	0.01	0.01	<0.01	0.01	0.01	0.08	0.08	0.08	0.08	<0.01	<0.01	0.01	0.08	0.08	<0.01	<0.01	<0.01	0.01	<0.01	<0.01	<0.01	<0.01	<0.01	<0.01
	Mn	*	0.01	0.01	<0.01	0.01	0.01	0.01	0.01	0.01	0.01	0.02	0.02	0.01	0.01	0.01	0.02	0.01	0.02	0.01	0.02	0.01	0.01	0.01	0.01	0.02
	Ti	*	<0.01	<0.01	<0.01	<0.01	<0.01	0.01	0.01	0.01	0.01	<0.01	<0.01	<0.01	0.01	0.01	<0.01	<0.01	<0.01	<0.01	<0.01	<0.01	<0.01	<0.01	<0.01	<0.01
	Fe	*	0.35	0.33	0.00	0.33	0.32	0.39	0.37	0.38	0.39	0.34	0.33	0.43	0.36	0.37	0.37	0.44	0.37	0.40	0.36	0.32	0.34	0.34	0.33	0.35
	Ni	*	<0.01	<0.01	0.01	<0.01	<0.01	<0.01	<0.01	<0.01	<0.01	<0.01	<0.01	<0.01	<0.01	<0.01	<0.01	<0.01	<0.01	<0.01	<0.01	<0.01	<0.01	<0.01	<0.01	<0.01
	Cr	*	<0.01	<0.01	<0.01	<0.01	<0.01	0.01	0.01	0.01	0.01	<0.01	<0.01	<0.01	0.01	0.01	<0.01	<0.01	<0.01	<0.01	<0.01	<0.01	<0.01	<0.01	<0.01	<0.01
	Fe3+	*	<0.01	<0.01	1.15	<0.01	<0.01	<0.01	0.01	<0.01	<0.01	<0.01	<0.01	<0.01	0.01	<0.01	<0.01	<0.01	<0.01	<0.01	<0.01	<0.01	<0.01	<0.01	<0.01	<0.01
	Total	*	3.99	3.99	4.25	3.99	3.98	3.99	4.00	3.99	3.99	4.00	3.99	3.99	3.99	3.99	3.99	3.99	3.99	3.98	3.99	3.99	3.99	3.99	3.99	3.99
	WO	%	0.38	0.37	0.03	0.44	0.43	3.91	3.95	3.98	3.92	0.12	0.13	0.35	3.86	3.97	0.18	0.11	0.18	0.25	0.16	0.17	0.17	0.13	0.19	0.11
	EN	%	81.75	82.52	99.74	82.53	83.00	75.82	76.77	76.21	75.58	81.84	81.90	77.19	77.44	76.89	80.05	76.92	80.27	79.05	80.51	82.88	82.03	82.21	82.27	80.87
	FS	%	17.87	17.11	0.23	17.04	16.57	20.27	19.28	19.81	20.50	18.04	17.97	22.46	18.69	19.15	19.77	22.96	19.55	20.70	19.33	16.95	17.81	17.67	17.54	19.02

	Sample		SC38	SC38	SC38	SC38	SC38	SC39	SC39	SC39	SC39	SC39	SC39	SC39	SC39	SC39	SC40A	SC40A	SC40A	SC40A	SC40A	SC40A	SC40A	SC40A	SC41	SC41
	Analysis		OPX3.1	OPX3.2	OPX4.1	OPX4.2	OPX4.3	OPX4.4	OPX1.1	OPX1.2	OPX1.3	OPX2.1	OPX2.2	OPX2.3	OPX3.1	OPX3.2	OPX1.1	OPX1.2	OPX1.3	OPX1.1	OPX1.2	OPX1.3	OPX1.4	OPX1.4	OPX1.1	OPX1.2
	Location	(m)	2029.0	2029.0	2029.0	2029.0	2029.0	2029.0	1998.0	1998.0	1998.0	1998.0	1998.0	1998.0	1998.0	1998.0	1930.0	1930.0	1930.0	1930.0	1930.0	1930.0	1930.0	1930.0	1850.0	1850.0
SERRA DO PUMA COMPLEX	Na2O	wt. %	<0.01	<0.01	<0.01	<0.01	<0.01	0.01	<0.01	0.01	<0.01	0.05	0.04	<0.01	0.05	0.02	<0.01	<0.01	<0.01	0.06	0.05	0.01	0.05	<0.01	<0.01	<0.01
	K2O	wt. %	0.03	0.01	0.01	<0.01	0.01	<0.01	<0.01	<0.01	<0.01	<0.01	<0.01	0.01	0.01	0.01	<0.01	0.03	<0.01	0.01	0.01	0.01	<0.01	<0.01	<0.01	<0.01
	Al2O3	wt. %	2.96	1.40	2.17	2.68	1.89	1.64	1.03	1.26	0.85	1.41	1.31	0.29	1.19	1.08	0.28	0.21	0.22	1.00	1.27	0.34	1.23	0.18	0.77	0.60
	MgO	wt. %	30.65	31.16	28.20	27.53	30.34	28.75	28.60	28.81	29.56	28.22	28.43	31.25	28.78	28.98	29.86	29.91	30.06	29.06	28.93	29.38	29.01	30.03	31.28	31.17
	SiO2	wt. %	55.46	56.21	55.12	54.20	55.32	55.79	55.76	55.45	55.85	54.97	55.11	57.53	55.32	55.31	56.86	57.04	57.33	55.71	55.78	56.25	55.62	57.38	57.75	56.82
	CaO	wt. %	0.07	0.06	0.17	0.19	0.04	0.06	0.15	1.36	0.83	2.05	1.99	0.10	1.91	0.10	0.31	0.28	0.22	1.88	1.92	0.09	1.94	0.28	0.08	0.10
	MnO	wt. %	0.39	0.41	0.34	0.35	0.44	0.58	0.32	0.27	0.26	0.27	0.24	0.38	0.28	0.38	0.36	0.34	0.35	0.24	0.24	0.37	0.28	0.37	0.41	0.39
	TiO2	wt. %	0.02	0.01	0.01	0.03	<0.01	<0.01	0.02	0.48	0.24	0.39	0.38	<0.01	0.35	<0.01	0.03	0.03	0.03	0.32	0.35	0.01	0.36	0.03	0.01	0.01
	FeO	wt. %	10.455	10.45	14.391	14.715	11.34	13.78	14.223	12.44	12.386	12.276	12.211	11.157	11.687	13.359	13.235	12.456	12.998	11.577	11.536	13.207	11.812	12.943	11.092	10.823
	NiO	wt. %	0.03	0.03	0.05	0.06	0.04	<0.01	0.03	0.05	0.05	0.04	0.09	0.01	0.05	0.04	0.04	0.02	0.03	0.06	0.06	0.01	0.05	0.04	0.03	0.04
	Cr2O3	wt. %	0.02	0.02	0.06	0.05	<0.01	0.02	0.06	0.26	0.17	0.40	0.40	<0.01	0.32	0.05	0.08	0.05	0.05	0.34	0.34	0.02	0.40	0.07	<0.01	0.02
	Fe2O3	wt. %	<0.01	<0.01	<0.01	<0.01	<0.01	<0.01	<0.01	<0.01	<0.01	<0.01	<0.01	<0.01	<0.01	<0.01	<0.01	<0.01	<0.01	<0.01	<0.01	<0.01	<0.01	<0.01	<0.01	<0.01
	Total	wt. %	100.06	99.76	100.53	99.80	99.41	100.62	100.19	100.38	100.19	100.06	100.19	100.73	99.94	99.30	101.06	100.36	101.28	100.25	100.47	99.69	100.76	101.32	101.41	99.98
	Na	*	<0.01	<0.01	<0.01	<0.01	<0.01	<0.01	<0.01	<0.01	<0.01	<0.01	<0.01	<0.01	<0.01	<0.01	<0.01	<0.01	<0.01	<0.01	<0.01	<0.01	<0.01	<0.01	<0.01	<0.01
	K	*	<0.01	<0.01	<0.01	<0.01	<0.01	<0.01	<0.01	<0.01	<0.01	<0.01	<0.01	<0.01	<0.01	<0.01	<0.01	<0.01	<0.01	<0.01	<0.01	<0.01	<0.01	<0.01	<0.01	<0.01
	Al	*	0.12	0.06	0.09	0.11	0.08	0.07	0.04	0.05	0.04	0.06	0.06	0.01	0.05	0.05	0.01	0.01	0.01	0.04	0.05	0.01	0.05	0.01	0.03	0.03
	Mg	*	1.60	1.63	1.49	1.47	1.60	1.52	1.52	1.52	1.56	1.50	1.51	1.63	1.53	1.55	1.57	1.57	1.57	1.53	1.52	1.56	1.53	1.57	1.62	1.63
	Si	*	1.95	1.98	1.96	1.95	1.96	1.98	1.99	1.97	1.98	1.96	1.96	2.01	1.97	1.98	2.00	2.01	2.01	1.97	1.97	2.00	1.96	2.01	2.00	2.00
	Ca	*	<0.01	<0.01	0.01	0.01	<0.01	<0.01	0.01	0.05	0.03	0.08	0.08	<0.01	0.07	<0.01	0.01	0.01	0.01	0.07	0.07	<0.01	0.07	0.01	<0.01	<0.01
	Mn	*	0.01	0.01	0.01	0.01	0.01	0.02	0.01	0.01	0.01	0.01	0.01	0.01	0.01	0.01	0.01	0.01	0.01	0.01	0.01	0.01	0.01	0.01	0.01	0.01
	Ti	*	<0.01	<0.01	<0.01	<0.01	<0.01	<0.01	<0.01	0.01	0.01	0.01	0.01	0.00	0.01	<0.01	<0.01	<0.01	<0.01	0.01	0.01	<0.01	0.01	<0.01	<0.01	<0.01
	Fe	*	0.31	0.31	0.43	0.44	0.34	0.41	0.42	0.37	0.37	0.37	0.36	0.33	0.35	0.40	0.39	0.37	0.38	0.34	0.34	0.39	0.35	0.38	0.32	0.32
	Ni	*	<0.01	<0.01	<0.01	<0.01	<0.01	<0.01	<0.01	<0.01	<0.01	<0.01	<0.01	<0.01	<0.01	<0.01	<0.01	<0.01	<0.01	<0.01	<0.01	<0.01	<0.01	<0.01	<0.01	<0.01
	Cr	*	<0.01	<0.01	<0.01	<0.01	<0.01	<0.01	<0.01	0.01	0.01	0.01	0.01	<0.01	0.01	<0.01	<0.01	<0.01	<0.01	0.01	0.01	<0.01	0.01	<0.01	<0.01	<0.01
	Fe3+	*	<0.01	<0.01	<0.01	<0.01	<0.01	<0.01	<0.01	<0.01	<0.01	<0.01	<0.01	<0.01	0.00	<0.01	<0.01	<0.01	<0.01	<0.01	<0.01	<0.01	<0.01	<0.01	<0.01	<0.01
	Total	*	3.99	3.99	3.99	3.99	3.99	3.99	3.99	3.99	3.99	3.99	3.99	3.98	3.99	3.99	3.99	3.98	3.98	3.99	3.99	3.98	3.99	3.98	3.98	3.98
	WO	%	0.14	0.12	0.34	0.39	0.07	0.11	0.29	2.64	1.60	4.01	3.88	0.18	3.73	0.19	0.59	0.53	0.42	3.65	3.74	0.17	3.75	0.53	0.15	0.20
	EN	%	83.32	83.54	77.07	76.21	82.05	78.01	77.58	78.04	79.35	76.82	77.16	82.68	78.06	78.84	79.18	80.20	79.71	78.45	78.36	79.27	78.00	79.65	82.77	83.03
	FS	%	16.54	16.34	22.60	23.40	17.88	21.88	22.13	19.32	19.05	19.17	18.96	17.13	18.21	20.97	20.24	19.27	19.87	17.90	17.90	20.56	18.25	19.82	17.08	16.77

	Sample		SC41	SC41	SC41	SC41	SC41	SC46	SC46	SC46	SC46	SC46	SC46	SC47A	SC47A	SC47A	SC47A	SC47A	SC48	SC48	SC48
	Analysis		OPX1.3	OPX1.4	OPX2.1	OPX2.1	OPX3.3	OPX1.1	OPX1.2	OPX1.3	OPX2.1	OPX2.2	OPX2.3	OPX1.1	OPX1.2	OPX1.3	OPX1.4	OPX1.5	OPX1.1	OPX2.1	OPX3.1
	Location	(m)	1850.0	1850.0	1850.0	1850.0	1850.0	1213.0	1213.0	1213.0	1213.0	1213.0	1213.0	1184.0	1184.0	1184.0	1184.0	1184.0	1145.0	1145.0	1145.0
SERRA DO PUMA COMPLEX	Na2O	wt. %	0.05	<0.01	0.35	0.01	<0.01	0.02	0.04	0.03	0.02	0.03	0.03	0.01	0.02	0.01	0.02	0.02	0.36	0.35	0.39
	K2O	wt. %	<0.01	<0.01	0.02	0.02	0.01	<0.01	<0.01	<0.01	<0.01	<0.01	0.01	<0.01	0.01	0.01	0.01	0.01	0.01	<0.01	0.02
	Al2O3	wt. %	1.18	1.22	2.80	1.18	0.09	0.91	0.87	0.87	0.89	0.89	0.88	0.91	0.88	0.76	0.95	0.88	2.10	2.25	2.58
	MgO	wt. %	28.94	29.55	15.86	27.60	30.77	29.26	29.45	29.30	29.12	29.49	29.41	30.13	30.04	30.21	30.23	29.92	17.84	17.13	16.56
	SiO2	wt. %	55.80	55.64	51.37	54.38	57.84	55.77	56.30	55.92	56.47	56.73	56.52	56.37	56.45	55.80	56.51	56.65	53.61	53.42	53.28
	CaO	wt. %	1.95	0.95	20.18	0.17	0.06	1.74	1.74	1.74	1.82	1.78	1.80	1.61	1.93	1.25	1.65	1.91	20.44	20.74	21.48
	MnO	wt. %	0.24	0.26	0.11	0.34	0.52	0.19	0.18	0.18	0.21	0.20	0.21	0.19	0.18	0.23	0.21	0.19	0.11	0.10	0.10
	TiO2	wt. %	0.33	0.34	0.24	0.00	0.01	0.30	0.28	0.28	0.29	0.31	0.27	0.17	0.18	0.13	0.18	0.18	0.15	0.19	0.21
	FeO	wt. %	11.641	11.933	4.948	12.77	11.965	11.846	12.076	11.988	11.957	11.759	11.696	10.386	10.227	10.461	10.171	10.346	4.364	4.413	4.266
	NiO	wt. %	0.08	0.06	0.03	0.03	0.02	0.08	0.12	0.10	0.09	0.09	0.11	0.10	0.10	0.09	0.08	0.11	0.07	0.08	0.03
	Cr2O3	wt. %	0.33	0.20	0.96	0.10	0.00	0.20	0.15	0.15	0.19	0.19	0.16	0.10	0.12	0.12	0.13	0.11	1.21	1.15	1.13
	Fe2O3	wt. %	<0.01	<0.01	<0.01	<0.01	<0.01	<0.01	<0.01	<0.01	<0.01	<0.01	<0.01	<0.01	<0.01	<0.01	<0.01	<0.01	<0.01	<0.01	<0.01
	Total	wt. %	100.54	100.15	96.86	96.59	101.28	100.32	101.18	100.54	101.06	101.45	101.10	99.99	100.13	99.08	100.14	100.33	100.28	99.83	100.05
	Na	*	<0.01	<0.01	0.03	<0.01	<0.01	<0.01	<0.01	<0.01	<0.01	<0.01	<0.01	<0.01	<0.01	<0.01	<0.01	<0.01	0.03	0.03	0.03
	K	*	<0.01	<0.01	<0.01	<0.01	<0.01	<0.01	<0.01	<0.01	<0.01	<0.01	<0.01	<0.01	<0.01	<0.01	<0.01	<0.01	<0.01	<0.01	<0.01
	Al	*	0.05	0.05	0.12	0.05	0.00	0.04	0.04	0.04	0.04	0.04	0.04	0.04	0.04	0.03	0.04	0.04	0.09	0.10	0.11
	Mg	*	1.52	1.56	0.89	1.51	1.60	1.54	1.54	1.54	1.53	1.54	1.54	1.58	1.58	1.60	1.58	1.57	0.97	0.93	0.90
	Si	*	1.97	1.97	1.94	2.00	2.02	1.98	1.98	1.98	1.98	1.98	1.98	1.99	1.99	1.99	1.99	1.99	1.95	1.95	1.94
	Ca	*	0.07	0.04	0.82	0.01	<0.01	0.07	0.07	0.07	0.07	0.07	0.07	0.06	0.07	0.05	0.06	0.07	0.80	0.81	0.84
	Mn	*	0.01	0.01	<0.01	0.01	0.02	0.01	0.01	0.01	0.01	0.01	0.01	0.01	0.01	0.01	0.01	0.01	<0.01	<0.01	<0.01
	Ti	*	0.01	0.01	0.01	<0.01	<0.01	0.01	0.01	0.01	0.01	0.01	0.01	0.01	0.01	<0.01	0.01	0.01	<0.01	0.01	0.01
	Fe	*	0.34	0.35	0.16	0.39	0.35	0.35	0.36	0.35	0.35	0.34	0.34	0.31	0.30	0.31	0.30	0.30	0.13	0.14	0.13
	Ni	*	<0.01	<0.01	<0.01	<0.01	<0.01	<0.01	<0.01	<0.01	<0.01	<0.01	<0.01	<0.01	<0.01	<0.01	<0.01	<0.01	<0.01	<0.01	<0.01
	Cr	*	0.01	0.01	0.03	<0.01	<0.01	0.01	<0.01	<0.01	0.01	0.01	<0.01	<0.01	<0.01	<0.01	<0.01	<0.01	0.04	0.03	0.03
	Fe3+	*	<0.01	<0.01	<0.01	<0.01	<0.01	<0.01	<0.01	<0.01	<0.01	<0.01	<0.01	<0.01	<0.01	<0.01	<0.01	<0.01	<0.01	<0.01	<0.01
	Total	*	3.99	3.99	3.99	3.97	3.98	3.99	3.99	3.99	3.99	3.99	3.98	3.98	3.98	3.99	3.98	3.98	3.99	3.99	3.99
	WO	%	3.79	1.84	43.69	0.35	0.11	3.35	3.32	3.34	3.52	3.42	3.47	3.12	3.72	2.43	3.19	3.68	41.93	43.12	44.81
	EN	%	78.19	79.70	47.76	78.68	81.36	78.52	78.37	78.39	78.16	78.67	78.66	80.94	80.61	81.41	81.16	80.42	50.91	49.55	48.07
	FS	%	18.01	18.46	8.55	20.98	18.54	18.13	18.30	18.27	18.32	17.91	17.88	15.95	15.68	16.17	15.65	15.90	7.16	7.33	7.12

SERRA DO ONÇA COMPLEX

Sample		SC22	SC22	SC22	SC23	SC23	SC23	SC23	SC23	SC23	SC24A	SC24A	SC24A	SC11	SC11	SC11	SC11	SC11	SC12	SC12	SC12	SC12	SC13	SC13	SC13
Analysis		CPX5.1	CPX5.2	CPX5.3	CPX1.1	CPX1.2	CPX2.2	CPX2.3	CPX3.2	CPX3.3	CPX3.1	CPX3.2	CPX4.1	CPX1.1	CPX2.1	CPX2.2	CPX3.1	CPX3.3	OPX1.4	CPX2.3	CPX2.1	CPX3.2	CPX1.2	CPX2.1	CPX2.2
Location (m)		1898.0	1898.0	1898.0	1987.0	1987.0	1987.0	1987.0	1987.0	1987.0	2081.0	2081.0	2081.0	1060.0	1060.0	1060.0	1060.0	1060.0	1120.0	1120.0	1120.0	1120.0	1135.0	1135.0	1135.0
Na2O	wt. %	0.27	0.33	0.34	0.26	0.28	0.25	0.28	0.27	0.25	0.32	0.35	0.38	0.21	0.23	0.24	0.22	0.22	0.26	0.24	0.27	0.26	0.26	0.26	0.25
K2O	wt. %	<0.01	<0.01	<0.01	<0.01	<0.01	0.01	<0.01	0.04	<0.01	<0.01	0.05	<0.01	0.01	<0.01	0.03	<0.01	<0.01	<0.01	<0.01	<0.01	<0.01	<0.01	<0.01	<0.01
Al2O3	wt. %	2.00	2.07	2.05	1.89	2.10	2.02	2.03	1.98	1.70	2.14	2.19	2.13	2.05	1.87	1.93	1.82	1.85	1.36	1.62	1.84	1.76	1.76	1.81	1.88
MgO	wt. %	17.09	14.72	15.03	14.65	13.39	14.19	13.86	13.65	15.24	14.32	13.96	13.97	16.26	16.15	15.59	16.06	15.87	15.30	15.05	14.87	14.85	15.42	15.08	15.87
SiO2	wt. %	51.69	50.84	51.14	50.78	50.99	51.09	51.10	51.21	51.28	50.45	50.65	51.15	51.95	51.79	52.08	51.89	52.08	52.18	52.14	52.08	51.96	52.82	52.68	52.55
CaO	wt. %	16.12	20.98	19.64	19.48	20.99	18.27	19.97	20.30	18.66	19.39	21.15	20.30	18.91	20.38	21.87	21.01	20.16	21.94	21.14	21.75	21.94	20.96	20.85	21.48
MnO	wt. %	0.22	0.21	0.17	0.26	0.29	0.24	0.23	0.23	0.24	0.22	0.22	0.18	0.16	0.21	0.14	0.15	0.14	0.14	0.20	0.17	0.17	0.18	0.23	0.19
TiO2	wt. %	0.35	0.38	0.41	0.42	0.42	0.38	0.45	0.39	0.38	0.43	0.43	0.38	0.13	0.15	0.13	0.18	0.15	0.21	0.21	0.24	0.22	0.18	0.18	0.19
FeO	wt. %	9.507	6.212	7.792	8.532	8.998	11.312	9.663	9.68	9.166	8.596	6.939	8.646	7.093	5.846	5.148	5.412	6.553	5.826	7.308	6.639	6.388	7.556	8.092	5.82
NiO	wt. %	0.03	0.04	0.05	0.05	0.02	0.02	0.04	0.01	0.03	0.04	0.05	0.02	0.06	0.06	0.06	0.06	0.08	0.01	0.03	0.05	0.02	0.04	0.02	0.03
Cr2O3	wt. %	0.29	0.28	0.29	0.03	0.01	0.03	0.02	0.04	0.03	0.36	0.35	0.34	0.08	0.07	0.08	0.08	0.11	0.02	0.04	0.05	0.05	0.03	0.06	0.10
Fe2O3	wt. %	1.22	1.99	0.97	2.71	1.70	0.75	1.21	1.19	2.47	2.38	2.59	1.10	<0.01	0.97	0.83	0.77	<0.01	1.08	0.23	0.86	0.88	0.79	0.17	2.04
Total	wt. %	98.78	98.05	97.86	99.05	99.18	98.55	98.85	98.98	99.45	98.63	98.92	98.60	96.91	97.72	98.12	97.64	97.20	98.33	98.20	98.83	98.49	100.00	99.44	100.40
Na	*	0.02	0.03	0.03	0.02	0.02	0.02	0.02	0.02	0.02	0.02	0.03	0.03	0.02	0.02	0.02	0.02	0.02	0.02	0.02	0.02	0.02	0.02	0.02	0.02
K	*	<0.01	<0.01	<0.01	<0.01	<0.01	<0.01	<0.01	<0.01	<0.01	<0.01	<0.01	<0.01	<0.01	<0.01	<0.01	<0.01	<0.01	<0.01	<0.01	<0.01	<0.01	<0.01	<0.01	<0.01
Al	*	0.09	0.09	0.09	0.08	0.09	0.09	0.09	0.09	0.08	0.10	0.10	0.10	0.09	0.08	0.09	0.08	0.08	0.06	0.07	0.08	0.08	0.08	0.08	0.08
Mg	*	0.95	0.83	0.85	0.82	0.75	0.80	0.78	0.77	0.85	0.81	0.79	0.79	0.92	0.91	0.87	0.90	0.89	0.86	0.84	0.83	0.83	0.85	0.84	0.87
Si	*	1.93	1.92	1.94	1.92	1.93	1.94	1.94	1.94	1.93	1.91	1.91	1.94	1.97	1.95	1.95	1.95	1.97	1.96	1.96	1.95	1.95	1.95	1.96	1.93
Ca	*	0.65	0.85	0.80	0.79	0.85	0.74	0.81	0.82	0.75	0.79	0.86	0.82	0.77	0.82	0.88	0.85	0.82	0.88	0.85	0.87	0.88	0.83	0.83	0.85
Mn	*	0.01	0.01	0.01	0.01	0.01	0.01	0.01	0.01	0.01	0.01	0.01	0.01	0.01	0.01	0.01	0.01	0.01	<0.01	0.01	0.01	0.01	0.01	0.01	0.01
Ti	*	0.01	0.01	0.01	0.01	0.01	0.01	0.01	0.01	0.01	0.01	0.01	0.01	<0.01	<0.01	<0.01	0.01	<0.01	0.01	0.01	0.01	0.01	0.01	0.01	0.01
Fe	*	0.30	0.20	0.25	0.27	0.28	0.36	0.31	0.31	0.29	0.27	0.22	0.27	0.22	0.18	0.16	0.17	0.21	0.18	0.23	0.21	0.20	0.23	0.25	0.18
Ni	*	<0.01	<0.01	<0.01	<0.01	<0.01	<0.01	<0.01	<0.01	<0.01	<0.01	<0.01	<0.01	<0.01	<0.01	<0.01	<0.01	<0.01	<0.01	<0.01	<0.01	<0.01	<0.01	<0.01	<0.01
Cr	*	0.01	0.01	0.01	<0.01	<0.01	<0.01	<0.01	<0.01	<0.01	0.01	0.01	0.01	<0.01	<0.01	<0.01	<0.01	<0.01	<0.01	<0.01	<0.01	<0.01	<0.01	<0.01	<0.01
Fe3+	*	0.03	0.06	0.03	0.08	0.05	0.02	0.03	0.03	0.07	0.07	0.07	0.03	<0.01	0.03	0.02	0.02	<0.01	0.03	0.01	0.02	0.03	0.02	0.01	0.06
Total	*																								
WO	%	33.95	45.14	42.00	41.70	44.79	38.85	42.50	43.17	39.53	41.97	45.82	43.54	40.07	42.83	45.86	44.05	42.47	45.83	44.11	45.55	45.98	43.26	43.14	44.52
EN	%	50.06	44.07	44.71	43.62	39.74	41.97	41.05	40.37	44.91	43.13	42.07	41.68	47.93	47.23	45.48	46.85	46.51	44.46	43.67	43.31	43.30	44.28	43.41	45.76
FS	%	15.99	10.80	13.30	14.68	15.47	19.18	16.45	16.46	15.56	14.90	12.11	14.79	12.00	9.95	8.66	9.10	11.02	9.72	12.23	11.14	10.72	12.47	13.45	9.72

SERRA DO ONÇA COMPLEX

Sample		SC13	SC14	SC14	SC14	SC14	SC15	SC15	SC15	SC15	SC16B	SC16B	SC16B	SC16B	SC16B	SC16B	SC17	SC17	SC17	SC17	SC17	SC17	SC18	SC18	SC18
Analysis		CPX2.3	CPX1.1	CPX1.3	CPX2.2	CPX3.1	CPX3.3	CPX1.1	CPX1.3	CPX2.1	CPX2.2	CPX1.1	CPX1.2	CPX2.1	CPX2.2	CPX3.1	CPX1.1	CPX1.2	CPX2.1	OPX2.1	CPX3.1	CPX3.3	CPX1.1	CPX2.1	CPX2.3
Location (m)		1135.0	1225.0	1225.0	1225.0	1225.0	1225.0	1370.0	1370.0	1370.0	1788.3	1445.0	1445.0	1445.0	1445.0	1445.0	1500.0	1500.0	1500.0	1500.0	1500.0	1500.0	1565.0	1565.0	1565.0
Na2O	wt. %	0.26	0.29	0.27	0.20	0.18	0.19	0.28	0.31	0.33	0.28	0.36	0.33	0.31	0.29	0.31	0.35	0.36	0.33	0.25	0.34	0.31	0.37	0.30	0.32
K2O	wt. %	0.01	<0.01	<0.01	<0.01	<0.01	<0.01	0.01	<0.01	0.02	0.01	0.02	<0.01	<0.01	<0.01	0.01	0.01	0.01	<0.01	0.01	0.01	<0.01	<0.01	<0.01	0.01
Al2O3	wt. %	1.89	1.84	1.91	1.66	1.79	1.82	1.76	1.81	1.84	1.82	2.08	1.93	1.71	1.66	1.80	2.24	2.36	2.63	1.84	2.35	2.59	2.68	2.42	2.54
MgO	wt. %	15.06	15.20	16.23	16.08	16.57	16.55	15.58	14.40	14.37	14.29	13.50	14.00	13.87	14.11	14.00	13.48	13.49	13.24	15.08	14.34	13.53	13.43	13.53	13.26
SiO2	wt. %	52.53	52.34	52.17	52.40	52.21	52.51	51.66	51.80	51.85	51.99	51.14	51.33	51.77	51.91	51.40	50.86	50.91	50.34	50.83	50.94	50.65	51.24	51.21	51.14
CaO	wt. %	22.04	21.67	21.08	17.52	15.05	17.35	19.01	21.34	21.91	21.55	21.96	20.58	21.10	20.75	21.00	20.27	21.50	20.01	20.67	18.62	18.92	20.60	21.42	20.99
MnO	wt. %	0.16	0.19	0.22	0.27	0.23	0.21	0.26	0.21	0.17	0.20	0.23	0.25	0.25	0.22	0.28	0.18	0.21	0.22	0.18	0.31	0.27	0.20	0.18	0.20
TiO2	wt. %	0.21	0.21	0.27	0.23	0.25	0.25	0.28	0.28	0.29	0.27	0.37	0.38	0.37	0.36	0.34	0.34	0.36	0.35	0.27	0.32	0.37	0.32	0.31	0.31
FeO	wt. %	6.492	6.353	5.223	10.519	12.279	10.193	8.27	7.479	6.789	7.739	7.312	8.618	8.8	9.078	8.142	9.258	7.713	9.51	6.276	9.877	10.852	9.288	8.343	9.199
NiO	wt. %	0.03	0.02	<0.01	0.04	0.04	0.01	0.06	0.07	0.02	0.06	0.02	0.01	<0.01	0.02	<0.01	0.06	<0.01	0.03	0.01	<0.01	<0.01	<0.01	0.01	<0.01
Cr2O3	wt. %	0.06	0.05	0.08	0.08	0.05	0.05	0.08	0.06	0.05	0.06	0.04	0.03	0.08	0.05	0.04	0.02	<0.01	<0.01	<0.01	0.01	<0.01	0.02	0.01	0.01
Fe2O3	wt. %	0.99	2.10	3.42	0.70	<0.01	0.50	2.44	1.71	1.98	0.94	2.12	2.00	1.27	1.43	2.09	1.81	2.49	2.00	3.59	2.51	1.34	2.03	1.91	1.87
Total	wt. %	99.72	100.25	100.88	99.68	98.66	99.63	99.68	99.45	99.62	99.21	99.15	99.47	99.52	99.88	99.41	98.86	99.40	98.65	99.00	99.62	98.83	100.18	99.65	99.84
Na	*	0.02	0.02	0.02	0.02	0.01	0.01	0.02	0.02	0.02	0.02	0.03	0.02	0.02	0.02	0.02	0.03	0.03	0.02	0.02	0.03	0.02	0.03	0.02	0.02
K	*	<0.01	<0.01	<0.01	<0.01	<0.01	<0.01	<0.01	<0.01	<0.01	<0.01	<0.01	<0.01	<0.01	<0.01	<0.01	<0.01	<0.01	<0.01	<0.01	<0.01	<0.01	<0.01	<0.01	<0.01
Al	*	0.08	0.08	0.08	0.07	0.08	0.08	0.08	0.08	0.08	0.08	0.09	0.09	0.08	0.07	0.08	0.10	0.11	0.12	0.08	0.10	0.12	0.12	0.11	0.11
Mg	*	0.83	0.84	0.89	0.89	0.93	0.92	0.87	0.80	0.80	0.80	0.76	0.78	0.78	0.79	0.78	0.76	0.76	0.75	0.85	0.80	0.77	0.75	0.76	0.74
Si	*	1.95	1.94	1.91	1.95	1.96	1.95	1.93	1.94	1.94	1.95	1.93	1.93	1.94	1.94	1.93	1.93	1.92	1.91	1.91	1.92	1.92	1.92	1.92	1.92
Ca	*	0.88	0.86	0.83	0.70	0.61	0.69	0.76	0.86	0.88	0.87	0.89	0.83	0.85	0.83	0.85	0.82	0.87	0.82	0.83	0.75	0.77	0.83	0.86	0.85
Mn	*	0.01	0.01	0.01	0.01	0.01	0.01	0.01	0.01	0.01	0.01	0.01	0.01	0.01	0.01	0.01	0.01	0.01	0.01	0.01	0.01	0.01	0.01	0.01	0.01
Ti	*	0.01	0.01	0.01	0.01	0.01	0.01	0.01	0.01	0.01	0.01	0.01	0.01	0.01	0.01	0.01	0.01	0.01	0.01	0.01	0.01	0.01	0.01	0.01	0.01
Fe	*	0.20	0.20	0.16	0.33	0.39	0.32	0.26	0.23	0.21	0.24	0.23	0.27	0.28	0.28	0.26	0.29	0.24	0.30	0.20	0.31	0.35	0.29	0.26	0.29
Ni	*	<0.01	<0.01	<0.01	<0.01	<0.01	<0.01	<0.01	<0.01	<0.01	<0.01	<0.01	<0.01	<0.01	<0.01	<0.01	<0.01	<0.01	<0.01	<0.01	<0.01	<0.01	<0.01	<0.01	<0.01
Cr	*	<0.01	<0.01	<0.01	<0.01	<0.01	<0.01	<0.01	<0.01	<0.01	<0.01	<0.01	<0.01	<0.01	<0.01	<0.01	<0.01	<0.01	<0.01	<0.01	<0.01	<0.01	<0.01	<0.01	<0.01
Fe3+	*	0.03	0.06	0.09	0.02	<0.01	0.01	0.07	0.05	0.06	0.03	0.06	0.06	0.04	0.04	0.06	0.05	0.07	0.06	0.10	0.07	0.04	0.06	0.05	0.05
Total	*																								
WO	%	45.74	45.22	44.00	36.27	31.45	35.78	40.16	45.05	46.29	45.24	47.09	43.81	44.46	43.55	44.63	43.70	46.29	43.47	44.28	40.03	40.76	44.13	45.67	44.87
EN	%	43.48	44.13	47.13	46.30	48.15	47.48	45.77	42.28	42.23	41.75	40.28	41.45	40.65	41.20	41.39	40.42	40.39	40.02	44.93	42.88	40.54	40.01	40.14	39.44
FS	%	10.78	10.66	8.88	17.43	20.41	16.74	14.07	12.67	11.48	13.01	12.63	14.74	14.89	15.24	13.98	15.88	13.32	16.51	10.79	17.10	18.70	15.86	14.19	15.69

SERRA DO ONÇA COMPLEX

Sample		SC18	SC19	SC19	SC19	SC19	SC19	SC19	SC20	SC20	SC20	SC20	SC20	SC20	SC21	SC21	SC21	SC21	SC21	SC25	SC25	SC25	SC26	SC26	SC26
Analysis		OPX1.1	CPX1.1	CPX1.2	CPX2.1	CPX2.2	CPX2.3	CPX3.1	CPX3.2	CPX1.1	CPX1.2	CPX1.3	CPX2.1	CPX2.2	CPX2.1	CPX1.1	CPX2.1	CPX2.2	CPX3.1	CPX3.1	CPX3.2	CPX3.3	CPX4.1	CPX2.1	CPX1.2
Location (m)		1565.0	1670.0	1670.0	1670.0	1670.0	1670.0	1670.0	1670.0	1748.0	1748.0	1748.0	1748.0	1748.0	1800.0	1800.0	1800.0	1800.0	1800.0	2171.0	2171.0	2171.0	2171.0	2278.0	2278.0
Na2O	wt. %	0.35	0.31	0.26	0.28	0.26	0.26	0.29	0.30	0.26	0.26	0.28	0.30	0.27	0.32	0.33	0.31	0.37	0.30	0.39	0.31	0.28	0.33	0.35	0.34
K2O	wt. %	<0.01	<0.01	<0.01	0.01	<0.01	<0.01	<0.01	<0.01	0.02	0.01	<0.01	0.01	0.01	<0.01	<0.01	<0.01	<0.01	<0.01	0.01	<0.01	0.01	0.01	<0.01	0.01
Al2O3	wt. %	2.53	1.71	1.70	1.93	1.94	1.80	1.85	1.70	1.90	1.87	1.93	1.71	1.83	1.84	2.01	1.87	1.96	1.74	2.31	2.05	1.84	2.10	1.99	2.03
MgO	wt. %	14.43	14.76	14.05	14.14	14.27	14.42	15.10	16.11	14.32	14.09	14.12	14.31	14.19	16.20	14.52	14.60	14.07	15.02	13.19	14.26	15.53	14.04	14.72	14.69
SiO2	wt. %	50.70	52.49	52.31	52.09	52.28	52.26	51.91	52.32	52.16	52.52	51.84	51.97	51.68	52.38	52.74	52.42	52.19	52.31	51.26	51.80	51.88	52.13	52.04	52.05
CaO	wt. %	19.68	21.77	21.89	21.82	19.66	20.11	21.33	20.51	19.10	20.10	20.87	20.71	20.40	19.56	20.70	20.90	21.88	19.57	21.47	19.25	17.68	20.03	18.82	17.91
MnO	wt. %	0.27	0.25	0.25	0.25	0.21	0.23	0.29	0.31	0.23	0.21	0.21	0.24	0.20	0.20	0.16	0.16	0.16	0.19	0.25	0.22	0.28	0.23	0.15	0.15
TiO2	wt. %	0.34	0.36	0.38	0.40	0.39	0.37	0.36	0.31	0.31	0.30	0.36	0.30	0.29	0.34	0.38	0.38	0.41	0.36	0.47	0.56	0.46	0.49	0.35	0.35
FeO	wt. %	8.077	7.176	8.353	7.927	9.854	9.711	6.475	6.133	11.104	10.44	8.863	8.691	9.143	7.27	8.844	8.607	7.784	9.434	8.597	10.697	10.442	10.262	9.773	10.189
NiO	wt. %	0.02	0.02	0.01	0.01	0.03	0.03	0.03	0.04	0.04	0.01	0.05	0.02	0.03	0.02	0.06	0.04	0.02	0.04	0.01	0.02	0.04	0.03	0.04	0.04
Cr2O3	wt. %	<0.01	0.03	0.07	0.06	0.06	0.08	0.10	0.06	0.04	0.06	0.04	0.04	0.06	0.17	0.22	0.21	0.24	0.20	0.21	0.24	0.25	0.33	0.49	0.38
Fe2O3	wt. %	3.29	1.81	0.70	1.08	<0.01	<0.01	3.12	3.89	<0.01	<0.01	1.07	1.09	0.79	2.17	<0.01	0.03	0.21	0.41	1.04	0.19	1.55	0.01	<0.01	<0.01
Total	wt. %	99.69	100.67	99.96	100.00	98.95	99.27	100.85	101.66	99.47	99.89	99.63	99.39	98.88	100.49	99.98	99.51	99.29	99.56	99.19	99.59	100.24	99.98	98.72	98.14
Na	*	0.03	0.02	0.02	0.02	0.02	0.02	0.02	0.02	0.02	0.02	0.02	0.02	0.02	0.02	0.02	0.02	0.03	0.02	0.03	0.02	0.02	0.02	0.03	0.03
K	*	<0.01	<0.01	<0.01	<0.01	<0.01	<0.01	<0.01	<0.01	<0.01	<0.01	<0.01	<0.01	<0.01	<0.01	<0.01	<0.01	<0.01	<0.01	<0.01	<0.01	<0.01	<0.01	<0.01	<0.01
Al	*	0.11	0.07	0.08	0.09	0.09	0.08	0.08	0.07	0.08	0.08	0.09	0.08	0.08	0.08	0.09	0.08	0.09	0.08	0.10	0.09	0.08	0.09	0.09	0.09
Mg	*	0.81	0.81	0.78	0.79	0.80	0.81	0.83	0.88	0.80	0.79	0.79	0.80	0.80	0.89	0.80	0.81	0.78	0.84	0.74	0.80	0.86	0.78	0.83	0.83
Si	*	1.90	1.94	1.95	1.94	1.97	1.96	1.92	1.91	1.96	1.96	1.94	1.95	1.95	1.93	1.96	1.96	1.95	1.95	1.93	1.94	1.93	1.95	1.96	1.97
Ca	*	0.79	0.86	0.87	0.87	0.79	0.81	0.84	0.80	0.77	0.81	0.84	0.83	0.82	0.77	0.82	0.84	0.88	0.78	0.87	0.77	0.71	0.80	0.76	0.73
Mn	*	0.01	0.01	0.01	0.01	0.01	0.01	0.01	0.01	0.01	0.01	0.01	0.01	0.01	0.01	0.01	0.01	0.01	0.01	0.01	0.01	0.01	0.01	0.01	0.01
Ti	*	0.01	0.01	0.01	0.01	0.01	0.01	0.01	0.01	0.01	0.01	0.01	0.01	0.01	0.01	0.01	0.01	0.01	0.01	0.02	0.01	0.01	0.01	0.01	0.01
Fe	*	0.25	0.22	0.26	0.25	0.31	0.31	0.20	0.19	0.35	0.33	0.28	0.27	0.29	0.22	0.28	0.27	0.24	0.30	0.27	0.34	0.33	0.32	0.31	0.32
Ni	*	<0.01	<0.01	<0.01	<0.01	<0.01	<0.01	<0.01	<0.01	<0.01	<0.01	<0.01	<0.01	<0.01	<0.01	<0.01	<0.01	<0.01	<0.01	<0.01	<0.01	<0.01	<0.01	<0.01	<0.01
Cr	*	<0.01	<0.01	<0.01	<0.01	<0.01	<0.01	<0.01	<0.01	<0.01	<0.01	<0.01	<0.01	<0.01	0.01	0.01	0.01	0.01	0.01	0.01	0.01	0.01	0.02	0.01	
Fe3+	*	0.09	0.05	0.02	0.03	<0.01	<0.01	0.09	0.11	<0.01	<0.01	0.03	0.03	0.02	0.06	<0.01	<0.01	0.01	0.01	0.03	0.01	0.04	<0.01	<0.01	<0.01
Total	*																								
WO	%	42.53	45.26	45.45	45.57	41.51	41.95	44.80	42.77	39.90	41.86	43.84	43.51	43.01	40.80	43.19	43.49	45.92	40.80	45.95	40.43	37.09	41.94	40.00	38.58
EN	%	43.38	42.69	40.60	41.09	41.91	41.86	44.11	46.73	41.62	40.82	41.27	41.84	41.62	47.03	42.15	42.27	41.07	43.55	39.28	41.68	45.34	40.90	43.53	44.03
FS	%	14.08	12.05	13.95	13.34	16.59	16.19	11.09	10.49	18.48	17.32	14.89	14.65	15.38	12.17	14.66	14.24	13.01	15.66	14.78	17.90	17.56	17.16	16.47	17.39

SERRA DO PUMA COMPLEX

Sample		SC33A	SC33A	SC33A	SC33A	SC33A	SC33A	SC33A	SC34A	SC34A	SC34A	SC34A	SC34A	SC34A	SC35	SC35	SC35	SC35	SC35	SC43	SC43	SC43	SC43	SC43	SC43
Analysis		CPX1.1	CPX1.2	CPX2.1	CPX2.2	CPX2.3	CPX3.1	CPX3.2	CPX1.1	CPX2.1	CPX2.2	CPX3.1	CPX3.2	CPX3.3	CPX3.1	CPX3.2	CPX3.3	CPX4.1	CPX4.2	CPX1.1	CPX2.1	CPX3.1	CPX3.2	CPX3.3	CPX4.1
Location	(m)	2391.0	2391.0	2391.0	2391.0	2391.0	2391.0	2391.0	2254.0	2254.0	2254.0	2254.0	2254.0	2254.0	2210.0	2210.0	2210.0	2210.0	2210.0	1585.0	1585.0	1585.0	1585.0	1585.0	1585.0
Na2O	wt. %	0.32	0.32	0.36	0.33	0.34	0.37	0.36	0.31	0.11	0.20	0.25	0.29	0.14	0.10	0.30	0.06	0.06	0.15	0.31	0.28	0.30	0.32	0.33	0.31
K2O	wt. %	0.01	<0.01	<0.01	<0.01	0.01	<0.01	0.01	<0.01	0.01	<0.01	0.01	0.05	0.01	0.01	<0.01	<0.01	<0.01	<0.01	0.01	<0.01	0.01	0.01	<0.01	<0.01
Al2O3	wt. %	1.95	1.85	1.60	1.85	1.87	1.87	1.91	0.66	0.08	0.23	0.46	0.39	0.14	0.10	0.45	0.12	0.10	0.20	1.65	1.33	1.77	2.52	1.78	1.93
MgO	wt. %	16.36	16.04	16.14	14.97	15.57	15.25	16.07	13.92	13.88	13.81	12.96	13.60	13.74	13.92	13.78	13.77	13.85	14.56	16.47	15.88	16.52	16.74	16.27	16.16
SiO2	wt. %	53.30	53.18	53.11	53.28	54.02	53.42	53.43	53.02	53.38	53.09	52.41	52.64	53.19	53.83	53.57	53.62	53.36	53.63	52.99	53.26	53.10	51.74	52.98	52.71
CaO	wt. %	21.86	21.96	21.00	22.73	22.96	22.89	21.85	23.40	24.42	24.14	23.93	23.53	24.24	24.53	24.08	24.65	24.22	23.66	21.60	23.29	21.61	20.37	21.56	21.98
MnO	wt. %	0.07	0.14	0.14	0.23	0.14	0.12	0.10	0.22	0.21	0.19	0.21	0.17	0.14	0.16	0.15	0.20	0.16	0.22	0.11	0.12	0.13	0.12	0.12	0.11
TiO2	wt. %	0.33	0.28	0.40	0.20	0.29	0.39	0.30	0.14	0.01	0.04	0.05	0.03	<0.01	<0.01	0.02	0.02	<0.01	0.01	0.27	0.25	0.27	0.24	0.39	0.25
FeO	wt. %	5.218	5.436	6.355	6.029	5.734	5.468	5.673	7.082	7.062	6.818	7.485	6.893	7.221	7.248	7.139	7.316	7.333	6.819	4.982	4.312	4.979	4.459	5.397	4.7
NiO	wt. %	0.04	0.04	0.06	0.01	<0.01	0.02	0.05	0.01	0.03	0.02	0.04	0.04	0.01	0.03	0.01	0.02	0.02	0.02	0.04	0.03	0.05	0.05	0.05	0.04
Cr2O3	wt. %	0.10	0.09	0.07	0.11	0.09	0.13	0.05	0.03	0.02	<0.01	0.02	0.03	0.03	0.03	0.05	0.03	0.04	0.05	0.09	0.13	0.11	0.06	0.09	0.10
Fe2O3	wt. %	0.29	0.62	0.25	<0.01	<0.01	<0.01	0.19	1.12	0.51	0.71	1.03	2.33	0.32	<0.01	0.30	<0.01	<0.01	<0.01	0.79	0.99	1.02	2.16	0.71	0.50
Total	wt. %	99.86	99.96	99.46	99.73	101.02	99.92	99.99	99.90	99.72	99.26	98.85	99.99	99.18	99.96	99.83	99.81	99.13	99.32	99.30	99.87	99.87	98.79	99.68	98.79
Na	*	0.02	0.02	0.03	0.02	0.02	0.03	0.03	0.02	0.01	0.02	0.02	0.02	0.01	0.01	0.02	0.01	<0.01	0.01	0.02	0.02	0.02	0.02	0.02	0.02
K	*	<0.01	<0.01	<0.01	<0.01	<0.01	<0.01	<0.01	<0.01	<0.01	<0.01	<0.01	<0.01	<0.01	<0.01	<0.01	<0.01	<0.01	<0.01	<0.01	<0.01	<0.01	<0.01	<0.01	<0.01
Al	*	0.08	0.08	0.07	0.08	0.08	0.08	0.08	0.03	<0.01	0.01	0.02	0.02	0.01	<0.01	0.02	0.01	<0.01	0.01	0.07	0.06	0.08	0.11	0.08	0.08
Mg	*	0.90	0.88	0.89	0.82	0.84	0.84	0.88	0.77	0.77	0.77	0.73	0.76	0.77	0.77	0.77	0.77	0.78	0.81	0.91	0.87	0.90	0.93	0.89	0.89
Si	*	1.96	1.95	1.96	1.97	1.97	1.96	1.96	1.98	1.99	1.99	1.98	1.97	2.00	2.00	2.00	2.00	2.00	2.00	1.96	1.96	1.95	1.92	1.95	1.95
Ca	*	0.86	0.87	0.83	0.90	0.90	0.90	0.86	0.94	0.98	0.97	0.97	0.94	0.98	0.98	0.96	0.99	0.97	0.95	0.85	0.92	0.85	0.81	0.85	0.87
Mn	*	<0.01	<0.01	<0.01	0.01	<0.01	<0.01	<0.01	0.01	0.01	0.01	0.01	0.01	0.01	0.01	0.01	0.01	0.01	0.01	<0.01	<0.01	<0.01	<0.01	<0.01	<0.01
Ti	*	0.01	0.01	0.01	0.01	0.01	0.01	0.01	<0.01	<0.01	<0.01	<0.01	<0.01	<0.01	<0.01	<0.01	<0.01	<0.01	<0.01	0.01	0.01	0.01	0.01	0.01	0.01
Fe	*	0.16	0.17	0.20	0.19	0.17	0.17	0.17	0.22	0.22	0.21	0.24	0.22	0.23	0.23	0.22	0.23	0.23	0.21	0.15	0.13	0.15	0.14	0.17	0.15
Ni	*	<0.01	<0.01	<0.01	<0.01	<0.01	<0.01	<0.01	<0.01	<0.01	<0.01	<0.01	<0.01	<0.01	<0.01	<0.01	<0.01	<0.01	<0.01	<0.01	<0.01	<0.01	<0.01	<0.01	<0.01
Cr	*	<0.01	<0.01	<0.01	<0.01	<0.01	<0.01	<0.01	<0.01	<0.01	<0.01	<0.01	<0.01	<0.01	<0.01	<0.01	<0.01	<0.01	<0.01	<0.01	<0.01	<0.01	<0.01	<0.01	<0.01
Fe3+	*	0.01	0.02	0.01	<0.01	<0.01	<0.01	0.01	0.03	0.01	0.02	0.03	0.07	0.01	<0.01	0.01	<0.01	<0.01	<0.01	0.02	0.03	0.03	0.06	0.02	0.01
Total	*	3.99	3.99	3.99	3.99	3.99	3.99	3.99	4.00	3.99	4.00	4.00	4.00	4.00	3.99	4.00	4.00	3.99	4.00	3.99	3.99	3.99	3.99	3.99	3.99
WO	%	44.88	45.29	43.37	47.09	46.79	47.32	44.93	48.45	49.57	49.59	50.05	49.19	49.47	49.49	49.33	49.80	49.22	48.04	44.62	47.76	44.57	43.25	44.55	45.66
EN	%	46.76	45.97	46.40	43.16	44.12	43.86	45.97	40.10	39.22	39.47	37.72	39.54	39.02	39.07	39.27	38.68	39.16	41.14	47.34	45.32	47.40	49.39	46.75	46.71
FS	%	8.36	8.74	10.23	9.74	9.10	8.81	9.10	11.45	11.21	10.94	12.23	11.27	11.52	11.44	11.40	11.53	11.62	10.82	8.05	6.92	8.02	7.37	8.69	7.64

SERRA DO PUMA COMPLEX

Sample		SC44	SC44	SC44	SC44	SC44	SC44	SC44	SC33B	SC33B	SC33B	SC33B	SC34B	SC34B	SC34B	SC34B	SC34B	SC34B	SC34B	SC36	SC36	SC36	SC36	SC36	SC36
Analysis		CPX1.1	CPX1.2	CPX2.1	CPX2.2	CPX3.1	CPX3.2	CPX4.1	CPX1.1	CPX1.2	CPX2.1	CPX2.2	CPX1.1	CPX1.2	CPX1.3	CPX2.1	CPX2.2	CPX3.1	CPX3.2	CPX1.1	CPX1.2	CPX1.3	CPX2.1	CPX2.2	CPX2.3
Location	(m)	1526.0	1526.0	1526.0	1526.0	1526.0	1526.0	1526.0	2391.0	2391.0	2391.0	2391.0	2254.0	2254.0	2254.0	2254.0	2254.0	2254.0	2254.0	2130.0	2130.0	2130.0	2130.0	2130.0	2130.0
Na2O	wt. %	0.28	0.27	0.30	0.35	0.27	0.27	0.26	0.39	0.41	0.37	0.39	0.39	0.36	0.40	0.37	0.41	0.09	0.48	0.33	0.37	0.32	0.35	0.35	0.36
K2O	wt. %	0.01	0.02	<0.01	0.08	<0.01	<0.01	<0.01	0.02	0.02	<0.01	<0.01	<0.01	<0.01	0.01	0.01	<0.01	0.07	0.01	0.01	<0.01	<0.01	0.01	<0.01	0.01
Al2O3	wt. %	1.91	1.89	1.72	2.23	2.02	1.91	1.75	2.13	2.67	2.55	2.37	3.63	2.11	2.11	2.56	3.46	0.82	1.88	2.86	2.73	2.81	3.00	3.11	3.01
MgO	wt. %	17.75	17.44	17.21	17.60	17.24	17.20	17.34	17.18	16.77	17.02	17.08	15.84	16.78	16.83	16.28	15.42	16.28	15.56	16.35	16.29	16.36	16.12	16.34	16.35
SiO2	wt. %	53.12	53.15	52.88	53.21	53.57	53.40	53.43	53.09	52.32	53.11	52.98	51.72	53.10	53.05	51.79	51.17	53.55	52.98	52.14	52.07	52.23	51.77	51.32	52.59
CaO	wt. %	20.70	21.13	20.90	19.81	21.01	21.26	21.15	21.47	21.40	21.60	21.48	20.48	20.92	21.07	20.63	20.87	24.09	22.42	21.40	21.01	21.38	21.07	20.66	21.36
MnO	wt. %	0.11	0.10	0.10	0.13	0.11	0.10	0.09	0.09	0.09	0.11	0.08	0.14	0.13	0.13	0.12	0.14	0.14	0.15	0.10	0.14	0.09	0.09	0.16	0.09
TiO2	wt. %	0.25	0.25	0.26	0.25	0.25	0.24	0.22	0.24	0.25	0.24	0.22	0.33	0.22	0.20	0.30	0.32	0.15	0.30	0.25	0.29	0.28	0.26	0.28	0.28
FeO	wt. %	4.123	4.156	4.472	5.048	5.252	4.814	4.671	3.577	3.391	3.81	3.599	5.716	5.142	4.57	4.864	5.132	3.372	4.724	4.351	4.67	4.53	4.611	4.206	4.824
NiO	wt. %	0.05	0.05	0.06	0.06	0.04	0.03	0.07	0.05	0.05	0.08	0.08	0.05	0.02	0.05	0.05	0.08	0.03	0.03	0.03	0.05	0.04	0.04	0.04	0.02
Cr2O3	wt. %	0.06	0.01	0.06	0.11	0.03	0.06	0.10	1.19	1.32	1.39	1.20	1.35	0.74	0.77	0.93	1.25	0.23	0.70	1.04	1.06	1.13	1.17	1.16	1.12
Fe2O3	wt. %	1.14	1.17	1.18	0.05	0.09	0.46	0.71	0.47	0.91	0.30	0.53	0.34	0.50	1.09	1.08	0.91	<0.01	0.69	1.05	1.12	0.85	0.69	1.16	0.67
Total	wt. %	99.49	99.65	99.14	98.93	99.87	99.73	99.79	99.89	99.60	100.57	100.00	99.98	100.02	100.26	98.98	99.15	98.83	99.91	99.90	99.81	100.01	99.18	98.79	100.69
Na	*	0.02	0.02	0.02	0.03	0.02	0.02	0.02	0.03	0.03	0.03	0.03	0.03	0.03	0.03	0.03	0.03	0.01	0.04	0.02	0.03	0.02	0.03	0.03	0.03
K	*	<0.01	<0.01	<0.01	<0.01	<0.01	<0.01	<0.01	<0.01	<0.01	<0.01	<0.01	<0.01	<0.01	<0.01	<0.01	<0.01	<0.01	<0.01	<0.01	<0.01	<0.01	<0.01	<0.01	<0.01
Al	*	0.08	0.08	0.08	0.10	0.09	0.08	0.08	0.09	0.12	0.11	0.10	0.16	0.09	0.09	0.11	0.15	0.04	0.08	0.12	0.12	0.12	0.13	0.14	0.13
Mg	*	0.97	0.95	0.95	0.97	0.94	0.94	0.95	0.94	0.92	0.92	0.93	0.87	0.92	0.92	0.90	0.85	0.90	0.85	0.89	0.89	0.89	0.89	0.90	0.89
Si	*	1.95	1.95	1.95	1.96	1.96	1.96	1.96	1.94	1.92	1.93	1.93	1.90	1.94	1.94	1.92	1.90	1.98	1.95	1.91	1.92	1.92	1.91	1.90	1.92
Ca	*	0.81	0.83	0.83	0.78	0.82	0.83	0.83	0.84	0.84	0.84	0.84	0.81	0.82	0.82	0.82	0.83	0.96	0.88	0.84	0.83	0.84	0.83	0.82	0.83
Mn	*	<0.01	<0.01	<0.01	<0.01	<0.01	<0.01	<0.01	<0.01	<0.01	<0.01	<0.01	<0.01	<0.01	<0.01	<0.01	0.01	<0.01	0.01	<0.01	<0.01	<0.01	<0.01	0.01	<0.01
Ti	*	0.01	0.01	0.01	0.01	0.01	0.01	0.01	0.01	0.01	0.01	0.01	0.01	0.01	0.01	0.01	0.01	<0.01	0.01	0.01	0.01	0.01	0.01	0.01	0.01
Fe	*	0.13	0.13	0.14	0.16	0.16	0.15	0.14	0.11	0.10	0.12	0.11	0.18	0.16	0.14	0.15	0.16	0.10	0.15	0.13	0.14	0.14	0.14	0.13	0.15
Ni	*	<0.01	<0.01	<0.01	<0.01	<0.01	<0.01	<0.01	<0.01	<0.01	<0.01	<0.01	<0.01	<0.01	<0.01	<0.01	<0.01	<0.01	<0.01	<0.01	<0.01	<0.01	<0.01	<0.01	<0.01
Cr	*	<0.01	<0.01	<0.01	<0.01	<0.01	<0.01	<0.01	0.03	0.04	0.04	0.04	0.04	0.02	0.02	0.03	0.04	0.01	0.02	0.03	0.03	0.03	0.03	0.03	0.03
Fe3+	*	0.03	0.03	0.03	<0.01	<0.01	0.01	0.02	0.01	0.03	0.01	0.02	0.01	0.01	0.03	0.03	0.03	<0.01	0.02	0.03	0.03	0.02	0.02	0.03	0.02
Total	*	3.99	3.99	3.99	3.99	3.99	4.00	3.99	3.99	3.99	4.00	4.00	4.00	4.00	3.99	3.99	4.00	3.99	4.00	4.00	3.99	4.00	4.00	4.00	4.00
WO	%	42.58	43.45	43.24	41.08	42.80	43.46	43.22	44.59	45.19	44.75	44.70	43.60	43.35	43.83	43.83	45.06	48.80	46.97	45.00	44.40	44.85	44.72	44.28	44.62
EN	%	50.81	49.90	49.53	50.76	48.83	48.88	49.32	49.63	49.22	49.07	49.44	46.89	48.36	48.72	48.10	46.31	45.89	45.32	47.83	47.88	47.73	47.61	48.71	47.51
FS	%	6.61	6.66	7.23	8.15	8.37	7.66	7.46	5.79	5.59	6.18	5.85	9.51	8.29	7.45	8.07	8.63	5.31	7.70	7.17	7.72	7.42	7.67	7.01	7.87

SERRA DO PUMA COMPLEX

Sample		SC38	SC38	SC38	SC38	SC38	SC38	SC38	SC39	SC39	SC39	SC39	SC39	SC39	SC40A	SC40A	SC40A	SC40A	SC40A	SC40A	SC40A	SC40A	SC41	SC41	SC41
Analysis		CPX1.1	CPX1.2	CPX2.3	CPX2.4	CPX2.5	CPX3.1	CPX3.2	CPX1.1	CPX1.2	CPX2.1	CPX2.2	CPX2.3	CPX3.1	CPX2.1	CPX2.3	CPX2.2	CPX2.4	CPX1.1	CPX1.2	CPX1.3	CPX1.4	CPX1.1	CPX1.2	CPX1.3
Location	(m)	2029.0	2029.0	2029.0	2029.0	2029.0	2029.0	2029.0	1998.0	1998.0	1998.0	1998.0	1998.0	1998.0	1930.0	1930.0	1930.0	1930.0	1930.0	1930.0	1930.0	1930.0	1850.0	1850.0	1850.0
Na2O	wt. %	0.41	0.35	0.42	0.06	0.46	0.37	0.39	0.41	0.44	0.35	0.33	0.37	0.35	0.32	0.39	0.35	0.34	0.37	0.38	0.43	0.42	0.38	0.45	0.35
K2O	wt. %	0.02	0.01	0.01	0.02	0.02	0.01	0.01	<0.01	<0.01	0.01	<0.01	<0.01	0.01	0.01	0.01	<0.01	0.01	0.01	0.01	<0.01	<0.01	<0.01	0.01	<0.01
Al2O3	wt. %	2.74	2.91	2.47	0.34	2.79	2.67	2.70	2.26	2.45	2.76	2.85	2.80	2.70	2.93	2.74	2.79	2.88	2.59	2.73	2.19	2.41	2.84	3.01	2.90
MgO	wt. %	15.70	15.94	15.61	17.61	15.53	16.44	16.55	17.14	16.34	16.20	16.36	16.21	16.23	16.56	16.40	16.22	16.01	16.36	16.55	16.04	15.87	16.04	16.12	16.34
SiO2	wt. %	52.59	51.96	51.81	55.19	52.14	52.54	52.24	52.99	52.83	52.33	52.58	52.60	52.31	52.64	52.69	52.63	52.44	52.22	52.94	53.42	52.85	52.07	51.98	53.09
CaO	wt. %	22.61	21.52	21.70	25.44	22.10	20.23	20.82	19.26	20.70	20.99	20.96	21.39	20.75	21.53	20.84	21.29	21.43	20.88	21.11	22.21	21.83	21.21	21.09	21.16
MnO	wt. %	0.12	0.08	0.13	0.10	0.11	0.10	0.13	0.13	0.12	0.13	0.13	0.11	0.11	0.08	0.15	0.11	0.11	0.14	0.14	0.17	0.15	0.11	0.11	0.10
TiO2	wt. %	0.28	0.26	0.51	0.07	0.30	0.30	0.32	0.48	0.42	0.30	0.27	0.25	0.33	0.23	0.31	0.28	0.25	0.32	0.31	0.57	0.42	0.27	0.26	0.24
FeO	wt. %	4.068	4.675	4.647	1.661	4.293	5.716	4.543	6.391	5.7	5.277	5.331	4.961	5.558	4.387	5.322	5.243	5.168	4.923	5.124	5.106	5.161	4.859	4.355	5.166
NiO	wt. %	0.05	<0.01	0.03	<0.01	0.04	0.07	0.06	0.04	0.06	0.02	0.04	0.03	0.04	0.05	0.05	0.04	0.05	0.01	0.04	0.03	0.04	0.03	0.04	0.02
Cr2O3	wt. %	1.08	1.02	0.95	0.03	0.76	0.99	1.00	0.91	0.88	1.03	1.05	1.03	1.03	1.07	1.02	0.91	1.04	1.04	0.97	0.80	1.01	1.13	1.12	1.07
Fe2O3	wt. %	1.23	0.61	1.13	0.51	0.57	<0.01	1.49	<0.01	<0.01	0.31	<0.01	0.55	0.22	0.93	0.19	<0.01	0.19	0.76	0.61	<0.01	0.29	0.09	1.01	<0.01
Total	wt. %	100.89	99.33	99.41	101.03	99.09	99.42	100.24	100.01	99.92	99.69	99.89	100.31	99.62	100.74	100.11	99.85	99.92	99.63	100.90	100.95	100.45	99.01	99.56	100.44
Na	*	0.03	0.03	0.03	<0.01	0.03	0.03	0.03	0.03	0.03	0.03	0.02	0.03	0.03	0.02	0.03	0.03	0.02	0.03	0.03	0.03	0.03	0.03	0.03	0.03
K	*	<0.01	<0.01	<0.01	<0.01	<0.01	<0.01	<0.01	<0.01	<0.01	<0.01	<0.01	<0.01	<0.01	<0.01	<0.01	<0.01	<0.01	<0.01	<0.01	<0.01	<0.01	<0.01	<0.01	<0.01
Al	*	0.12	0.13	0.11	0.02	0.12	0.12	0.12	0.10	0.11	0.12	0.12	0.12	0.12	0.13	0.12	0.12	0.13	0.11	0.12	0.09	0.10	0.12	0.13	0.12
Mg	*	0.85	0.88	0.86	0.94	0.86	0.90	0.90	0.94	0.89	0.89	0.89	0.88	0.89	0.90	0.90	0.89	0.88	0.90	0.90	0.87	0.87	0.89	0.89	0.89
Si	*	1.92	1.92	1.92	1.99	1.93	1.94	1.91	1.94	1.94	1.93	1.93	1.92	1.93	1.91	1.93	1.93	1.93	1.92	1.92	1.94	1.93	1.93	1.91	1.93
Ca	*	0.88	0.85	0.86	0.98	0.88	0.80	0.82	0.76	0.81	0.83	0.82	0.84	0.82	0.84	0.82	0.84	0.84	0.82	0.82	0.87	0.86	0.84	0.83	0.83
Mn	*	<0.01	<0.01	<0.01	<0.01	<0.01	<0.01	<0.01	<0.01	<0.01	<0.01	<0.01	<0.01	<0.01	<0.01	0.01	<0.01	<0.01	<0.01	<0.01	0.01	0.01	<0.01	<0.01	<0.01
Ti	*	0.01	0.01	0.01	<0.01	0.01	0.01	0.01	0.01	0.01	0.01	0.01	0.01	0.01	0.01	0.01	0.01	0.01	0.01	0.01	0.02	0.01	0.01	0.01	0.01
Fe	*	0.12	0.14	0.14	0.05	0.13	0.18	0.14	0.20	0.18	0.16	0.16	0.15	0.17	0.13	0.16	0.16	0.16	0.15	0.16	0.16	0.16	0.15	0.13	0.16
Ni	*	<0.01	<0.01	<0.01	<0.01	<0.01	<0.01	<0.01	<0.01	<0.01	<0.01	<0.01	<0.01	<0.01	<0.01	<0.01	<0.01	<0.01	<0.01	<0.01	<0.01	<0.01	<0.01	<0.01	<0.01
Cr	*	0.03	0.03	0.03	<0.01	0.02	0.03	0.03	0.03	0.03	0.03	0.03	0.03	0.03	0.03	0.03	0.03	0.03	0.03	0.03	0.02	0.03	0.03	3.00	0.03
Fe3+	*	0.03	0.02	0.03	0.01	0.02	<0.01	0.04	<0.01	<0.01	0.01	<0.01	0.02	0.01	0.03	0.01	<0.01	0.01	0.02	0.02	<0.01	0.01	<0.01	0.03	<0.01
Total	*	4.00	4.00	4.00	3.99	3.99	3.99	3.99	3.99	4.00	4.00	3.99	4.00	4.00	4.00	4.00	4.00	3.99	4.00	4.00	4.00	4.00	3.99	6.96	3.99
WO	%	47.50	45.49	46.14	49.67	46.97	42.51	43.95	40.06	43.23	44.07	43.75	44.74	43.54	44.87	43.57	44.40	44.89	43.97	43.86	45.79	45.56	44.83	44.95	44.17
EN	%	45.83	46.82	46.14	47.80	45.90	48.11	48.57	49.55	47.48	47.31	47.53	47.14	47.37	48.02	47.73	47.06	46.65	47.92	47.81	46.00	46.04	47.17	47.81	47.43
FS	%	6.67	7.69	7.72	2.53	7.13	9.38	7.48	10.39	9.29	8.62	8.72	8.12	9.09	7.11	8.69	8.54	8.47	8.11	8.32	8.21	8.41	8.00	7.24	8.40

SERRA DO PUMA COMPLEX

Sample		SC45	SC45	SC45	SC45	SC45	SC45	SC46	SC46	SC46	SC46	SC46	SC46	SC47A	SC47A	SC47A	SC47A	SC47A	SC47A	SC47A	SC47A	SC47B	SC47B	SC47B	SC47B
Analysis		CPX1.1	CPX1.2	CPX2.1	CPX2.2	CPX3.1	CPX3.2	CPX1.1	CPX1.2	CPX1.3	CPX1.4	CPX2.1	CPX2.2	CPX1.1	CPX1.2	CPX2.1	CPX2.2	CPX3.1	CPX3.2	CPX4.1	CPX4.2	CPX1.1	CPX2.1	CPX2.2	CPX3.1
Location	(m)	1473.0	1473.0	1473.0	1473.0	1473.0	1473.0	1213.0	1213.0	1213.0	1213.0	1213.0	1213.0	1184.0	1184.0	1184.0	1184.0	1184.0	1184.0	1184.0	1184.0	1184.0	1184.0	1184.0	1184.0
Na2O	wt. %	0.29	0.30	0.30	0.32	0.31	0.25	0.27	0.35	0.36	0.36	0.33	0.38	0.29	0.29	0.27	0.27	0.25	0.26	0.28	0.31	0.25	0.25	0.27	0.28
K2O	wt. %	<0.01	<0.01	<0.01	<0.01	<0.01	<0.01	<0.01	0.01	0.01	<0.01	<0.01	<0.01	0.01	<0.01	0.01	0.01	0.01	0.01	0.01	0.01	0.01	0.01	0.01	0.02
Al2O3	wt. %	1.94	1.91	1.68	1.78	1.97	1.93	1.68	2.16	1.89	2.23	2.44	1.76	1.71	2.05	2.15	2.00	1.89	1.93	1.96	2.15	1.87	1.82	1.87	2.16
MgO	wt. %	17.17	17.33	16.93	16.38	16.86	17.54	17.80	16.94	16.90	16.65	17.21	17.67	17.30	17.57	17.71	17.70	17.53	17.81	17.86	17.44	17.47	18.09	17.89	17.94
SiO2	wt. %	53.87	53.97	53.73	53.80	53.77	53.81	53.45	53.41	53.86	53.45	53.94	54.43	54.22	53.67	53.92	53.84	54.06	54.20	54.10	53.68	52.89	53.34	53.89	53.56
CaO	wt. %	20.77	21.14	20.78	22.06	21.49	20.84	20.66	21.48	21.73	21.90	21.21	20.19	21.39	20.89	20.86	21.30	21.02	21.07	21.05	21.14	20.97	21.21	20.89	20.79
MnO	wt. %	0.12	0.11	0.13	0.12	0.13	0.12	0.13	0.11	0.11	0.09	0.07	0.11	0.13	0.11	0.11	0.08	0.12	0.12	0.10	0.09	0.06	0.10	0.10	0.06
TiO2	wt. %	0.26	0.24	0.42	0.40	0.27	0.21	0.24	0.23	0.27	0.31	0.33	0.33	0.18	0.25	0.25	0.11	0.16	0.15	0.14	0.27	0.14	0.21	0.15	0.19
FeO	wt. %	5.545	5.2	5.963	5.345	5.337	5.259	4.543	4.569	4.8	4.623	5.025	5.379	4.446	4.719	4.407	4.279	4.4	4.388	4.384	4.346	3.3	3.207	3.831	3.831
NiO	wt. %	0.02	0.06	0.03	0.05	0.04	0.05	0.03	0.04	0.06	0.06	0.01	0.06	0.06	0.06	0.04	0.02	0.03	0.05	0.03	0.05	0.07	0.03	0.03	0.07
Cr2O3	wt. %	0.22	0.19	0.18	0.20	0.20	0.25	0.18	0.40	0.38	0.31	0.21	0.39	0.25	0.23	0.24	0.27	0.26	0.28	0.29	0.22	0.19	0.15	0.17	0.23
Fe2O3	wt. %	<0.01	0.05	<0.01	<0.01	0.06	<0.01	0.71	0.21	0.15	0.50	<0.01	<0.01	<0.01	<0.01	<0.01	0.01	<0.01	<0.01	<0.01	<0.01	<0.01	0.51	<0.01	<0.01
Total	wt. %	100.20	100.51	100.15	100.45	100.44	100.24	99.70	99.91	100.53	100.48	100.78	100.70	99.97	99.82	99.95	99.88	99.74	100.27	100.20	99.71	97.21	98.93	99.09	99.14
Na	*	0.02	0.02	0.02	0.02	0.02	0.02	0.02	0.03	0.03	0.03	0.02	0.03	0.02	0.02	0.02	0.02	0.02	0.02	0.02	0.02	0.02	0.02	0.02	0.02
K	*	<0.01	<0.01	<0.01	<0.01	<0.01	<0.01	<0.01	<0.01	<0.01	<0.01	<0.01	<0.01	<0.01	<0.01	<0.01	<0.01	<0.01	<0.01	<0.01	<0.01	<0.01	<0.01	<0.01	<0.01
Al	*	0.08	0.08	0.07	0.08	0.08	0.08	0.07	0.09	0.08	0.10	0.10	0.08	0.07	0.09	0.09	0.09	0.08	0.08	0.08	0.09	0.08	0.08	0.08	0.09
Mg	*	0.93	0.94	0.92	0.89	0.92	0.95	0.97	0.92	0.92	0.90	0.93	0.95	0.94	0.96	0.96	0.96	0.95	0.96	0.97	0.95	0.97	0.99	0.98	0.98
Si	*	1.96	1.96	1.96	1.96	1.96	1.96	1.95	1.95	1.96	1.95	1.95	1.97	1.97	1.96	1.96	1.96	1.97	1.96	1.96	1.96	1.97	1.96	1.97	1.96
Ca	*	0.81	0.82	0.81	0.86	0.84	0.81	0.81	0.84	0.85	0.85	0.82	0.78	0.83	0.82	0.81	0.83	0.82	0.82	0.82	0.83	0.84	0.83	0.82	0.81
Mn	*	<0.01	<0.01	<0.01	<0.01	<0.01	<0.01	<0.01	<0.01	<0.01	<0.01	<0.01	<0.01	<0.01	<0.01	<0.01	<0.01	<0.01	<0.01	<0.01	<0.01	<0.01	<0.01	<0.01	<0.01
Ti	*	0.01	0.01	0.01	0.01	0.01	0.01	0.01	0.01	0.01	0.01	0.01	0.01	0.01	0.01	0.01	<0.01	<0.01	<0.01	<0.01	0.01	<0.01	0.01	<0.01	0.01
Fe	*	0.17	0.16	0.18	0.16	0.16	0.16	0.14	0.14	0.15	0.14	0.15	0.16	0.14	0.14	0.13	0.13	0.13	0.13	0.13	0.13	0.10	0.10	0.12	0.70
Ni	*	<0.01	<0.01	<0.01	<0.01	<0.01	<0.01	<0.01	<0.01	<0.01	<0.01	<0.01	<0.01	<0.01	<0.01	<0.01	<0.01	<0.01	<0.01	<0.01	<0.01	<0.01	<0.01	<0.01	<0.01
Cr	*	0.01	0.01	0.01	0.01	0.01	0.01	0.01	0.01	0.01	0.01	0.01	0.01	0.01	0.01	0.01	0.01	0.01	0.01	0.01	0.01	0.01	<0.01	0.01	0.01
Fe3+	*	<0.01	<0.01	<0.01	<0.01	<0.01	<0.01	0.02	0.01	<0.01	0.01	<0.01	<0.01	<0.01	<0.01	<0.01	<0.01	<0.01	<0.01	<0.01	<0.01	<0.01	0.01	<0.01	<0.01
Total	*	3.99	4.00	3.99	3.99	3.99	3.99	4.00	4.00	3.99	4.00	4.00	3.99	3.99	4.00	3.99	3.99	3.98	3.99	3.99	3.99	3.99	3.99	3.99	4.58
WO	%	42.42	42.89	42.41	45.01	43.74	42.23	42.18	44.19	44.36	44.99	43.22	41.20	43.73	42.61	42.62	43.23	43.02	42.76	42.69	43.31	43.82	43.41	42.83	32.66
EN	%	48.74	48.88	48.10	46.48	47.76	49.45	50.57	48.45	47.98	47.58	48.79	50.21	49.19	49.87	50.34	50.00	49.95	50.29	50.37	49.71	50.79	51.49	51.05	39.25
FS	%	8.84	8.23	9.49	8.51	8.51	8.32	7.25	7.36	7.66	7.43	7.99	8.59	7.08	7.52	7.03	6.77	7.03	6.95	6.94	6.97	5.39	5.11	6.13	28.09

SERRA DO PUMA COMPLEX

Sample		SC47B	SC47B	SC47B	SC47B	SC47B	SC47B	SC50	SC50	SC50	SC50	SC50	SC48	SC48	SC48	SC48	SC48	SC48	SC48	SC48
Analysis		CPX3.2	CPX1.1	CPX3.2	CPX4.1	CPX4.2	CPX4.3	CPX1.1	CPX1.2	CPX1.3	CPX1.4	CPX1.5	CPX1.1	CPX1.2	CPX1.3	CPX2.1	CPX2.2	CPX1.1	CPX2.1	CPX3.1
Location	(m)	1184.0	1184.0	1184.0	1184.0	1184.0	1184.0	790.0	790.0	790.0	790.0	790.0	1145.0	1145.0	1145.0	1145.0	1145.0	1145.0	1145.0	1145.0
Na2O	wt. %	0.27	0.26	0.27	0.24	0.26	0.25	0.49	0.50	0.54	0.44	0.56	0.36	0.31	0.36	0.37	0.44	0.36	0.35	0.39
K2O	wt. %	0.02	<0.01	0.01	<0.01	<0.01	0.01	0.01	<0.01	0.01	0.02	<0.01	0.01	<0.01	0.01	0.01	<0.01	0.01	<0.01	0.02
Al2O3	wt. %	1.90	1.79	1.88	1.86	1.91	1.83	2.43	2.35	2.66	2.46	2.25	2.19	2.06	2.17	2.19	2.17	2.10	2.25	2.58
MgO	wt. %	18.48	18.40	17.94	17.84	18.00	18.12	17.23	17.84	16.43	17.25	16.94	17.14	19.34	17.68	17.45	17.61	17.84	17.13	16.56
SiO2	wt. %	53.86	54.51	54.51	54.52	54.69	54.46	51.87	53.16	52.26	52.95	52.89	53.14	53.71	53.47	54.04	53.31	53.61	53.42	53.28
CaO	wt. %	19.59	21.19	21.67	21.00	21.41	21.10	20.17	20.37	21.66	20.58	21.60	21.34	18.63	20.77	20.26	19.31	20.44	20.74	21.48
MnO	wt. %	0.09	0.09	0.11	0.12	0.09	0.09	0.08	0.08	0.06	0.09	0.08	0.11	0.10	0.13	0.11	0.11	0.11	0.10	0.10
TiO2	wt. %	0.16	0.17	0.11	0.15	0.13	0.17	0.38	0.36	0.40	0.36	0.41	0.16	0.16	0.20	0.16	0.26	0.15	0.19	0.21
FeO	wt. %	3.872	4.049	3.916	4.46	4.038	4.157	3.369	3.529	3.163	3.561	3.008	3.922	4.413	4.123	4.57	5.084	4.364	4.413	4.266
NiO	wt. %	0.04	0.06	0.01	0.05	0.08	0.06	0.07	0.06	0.06	0.02	0.05	0.07	0.06	0.03	0.08	0.04	0.07	0.08	0.03
Cr2O3	wt. %	0.16	0.19	0.15	0.19	0.18	0.16	1.30	1.22	1.31	1.19	1.26	1.14	1.17	1.20	1.17	1.07	1.21	1.15	1.13
Fe2O3	wt. %	<0.01	0.11	<0.01	<0.01	<0.01	<0.01	0.31	0.01	0.27	<0.01	0.20	0.28	0.26	0.16	<0.01	<0.01	0.03	<0.01	<0.01
Total	wt. %	98.44	100.82	100.57	100.44	100.79	100.42	97.71	99.47	98.82	98.92	99.24	99.85	100.20	100.30	100.43	99.41	100.31	99.83	100.05
Na	*	0.02	0.02	0.02	0.02	0.02	0.02	0.04	0.04	0.04	0.03	0.04	0.03	0.02	0.03	0.03	0.03	0.03	0.03	0.03
K	*	<0.01	<0.01	<0.01	<0.01	<0.01	<0.01	<0.01	<0.01	<0.01	<0.01	<0.01	<0.01	<0.01	<0.01	<0.01	<0.01	<0.01	<0.01	<0.01
Al	*	0.08	0.08	0.08	0.08	0.08	0.08	0.11	0.10	0.12	0.11	0.10	0.09	0.09	0.09	0.09	0.09	0.09	0.10	0.11
Mg	*	1.01	0.99	0.97	0.96	0.97	0.98	0.96	0.97	0.90	0.94	0.93	0.93	1.04	0.96	0.94	0.96	0.97	0.93	0.90
Si	*	1.98	1.96	1.97	1.97	1.97	1.97	1.93	1.94	1.93	1.94	1.94	1.94	1.94	1.94	1.96	1.95	1.95	1.95	1.94
Ca	*	0.77	0.82	0.84	0.81	0.83	0.82	0.80	0.80	0.86	0.81	0.85	0.84	0.72	0.81	0.79	0.76	0.80	0.81	0.84
Mn	*	<0.01	<0.01	<0.01	<0.01	<0.01	<0.01	<0.01	<0.01	<0.01	<0.01	<0.01	<0.01	<0.01	<0.01	<0.01	<0.01	<0.01	<0.01	<0.01
Ti	*	<0.01	0.01	<0.01	<0.01	<0.01	0.01	0.01	0.01	0.01	0.01	0.01	<0.01	<0.01	0.01	<0.01	0.01	<0.01	0.01	0.01
Fe	*	0.12	0.12	0.12	0.14	0.12	0.13	0.11	0.11	0.10	0.11	0.09	0.12	0.13	0.13	0.14	0.16	0.13	0.14	0.13
Ni	*	<0.01	<0.01	<0.01	<0.01	<0.01	<0.01	<0.01	<0.01	<0.01	<0.01	<0.01	<0.01	<0.01	<0.01	<0.01	<0.01	<0.01	<0.01	<0.01
Cr	*	0.01	0.01	<0.01	0.01	0.01	<0.01	0.04	0.04	0.04	0.04	0.04	0.03	0.03	0.03	0.03	0.03	0.04	0.03	0.03
Fe3+	*	<0.01	<0.01	<0.01	<0.01	<0.01	<0.01	0.01	<0.01	0.01	<0.01	0.01	0.01	0.01	<0.01	<0.01	<0.01	<0.01	<0.01	<0.01
Total	*	3.98	3.99	3.99	3.98	3.99	3.99	4.00	4.00	4.00	3.99	4.00	3.99	3.99	3.99	3.98	3.99	3.99	3.99	3.99
WO	%	40.55	42.42	43.62	42.59	43.16	42.57	43.11	42.48	46.10	43.45	45.47	44.23	38.04	42.75	42.12	40.43	42.02	43.18	44.89
EN	%	53.19	51.25	50.23	50.34	50.47	50.86	51.26	51.76	48.63	50.70	49.60	49.42	54.95	50.63	50.48	51.25	51.00	49.63	48.15
FS	%	6.27	6.33	6.14	7.07	6.37	6.57	5.63	5.76	5.28	5.85	4.93	6.36	7.01	6.61	7.40	8.32	6.98	7.19	6.96

SERRA DO ONÇA COMPLEX

Sample		SC22	SC22	SC22	SC22	SC22	SC22	SC23	SC23	SC23	SC23	SC23	SC23	SC24A	SC24A	SC24A	SC24A	SC24A	SC24A	SC24A	SC11	SC11	SC11	SC11	SC11
Analysis		PL1.1	PL1.2	PL2.1	PL2.2	PL3.1	PL2.2	PL1.1	PL1.2	PL2.1	PL2.2	PL3.1	PL3.2	PL1.1	PL1.2	PL2.1	PL2.2	PL2.3	PL3.1	PL3.2	PL1.1	PL1.2	PL2.1	PL2.2	PL3.1
Location	(m)	1898.0	1898.0	1898.0	1898.0	1898.0	1898.0	1987.0	1987.0	1987.0	1987.0	1987.0	1987.0	2081.0	2081.0	2081.0	2081.0	2081.0	2081.0	2081.0	1060.0	1060.0	1060.0	1060.0	1060.0
Na2O	wt. %	5.41	5.00	4.83	4.92	4.97	5.01	4.36	4.42	4.58	4.88	4.63	4.43	4.81	4.60	4.57	4.13	4.65	4.98	5.40	4.14	4.31	4.26	4.16	4.20
K2O	wt. %	0.26	0.25	0.26	0.26	0.19	0.23	0.25	0.20	0.24	0.27	0.27	0.25	0.23	0.26	0.29	0.24	0.25	0.27	0.35	0.08	0.06	0.07	0.07	0.07
SiO2	wt. %	54.64	54.05	53.38	53.51	53.44	53.75	53.40	53.10	53.87	53.81	53.11	53.09	53.77	53.63	52.88	52.58	53.23	54.02	54.24	51.60	52.25	51.67	51.69	52.14
Al2O3	wt. %	28.82	28.87	29.50	28.77	29.08	28.90	29.72	29.94	29.07	29.11	29.72	29.71	29.10	29.21	29.32	29.49	29.08	28.67	28.24	30.09	29.90	30.41	30.35	30.28
FeO	wt. %	0.30	0.38	0.27	0.40	0.36	0.27	0.40	0.40	0.82	0.36	0.43	0.39	0.48	0.45	0.40	0.38	0.37	0.41	0.39	0.31	0.38	0.33	0.31	0.36
CaO	wt. %	11.12	11.51	11.89	11.49	11.64	11.69	12.36	12.55	11.74	11.61	12.37	12.33	12.21	12.01	11.99	12.39	12.14	11.49	11.08	13.08	13.13	13.40	13.30	13.15
BaO	wt. %	0.04	>0.01	0.13	>0.01	>0.01	0.09	>0.01	0.10	0.09	>0.01	>0.01	>0.01	0.03	>0.01	>0.01	>0.01	0.07	0.11	0.06	>0.01	>0.01	0.18	>0.01	>0.01
SrO	wt. %	>0.01	0.04	0.01	>0.01	0.01	>0.01	>0.01	>0.01	>0.01	0.05	>0.01	>0.01	>0.01	>0.01	0.05	>0.01	>0.01	>0.01	>0.01	>0.01	0.06	>0.01	>0.01	>0.01
Total	wt. %	100.595	100.089	100.254	99.344	99.689	99.93	100.482	100.706	100.392	100.087	100.526	100.214	100.615	100.15	99.495	99.209	99.783	99.951	99.765	99.3	100.098	100.32	99.868	100.197
Na	*	0.47	0.44	0.42	0.44	0.44	0.44	0.38	0.39	0.40	0.43	0.41	0.39	0.42	0.40	0.40	0.37	0.41	0.44	0.48	0.37	0.38	0.38	0.37	0.37
K	*	0.02	0.01	0.02	0.02	0.01	0.01	0.01	0.01	0.01	0.02	0.02	0.02	0.01	0.02	0.02	0.01	0.01	0.02	0.02	0.01	>0.01	>0.01	>0.01	>0.01
Si	*	2.46	2.45	2.42	2.44	2.43	2.44	2.41	2.40	2.44	2.44	2.40	2.40	2.43	2.43	2.41	2.40	2.42	2.45	2.46	2.36	2.38	2.35	2.36	2.37
Al	*	1.53	1.54	1.57	1.55	1.56	1.55	1.58	1.59	1.55	1.55	1.58	1.59	1.55	1.56	1.58	1.59	1.56	1.53	1.51	1.62	1.60	1.63	1.63	1.62
Fe	*	0.01	0.01	0.01	0.02	0.01	0.01	0.02	0.02	0.03	0.01	0.02	0.02	0.02	0.02	0.02	0.02	0.01	0.02	0.02	0.01	0.02	0.01	0.01	0.01
Ca	*	0.54	0.56	0.58	0.56	0.57	0.57	0.60	0.61	0.57	0.56	0.60	0.60	0.59	0.58	0.59	0.61	0.59	0.56	0.54	0.64	0.64	0.65	0.65	0.64
Ba	*	>0.01	>0.01	>0.01	>0.01	>0.01	>0.01	>0.01	>0.01	>0.01	>0.01	>0.01	>0.01	>0.01	>0.01	>0.01	>0.01	>0.01	>0.01	>0.01	>0.01	>0.01	>0.01	>0.01	>0.01
Sr	*	>0.01	>0.01	>0.01	>0.01	>0.01	>0.01	>0.01	>0.01	>0.01	>0.01	>0.01	>0.01	>0.01	>0.01	>0.01	>0.01	>0.01	>0.01	>0.01	>0.01	>0.01	>0.01	>0.01	>0.01
Total	*	5.02	5.01	5.02	5.01	5.02	5.02	5.00	5.01	5.00	5.01	5.02	5.01	5.02	5.00	5.01	4.99	5.01	5.01	5.03	5.01	5.02	5.03	5.02	5.01
AB	%	46.15	43.36	41.74	43.03	43.08	43.10	38.41	38.49	40.77	42.55	39.75	38.84	41.07	40.32	40.14	37.09	40.35	43.26	45.95	36.23	37.16	36.37	36.02	36.49
OR	%	1.47	1.40	1.45	1.47	1.11	1.31	1.42	1.13	1.39	1.57	1.52	1.46	1.31	1.48	1.66	1.43	1.40	1.54	1.96	0.45	0.33	0.37	0.38	0.40
AN.	%	52.38	55.24	56.81	55.50	55.82	55.59	60.17	60.38	57.83	55.88	58.73	59.70	57.63	58.20	58.20	61.49	58.25	55.19	52.09	63.33	62.51	63.26	63.60	63.11

SERRA DO ONÇA COMPLEX

Sample		SC11	SC12	SC12	SC12	SC12	SC12	SC12	SC12	SC12	SC13	SC13	SC13	SC13	SC13	SC13	SC14	SC14	SC14	SC14	SC14	SC14	SC15	SC15	SC15
Analysis		PL3.2	PL1.1	PL1.2	PL2.1	PL2.2	PL2.1	PL2.2	PL3.1	PL3.2	PL1.1	PL1.2	PL2.1	PL2.2	PL2.1	PL2.2	PL1.1	PL1.2	PL2.1	PL2.2	PL3.1	PL4.1	PL1.1	PL1.1	PL3.1
Location	(m)	1060.0	1120.0	1120.0	1120.0	1120.0	1120.0	1120.0	1120.0	1120.0	1135.0	1135.0	1135.0	1135.0	1135.0	1135.0	1225.0	1225.0	1225.0	1225.0	1225.0	1225.0	1370.0	1370.0	1370.0
Na2O	wt. %	4.16	4.58	4.81	4.24	4.57	4.60	4.52	4.22	4.49	5.25	5.07	4.69	4.60	4.79	4.78	4.87	4.73	4.96	5.31	5.03	4.71	4.77	4.71	4.76
K2O	wt. %	0.07	0.22	0.23	0.22	0.20	0.19	0.21	0.25	0.20	0.13	0.18	0.13	0.11	0.11	0.09	0.19	0.16	0.10	0.16	0.14	0.16	0.27	0.27	0.22
SiO2	wt. %	51.75	52.85	53.25	52.73	52.58	53.49	53.15	52.46	52.68	54.33	53.95	53.28	52.47	53.08	52.85	52.88	52.87	53.36	54.24	53.75	53.19	53.43	52.82	52.89
Al2O3	wt. %	30.22	29.89	29.63	30.08	29.76	29.26	29.31	29.76	29.84	29.37	29.16	29.69	29.91	29.76	30.06	29.12	29.30	29.12	28.93	29.29	29.39	29.54	29.43	29.66
FeO	wt. %	0.43	0.35	0.27	0.26	0.37	0.37	0.58	0.37	0.41	0.30	0.35	0.34	0.38	0.39	0.23	0.43	0.24	0.27	0.38	0.34	0.47	0.46	0.30	0.38
CaO	wt. %	13.34	12.27	12.05	12.99	12.34	12.28	12.33	12.51	12.60	11.68	11.67	12.22	12.37	12.43	12.54	12.09	12.22	11.85	11.37	11.79	12.30	12.12	12.23	12.26
BaO	wt. %	0.06	0.03	0.04	>0.01	0.01	>0.01	0.11	>0.01	0.06	0.06	>0.01	0.11	0.27	0.14	>0.01	>0.01	0.09	0.07	>0.01	0.11	0.09	>0.01	0.01	0.11
SrO	wt. %	>0.01	>0.01	0.05	0.02	0.01	>0.01	>0.01	>0.01	>0.01	0.03	>0.01	>0.01	>0.01	>0.01	>0.01	>0.01	>0.01	>0.01	>0.01	>0.01	>0.01	>0.01	>0.01	>0.01
Total	wt. %	100.024	100.193	100.336	100.54	99.847	100.183	100.201	99.563	100.275	101.136	100.372	100.454	100.11	100.695	100.542	99.581	99.602	99.733	100.391	100.438	100.3	100.585	99.772	100.284
Na	*	0.37	0.40	0.42	0.37	0.40	0.40	0.40	0.37	0.40	0.46	0.44	0.41	0.41	0.42	0.42	0.43	0.42	0.44	0.47	0.44	0.41	0.42	0.42	0.42
K	*	>0.01	0.01	0.01	0.01	0.01	0.01	0.01	0.01	0.01	0.01	0.01	0.01	0.01	0.01	0.01	0.01	0.01	0.01	0.01	0.01	0.01	0.02	0.02	0.01
Si	*	2.36	2.39	2.41	2.38	2.39	2.42	2.41	2.39	2.39	2.43	2.44	2.41	2.39	2.40	2.39	2.41	2.41	2.43	2.45	2.43	2.41	2.41	2.40	2.40
Al	*	1.62	1.60	1.58	1.60	1.60	1.56	1.57	1.60	1.59	1.55	1.55	1.58	1.60	1.58	1.60	1.57	1.57	1.56	1.54	1.56	1.57	1.57	1.58	1.59
Fe	*	0.02	0.01	0.01	0.01	0.01	0.01	0.02	0.01	0.02	0.01	0.01	0.01	0.01	0.02	0.01	0.02	0.01	0.01	0.01	0.01	0.02	0.02	0.01	0.01
Ca	*	0.65	0.60	0.58	0.63	0.60	0.60	0.60	0.61	0.61	0.56	0.56	0.59	0.60	0.60	0.61	0.59	0.60	0.58	0.55	0.57	0.60	0.59	0.60	0.60
Ba	*	>0.01	>0.01	>0.01	>0.01	>0.01	>0.01	>0.01	>0.01	>0.01	>0.01	>0.01	>0.01	0.01	>0.01	>0.01	>0.01	>0.01	>0.01	>0.01	>0.01	>0.01	>0.01	>0.01	>0.01
Sr	*	>0.01	>0.01	>0.01	>0.01	>0.01	>0.01	>0.01	>0.01	>0.01	>0.01	>0.01	>0.01	>0.01	>0.01	>0.01	>0.01	>0.01	>0.01	>0.01	>0.01	>0.01	>0.01	>0.01	>0.01
Total	*	5.02	5.02	5.02	5.01	5.02	5.01	5.01	5.00	5.02	5.02	5.02	5.01	5.02	5.02	5.03	5.03	5.02	5.02	5.02	5.02	5.02	5.02	5.02	5.03
AB	%	35.96	39.83	41.40	36.64	39.69	39.94	39.42	37.36	38.75	44.54	43.56	40.71	39.99	40.83	40.62	41.71	40.81	42.86	45.39	43.22	40.56	40.95	40.47	40.76
OR	%	0.37	1.23	1.30	1.25	1.13	1.10	1.18	1.45	1.16	0.72	1.00	0.72	0.65	0.62	0.48	1.09	0.89	0.59	0.90	0.79	0.92	1.55	1.53	1.26
AN.	%	63.68	58.94	57.30	62.12	59.18	58.96	59.40	61.19	60.09	54.74	55.44	58.58	59.37	58.55	58.90	57.20	58.29	56.55	53.70	55.99	58.52	57.50	58.00	57.98

SERRA DO ONÇA COMPLEX

Sample		SC15	SC15	SC15	SC16B	SC16B	SC16B	SC16B	SC16B	SC16B	SC17	SC17	SC17	SC17	SC17	SC17	SC18	SC18	SC18	SC18	SC18	SC18	SC18	SC19	SC19
Analysis		PL3.2	PL4.1	PL4.2	PL1.1	PL1.2	PL2.1	PL2.2	PL3.1	PL3.2	PL1.1	PL1.2	PL2.1	PL2.2	PL3.1	PL3.2	PL1.2	PL1.3	PL2.1	PL3.1	PL4.1	PL4.2	PL5.1	PL1.1	PL1.2
Location	(m)	1370.0	1370.0	1370.0	1445.0	1445.0	1445.0	1445.0	1445.0	1445.0	1500.0	1500.0	1500.0	1500.0	1500.0	1500.0	1565.0	1565.0	1565.0	1565.0	1565.0	1565.0	1565.0	1670.0	1670.0
Na2O	wt. %	4.90	4.56	4.55	5.28	5.28	5.34	5.29	5.17	5.25	5.38	5.24	5.46	5.36	5.30	5.25	5.41	5.41	5.97	5.30	5.66	5.71	5.31	5.00	5.06
K2O	wt. %	0.25	0.30	0.24	0.26	0.24	0.28	0.29	0.21	0.22	0.29	0.27	0.25	0.26	0.23	0.31	0.23	0.28	0.32	0.23	0.23	0.25	0.20	0.31	0.29
SiO2	wt. %	53.01	52.76	52.39	54.37	54.36	54.22	54.14	53.82	54.08	55.22	55.11	55.79	55.59	55.64	55.59	54.56	55.80	56.43	55.23	55.49	55.26	54.81	54.64	54.63
Al2O3	wt. %	29.46	29.74	29.59	29.00	28.88	28.70	28.54	28.98	28.94	28.10	28.04	28.29	28.15	27.99	28.15	28.49	28.29	27.64	28.48	28.26	28.24	28.59	29.32	29.00
FeO	wt. %	0.35	0.40	0.47	0.35	0.29	0.35	0.35	0.31	0.27	0.45	0.43	0.47	0.50	0.40	0.48	0.46	0.45	0.35	0.49	0.39	0.36	0.44	0.40	0.44
CaO	wt. %	12.13	12.43	12.36	11.44	11.22	11.22	11.35	11.45	11.32	10.69	11.19	10.96	10.89	11.24	11.16	11.15	10.97	10.11	11.08	10.51	10.51	11.12	11.70	11.50
BaO	wt. %	0.04	0.09	0.09	0.01	>0.01	0.06	0.01	0.06	0.10	>0.01	>0.01	0.04	0.06	>0.01	0.06	0.03	>0.01	0.09	0.07	0.04	0.06	0.10	>0.01	>0.01
SrO	wt. %	>0.01	>0.01	>0.01	0.02	>0.01	>0.01	>0.01	>0.01	0.01	0.04	>0.01	>0.01	>0.01	>0.01	>0.01	>0.01	>0.01	>0.01	>0.01	>0.01	0.01	0.01	>0.01	>0.01
Total	wt. %	100.136	100.269	99.695	100.733	100.267	100.149	99.977	99.989	100.18	100.165	100.282	101.256	100.802	100.805	100.981	100.329	101.198	100.912	100.864	100.562	100.387	100.578	101.361	100.905
Na	*	0.43	0.40	0.40	0.46	0.46	0.47	0.47	0.45	0.46	0.47	0.46	0.47	0.47	0.46	0.46	0.47	0.47	0.52	0.46	0.49	0.50	0.46	0.43	0.44
K	*	0.01	0.02	0.01	0.02	0.01	0.02	0.02	0.01	0.01	0.02	0.02	0.01	0.02	0.01	0.02	0.01	0.02	0.02	0.01	0.01	0.01	0.01	0.02	0.02
Si	*	2.41	2.39	2.39	2.45	2.45	2.45	2.45	2.44	2.45	2.49	2.49	2.49	2.49	2.50	2.49	2.46	2.49	2.52	2.48	2.49	2.49	2.47	2.44	2.45
Al	*	1.58	1.59	1.59	1.54	1.54	1.53	1.53	1.55	1.54	1.49	1.49	1.49	1.49	1.48	1.49	1.52	1.49	1.46	1.51	1.50	1.50	1.52	1.54	1.53
Fe	*	0.01	0.02	0.02	0.01	0.01	0.01	0.01	0.01	0.01	0.02	0.02	0.02	0.02	0.02	0.02	0.02	0.02	0.01	0.02	0.01	0.01	0.02	0.02	0.02
Ca	*	0.59	0.60	0.60	0.55	0.54	0.54	0.55	0.56	0.55	0.52	0.54	0.52	0.52	0.54	0.54	0.54	0.53	0.48	0.53	0.51	0.51	0.54	0.56	0.55
Ba	*	>0.01	>0.01	>0.01	>0.01	>0.01	>0.01	>0.01	>0.01	>0.01	>0.01	>0.01	>0.01	>0.01	>0.01	>0.01	>0.01	>0.01	>0.01	>0.01	>0.01	>0.01	>0.01	>0.01	>0.01
Sr	*	>0.01	>0.01	>0.01	>0.01	>0.01	>0.01	>0.01	>0.01	>0.01	>0.01	>0.01	>0.01	>0.01	>0.01	>0.01	>0.01	>0.01	>0.01	>0.01	>0.01	>0.01	>0.01	>0.01	>0.01
Total	*	5.03	5.02	5.02	5.02	5.02	5.03	5.03	5.02	5.02	5.01	5.01	5.01	5.00	5.00	5.00	5.02	5.01	5.02	5.01	5.01	5.02	5.01	5.01	5.01
AB	%	41.65	39.19	39.44	44.86	45.34	45.58	45.02	44.44	45.08	46.89	45.19	46.71	46.43	45.43	45.20	46.13	46.41	50.74	45.83	48.75	48.88	45.84	42.82	43.59
OR	%	1.38	1.72	1.38	1.45	1.36	1.55	1.63	1.18	1.23	1.65	1.52	1.41	1.48	1.31	1.73	1.31	1.59	1.79	1.29	1.28	1.39	1.14	1.77	1.65
AN.	%	56.97	59.09	59.17	53.69	53.30	52.87	53.36	54.38	53.69	51.46	53.29	51.88	52.09	53.26	53.06	52.56	52.00	47.48	52.88	49.97	49.73	53.02	55.41	54.76

SERRA DO ONÇA COMPLEX

Sample		SC19	SC19	SC19	SC19	SC19	SC20	SC20	SC20	SC20	SC20	SC20	SC21	SC21	SC21	SC21	SC21	SC25	SC25	SC25	SC25	SC25	SC25	SC25	SC26
Analysis		PL2.1	PL2.2	PL3.1	PL3.2	PL3.3	PL1.1	PL1.2	PL2.1	PL2.2	PL3.1	PL3.2	PL1.1	PL1.2	PL2.1	PL2.2	PL3.1	PL1.1	PL2.1	PL2.2	PL3.1	PL3.2	PL4.1	PL4.2	PL1.1
Location	(m)	1670.0	1670.0	1670.0	1670.0	1670.0	1748.0	1748.0	1748.0	1748.0	1748.0	1748.0	1800.0	1800.0	1800.0	1800.0	1800.0	2171.0	2171.0	2171.0	2171.0	2171.0	2171.0	2171.0	2278.0
Na2O	wt. %	4.94	5.01	4.40	4.86	4.84	4.83	5.11	5.00	4.97	4.72	4.86	4.14	4.08	4.51	4.38	4.61	5.12	5.28	4.60	5.30	4.53	4.89	5.37	4.44
K2O	wt. %	0.31	0.24	0.24	0.25	0.25	0.22	0.19	0.16	0.20	0.24	0.20	0.30	0.24	0.22	0.21	0.21	0.17	0.18	0.17	0.20	0.22	0.16	0.22	0.26
SiO2	wt. %	54.38	54.64	52.55	53.75	54.15	53.08	54.04	53.89	54.02	53.94	54.10	52.80	52.39	53.70	53.17	53.33	54.30	54.90	53.44	54.58	53.05	53.97	55.04	53.44
Al2O3	wt. %	29.09	29.06	29.94	29.52	29.14	29.00	28.72	28.88	29.09	29.17	28.97	29.93	30.28	29.79	29.78	29.74	28.88	29.08	29.81	28.82	29.58	29.44	29.04	29.95
FeO	wt. %	0.71	0.41	0.34	0.36	0.34	0.43	0.38	0.49	0.47	0.47	0.48	0.34	0.39	0.22	0.26	0.27	0.39	0.34	0.34	0.38	0.40	0.42	0.21	0.21
CaO	wt. %	11.67	11.44	12.51	11.90	11.83	11.77	11.40	11.74	11.62	11.97	11.65	12.90	13.48	12.46	12.49	12.33	11.54	11.70	12.55	11.18	12.63	11.83	11.42	12.46
BaO	wt. %	>0.01	0.01	0.03	>0.01	>0.01	>0.01	>0.01	0.01	0.01	>0.01	0.01	>0.01	>0.01	>0.01	>0.01	>0.01	0.13	>0.01	0.10	0.06	0.11	0.03	>0.01	>0.01
SrO	wt. %	>0.01	>0.01	0.02	>0.01	>0.01	>0.01	>0.01	>0.01	>0.01	>0.01	>0.01	>0.01	0.01	>0.01	>0.01	0.03	>0.01	>0.01	>0.01	>0.01	>0.01	>0.01	>0.01	>0.01
Total	wt. %	101.088	100.817	100.035	100.631	100.546	99.325	99.832	100.162	100.384	100.499	100.271	100.416	100.859	100.911	100.291	100.518	100.519	101.488	101.009	100.511	100.525	100.729	101.299	100.763
Na	*	0.43	0.44	0.39	0.43	0.42	0.43	0.45	0.44	0.44	0.41	0.43	0.36	0.36	0.39	0.38	0.40	0.45	0.46	0.40	0.46	0.40	0.43	0.47	0.39
K	*	0.02	0.01	0.01	0.01	0.01	0.01	0.01	0.01	0.01	0.01	0.01	0.02	0.01	0.01	0.01	0.01	0.01	0.01	0.01	0.01	0.01	0.01	0.01	0.02
Si	*	2.44	2.45	2.39	2.42	2.44	2.42	2.45	2.44	2.44	2.43	2.44	2.39	2.37	2.41	2.40	2.41	2.45	2.45	2.40	2.46	2.40	2.43	2.46	2.40
Al	*	1.54	1.54	1.60	1.57	1.55	1.56	1.53	1.54	1.55	1.55	1.54	1.60	1.61	1.58	1.59	1.58	1.53	1.53	1.58	1.53	1.58	1.56	1.53	1.59
Fe	*	0.03	0.02	0.01	0.01	0.01	0.02	0.01	0.02	0.02	0.02	0.02	0.01	0.02	0.01	0.01	0.01	0.02	0.01	0.01	0.01	0.02	0.02	0.01	0.01
Ca	*	0.56	0.55	0.61	0.58	0.57	0.58	0.55	0.57	0.56	0.58	0.56	0.63	0.65	0.60	0.61	0.60	0.56	0.56	0.61	0.54	0.61	0.57	0.55	0.60
Ba	*	>0.01	>0.01	>0.01	>0.01	>0.01	>0.01	>0.01	>0.01	>0.01	>0.01	>0.01	>0.01	>0.01	>0.01	>0.01	>0.01	>0.01	>0.01	>0.01	>0.01	>0.01	>0.01	>0.01	>0.01
Sr	*	>0.01	>0.01	>0.01	>0.01	>0.01	>0.01	>0.01	>0.01	>0.01	>0.01	>0.01	>0.01	>0.01	>0.01	>0.01	>0.01	>0.01	>0.01	>0.01	>0.01	>0.01	>0.01	>0.01	>0.01
Total	*	5.02	5.00	5.01	5.02	5.01	5.02	5.01	5.02	5.01	5.01	5.00	5.00	5.01	5.00	5.00	5.01	5.01	5.02	5.01	5.02	5.02	5.01	5.02	5.00
AB	%	42.64	43.58	38.36	41.90	41.96	42.08	44.29	43.14	43.13	41.06	42.52	36.11	34.91	39.06	38.33	39.87	44.10	44.50	39.50	45.67	38.86	42.40	45.43	38.63
OR	%	1.75	1.40	1.39	1.40	1.43	1.28	1.09	0.90	1.15	1.35	1.17	1.72	1.36	1.27	1.20	1.17	0.96	1.01	0.94	1.14	1.27	0.90	1.21	1.51
AN.	%	55.62	55.02	60.26	56.70	56.62	56.64	54.63	55.97	55.73	57.59	56.31	62.16	63.73	59.67	60.47	58.97	54.94	54.49	59.57	53.19	59.87	56.70	53.35	59.86

SERRA DO ONÇA COMPLEX

Sample		SC26	SC26	SC26	SC26	SC26	SC27	SC27	SC27	SC27	SC27	SC27
Analysis		PL1.2	PL1.3	PL2.1	PL2.2	PL2.3	PL1.1	PL1.2	PL2.1	PL2.2	PL3.1	PL4.1
Location	(m)	2278.0	2278.0	2278.0	2278.0	2278.0	2448.0	2448.0	2448.0	2448.0	2448.0	2448.0
Na2O	wt. %	4.50	4.47	4.91	4.83	4.69	5.08	5.21	5.78	5.65	5.33	5.35
K2O	wt. %	0.25	0.39	0.16	0.15	0.21	0.31	0.29	0.37	0.35	0.25	0.32
SiO2	wt. %	53.07	53.52	53.66	53.70	53.61	54.76	54.98	56.14	56.37	55.24	55.72
Al2O3	wt. %	30.02	29.34	29.19	29.24	29.51	28.72	28.93	28.10	28.11	28.51	28.26
FeO	wt. %	0.22	0.29	0.41	0.35	0.34	0.15	0.23	0.25	0.30	0.31	0.24
CaO	wt. %	12.67	12.44	11.94	11.94	12.26	11.55	11.30	10.51	10.51	11.20	11.08
BaO	wt. %	0.26	>0.01	>0.01	0.03	>0.01	>0.01	0.09	>0.01	0.01	0.16	0.11
SrO	wt. %	>0.01	>0.01	>0.01	>0.01	>0.01	>0.01	0.03	0.03	>0.01	>0.01	>0.01
Total	wt. %	100.988	100.445	100.255	100.225	100.618	100.582	101.058	101.179	101.299	100.988	101.08
Na	*	0.39	0.39	0.43	0.42	0.41	0.44	0.45	0.50	0.49	0.46	0.46
K	*	0.01	0.02	0.01	0.01	0.01	0.02	0.02	0.02	0.02	0.01	0.02
Si	*	2.39	2.42	2.43	2.43	2.42	2.46	2.46	2.51	2.51	2.48	2.49
Al	*	1.59	1.56	1.56	1.56	1.57	1.52	1.53	1.48	1.48	1.51	1.49
Fe	*	0.01	0.01	0.02	0.01	0.01	0.01	0.01	0.01	0.01	0.01	0.01
Ca	*	0.61	0.60	0.58	0.58	0.59	0.56	0.54	0.50	0.50	0.54	0.53
Ba	*	0.01	>0.01	>0.01	>0.01	>0.01	>0.01	>0.01	>0.01	>0.01	>0.01	>0.01
Sr	*	>0.01	>0.01	>0.01	>0.01	>0.01	>0.01	>0.01	>0.01	>0.01	>0.01	>0.01
Total	*	5.02	5.01	5.02	5.01	5.01	5.01	5.01	5.02	5.01	5.01	5.01
AB	%	38.54	38.54	42.27	41.92	40.44	43.55	44.73	48.87	48.33	45.61	45.79
OR	%	1.42	2.24	0.88	0.84	1.19	1.75	1.64	2.06	1.95	1.40	1.82
AN.	%	60.04	59.22	56.84	57.24	58.37	54.70	53.63	49.07	49.72	52.99	52.39

SERRA DO PUMA COMPLEX	Sample		SC33A	SC33A	SC33A	SC33A	SC33A	SC33A	SC34A	SC34A	SC34A	SC34A	SC34A	SC34A	SC34A	SC34A	SC34A	SC35	SC35	SC35	SC35	SC35	SC35	SC35	SC35	SC35
	Analysis		PL1.1	PL1.2	PL1.3	PL2.1	PL2.2	PL3.1	PL1.1	PL1.2	PL1.3	PL2.1	PL2.2	PL3.1	PL4.1	PL4.2	PL5.1	PL1.1	PL1.2	PL2.1	PL2.2	PL3.1	PL3.1	PL3.2	PL4.1	PL4.2
	Location	(m)	2391.0	2391.0	2391.0	2391.0	2391.0	2391.0	2254.0	2254.0	2254.0	2254.0	2254.0	2254.0	2254.0	2254.0	2254.0	2210.0	2210.0	2210.0	2210.0	2210.0	2210.0	2210.0	2210.0	2210.0
	Na2O	wt. %	5.44	5.38	5.52	5.25	5.42	5.50	7.14	6.54	6.32	6.60	6.60	4.75	6.73	4.98	6.33	5.72	5.76	6.05	5.92	7.13	6.00	5.96	5.53	5.24
	K2O	wt. %	0.06	0.11	0.04	0.07	0.06	0.13	0.06	0.02	0.07	0.22	0.06	0.03	0.06	0.04	0.10	0.09	0.05	0.08	0.06	0.08	0.12	0.06	0.22	0.08
	SiO2	wt. %	55.21	54.77	54.93	53.99	54.73	54.53	58.65	57.54	56.57	56.90	57.04	53.82	57.81	54.34	56.03	55.74	55.57	56.78	56.16	58.90	55.44	56.73	53.32	55.13
	Al2O3	wt. %	28.65	28.45	29.01	29.38	29.13	29.10	26.49	27.63	28.19	26.52	27.53	30.24	27.10	29.82	27.81	28.72	28.84	28.56	28.59	26.84	28.38	28.36	27.36	29.29
	FeO	wt. %	0.07	0.25	0.08	0.35	0.15	0.45	0.12	0.12	0.18	0.88	0.14	0.23	0.30	0.14	0.55	0.06	0.04	>0.01	0.15	0.12	1.59	0.22	2.10	0.25
	CaO	wt. %	11.05	11.28	11.05	11.70	11.40	11.12	8.38	9.35	9.70	8.88	9.35	12.54	9.06	11.82	9.87	10.94	11.06	10.27	10.41	8.48	9.91	10.23	11.35	11.32
	BaO	wt. %	>0.01	0.10	>0.01	>0.01	>0.01	>0.01	0.10	>0.01	>0.01	>0.01	>0.01	0.14	0.19	0.08	0.11	0.08	>0.01	0.04	>0.01	0.13	0.11	>0.01	>0.01	>0.01
	SrO	wt. %	0.02	>0.01	>0.01	>0.01	>0.01	>0.01	0.05	>0.01	>0.01	>0.01	>0.01	>0.01	>0.01	0.07	>0.01	>0.01	0.02	>0.01	>0.01	>0.01	>0.01	>0.01	>0.01	>0.01
	Total	wt. %	100.499	100.34	100.631	100.743	100.881	100.821	100.989	101.191	101.028	99.995	100.709	101.739	101.258	101.288	100.805	101.344	101.337	101.778	101.295	101.667	101.542	101.547	99.878	101.315
	Na	*	0.47	0.47	0.48	0.46	0.47	0.48	0.61	0.56	0.55	0.58	0.57	0.41	0.58	0.43	0.55	0.49	0.50	0.52	0.51	0.61	0.52	0.51	0.49	0.45
	K	*	>0.01	0.01	>0.01	>0.01	>0.01	0.01	>0.01	>0.01	0.01	>0.01	0.01	>0.01	>0.01	>0.01	0.01	0.01	>0.01	>0.01	>0.01	>0.01	0.01	>0.01	0.01	0.01
	Si	*	2.48	2.47	2.46	2.43	2.45	2.45	2.60	2.55	2.52	2.57	2.55	2.40	2.57	2.43	2.51	2.48	2.48	2.51	2.50	2.60	2.48	2.51	2.45	2.46
	Al	*	1.52	1.51	1.53	1.56	1.54	1.54	1.39	1.44	1.48	1.41	1.45	1.59	1.42	1.57	1.47	1.51	1.51	1.49	1.50	1.40	1.50	1.48	1.48	1.54
	Fe	*	>0.01	0.01	>0.01	0.01	0.01	0.02	0.01	>0.01	0.01	0.03	0.01	0.01	0.01	0.01	0.02	>0.01	>0.01	>0.01	0.01	>0.01	0.06	0.01	0.08	0.01
	Ca	*	0.53	0.55	0.53	0.56	0.55	0.54	0.40	0.44	0.46	0.43	0.45	0.60	0.43	0.57	0.47	0.52	0.53	0.49	0.50	0.40	0.48	0.49	0.56	0.54
	Ba	*	>0.01	>0.01	>0.01	>0.01	>0.01	>0.01	>0.01	>0.01	>0.01	>0.01	>0.01	>0.01	>0.01	>0.01	>0.01	>0.01	>0.01	>0.01	>0.01	>0.01	>0.01	>0.01	>0.01	>0.01
	Sr	*	>0.01	>0.01	>0.01	>0.01	>0.01	>0.01	>0.01	>0.01	>0.01	>0.01	>0.01	>0.01	>0.01	>0.01	>0.01	>0.01	>0.01	>0.01	>0.01	>0.01	>0.01	>0.01	>0.01	>0.01
	Total	*	5.00	5.01	5.01	5.02	5.02	5.03	5.01	5.01	5.02	5.03	5.02	5.01	5.02	5.00	5.03	5.01	5.02	5.01	5.01	5.01	5.04	5.01	5.07	5.00
	AB	%	46.94	46.06	47.37	44.65	46.12	46.89	60.43	55.83	53.91	56.63	55.91	40.57	57.15	43.13	53.43	48.38	48.38	51.39	50.52	60.10	51.91	51.13	46.28	45.38
	OR	%	0.33	0.61	0.22	0.40	0.31	0.73	0.35	0.10	0.38	1.23	0.31	0.17	0.36	0.25	0.55	0.48	0.29	0.45	0.35	0.42	0.71	0.36	1.19	0.47
	AN.	%	52.73	53.34	52.41	54.96	53.57	52.38	39.22	44.07	45.71	42.14	43.78	59.26	42.50	56.62	46.02	51.14	51.34	48.17	49.14	39.48	47.38	48.51	52.52	54.15
SERRA DO PUMA COMPLEX	Sample		SC35	SC43	SC43	SC43	SC43	SC43	SC43	SC44	SC44	SC44	SC44	SC44	SC44	SC44	SC34B	SC34B	SC34B	SC34B	SC38	SC38	SC38	SC38	SC40A	SC40A	SC40A
	Analysis		PL5.1	PL1.1	PL1.2	PL2.1	PL2.2	PL3.1	PL4.2	PL1.1	PL1.2	PL2.1	PL2.2	PL3.1	PL3.2	PL1.1	PL1.2	PL1.3	PL2.1	PL2.1	PL2.2	PL2.3	PL2.4	PL1.1	PL1.2	PL1.3
	Location	(m)	2210.0	1585.0	1585.0	1585.0	1585.0	1585.0	1585.0	1526.0	1526.0	1526.0	1526.0	1526.0	1526.0	2254.0	2254.0	2254.0	2254.0	2029.0	2029.0	2029.0	2029.0	1930.0	1930.0	1930.0
	Na2O	wt. %	6.04	5.40	5.26	5.20	5.23	4.95	4.93	4.50	4.63	4.58	4.66	4.56	4.77	4.74	4.71	4.72	0.46	3.15	4.22	3.80	4.88	4.15	4.85	4.92
	K2O	wt. %	0.04	0.06	0.08	0.03	0.05	0.02	0.08	0.09	0.14	0.08	0.10	0.11	0.09	0.07	0.06	0.07	>0.01	0.03	0.05	0.05	0.09	0.05	0.13	0.07
	SiO2	wt. %	56.57	54.32	53.59	54.90	55.06	53.85	53.21	53.00	53.14	53.12	54.01	52.90	53.11	53.85	53.36	53.66	50.84	50.60	52.55	51.56	54.22	53.67	54.27	54.80
	Al2O3	wt. %	27.70	29.36	28.71	29.30	29.13	29.47	29.44	30.07	29.54	29.95	30.26	30.01	29.74	30.04	29.88	30.10	2.77	31.92	31.11	31.16	29.74	29.52	29.08	29.63
	FeO	wt. %	0.18	0.22	0.32	0.07	0.21	0.03	0.24	0.28	0.36	0.01	0.19	0.29	0.11	0.19	0.34	0.20	5.93	0.25	0.27	0.25	0.23	0.23	0.22	0.19
	CaO	wt. %	9.95	11.23	11.30	11.68	11.36	12.08	12.30	12.89	12.36	12.37	12.23	12.90	12.52	12.33	12.40	12.66	21.10	15.28	13.45	13.87	12.09	12.45	11.18	11.86
	BaO	wt. %	0.03	>0.01	0.14	0.13	>0.01	0.07	0.14	0.04	>0.01	>0.01	0.03	0.06	0.03	>0.01	>0.01	>0.01	0.15	0.07	>0.01	0.07	0.01	>0.01	>0.01	0.01
	SrO	wt. %	>0.01	>0.01	>0.01	>0.01	>0.01	0.01	>0.01	>0.01	>0.01	>0.01	>0.01	0.01	>0.01	>0.01	>0.01	>0.01	>0.01	>0.01	>0.01	>0.01	0.01	>0.01	>0.01	>0.01
	Total	wt. %	100.503	100.58	99.397	101.305	101.051	100.475	100.332	100.862	100.162	100.121	101.466	100.826	100.374	101.221	100.755	101.397	81.252	101.29	101.654	100.746	101.258	100.078	99.728	101.476
	Na	*	0.52	0.47	0.47	0.45	0.45	0.43	0.43	0.39	0.41	0.40	0.40	0.40	0.42	0.41	0.41	0.41	0.05	0.28	0.37	0.33	0.42	0.36	0.43	0.43
	K	*	>0.01	>0.01	>0.01	>0.01	>0.01	>0.01	0.01	0.01	0.01	0.01	0.01	0.01	0.01	>0.01	>0.01	>0.01	>0.01	>0.01	>0.01	>0.01	0.01	>0.01	0.01	>0.01
	Si	*	2.53	2.44	2.44	2.45	2.46	2.43	2.41	2.39	2.41	2.40	2.41	2.39	2.40	2.41	2.40	2.40	3.02	2.28	2.35	2.33	2.42	2.42	2.45	2.44
	Al	*	1.46	1.56	1.54	1.54	1.53	1.56	1.57	1.60	1.58	1.60	1.59	1.60	1.58	1.58	1.59	1.59	0.19	1.70	1.64	1.66	1.57	1.57	1.55	1.56
	Fe	*	0.01	0.01	0.01	>0.01	0.01	>0.01	0.01	0.01	0.01	>0.01	0.01	0.01	>0.01	0.01	0.01	0.01	0.29	0.01	0.01	0.01	0.01	0.01	0.01	0.01
	Ca	*	0.48	0.54	0.55	0.56	0.54	0.58	0.60	0.62	0.60	0.60	0.58	0.62	0.61	0.59	0.60	0.61	1.34	0.74	0.65	0.67	0.58	0.60	0.54	0.57
	Ba	*	>0.01	>0.01	>0.01	>0.01	>0.01	>0.01	>0.01	>0.01	>0.01	>0.01	>0.01	>0.01	>0.01	>0.01	>0.01	>0.01	>0.01	>0.01	>0.01	>0.01	>0.01	>0.01	>0.01	>0.01
	Sr	*	>0.01	>0.01	>0.01	>0.01	>0.01	>0.01	>0.01	>0.01	>0.01	>0.01	>0.01	>0.01	>0.01	>0.01	>0.01	>0.01	>0.01	>0.01	>0.01	>0.01	>0.01	>0.01	>0.01	>0.01
	Total	*	5.00	5.02	5.02	5.01	5.00	5.01	5.03	5.01	5.01	5.00	5.00	5.02	5.02	5.01	5.01	5.01	4.91	5.01	5.01	5.01	5.01	4.97	4.99	5.00
	AB	%	52.22	46.38	45.51	44.54	45.31	42.55	41.86	38.50	40.09	39.94	40.60	38.76	40.60	40.88	40.58	40.11	3.82	27.13	36.11	33.03	41.99	37.54	43.63	42.72
	OR	%	0.22	0.31	0.43	0.16	0.31	0.13	0.46	0.50	0.80	0.48	0.56	0.63	0.51	0.38	0.36	0.39	>0.01	0.16	0.25	0.26	0.49	0.28	0.76	0.37
	AN.	%	47.56	53.31	54.07	55.30	54.38	57.32	57.68	60.99	59.12	59.58	58.84	60.61	58.89	58.74	59.06	59.50	96.18	72.71	63.64	66.71	57.52	62.18	55.62	56.91
SERRA DO PUMA COMPLEX	Sample		SC40A	SC40A	SC41	SC41	SC41	SC41	SC41	SC41	SC41	SC41	SC41	SC41	SC41	SC41	SC45	SC45	SC45	SC45	SC45	SC45	SC45	SC46	SC46	SC46	SC46
	Analysis		PL1.4	PL1.5	PL1.1	PL1.2	PL1.3	PL1.4	PL1.5	PL2.1	PL2.2	PL3.1	PL3.2	PL4.1	PL4.2	PL1.1	PL1.2	PL1.3	PL2.1	PL2.2	PL3.1	PL3.2	PL1.1	PL1.2	PL1.3	PL2.1
	Location	(m)	1930.0	1930.0	1850.0	1850.0	1850.0	1850.0	1850.0	1850.0	1850.0	1850.0	1850.0	1850.0	1850.0	1473.0	1473.0	1473.0	1473.0	1473.0	1473.0	1473.0	1213.0	1213.0	1213.0	1213.0
	Na2O	wt. %	4.99	4.74	0.45	3.97	2.82	4.55	4.14	5.18	5.06	3.79	3.89	3.02	3.84	4.09	4.75	4.98	4.49	4.71	4.43	4.44	5.89	5.78	5.80	7.06
	K2O	wt. %	0.06	0.27	>0.01	0.05	0.12	0.09	0.09	0.07	0.06	0.08	0.04	0.16	0.53	0.05	0.08	0.06	0.11	0.05	0.09	0.06	0.14	0.25	0.18	0.16
	SiO2	wt. %	53.93	53.82	50.30	51.44	47.43	52.78	51.99	53.54	53.83	50.46	51.31	49.23	51.04	51.89	52.64	53.25	52.27	52.87	52.30	52.62	55.43	55.74	55.97	58.21
	Al2O3	wt. %	29.39	29.58	2.32	30.38	29.08	29.77	30.52	29.15	29.28	30.56	30.55	31.95	30.14	30.65	29.84	29.40	30.05	29.75	30.02	30.23	28.02	28.32	28.28	26.41
	FeO	wt. %	0.25	0.76	6.01	0.22	0.31	0.33	0.39	0.26	0.27	0.37	0.37	0.73	0.26	0.27	0.27	0.22	0.31	0.18	0.62	0.16	0.22	0.25	0.19	0.33
	CaO	wt. %	11.89	12.18	19.78	12.92	13.48	12.53	13.11	11.29	11.75	13.46	13.44	14.82	12.91	13.09	12.34	11.95	12.38	12.18	12.80	12.80	10.42	10.08	10.39	8.40
	BaO	wt. %	0.03	0.06	>0.01	0.05	>0.01	>0.01	>0.01	0.01	>0.01	0.02	>0.01	0.02	0.10	>0.01	0.01	0.06	0.04	>0.01	>0.01	>0.01	>0.01	>0.01	0.13	0.02	0.02
	SrO	wt. %	>0.01	>0.01	>0.01	>0.01	>0.01	>0.01	>0.01	>0.01	>0.01	>0.01	>0.01	>0.01	>0.01	>0.01	>0.01	>0.01	>0.01	>0.01	>0.01	>0.01	>0.01	>0.01	>0.01	>0.01
	Total	wt. %	100.542	101.395	78.866	99.018	93.235	100.048	100.232	99.497	100.241	98.734	99.606	99.918	98.817	100.03	99.93	99.913	99.642	99.742	100.252	100.308	100.117	100.557	100.834	100.59
	Na	*	0.44	0.41	0.05	0.35	0.27	0.40	0.36	0.46	0.44	0.34	0.35	0.27	0.34	0.36	0.42	0.44	0.40	0.42	0.39	0.39	0.51	0.50	0.50	0.61
	K	*	>0.01	0.02	>0.01	>0.01	0.01	0.01	0.01	>0.01	>0.01	0.01	>0.01	0.01	0.03	>0.01	>0.01	>0.01	0.01	>0.01	0.01	>0.01	0.01	0.01	0.01	0.01
	Si	*	2.43	2.41	3.06	2.36	2.32	2.39	2.36	2.43	2.43	2.33	2.34	2.26	2.35	2.36	2.39	2.42	2.38	2.40	2.37	2.38	2.50	2.50	2.50	2.60
	Al	*	1.56	1.56	0.17	1.64	1.67	1.59	1.63	1.56	1.56	1.66	1.65	1.73	1.64	1.64	1.60	1.57	1.61	1.59	1.61	1.61	1.49	1.50	1.49	1.39
	Fe	*	0.01	0.03	0.31	0.01	0.01	0.01	0.02	0.01	0.01	0.01	0.01	0.03	0.01	0.01	0.01	0.01	>0.01	0.01	0.02	0.01	0.01	0.01	0.01	0.01
	Ca	*	0.57	0.59	1.29	0.64	0.71	0.61	0.64	0.55	0.57	0.67	0.66	0.73	0.64	0.64	0.60	0.58	0.60	0.59	0.62	0.62	0.50	0.48	0.50	0.40
	Ba	*	>0.01	>0.01	>0.01	>0.01	>0.01	>0.01	>0.01	>0.01	>0.01	>0.01	>0.01	>0.01	>0.01	>0.01	>0.01	>0.01	>0.01	>0.01	>0.01	>0.01	>0.01	>0.01	>0.01	>0.01
	Sr	*	>0.01	>0.01	>0.01	>0.01	>0.01	>0.01	>0.01	>0.01	>0.01	>0.01	>0.01	>0.01	>0.01	>0.01	>0.01	>0.01	>0.01	>0.01	>0.01	>0.01	>0.01	>0.01	>0.01	>0.01
	Total	*	5.01	5.02	4.88	5.00	4.98	5.01	5.01	5.02	5.01	5.01	5.01	5.02	5.02	5.01	5.02	5.02	5.00	5.01	5.02	5.01	5.02	5.01	5.01	5.02
	AB	%	43.01	40.71	3.99	35.62	27.30	39.43	36.16	45.15	43.63	33.59	34.32	26.69	33.92	35.99	40.89	42.86	39.39	41.08	38.31	38.46	50.16	50.20	49.72	59.82
	OR	%	0.32	1.52	>0.01	0.28	0.74	0.54	0.51	0.41	0.34	0.46	0.23	0.90	3.09	0.29	0.44	0.32	0.61	0.27	0.52	0.32	0.80	1.42	1.03	0.87
	AN.	%	56.663	57.778	96.015	64.1	71.962	60.03	63.335	54.436	56.034	65.959	65.453	72.407	62.984	63.727	58.673	56.822	59.999	58.65	61.175	61.218	49.042	48.382	49.257	39.31
SERRA DO PUMA COMPLEX	Sample		SC46	SC46	SC46	SC46	SC46	SC47A	SC47A	SC47A	SC47A	SC47A	SC47A	SC47A	SC47A	SC47B	SC47B	SC47B	SC47B	SC47B	SC47B	SC47B	SC47B				
	Analysis		PL2.2	PL3.1	PL3.2	PL4.1	PL4.2	PL1.1	PL1.2	PL2.1	PL2.2	PL3.1	PL3.2	PL4.1	PL4.2	PL1.1	PL1.2	PL2.1	PL2.2	PL3.1	PL3.2	PL4.1	PL4.2				
	Location	(m)	1213.0	1213.0	1213.0	1213.0	1213.0	1184.0	1184.0	1184.0	1184.0	1184.0	1184.0	1184.0	1184.0	1184.0	1184.0	1184.0	1184.0	1184.0	1184.0	1184.0	1184.0				
	Na2O	wt. %	6.83	6.18	6.16	5.73	5.55	4.10	4.25	4.54	4.41	3.98	4.28	4.38	4.42	4.18	4.40	4.15	4.38	4.14	4.34	4.18	4.25				
	K2O	wt. %	0.11	0.11	0.11	0.15	0.15	0.07	0.10	0.09	0.12	0.06	0.06	0.05	0.05	0.07	0.11	0.05	0.10	0.06	0.08	0.09	0.10				
	SiO2	wt. %	57.96	56.32	55.69	55.67	55.26	51.71	51.96	52.76	52.33	51.69	51.73	52.32	52.64	51.64	51.77	51.57	51.43	51.97	52.19	51.82	52.30				
	Al2O3	wt. %	26.84	27.83	27.98	28.26	28.44	30.42	30.18	29.92	29.97	30.43	30.27	30.10	30.12	30.11	29.63	29.93	30.02	30.55	30.02	30.70	30.40				
	FeO	wt. %	0.18	0.20	0.19	0.21	0.24	0.27	0.23	0.21	0.18	0.30	0.29	0.26	0.33	0.24	0.49	0.16	0.15	0.24	0.27	0.26	0.30				
	CaO	wt. %	8.42	9.81	9.85	10.40	10.99	13.33	12.92	12.59	12.54	13.10	13.03	12.76	12.70	12.87	12.42	12.94	12.62	13.30	13.22	13.35	12.84				
	BaO	wt. %	0.05	>0.01	>0.01	0.04	0.04	>0.01	0.05	0.09	0.05	>0.01	0.08	>0.01	0.01	0.04	>0.01	>0.01	0.07	0.20	0.09	0.01	>0.01				
	SrO	wt. %	>0.01	>0.01	>0.01	>0.01	>0.01	>0.01	>0.01	>0.01	>0.01	>0.01	>0.01	>0.01	>0.01	>0.01	>0.01	>0.01	>0.01	>0.01	>0.01	>0.01	>0.01				
	Total	wt. %	100.388	100.441	99.984	100.458	100.668	99.894	99.682	100.198	99.593	99.557	99.743	99.866	100.267	99.149	98.817	98.801	98.766	100.467	100.194	100.423	100.192				
	Na	*	0.59	0.54	0.54	0.50	0.48	0.36	0.38	0.40	0.39	0.35	0.38	0.39	0.39	0.37	0.39	0.37	0.39	0.36	0.38	0.37	0.37				
	K	*	0.01	0.01	0.01	0.01	0.01	>0.01	0.01	0.01	0.01	>0.01	>0.01	>0.01	>0.01	>0.01	0.01	>0.01	0.01	>0.01	>0.01	0.01	0.01				
	Si	*	2.59	2.52	2.51	2.50	2.48	2.35	2.37	2.39	2.38	2.36	2.36	2.38	2.38	2.37	2.38	2.37	2.37	2.36	2.37	2.35	2.37				
	Al	*	1.41	1.47	1.49	1.50	1.50	1.63	1.62	1.60	1.61	1.64	1.63	1.61	1.61	1.63	1.61	1.62	1.63	1.63	1.61	1.64	1.62				
	Fe	*	0.01	0.01	0.01	0.01	0.01	0.01	0.01	0.01	0.01	0.01	0.01	0.01	0.01	0.01	0.02	0.01	0.01	0.01	0.01	0.01	0.01				
	Ca	*	0.40	0.47	0.48	0.50	0.53	0.65	0.63	0.61	0.61	0.64	0.64	0.62	0.62	0.63	0.61	0.64	0.62	0.65	0.64	0.65	0.62				
	Ba	*	>0.01	>0.01	>0.01	>0.01	>0.01	>0.01	>0.01	>0.01	>0.01	>0.01	>0.01	>0.01	>0.01	>0.01	>0.01	>0.01	>0.01	>0.01	>0.01	>0.01	>0.01				
	Sr	*	>0.01	>0.01	>0.01	>0.01	>0.01	>0.01	>0.01	>0.01	>0.01	>0.01	>0.01	>0.01	>0.01	>0.01	>0.01	>0.01	>0.01	>0.01	>0.01	>0.01	>0.01				
	Total	*	5.01	5.01	5.02	5.01	5.01	5.01	5.01	5.01	5.01	5.00	5.02	5.01	5.01	5.01	5.02	5.01	5.02	5.01	5.02	5.02	5.01				
	AB	%	59.12	52.95	52.76	49.51	47.36	35.61	37.12	39.28	38.60	35.35	37.19	38.24	38.54	36.85	38.84	36.59	38.35	35.91	37.10	35.99	37.26				
	OR	%	0.61	0.61	0.63	0.87	0.84	0.39	0.57	0.53	0.67	0.33	0.33	0.26	0.28	0.43	0.62	0.30	0.56	0.36	0.44	0.52	0.56				
	AN.	%	40.28	46.44	46.60	49.62	51.80	64.00	62.31	60.20	60.74	64.32	62.48	61.50	61.18	62.72	60.54	63.11	61.09	63.73	62.47	63.48	62.18				